UNIVERSITY OF LONDON THESIS

Degree PhD Year 2008 Name of Author SALEH-HADDADI, ALI, AFRAIM.

EEG-Correlated Functional MRI in Epilepsy

by

Dr Afraim Salek-Haddadi

Department of Clinical & Experimental Epilepsy

INSTITUTE OF NEUROLOGY

University College London (UCL)

Thesis submitted for the degree of Doctor of Philosophy

UNIVERSITY OF LONDON

2008

ProQuest LLC
789 East Eisenhower Parkway
P.O. Box 1346
Ann Arbor, MI 48106-1346

Declaration of own work

I Afraim Salek-Haddadi, confirm that the work presented in this thesis is my own and that I am the sole author. Where information has been derived from other sources, I confirm that this has been indicated in the thesis.

I have outlined my own individual contribution to the published work in chapter 1, alongside those of co-workers and collaborators.

Signed:

Date: 27.11.06

To

Jane, Skye & Siena

Preface

This dissertation is the result of 4 years work as a full-time Clinical Research Fellow of the Department of Clinical and Experimental Epilepsy, UCL Institute of Neurology, based primarily at the MRI Unit, National Society of Epilepsy, Chalfont St Peter. A further 4 years was spent analyzing the remaining data, finalizing the publications and drafting this thesis during full-time training as a Specialist Registrar in Clinical Neurology, at the National Hospital for Neurology & Neurosurgery, Queen Square, St George's Hospital, Tooting, St Mary's Hospital, Paddington, and Charing Cross Hospital, Hammersmith.

The first two years was funded as part of a co-operative group component grant from the Medical Research Council, UK, awarded to Professor David Fish and Professor Louis Lemieux, and the next two years from a combination of two UCL CRDC grants awarded to Professor David Fish, Dr Matthias Koepp and Professor Mark Richardson. I am indebted to the grant holders for providing me with the opportunity to do cutting edge research in a world-class environment.

The bulk of the experimental work was carried out at the MRI Unit at the National Society for Epilepsy (NSE), Chalfont St Peter with excellent support from the radiographers, Philippa Bartlett, Jane Burdette, and Penny Hitchings, and physics team Dr Mark Symms, Dr Phil Boulby, and Professor Gareth Barker, under the directorship of Professor John Duncan. The research was made possible by the efforts of Mr Philip Allen and his team of engineers are the Department of Clinical Neurophysiology, National Hospital for Neurology & Neurosurgery (NHNN) who built and developed the necessary hardware and software for recording simultaneous EEG. I am indebted to them for their very generous support throughout the project. I was fortunate enough to be able to work closely with the methods group at the Welcome Trust Centre for Neuroimaging (formerly the FIL), headed by Professor Karl Friston, over several of the more technical aspects of the project and am grateful to Professor Robert Tuner and Mr Oliver Josephs for key ideas.

During my time at the NSE I had the privilege of working and collaborating with several researchers and visiting fellows, many of whom are now personal friends including Dr Tejal Mitchell, Dr Rebecca Liu, Dr Robert Simister, Dr Fergus Rugg-Gunn, Dr Sofia Eriksson, Dr Robert Powell, Dr Athanasos Gaitatsis, Dr Khalid

Hamandi, Dr Torben Lund, Dr Beate Diehl, Dr Martin Merschhemke, and Dr Alexander Hammers. I would like to thank my predecessor Dr Karsten Krakow for introducing me to what would have been a very daunting field and my successors, Dr Khalid Hamandi and Dr Helmut Laufs, for keeping me up to date with such a fast moving field. I am grateful to the clinical staff at the NSE and NHNN for referring patients and thank the many dozens of patients who gave freely and willingly of their time.

Finally, I would like to thank my supervisors, professors David Fish and Louis Lemieux for their patience, guidance, wisdom, support and encouragement.

Abstract

This thesis concerns the application of simultaneous EEG-correlated functional MRI (EEG/fMRI) to imaging epileptiform activity in vivo. The limitations of fMRI and scalp EEG are discussed together with the key advantages and limitations of combining the two.

Findings are presented from work on over 100 patient volunteers with epilepsy, including the first continuous EEG/fMRI patient study, and results from imaging focal electrographic seizures and absence seizures (serving as human evidence for the reciprocal participation of focal thalamic and widespread cortical networks during generalized spike-wave activity).

The core comprises a study of interictal epileptiform EEG activity (IEDs) in 63 patients with focal epilepsy. Semi-automated spike detection and advanced modeling strategies are introduced to account for different EEG event types, and to minimize false activations from uncontrolled motion. We show that: (1) significant hemodynamic correlates were detectable in over 68% of patients in whom discharges were captured and were highly, but not entirely, concordant with site(s) of presumed seizure generation where known; (2) deactivations were less concordant and may non-specifically reflect the consequential or downstream effects of IEDs on brain activity; (3) a striking pattern of retrosplenial deactivation was observed in 7 cases mainly with focal discharges; (4) the general hemodynamic response to IEDs is physiological; (5) incorporating information about different types of IEDs, their durations and saturation effects resulted in more powerful models for the detection of fMRI correlates; (6) focal activations were more likely when there was good electroclinical localization, frequent stereotyped spikes, less head motion and less background EEG abnormality, but were also seen in patients in whom the electroclinical focus localization was uncertain.

Data is also presented from patients with generalized epilepsy and from a study of primary reading epilepsy using simultaneous EMG and voice recordings, exploring the relationship between cognitive and epileptic activity.

Table of contents

DECLARATION OF OWN WORK 2

PREFACE 4

ABSTRACT 6

TABLE OF CONTENTS 7

LIST OF FIGURES 10

LIST OF TABLES 12

GLOSSARY 13

1. CHAPTER 1: INTRODUCTION & OWN CONTRIBUTION 15

2. CHAPTER 2: BACKGROUND 20

2.1 BOLD fMRI AND ITS LIMITATIONS 20
2.1.1 Susceptibility artefacts 21
2.1.2 Head motion 21
2.2 SCALP EEG AND THE INVERSE PROBLEM 22
2.3 EEG-CORRELATED fMRI 23
2.3.1 Rational & History 24
2.3.2 Technical Issues 27
2.3.2.1 Patient safety 28
2.3.2.2 Effects of EEG acquisition on MRI 29
2.3.2.3 Effects of MRI acquisition on EEG 29
2.3.3 Modes of acquisition 30
2.4 fMRI IN EPILEPSY 34
2.4.1 Motor mapping 34
2.4.2 Language mapping 34
2.4.3 Memory mapping 34
2.5 EEG/CORRELATED fMRI IN EPILEPSY 34
2.5.1 Interictal EEG/fMRI 34
2.5.2 Ictal EEG/fMRI 37
2.6 OTHER APPLICATIONS 38
2.6.1 Sleep 38
2.6.2 Alpha rhythm 39

3. CHAPTER 3: SPECIFIC METHODOLOGICAL ISSUES 42

3.1 WHAT DEFINES fMRI ACTIVATION 42
3.1.1 Is rest, rest? 43
3.1.2 Are all spikes equal? 47
3.2 THE NEUROVASCULAR COUPLING IN EPILEPSY 49
3.2.1 What are the potentially relevant metabolic implications of IEDs? 50
3.2.2 Is the coupling affected? 50
3.3 MODELING SPONTANEOUS EEG ACTIVITY 53
3.3.1 How efficient are spontaneous EEG paradigms (how may spikes constitute a study?) 53
3.3.2 What are the essential modeling requirements? 55
3.4 HOW CAN ONE JUDGE THE VALIDITY OF ACTIVATIONS? 56
3.5 CAN INTERICTAL EEG/fMRI BE USED TO STUDY CONNECTIVITY? 59

4. CHAPTER 4: COMMON METHODS 62

4.1 RECRUITMENT AND ETHICS 62
4.2 EXPERIMENTAL SET-UP 62
4.2.1 EEG recording 62
4.2.2 MRI acquisition 63
4.2.3 Pre-processing 65

5. CHAPTER 5: EVENT-RELATED EEG/FMRI 67

5.1 SUMMARY 67

5.2 INTRODUCTION ... 67
5.3 METHODS ... 68
5.3.1 Patient and data ... *68*
5.3.2 Continuous EEG/fMRI ... *69*
5.3.3 EEG source analysis ... *69*
5.3.4 EEG and fMRI analysis ... *70*
5.4 RESULTS ... 70
5.5 DISCUSSION ... 74

6. CHAPTER 6: EEG QUALITY DURING EEG/FMRI ... **75**

6.1 SUMMARY ... 75
6.2 INTRODUCTION ... 75
6.3 METHODS ... 79
6.4 RESULTS ... 82
6.5 DISCUSSION ... 82

7. CHAPTER 7: ICTAL EEG/FMRI ... **86**

7.1 SUMMARY ... 86
7.2 INTRODUCTION ... 86
7.3 METHODS ... 90
7.4 RESULTS ... 92
7.5 DISCUSSION ... 95

8. CHAPTER 8: EEG/FMRI OF HUMAN ABSENCE SEIZURES ... **101**

8.1 SUMMARY ... 101
8.2 INTRODUCTION ... 101
8.3 METHODS ... 102
8.4 RESULTS & DISCUSSION ... 106

9. CHAPTER 9: INTERICTAL EEG/FMRI IN FOCAL EPILEPSY ... **111**

9.1 SUMMARY ... 111
9.2 INTRODUCTION ... 111
9.3 METHODS ... 113
9.3.1 Patients ... *113*
9.3.2 Data acquisition ... *113*
9.3.3 Pre-processing ... *114*
9.3.4 EEG analysis ... *116*
9.3.5 fMRI analysis ... *116*
9.3.5.1 - Step 1: Are there areas that display a conventional hemodynamic response to IEDs? ... 117
9.3.5.2 - Step 2: Are there areas that display any time-locked activity linked to IED, other than the above? ... 117
9.3.5.3 - Step 3: Are the activated areas concordant with seizure focus? ... 118
9.3.5.4 - Step 4: What is the hemodynamic response to IEDs? ... 118
9.3.5.5 - Step 5: Do IED characteristics influence the BOLD response? ... 118
9.3.5.6 – Step 6: What are the factors that influence the likelihood of activation? ... 119
9.4 RESULTS ... 120
9.4.1 fMRI activation and concordance ... *149*
9.4.2 The hemodynamic response to IEDs ... *150*
9.4.3 IED characteristics and the BOLD response ... *150*
a. Cases with multiple IED types ... 150
c. Cases with very frequent IEDs ... 152
9.4.4 Factors influencing activation ... *152*
9.5 DISCUSSION ... 153
9.5.1 Methodological Aspects ... *153*
9.5.1.1 Choice of Subjects and EEG recording ... 153
9.5.1.2 EEG Classification & Automatic spike detection ... 153
9.5.1.3 Motion & Modeling implications ... 154
9.5.1.4 The assessment of concordance ... 155
9.5.2 Clinical and neurobiological aspects ... *156*
9.5.2.1 Yield, localization and clinical relevance ... 156
9.5.2.2 The Hemodynamic response to IEDs ... 157
9.5.2.3 Clinical relevance ... 158

9.5.3 Future work *158*

10. CHAPTER 10: INTERICTAL EEG/FMRI OF IDIOPATHIC & SECONDARILY GENERALIZED EPILEPSIES **159**

10.1 SUMMARY 159
10.2 INTRODUCTION 159
10.3 METHODS 161
10.3.1 Patients *161*
10.3.2 Data acquisition *161*
10.4 RESULTS 165
10.4.1 Clinical features *165*
10.4.2 Single subject results *165*
10.4.3 Group results *171*
10.5 DISCUSSION 173

11. CHAPTER 11: ICTAL FMRI IN PRIMARY READING EPILEPSY **178**

11.1 SUMMARY 178
11.2 INTRODUCTION 178
11.3 METHODS 180
11.3.1 Subjects *180*
11.3.2 Pre- assessment *180*
11.3.3 Experiment design *180*
11.3.4 Data acquisition *181*
11.3.5 Simultaneous EEG/EMG recording during fMRI *181*
11.3.6 Simultaneous voice recording and communication during fMRI *181*
11.3.7 Ictal EEG-fMRI acquisition *182*
11.3.8 fMRI analysis *182*
11.3.9 VBM *183*
11.4 RESULTS 184
11.4.1 Clinical features *184*
11.4.2 Motor and language mapping *184*
11.4.3 Ictal fMRI *186*
11.4.4 Voxel-based-morphometry *188*
11.5 DISCUSSION 191
11.5.1 Methodological considerations & limitations 193

12. CHAPTER 12: DISCUSSION **195**

12.1 SUMMARY OF FINDINGS 195
12.2 FURTHER WORK 196
12.2.1 EEG/fMRI in paediatric epiliepsies *196*
12.2.2 GSW, deactivations & the default mode hypothesis *197*
12.2.3 EEG/fMRI & neurobiology *198*
12.2.4 EEG/fMRI vs Intracranial EEG *199*
12.2.5 EEG/fMRI in epilepsy surgery *200*
12.2.6 Early BOLD responses *201*
12.2.7 Data Driven Analysis Techniques (TCA & ICA) *203*
12.2.8 Functional connectivity & DCM *204*
12.3 FUTURE WORK & CONCLUSIONS 205

13. APPENDICES **207**

13.1 APPENDIX I - PREVIOUS EEG/FMRI STUDIES IN EPILEPSY 207
13.2 APPENDIX II - RECENT EEG/FMRI STUDIES IN EPILEPSY 209
13.3 APPENDIX III - ICA ON CHAPTER 8 DATA 211

REFERENCES **219**

List of Figures

Figure 2-1 EEG recorded during fMRI. 24
Figure 2-2 EEG Electrodes and signal drop-out. 29
Figure 2-3 Complex EEG recorded during fMRI 30
Figure 2-4 Spike-triggered fMRI 32
Figure 3-1 Simultaneously recorded scalp and invasive EEG 45
Figure 4-1 EEG Electrodes 63
Figure 4-2 EEG Transmitter 63
Figure 4-4 Patient connected to headbox 65
Figure 4-5 Online EEG Display 65
Figure 4-6 Scanner Console 65
Figure 4-7 Equipment Trolley 65
Figure 5-1 EEG during fMRI 71
Figure 5-2 fMRI activation 72
Figure 5-3 Dipoles vs BOLD 73
Figure 5-4 Timecourse 73
Figure 6-1 EEG recorded during the experiment 80
Figure 6-2 Amplitude distributions 83
Figure 6-3 Inter-event interval distributions 84
Figure 7-1 EEG recorded during the experiment. 93
Figure 7-2 SPM 95
Figure 7-3 Regional timeseries and realignment parameters 96
Figure 7-4 Anatomical Overlay 97
Figure 8-1 EEG from the experiment. 103
Figure 8-2 Experimental parameters. 103
Figure 8-3 Statistical parametric maps. 107
Figure 8-4 Anatomical overlay 108
Figure 9-1 EEG recorded during fMRI from patient #25 114
Figure 9-2 Summary of scanning and activation findings for basic model 132
Figure 9-3 *Concordant* activation and *Discordant* deactivation 132
Figure 9-4 *Concordant Plus* activation / *Discordant* deactivation 135
Figure 9-5 *Concordant* activation / *Discordant* deactivation 136

Figure 9-6 Bilateral precuneus deactivation 138
Figure 9-7 Other EEG/fMRI activations 139
Figure 10-1 (below) Cortical signal change with GSW 169
Figure 10-2 (overleaf) Examples from 2 patients with SGE 169
Figure 10-3 IGE group analysis 173
Figure 11-1 EEG in reading epilepsy. 187
Figure 11-2 fMRI activation during reading induced seizures 188
Figure 11-3 Activations during conversation induced seizures 190
Figure 11-4 Subcortical activations with reading induced seizures 190
Figure 13-1 Thresholded IC maps. 212

List of Tables

Table 2-1 Summary of technical problems and solutions 28
Table 3-1 Essential conditions and assumptions in interictal EEG/fMRI. 57
Table 7-1 Summary of published ictal fMRI time series 88
Table 9-1 Electroclinical data 121
Table 9-2 fMRI results for basic model 124
Table 9-3 fMRI models and statistics 126
Table 9-4 Hemodynamic response characteristics. 151
Table 9-5 Experimental factors and presence of fMRI activation. 152
Table 10-1 Clinical Details 161
Table 10-2 Summary of results 166
Table 10-3 Group Analysis 172
Table 11-1 Clinical demographics in nine patients with reading epilepsy 185
Table 11-2 EEG-fMRI results 189

Glossary

AED	Antiepileptic drug
AVM	Arteriovenous malformation
BA	Brodmann area
BECTS	Benign epilepsy with centrotemporal spikes
BOLD	Blood oxygenation level dependent
CAE	Childhood absence epilepsy
CBF	Cerebral blood flow
CNS	Central nervous system
CPS	Complex partial seizure
CSF	Cerebrospinal fluid
CT	Computed tomography
DCM	Dynamic Causal Modeling
DNET	Dysembryoplastic neuroepithelial tumor
ECG	Electrocardiogram
ECoG	Electrocorticography
EEG	Electroencephalogram
EMG	Electromyography
EPI	Echo planar imaging
FDG	[^{18}F]-fluorodeoxyglucose
FLE	Frontal Lobe Epilepsy
fMRI	Functional magnetic resonance imaging
FOV	Field of view
FWHM	Full-width half maximum
GAERS	Genetic Absence Epilepsy Rats of Strasbourg
GE	The General Electric Company
GLM	General Linear Model
GTCS	Generalized tonic-clonic seizure
HRF	Haemodynamic response function
HS	Hippocampal sclerosis
IA	Imaging Artefact

IC	Independent Component
ICA	Independent component analysis
IED	Interictal epileptiform discharge
IGE	Idiopathic generalized epilepsy
ILAE	International league against epilepsy
JAE	Juvenile absence epilepsy
JME	Juvenile myoclonic epilepsy
MCD	Malformation of cortical development
MNI	Montreal neurological institute
MRI	Magnetic resonance imaging
MTL	Mesial temporal lobe
NHNN	National Hospital for Neurology & Neurosurgery
NIRS	Near Infrared Spectroscopy
NSE	National Society for Epilepsy
OLE	Occipital lobe epilepsy
PA	Pulse Artefact
PCA	Principle component analysis
PET	Positron emission tomography
RSN	Resting State Networks
RF	Radiofrequency
ROI	Region of interest
SGE	Secondary generalized epilepsy
SNR	Signal to noise ratio
SPECT	Single photon emission tomography
SPM	Statistical parametric mapping
SPS	Simple partial seizure
TCA	Temporal cluster analysis
TE	Echo time
TR	Repetition time
TLE	Temporal lobe epilepsy

1. Chapter 1: Introduction & own contribution

This thesis introduces and builds on a number of technological and methodological advances which have allowed the simultaneous acquisition of EEG and fMRI data. The key advantage conferred is the ability to use functional MRI to study and localize *spontaneous* EEG activity, both physiological (e.g. brain rhythms, sleep phenomenon) and pathological. Clinically, this is hugely exciting because efforts to localize interictal and ictal epileptiform activity are central to both the syndromic diagnosis and treatment of seizure disorders. EEG/fMRI as a technique, has the potential to bring a whole new dimension to seizure localization efforts which lie at the heart of epilepsy surgery programs. There are wider applications still in many areas of neuroscience but the focus of this thesis is on applications in epilepsy, specifically the study of interictal epileptiform discharges in both focal and generalized epilepsy, studying seizure activity (ictal fMRI) and a novel application to reading epilepsy where epilepsy meets cognitive neuroscience.

Chapter 2 introduces functional MRI and scalp EEG together with their individual limitations and explores the technical challenges of simultaneous acquisition. The role of fMRI in the pre-surgical evaluation of epilepsy is briefly outlined before reviewing previous work based on *spike-triggered* fMRI. Portions of this chapter feature in various publications:

- Salek-Haddadi A, Lemieux L, Merschhemke M, Allen PJ, Fish DR. Continuous EEG-correlated fMRI in epilepsy. In: Hirata K, editor. 12th World Congress of the International Society of Brain Electromagnetic Topography, Tochigi, 8 - 10 March 2001 – International Congress Series 1232. Amsterdam: Elsevier Science B.V., 2002.

- Lemieux L, Salek-Haddadi A, Hoffmann A, Gotman J, Fish DR. EEG-Correlated Functional MRI: Recent Methodologic Progress and Current Issues. Epilepsia 2002; 43(Suppl.1):64-68.

- Salek-Haddadi A, Lemieux L, Fish DR. Role of functional magnetic resonance imaging in the evaluation of patients with malformations caused by cortical development. Neurosurg Clin N Am 2002; 13(1):63-69.

- Salek-Haddadi A, Friston KJ, Lemieux L, Fish DR. Studying spontaneous EEG activity with fMRI. Brain Res Brain Res Rev 2003; 43(1):110-133.

- Hamandi K, Salek-Haddadi A, Fish DR, Lemieux L. EEG-correlated fMRI: Update on the Queen Square experience. J Clin Neurophysiol 2004; 21(4):241-8

Chapter 3 explores the core biological and methodological considerations central to the statistical analysis and clinical interpretation of simultaneously acquired EEG/fMRI data from patients with epilepsy. Many of these issues were brought together for the first time in:

- Salek-Haddadi A, Friston KJ, Lemieux L, Fish DR. Studying spontaneous EEG activity with fMRI. Brain Res Brain Res Rev 2003; 43(1):110-133.

Chapter 4 presents the methodology common to all subsequent patient studies. In general, contribution to the individual chapters is reflected in the authorship lists of the published papers.
Chapters 5 – 11 are based on several papers published between 2001 and 2008 which are listed together with a statement of my own individual contribution.

Chapter 5 describes the first ever simultaneous and continuous EEG/fMRI study in a patient with epilepsy.

- Lemieux L, Salek-Haddadi A, Josephs O, Allen P, Toms N, Scott C, Krakow K, Turner R, Fish DR. Event-Related fMRI with Simultaneous and Continuous EEG: Description of the Method and Initial Case Report. Neuroimage 2001; 14(3):780-787.

I was responsible for recruitment, experimental set up, and EEG coding. The principle investigator was Professor Louis Lemieux.

Chapter 6 is an EEG quality study based on data from the same experiment.

- Salek-Haddadi A, Lemieux L, Merschhemke M, Diehl B, Allen PJ, Fish DR. EEG Quality during simultaneous functional MRI of interictal epileptiform discharges. Magn Reson Imaging 2003; 21:1159-1166.

I was primarily responsible for the study design and data analysis with statistical input from Professor Stephen Senn.

Chapter 7 described the first ictal EEG/fMRI study in a patient with epilepsy.

- Salek-Haddadi A, Merschhemke M, Lemieux L, Fish DR. Simultaneous EEG-Correlated Ictal fMRI. Neuroimage 2002; 16(1):32-40.

The recruitment, experimental setup and data analysis were primarily my own work. A Matlab routine, written by myself, was used to interrogate some of the data.

Chapter 8 describes the first EEG/fMRI study of human generalized spike-wave activity.

- Salek-Haddadi A, Lemieux L, Merschhemke M, Friston KJ, Duncan JS, Fish DR. Functional magnetic resonance imaging of human absence seizures. Ann Neurol 2003; 53(5):663-667.

The recruitment, experimental setup and data analysis was my own work with some key ideas from co-workers on analysis and interpretation. A Matlab routine, written by myself, was used to perform the EEG spectral analysis and interrogate some of the data.

Chapter 9 is the largest published interictal EEG/fMRI study of patients with focal epilepsy.

- Salek-Haddadi A, Diehl B, Hamandi K, Merschhemke M, Liston A, Friston K, Duncan JS, Fish DR, Lemieux L. Hemodynamic correlates of epileptiform discharges: an EEG-fMRI study of 63 patients with focal epilepsy. Brain Res. 2006 May 9;1088(1):148-66.

I was responsible for recruitment, experimental set up, data acquisition and analysis. BD and MM assisted me with reviewing and coding EEGs. Several key ideas regarding the presentation and interpretation of the findings were provided by the co-

authors. I was responsible for producing the figures and for graphical presentation of the data. Several batch scripts, developed by myself, were used for off-line data processing and analysis using SPM subroutines. Many were used department wide. Further scripts were written to allow pseudo-normalization of the results for presentation and allow access to the maximum intensity projection (MIP) sub routines of SPM for further interrogation of the data.

Chapter 10 is an interictal EEG/fMRI study of patients with generalized epilepsy.

- Hamandi K, Salek-Haddadi A, Laufs H, Liston A, Friston K, Fish DR, Duncan JS, Lemieux L. EEG-fMRI of idiopathic and secondarily generalized epilepsies. Neuroimage. 2006 Jul 15;31(4):1700-10.

I was responsible for study design and conception. I recruited and scanned the fist 26 patients before handing over to KH as principle investigator. The core methodology was as per chapter 9.

Chapter 11 is novel a study of language-induced seizures in patients with reading epilepsy using a different techniques.

- Salek-Haddadi A, Mayer T, Hamandi K, Symms, M, Josephs O, Fluegel D, Woermann F, Richardson MP, Noppeney U, Wolf P, Koepp MJ. Imaging seizure activity: a combined EEG/EMG-fMRI study in reading epilepsy. Epilepsia. 2008 Aug (in press).

The study was conceived and designed jointly with MJK. I was responsible for recruiting UK patients, experimental set up, data acquisition and analysis. OJ and MS developed the audio recording technology. Together with MK, I was responsible for clinical assessment and paradigm design. The online stimulus presentation system, which interfaced with the scanner via the serial port, was written by me in Matlab using some of the Cogent subroutines. The VBM work was done by DF. The write-up was done jointly with MJK and included key ideas from all co-authors.

Chapter 12 contains a critical discussion of the recent literature followed by general conclusions. It includes several studies in which I was peripherally involved, and which have built directly upon or extended the work presented in this thesis. The ones co-authored by myself include:

- Laufs H, Hamandi K, Salek-Haddadi A, Kleinschmidt AK, Duncan JS, Lemieux L. Temporal lobe interictal epileptic discharges affect cerebral activity in "default mode" brain regions. Hum Brain Mapp. 2007 Oct;28(10):1023-32.

- Lemieux L, Salek-Haddadi A, Lund TE, Laufs H, Carmichael D. Modeling large motion events in fMRI studies of patients with epilepsy. Magn Reson Imaging. 2007 Jul;25(6):894-901.

- Liston AD, Lund, TE, Salek-Haddadi A, Hamandi K, Friston KJ, Lemieux L. Modeling Cardiac Signal as a Confound in EEG-fMRI and its Application in Focal Epilepsy Studies. Neuroimage. 2006 Apr 15;30(3):827-34.

- Hamandi K, Salek Haddadi A, Liston A, Laufs H, Fish DR, Lemieux L. fMRI temporal clustering analysis in patients with frequent interictal epileptiform discharges: comparison with EEG-driven analysis. Neuroimage. 2005 May 15;26(1):309-16.

- Laufs H, Krakow K, Sterzer P, Eger E, Beyerle A, Salek-Haddadi A et al. Electroencephalographic signatures of attentional and cognitive default modes in spontaneous brain activity fluctuations at rest. Proc Natl Acad Sci USA 2003; 100(19):11053-11058.

* * *

2. Chapter 2: Background

2.1 BOLD fMRI and its limitations

Blood Oxygen Level Dependent (BOLD) fMRI has revolutionized the field of human brain mapping by providing the means to study focal neuronal activity non-invasively and with sub-millimeter resolution.

BOLD-fMRI relies on the detection of local fluctuations in magnetic susceptibility, mainly through T2*-weighted gradient-echo echo-planar imaging (GE-EPI), attributable to changes in the concentration of paramagnetic deoxyhaemoglobin - the BOLD effect (Ogawa et al., 1990). Focal neural activity, by way of the neurovascular coupling, drives a complex interplay between blood flow, blood volume and oxygen consumption which, ultimately determines measured signal (Buxton et al., 1998) though the exact mechanisms and mediators remain incompletely understood (Buxton et al., 1998;Villringer and Dirnagl, 1995). The end result is a subtle (few percent at 1.5 Tesla) but prolonged and characteristic pattern of MR signal change referred to as the Haemodynamic Response Function (HRF).

The precise aspects of neural activity which engender the changes in BOLD are still debated (Arthurs and Boniface, 2002). Likely candidates include both action potentials (neuronal spiking) (Heeger et al., 2000), and population synaptic activity (local field potentials) (Logothetis et al., 2001). However, matters are complicated by interdependencies between these measures, the relative weightings and effects of excitatory versus inhibitory activity (Jueptner and Weiller, 1995;Waldvogel et al., 2000), and the modulating influences of remote inputs as integrated and observed over the local neuronal population as a whole (Scannell and Young, 1999). In addition, many neuronal transaction involving functional integration and feature linking are probably accomplished through changes in fast dynamic synchronous interactions or phase-locking, as opposed to changes in firing rate or rate coding (See (Friston, 2000) for review). Whether or not such mechanisms underlie spontaneous brain rhythms (Nunez et al., 2001;von Stein et al., 2000), and whether they necessarily entail focal changes in BOLD are open questions, though theoretical reasons do exist for assuming a direct coupling between mean synaptic activity and synchronization (Chawla et al., 1999).

Another important limitation to mapping neuronal activity through BOLD arises from the fact that, at field strengths below 4 Tesla, the signal is dominated by venous contributions. This 'brain or vein problem' (Frahm et al., 1994) implies that BOLD changes may manifest downstream from neuronal activity (Disbrow et al., 2000), thereby imposing a fundamental biophysical constraint on spatial resolution, especially for larger activations (Turner, 2002).

Physical and hardware considerations limitat all MRI studies and EEG/fMRI is no exception. Two specific issues however, are particularly important in the present context, susceptibility artefacts and head motion.

2.1.1 Susceptibility artefacts

Susceptibility-based gradient-echo sequences - as used widely for BOLD-fMRI - are plagued by macroscopic susceptibility-artefacts arising from magnetic field inhomogeneities at air-tissue interfaces (e.g. surrounding orbitofrontal cortex and mesiotemporal structures) (Ojemann et al., 1997). Consequences include signal dropouts, image distortions, and reduced BOLD contrast-to-noise, extending even beyond the visible defects (Gorno-Tempini et al., 2002). It has already been shown that as a consequence, fMRI experiments show far less activation within the temporal lobes during cognitive studies than would otherwise have been expected from PET (Devlin et al., 2000) and the abundance of extra-temporal vs mesial temporal lobe activations in the epilepsy EEG/fMRI literature is noteworthy. Certainly, there are important trade-offs to be made and one must wonder as to the proportion of temporal lobe epilepsy patients, for example, whom may better have been served by sequences optimized for mesial temporal lobe coverage. Recent advances in MRI technology such as in parallel imaging, may provide important improvements in this area (De Zwart et al., 2002).

2.1.2 Head motion

The adverse effects of head motion on MR images are complex asnd extend beyond simple misregistrations (Andersson et al., 2001;Friston et al., 1996;Grootoonk et al., 2000;Kim et al., 1999). The result is a two-pronged attack on both sensitivity, through added residual variance, and specificity whereby stimulus-correlated motion

in particular, may give rise to false activation*. Patient studies of course are more prone to such effects and there are often difficulties in repeating corrupted fMRI sessions.

In theory, stimulus-correlated motion, ought not to pose a problem to paradigmless fMRI. In epilepsy however, subtle [epileptic] myoclonus (Hallet, 1997) may accompany EEG events, thereby creating a similar problem (e.g. in Juvenile Myoclonic Epilepsy, during polyspike-wave epochs). Co-operation may also be limited by physical disability or learning disability (again more prevalent in epilepsy). Subject discomfort from noise, long scanning times, EEG electrodes, or paradoxically even head restraints/cushioning may also pre-dispose to motion, as do boredom, drowsiness & sleep during paradigmless studies. The potential problems of head motion during sleep are obvious.

Strategies for dealing with motion fall under (1) Pre-imaging: patient selection, explanation, positioning, sedation (see caveats below), ear protection, gentle head restraint or cushioning; (2) Imaging: faster acquisition sequences, silent sequences, shorter imaging times; and (3) Post-imaging methods: co-registration (Friston et al., 1995a), spin-history correction (Grootoonk et al., 2000), unwarping (Andersson et al., 2001), de-noising e.g. using independent component analysis (McKeown et al., 1998), and modeling motion related signal changes explicitly within the design matrix (Friston et al., 1996). Irrespective of the above however, head motion remain a significant problem in EEG/fMRI and the question of 'How much motion is bad?', a difficult one to answer.

2.2 Scalp EEG and the inverse problem

The physical principles behind the theoretical limitations of scalp EEG are well established (see (Gloor, 1985;Niedermeyer and Lopes da Silva, 1999;Nunez, 1981) for reviews). Briefly, synaptic current sources give rise to instantaneous dipole-like generators of varying magnitude, orientation, and position (dipole sheets) in accordance with cortical geometry and functional organization. Scalp potentials arise from the spatial summation of synchronous dipole moments over the neocortical volume with a weighting that depends upon the anisotropic conductivity of the cranium. It follows that radial sources, aligned in parallel, closest to the scalp and

* These arise particularly at intensity boundaries like those between CSF and brain and around susceptibility and flow-related areas of artefact (Hajnal et al., 1994).

synchronously active (i.e. gyral dipole sheets) would be expected to supervene over tangential sources arising, for example, from the sulcal walls where opposing dipoles may cancel out (Gloor, 1985;Nunez, 1981). The 'smearing' effects of skull and scalp however, are not simple in relation to convoluted dipole sheets (Gloor, 1985) and depth is critical (probably more so for radial dipoles (Fuchs et al., 1998)).

Temporal considerations are equally important in relation to the EEG manifestations of neuronal activity. Preconditions of 'synchronicity' explain, for example, why longer (but lower-amplitude) synaptic potentials dominate over much larger (but shorter lasting) action potentials on scalp EEG (Nunez, 1995) and likewise, the inverse relationship between EEG frequency and amplitude in general (Cooper et al., 1965;Gloor, 1985). Interestingly, Nunez & Silberstein (Nunez and Silberstein, 2000) estimate the instantaneous contribution to scalp potentials as being proportional to the number of synchronous cortical columns plus the square-root of the number of asynchronous columns; a relationship that would not necessarily extend to concomitant metabolic/haemodynamic demands.

2.3 EEG-correlated fMRI

Virtually every aspect of normal brain activity has been or is being investigated using fMRI and increasingly, attention is focusing on studies of abnormal activity such as in stroke and epilepsy. Simply speaking, the localization of seizure-activity should present an obvious application, given the enormous clinical interest in mapping the 'epileptogenic zone', even if invasively. Clinically, the potential exists for such findings to help guide invasive-studies and help tailor surgical resections in focal epilepsy. Scientifically, the opportunity also exists to study the metabolic and neurovascular responses to epileptiform activity *in vivo*.

The use of fMRI for mapping eloquent cortex in the presurgical evaluation of epilepsy, is covered elsewhere in this chapter. Conventional fMRI studies rely on specific experimental manipulations or paradigms, to optimally elicit the relevant pattern of neuronal activity and hence focal changes in BOLD, for subsequent detection and localization. In contrast however, 'spontaneous' patterns of human EEG-activity (e.g. epileptiform activity), in general, can neither be replicated nor manipulated. 'Paradigmless' EEG/fMRI studies therefore need be performed within the same session. This means simultaneous recording and there are several difficulties.

2.3.1 Rational & History

What is spontaneous neural activity?

For the purposes of this chapter we shall define spontaneous neural activity as that occurring unprovoked, in the absence of an identifiable stimulus, with or without behavioral manifestations. Such phenomena are best characterized electrophysiologically through scalp electroencephalography (EEG) and span: the 'normal' brain rhythms linked to arousal, alpha (8-13 Hz), beta (>13Hz), theta (4-8 Hz), delta (<4Hz) and gamma (>20Hz) band activity; spontaneous sleep events, sleep spindles and K complexes; and [abnormal] epileptiform activity, both ictal (during seizures) and inter-ictal (between seizures). Examples of some of these features, as recorded during fMRI are shown in Figure 2-1. Evoked responses and other stimulus-linked phenomena will not be considered explicitly here, though many of the arguments below still apply.

Why study spontaneous neural activity?

In essence, spontaneous EEG phenomena represent endogenous patterns of neural activity and are of interest both scientifically and clinically. Scientifically, multimodal imaging - the fusion of information from different imaging techniques - remains something of a holy grail (Dale and Halgren, 2001;Horwitz and Poeppel, 2002). The promise is of multimodal observations of neuronal activity that have both high temporal and spatial resolution. Multimodal, in the sense that different aspects of neuronal activity (e.g. local field potentials, spiking, oxygen consumption and neurovascular coupling) may be integrated to make more precise and biologically meaningful inferences about their underlying cause.

Figure 2-1 EEG recorded during fMRI.
EEG recorded during fMRI from a patient with focal epilepsy in the eyes-closed rest condition. Pulse and imaging artefact have been removed. Two bi-temporal chains are shown, referenced to Pz in the top ten channels, followed by a bipolar montage in the next eight. ECG and slice timing signals (OSC) are shown at the bottom. Vertical eye movements are evident at (A). A focal left anterior-temporal sharp-wave complex is seen to arise at (B). The record is dominated by posterior 8-9 Hz alpha activity (C). The magnetohydrodynamic effects of systolic blood flow give rise to large T-waves, a normal feature of scanner ECG.

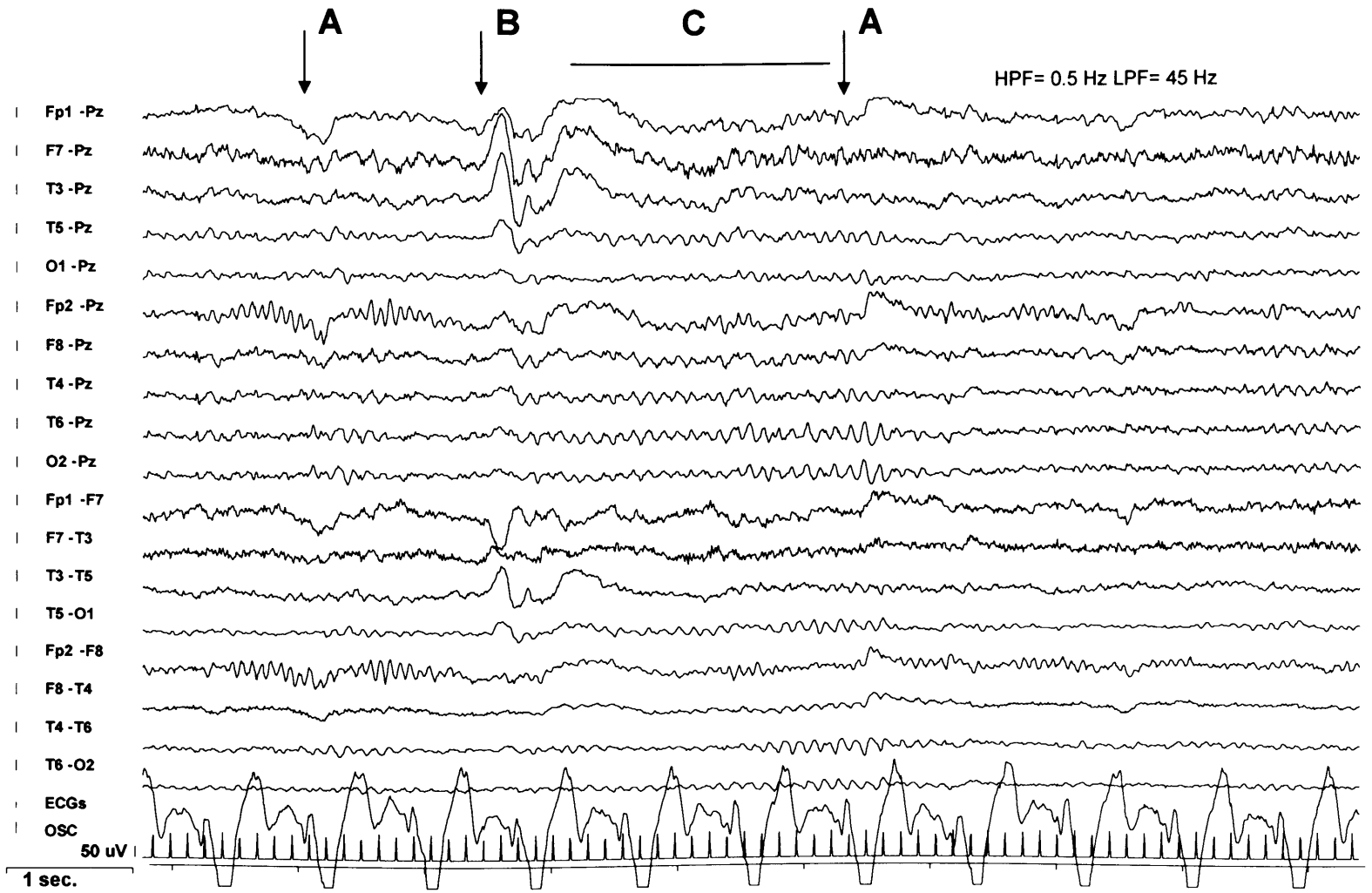
A
B
C
A
HPF= 0.5 Hz LPF= 45 Hz
Fp1 -Pz
F7 -Pz
T3 -Pz
T5 -Pz
O1 -Pz
Fp2 -Pz
F8 -Pz
T4 -Pz
T6 -Pz
O2 -Pz
Fp1 -F7
F7 -T3
T3 -T5
T5 -O1
Fp2 -F8
F8 -T4
T4 -T6
T6 -O2
ECGs
OSC
50 uV
1 sec.

Figure 2-1

The use of spatial information from fMRI to constrain EEG source solutions for example, is an area of active research (Dale et al., 2000;Phillips et al., 2002) and the advantages of multimodal imaging are not limited to data acquired simultaneously. Simultaneous acquisitions do however provide the only means of studying spontaneous EEG activity using fMRI. This is because evoked responses cannot be estimated in relation to experimental manipulation or input, but only in relation to each other. In this context, one is mainly concerned with the use of EEG measurements to 'predict' changes on fMRI.

Spontaneous EEG activity holds the key to unraveling the patterns of connectivity and synchronicity underlying states of consciousness and, together with fMRI, the potential exists for their generators to be localized anatomically. Whether spontaneous EEG rhythms such as alpha arise from anatomically distinct networks (Makeig et al., 2002;Niedermeyer, 1997;Nunez et al., 2001) or as a consequence of global dynamics (Lopes da Silva et al., 1997) are important questions with fundamental implications for understanding higher order processes and indeed consciousness. In sleep, EEG/fMRI recordings are not only of interest in localizing the hitherto undisclosed generators of specific phenomena such as spindles and K-complexes, but also in observing the effects of sleep stages and changes in arousal on other aspects of stimulus processing (Czisch et al., 2002;Matsuda et al., 2002;Portas et al., 2000) and cerebral physiology.

Clinically, spontaneous EEG is arguably most useful in the evaluation of seizure disorders. In fact, scalp EEG remains the principal tool in the diagnosis and classification of epilepsy syndromes. These divide broadly into two categories: In generalized seizure disorders, seizure onset is bilateral and synchronous with no obvious focus. By contrast, partial epilepsy is characterized by onset within distinct areas (which may or may not be structurally abnormal) and secondary spread. This [EEG] distinction is critical, as focal epilepsy is potentially amenable to surgery with the chances of a successful outcome depending on the confidence with which an 'epileptogenic zone'* can be identified (Rosenow and Luders, 2001). This generally relies on convergence of the results from a number of investigations, but electrophysiological studies (either scalp or invasive EEG) of spontaneous

* The epileptogenic zone is defined, in theoretical terms, as the area of cortex necessary and sufficient for initiating seizures, and whose removal or disconnection is necessary for abolition (Luders et al., 1993;Rosenow and Luders, 2001).

epileptiform activity remain the most important. Hence any technique that could finesse this information in terms of spatial resolution and coverage is of immediate clinical interest and through mapping complementary changes in Blood Oxygen Dependent (BOLD) signal, simultaneous EEG/fMRI promises to deliver exactly this. Whilst the 'ictal onset zone' is generally regarded as the best surrogate for the epileptogenic zone, ictal fMRI poses many challenges (Salek-Haddadi et al., 2002). The irritative zone is defined as that generating IEDs, and while it is not always concordant with the epileptogenic zone (e.g. as influenced by non-REM sleep (Sammaritano et al., 1991)) the relationship is generally close enough to be of diagnostic value (Engel, Jr., 1993;Luders et al., 1993;Rosenow and Luders, 2001). This is especially so in temporal lobe epilepsy (Blume et al., 1993;Chung et al., 1991) and a number of centers frequently use information from source models of IEDs during presurgical evaluation (Ebersole, 1997a;Michel et al., 1999). Mapping the 'irritative zone' therefore using interictal EEG/fMRI, offers a more practical alternative in epilepsy and not surprisingly, epilepsy has provided the main impetus for developments in this field to date. Beyond tailoring surgical resections, several additional possibilities exist. These include the guiding of invasive electrode placements and recordings, and the reciprocal use of such measures, perhaps in the context of interventional MRI, to better resolve areas of BOLD activation. In scientific terms, understanding how the irritative zone is influenced by different pathologies (and drugs), how it relates to the epileptogenic zone as defined by other investigations and surgical outcome measures, and how it may subdivide in response to different types of IEDs, are central questions in epileptology. More recently, EEG/fMRI has been applied to generalized spike-wave activity, the hallmark of generalized epileptic disorders (Salek-Haddadi et al., 2003d) (see Chapter 8). The BOLD changes observed here (thalamic activation and with widespread cortical deactivation) are very different to the focal changes seen during IEDs. An exciting prospect therefore is the application of EEG/fMRI to distinguish between epilepsy syndromes, both in the broadest sense (partial vs generalized) but potentially also between the individual syndromes (explored in Chapter 9).

2.3.2 Technical Issues

Briefly, the technical problems of simultaneous EEG/fMRI acquisition fall under three categories: patient safety, the effects of EEG on MRI acquisition, and the effects of MRI on EEG recording. These are summarized in Table 2-1.

Table 2-1 Summary of technical problems and solutions

Problem		Solutions
Patient Safety		
	Risk of electrode heating from RF-induced currents and changes in magnetic flux.	Current limiting resistors, and fibre optic isolation of patients
Influence of EEG on MRI		
	RF noise from electronics/digitizer	Shielding, RF filters
	Susceptibility artefacts and eddy currents from EEG electrodes	MR-compatible electrodes
Influence of MRI on EEG		
	Motion artefacts from static field	Head support, subject selection, cable arrangement
	Pulse artefact (Ballistocardiogram)	Twisted leads, pulse artefact subtraction algorithm
	Imaging artefact	Bipolar recording. Interleaved acquisition or imaging artefact subtraction algorithm with hardware modifications.

2.3.2.1 Patient safety

The first issue here is a general one, namely that all equipment within the vicinity of the superconducting magnet needs to be tested for MR compatibility and be appropriately secured so as not to pose a safety risk. The second set of issues concern the scanning of patients with EEG electrodes attached. There are three mechanisms by which risks may be posed to the patient, namely (1) current induction within the EEG electrodes by the static magnetic field, (2) current induction by the time-varying magnetic field (the gradients), (3) the radiofrequency (RF) field. In relation to our set-up, these issues were explored in (Lemieux et al., 1997). The main source of hazard was found to be the RF field. The use of current-limiting safety resistors was recommended with a minimum value of 11.9 kΩ. For standard electrodes and gel, the effects of heating were found to be negligible, even with high-RF output sequences. By avoiding loops within the electrodes, keeping leads short, avoiding crossed wires, using MR-compatible electrodes, paste, and current-limiting safety resistors,

excellent patient-safety may be achieved (Huang-Hellinger et al., 1995;Lemieux et al., 1997). This does however come at a premium, as resistors and longer leads incur a signal to noise penalty. The fibre-optic isolation of all equipment within the scanner room which is battery powered with 12 Volts adds yet another layer of safety. Indeed, we know of no adverse incidents to date involving the recording of scalp EEG within the MRI scanner.

2.3.2.2 Effect of EEG acquisition on MRI

There are two mechanisms by which EEG recording can affect image quality. The first of these is by generating RF interference which can be minimized by careful shielding and using low currents. The second is the generation of susceptibility artefacts at the scalp by electrodes or conducting gels/pasts and possibly eddy currents. Such artefacts give rise to drop-outs. The effects of the materials employed here were formally explored in (Krakow et al., 2000b) and the results have informed our choices such as the use of gold electrodes (See Figure 2-2 and Chapter 4).

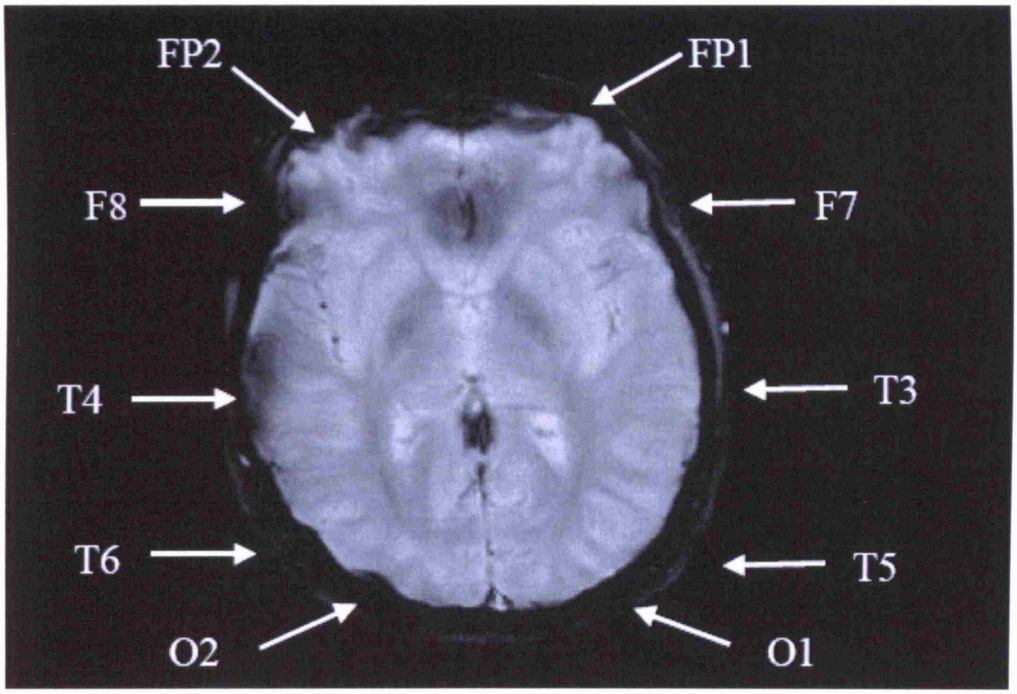

Figure 2-2 EEG Electrodes and signal drop-out.
High resolution EPI with two electrode assemblies on either side. At FP2, F8, T4, T6, O2, non-optimized electrode assemblies (silver/silver chloride electrodes, carbon composition resistor) give rise to areas of drop-out extending to the cortex. The optimized electrode assemblies (gold electrodes, cermet film resistors) on the opposite side did not compromise image quality. (From (Krakow et al., 2000b))

2.3.2.3 Effect of MRI acquisition on EEG

Beyond the main sources of noise, familiar to most electroencephalographers (muscle artefact, eye movement, perspiration, mains interference etc.), scanner-recorded EEG is exquisitely prone to motion-related artefacts. These are evident irrespective of whether or not imaging is taking place and arise by virtue of Faraday's law*. In particular, pulse artefact (PA; often referred to as the cardiobalistogram) is usually visible from subtle motion in relation to the cardiac cycle (Ives et al., 1993) and may resemble interictal epileptiform discharges, despite a fixed temporal relation to the QRS complex. Unsupervised algorithms for online PA removal (Allen PJ et al., 1998;Bonmassar et al., 2002) generally result in excellent scanner-EEG quality, though occasional bursts of PA may survive through short breaches during re-averaging following ECG noise, re-posturing or drifts in QRS morphology. In our experience, at 1.5 Tesla, gross head movements, vocalization, coughing, hiccups, sniffing, or swallowing may also result in often difficult-to-classify artefacts. Such artefacts may vary unpredictably depending on the distribution of the conspiring leads, occurring focally, unilaterally, or bilaterally. They may also decay slowly with physiological time constants, where disturbed leads are allowed to oscillate and may overlap considerably with bona fide EEG features. As such they may not be amenable to linear noise separation techniques. Figure 2-3 illustrates some of these difficulties.

2.3.3 Modes of EEG/fMRI acquisition

During image acquisition, the voltages induced by the time-varying magnetic fields (gradients and radio-frequency pulses) obscure the EEG completely with so-called 'imaging (or gradient) artefact'. The majority of early EEG/fMRI recordings were therefore interleaved combining epochs of acquisition and rest for EEG recording. Interleaved acquisitions may be either periodic, with a duty-cycle sufficient to allow for limited EEG interpretation in between bursts of imaging

Figure 2-3 Complex EEG recorded during fMRI
A segment of more complex EEG is shown as recorded during fMRI, from a patient with idiopathic generalized epilepsy. A brief burst of generalized spike-wave activity is marked by (A). In addition, pulse artefact (*) is seen intermittently (though always in fixed relation to the QRS complex) and swallowing artefacts (B) were a regular feature of this recording. These can make interpretation difficult.

* Faraday's law of electromagnetic induction (1831) states that for a closed circuit within a magnetic field, voltage is induced in proportional to the rate of change in magnetic flux. This may be influenced by varying the magnitude of field, the size of the circuit, or its orientation relative to the field.

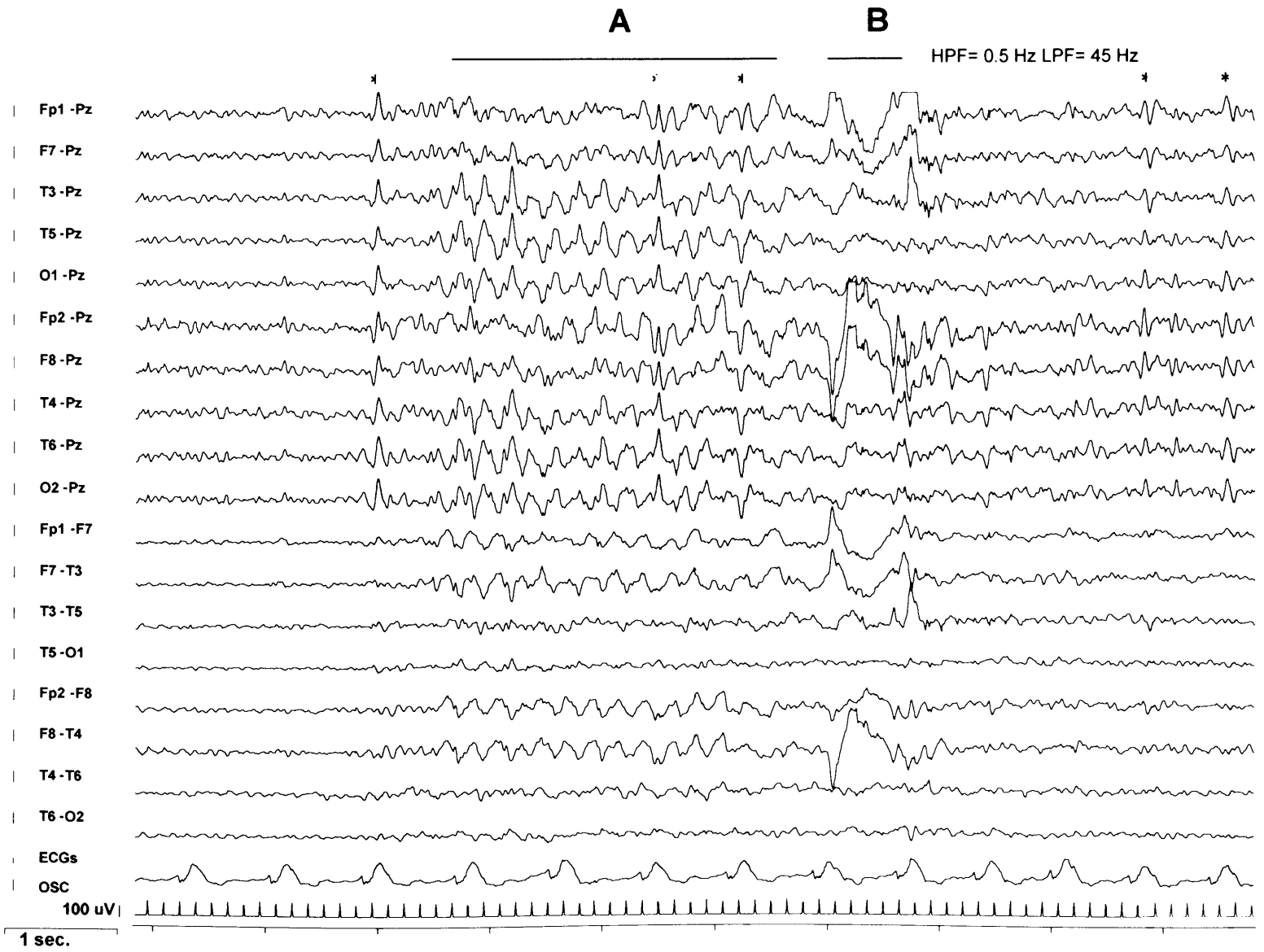
A
B
HPF= 0.5 Hz LPF= 45 Hz
Fp1 -Pz
F7 -Pz
T3 -Pz
T5 -Pz
O1 -Pz
Fp2 -Pz
F8 -Pz
T4 -Pz
T6 -Pz
O2 -Pz
Fp1 -F7
F7 -T3
T3 -T5
T5 -O1
Fp2 -F8
F8 -T4
T4 -T6
T6 -O2
ECGs
OSC
100 uV
1 sec.

Figure 2-3

Figure 2-4 Spike-triggered fMRI
BOLD responses are sampled irregularly at discrete time points and in delayed relation to the EEG. Haemodynamic latency allows for 'Activation scans' to be triggered following events of interest so as to capture the peak responses that ensue. At the same time, protection is afforded against conflation by 'invisible' EEG events occurring during acquisition itself (dashed lines). 'Resting scans' are acquired following periods devoid of activity for statistical comparison. A minimum lockout ensures equal T1-weighting throughout.

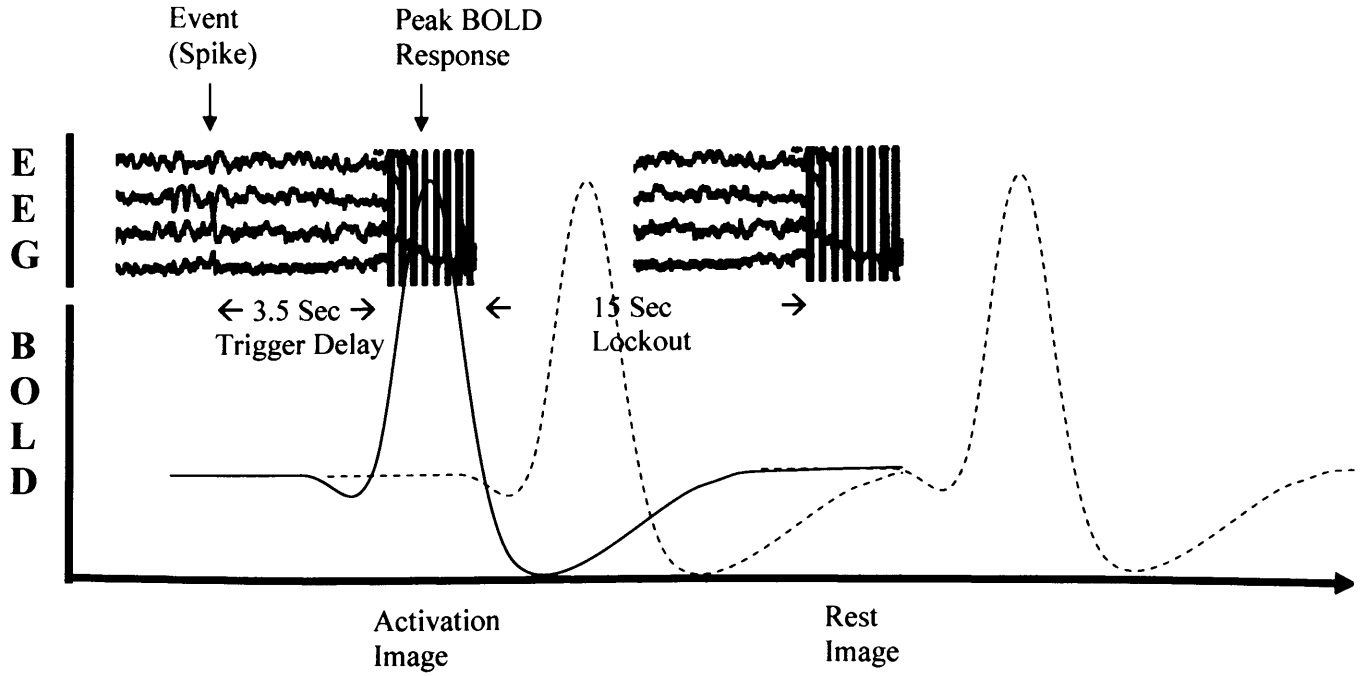

Figure 2-4

(Goldman et al., 2000), or more commonly aperiodic (i.e. EEG-triggered fMRI) (Krakow et al., 2000a). The principles of spike-triggered fMRI are demonstrated in Figure 2-4, but more recently advances in hardware and post processing technology have facilitated the removal of imaging artefact allowing for continuous, non-interleaved EEG/fMRI of the type shown in Figure 2-1 and Figure 2-3. For the purposes of detecting discrete events, this has been achieved both through (i) the accurate subtraction of an adequately-sampled channel-specific artefact waveform from an unsaturated EEG trace, in combination with adaptive noise cancellation (Allen et al., 2000) (used here) and (ii) through targeting the dominant imaging artefact frequencies with a series of band-stop filters (Hoffmann et al., 2000). These methods may be used online, and in combination with pulse-artefact removal, to provide diagnostic-quality EEG throughout imaging experiments.

The theoretical advantages of continuous acquisition are that BOLD-changes may be studied prior to, during, and after a host of EEG-phenomena within the same experimental session and signal dynamics may be fully explored. Therefore, a whole new 'physiological' dimension is added to the 'anatomical'. At a practical level, experiments are also easier to perform as EEG analyses need no longer be done at the scanner console and in real time.

The analysis of continuous fMRI time-series is however, substantially more complex. A lot of this added complexity centers on the implementation of strategies for dealing with the complex spatio-temporal autocorrelation structure of the data so that significance testing may take place in an unbiased manner. There are several dynamic sources of noise that also need to be dealt with. These may be physical (hardware-related), physiological (e.g. cardiac, respiratory, vasomotor etc) or neuronal (i.e. other unaccounted neuronal activity). Statistical modeling is also problematic. In contrast to studying state-related changes (e.g. finger tapping vs no finger-tapping), event-related signal changes are both more subtle (more difficult to detect above noise), and within the context of spontaneous EEG-events, more enigmatic. Indeed there are several unknowns regarding the precise manner in which the generators of EEG-phenomena may engender changes in BOLD. These issues are explored further in Chapter 3.

Clearly, future advances in signal processing and the design of new MR-compatible systems with simultaneous high-density EEG are likely to bring ever more subtle features within reach.

2.4 fMRI in epilepsy

2.4.1 Motor mapping

The main application of fMRI in the clinical setting is in the non-invasive mapping of brain function. Sensory-motor or central sulcus mapping performed with fMRI has repeatedly been found to be in agreement with intraoperative cortical stimulation studies (Achten et al., 1999;Dymarkowski et al., 1998;Fandino et al., 1999;Jack, Jr. et al., 1994;Puce et al., 1995;Pujol et al., 1998;Schulder et al., 1998;Yousry et al., 1995) and most centers now possess an additional wealth of unpublished experience.

2.4.2 Language mapping

A number of studies have found lateralization indices for language dominance based on fMRI to be in close agreement with measures derived from intra-carotid amylobarbitone (Wada) testing (Bahn et al., 1997;Binder et al., 1996;Desmond et al., 1995;Hertz-Pannier et al., 1997;Worthington et al., 1997;Yetkin et al., 1998) (Benson et al., 1999;Lehericy et al., 2000) and results from intraoperative cortical stimulation (FitzGerald et al., 1997;Lurito et al., 2000;Rutten et al., 1999;Schlosser et al., 1999;Yetkin et al., 1997). fMRI has been long hailed the successor to WADA testing. Existing paradigms however differ widely depending on available hardware and expertise with subtle differences in the brain areas targeted. Like many issues in fMRI there is a general lack of consensus but a move towards integrating information across different paradigms is evident. Validation is also less well developed for patients with mixed or right-hemisphere language dominance.

2.4.3 Memory mapping

Routine fMRI mapping of memory function is farther still from the clinical arena. Structures such as the hippocampus are both technically more difficult to image (see above) and more difficult to selectively target with cognitive paradigms (Bookheimer, 1996) but the benefits of new research techniques (Zeineh et al., 2000) are destined to spill over soon.

2.5 EEG/Correlated fMRI in epilepsy

2.5.1 Interictal EEG/fMRI

In 1996, Warach *et al.* described the first attempts at imaging inter-ictal epileptiform activity using EEG-triggered fMRI. Several 'spike' and 'rest' images were successfully acquired and a simple comparison was attempted using percentage change images. Several bilateral clusters of activation were noted but methodological limitations and uncertainties surrounding both the clinical syndromes and the sources of EEG activity, made interpretation rather difficult. Two imaging sequences were used, no motion correction was applied and significance testing was not employed. Seeck *et al.* (Seeck et al., 1998) used EEG-triggered fMRI to study a patient with focal epilepsy, bilateral (L>R) frontal spikes and an area of left frontal gliosis on subsequent resection. Three clusters of activation were described and good concordance was reported with both subdural recordings over the focus, and current density source reconstructions of scalp EEG data. However, despite a high level of thresholding (Bonferroni correction plus cluster threshold), more widespread changes were also evident raising concerns as to both the level of false positive error control and the effects of IV Clonazepam administration, routinely used by this group to acquire 'rest' images (see Chapter 3.2.2). Patel *et al.* (Patel et al., 1999) analyzed inter-ictal EEG-triggered fMRI data from ten patients, reporting activation 'corresponding to the EEG focus' in nine. Several subjects were excluded from the final analysis, no motion correction was applied and significance testing was not employed. Moreover, the two illustrated data sets pertained only to 'individual' spikes so it was difficult to see an overall picture.

At our own centre, the implementation of interictal EEG/fMRI has developed incrementally beginning with an initial safety/feasibility study (Lemieux et al., 1997). This was followed by the implementation of a pulse artefact removal (Allen PJ et al., 1998) allowing for EEG-triggered fMRI and later imaging artefact removal (Allen et al., 2000) allowing for continuous EEG/fMRI. Symms *et al.* (Symms et al., 1999) reported on the reproducible localization of interictal activity across four separate EEG-triggered fMRI sessions from the same patient. In a larger study by Krakow *et al.* (Krakow et al., 1999b;Krakow et al., 1999a;Krakow et al., 2001b) reproducible and concordant BOLD activation was found in 12 out of 24 patients with partial epilepsy. In 7 out of 12, where a structural abnormality was evident, activation was within or overlapping the lesion. Of the remaining 12 patients, no significant activation was observed in 10 but activation was discordant in 2. In six patients with well defined spike-related BOLD activations, 64-channel scalp EEG

recordings were made in separate sessions and equivalent current dipole locations found to correspond broadly with areas of activation, apart from one case with a deep mesial temporal activation (Lemieux et al., 2001a). Definitions of concordance however, were necessarily broad i.e. 'within the same lobe' and the use of global normalization/ intensity scaling may have curtailed the extent of larger activations. Using burst-mode fMRI (Josephs et al., 1999), attempts were made at imaging the timecourses of the haemodynamic response in four patients (Krakow et al., 2001b) and in one patient, individual spike images were effectively compared to the 'average' activation in an attempt to study individual events (Krakow et al., 2001c), though arguably revealing nothing more than the standard error of the response.

Lazeyras *et al.* (Lazeyras et al., 2000a) (see also (Lazeyras et al., 2000b)) were able to relate EEG-triggered fMRI findings in 11 patients with focal epilepsy to several measures of the epileptogenic zone, as part of a comprehensive study. The presence of activation was reported to have confirmed the clinical diagnosis in seven out of eleven patients, and in five out of six, intracranial EEG was also confirmatory. A number of compelling cases were illustrated but the numbers of false positive voxels are again surprising given the high degree of thresholding employed and the use of Clonazepam may have contributed to this. Definitions of concordance were again rather broad and large structural lesions in particular may not leave much scope for discordance.

Baudewig *et al.* (Baudewig et al., 2001a) used interleaved EEG/fMRI to study a patient with post-traumatic epilepsy and an abnormal background EEG with generalized polyspike and slow waves. Data from one of four sessions was shown; acquisition was complicated by the use of two interleaved slabs and motion correction was by way of removing individual scans only. Although the authors reported a right insular activation, the lack of proper significance testing combined with the ambiguous nature of the clinical syndrome complicates interpretation.

Benar *et al.*(Benar et al., 2002) used a different acquisition technique to record six-minute blocks of continuous EEG/fMRI data in a group of patients with focal epilepsy. EEG was filtered offline (Hoffmann et al., 2000) but, despite some distortion, was good enough to identify IEDs. They reported exclusively on a subgroup of four patients with good BOLD activations. These were modeled initially in an event-related manner using a canonical HRF to construct t-statistic maps of activation but thresholding was essentially carried out independently of the data

using a combination of Bonferroni correction and four-neighbor connectivity (except for one patient in whom 1 or 2 voxels were seen per cluster). However, this correction was not applied to the illustrated results. Multiple clusters of activation were shown and defined as regions of interest (ROIs). Within these, raw signals were extracted (following isolated IEDs only) and mean HRFs derived per cluster, per session, and per subject. An attempt was made to relate the size of the HRFs to those of the EEG spikes (see also (Krakow et al., 2001c)) but no significant relationship was established (see Chapter 3.1.2).

A similar recording setup was also used by Jager *et al.* (Jager et al., 2002) to perform burst-mode spike-triggered fMRI in 10 patients with focal epilepsy, successful in five. The signal changes however, were far in excess of anything previously reported (up to 31% BOLD increase at 1.5 Tesla) raising questions as to the exact nature of the effects observed (Lemieux et al., 2003).

Archer *et al.* (Archer et al., 2003b) performed EEG-triggered fMRI on a young patient with Rolandic spikes at 3 Tesla. Their report focused upon an area of activation within the left face sensorimotor cortex and deactivation adjacent to the cingulate gyrus, but widespread changes were also visible with maximal activation within occipital cortex. The results, as illustrated, were not corrected for multiple comparisons and there may have been uncertainties surrounding the EEG events triggered upon as half of the twenty acquired spike-images were later discarded.

A summary of these studies is provided in Appendix I.

2.5.2 Ictal EEG/fMRI

The first reported attempt at imaging spontaneous seizure activity using fMRI was by Jackson *et al.* in 1994 (Connelly, 1995;Jackson et al., 1994). Their study did not benefit from simultaneous EEG recording, which had only been attempted for the first time a year earlier by Ives *et al.* (Ives et al., 1993). Although methodologically simplistic by today's standards (see table 1), their reports of concordant BOLD changes in relation to focal motor seizures did fuel major efforts to image both ictal and interictal activity further. Detre *et al.* (Detre et al., 1995;Detre et al., 1996) described an interesting experiment where a patient, known to suffer with partial motor seizures, underwent fMRI alone. Despite no documented seizure activity during the study, the authors were able to identify areas of activation from visual inspection of percentage change images. These were later found to be concordant

with ictal SPECT and intracranial EEG localizations of the epileptogenic zone. Similarly using fMRI alone, Krings *et al.* studied a patient with a well defined structural lesion (glioma) during partial motor seizures (Jacksonian marches). Interesting peri-lesional clusters were selected from percentage change images and found to display a range of signal changes, both positive and negative. Some changes were attributed to the possibility of subclinical seizure activity, others to a mismatch between oxygen consumption and delivery. It was concluded that functional MRI can demonstrate seizure evolution and spread, but together these studies also highlight the need for objective means of assessing seizure activity to identify time-locked changes in BOLD. The difficulties in performing studies of this type have been outlined above, but the scope for more detailed physiological imaging in selected patients, is also apparent.

Induced seizure activity is of course more conducive to fMRI in a number of ways and the reflex epilepsies provide unique opportunities in this regard. Morocz *et al.* (Morocz et al., 2003) compared the effects of epileptogenic versus non-epileptogenic music in a patient with musicogenic epilepsy. Scanning took place over ten separate sessions and there was no EEG recording, but the patient was able to indicate six auras using a button. Whereas the study design did not permit the study of the seizure activity itself, it did allow for a comparison between sessions with and without aura. By averaging across all sessions, signal differences were reported within the left anterior temporal lobe (concordant with previous ictal EEG and SPECT) and the right gyrus rectus.

Archer *et al.* (Archer et al., 2003c) studied two patients with reading epilepsy using EEG-triggered fMRI during a reading task. For one of the subjects, activation was reported bilaterally within the inferior precentral gyrus, central sulcus, and globus pallidus in relation to epileptiform EEG activity which was known to be associated with jerks of the masseter and sternomastoid. These were not felt to have induced any significant motion but the results were not thresholded to correct for multiple comparisons and the use of global intensity normalization in fMRI is problematic (Aguirre et al., 1998a). It was suggested that the spikes of reading epilepsy 'spread' from frontal working memory areas into the adjacent motor cortex.

2.6 Other applications

2.6.1 Sleep

The first published report of EEG/fMRI during sleep was essentially a feasibility study by Huang-Hellinger *et al.* (Huang-Hellinger et al., 1995). Lovblad *et al.* (Lovblad et al., 1999) used a low-noise fMRI sequence (BURST) to acquire a single cardiac-gated BOLD-weighted slice every 10 seconds, interleaved with polysomnogram recordings. Three out of five subjects were observed to enter REM sleep, one of whom was excluded due to motion. The remaining subjects were scanned for 5-7 hours and voxel timeseries were cross-correlated with a step function representing REM and non-REM sleep states. The authors reported occipital activation and frontal deactivation during REM sleep but a number of limitations were apparent. It was not clear how residual motion was quantified and dealt with, an important consideration in single-slice studies. From the small segment of data shown, it was also unclear how many state changes were captured and how scanner noise - a significant problem in studying low frequency fluctuations – was dealt with/filtered. Later groups used EEG/fMRI to successfully stage sleep (Born et al., 2002;Czisch et al., 2002;Portas et al., 2000), but not to address the fMRI changes associated with the various specific sleep EEG phenomena. This was done successfully for sleep spindles by Schabus et al. (Schabus et al., 2007) and for sleep stages by Laufs et al. (Laufs et al., 2007b) (though in a single subject only).

Schabus et al. further demonstrated the existence of two different activation patterns corresponding to human fast (13-15Hz) and slow (11-13Hz) spindles. Activations common to both involved the thalami, anterior cingulate and insular and cortices together with superior temporal gyri, with the former recruiting sensorimotor motor and mesial frontal cortex together with hippocampus, and the later, the superior frontal gyrus, with potentially different functional significances. The involvement of sensory motor cortex is particularly interesting as sleep spindles and the sensory-motor cortex-generated human μ rhythm share a close functional relationship (Sterman et al., 1970). Similarly the hippocampal and prefrontal involvement was speculated to reflect memory processing during sleep (Gais et al., 2007).

2.6.2 Alpha rhythm

The first EEG/fMRI study of the generators of the alpha rhythm was by Goldman *et al.* (Goldman et al., 2002). By limiting brain coverage mainly to occipital cortex and thalamus, they used a temporally-interleaved periodic acquisition to enable EEG

monitoring between fMRI scans at 3 Tesla. Eleven subjects were scanned over a number of sessions and a running estimate of the occipital alpha power was derived. fMRI timeseries were essentially analyzed by way of cross-correlation with the HRF-convolved alpha power.

Negative correlations were reported within occipital, superior temporal, inferior frontal and anterior cingulated regions. Positive correlations were reported within the thalamus and insula. The results were interpreted as reflecting (1) the generators of the cortical rhythm, such as the occipital cortex; (2) areas forming part of the circuit but not directly generating the scalp-detectable rhythms (e.g. thalamus); and (3) other areas correlated with alpha but not causally linked., for example as relating to changes in arousal only.

Their data analysis however was quite complex. Epochs of artefact-contaminated EEG were discarded, along with sessions devoid of substantial alpha activity, images contaminated with motion, and results showing strong correlation within non-brain areas. Several different software packages were used, and an ROI approach was adopted instead of spatial normalization to enable inter-subject comparisons. Cluster thresholds were applied to the individual ROIs and group statistics were compiled using weighted results.

As the [occipital] alpha rhythm is essentially a universal phenomenon (Niedermeyer, 1997), in stark contrast to studies of focal epilepsy, one is specifically interested in group effects and inferences at the population level. In (Laufs et al., 2003a;Laufs et al., 2003b) we used a similar technique in 10 awake subjects with eyes closed. Spontaneous power fluctuations of electrical rhythms were determined for multiple discrete frequency bands, and associated fMRI signal modulations were mapped. We found little positive correlation of localized brain activity with alpha power (8–12 Hz), but strong and widespread negative correlation in lateral frontal and parietal cortices, known to support attentional processes. Power in the 17–23 Hz range of beta activity was positively correlated with activity in retrosplenial, temporo-parietal, and dorsomedial prefrontal cortices, areas previously characterized by high but coupled metabolism and blood flow at rest that decreases whenever subjects engage in explicit perception or action. The distributed patterns of fMRI activity that were correlated with power in different EEG bands overlapped strongly with those of functional connectivity, i.e., intrinsic covariations of regional activity at rest. The

result indicated that, during resting wakefulness, and hence the absence of a task, these areas constitute separable and dynamic functional networks, and that activity in these networks is associated with distinct EEG signatures. Taken together with studies that have explicitly characterized the response properties of these distributed cortical systems, the findings suggested that alpha oscillations signal a neural baseline with ''inattention'' whereas beta rhythms index spontaneous cognitive operations during conscious rest. This was also the first interpretation of cortical deactivations in EEG/fMRI studies in terms of the so called 'default mode hypothesis'.

Moosmann et al. (Moosmann et al., 2003) were able to further confirm the alpha-linked deactivation phenomenon and using NIRS confirmed that this phenomenon was due to a physiological increase in cortical deoxyhaemoglobin concentration. De Munck et al. (De Munck et al., 2007) have more recently studied the nature of the alpha-BOLD coupling and its variations across the cortex, confirming, amongst other things, that the so called 'alpha response function' was indeed positive in the thalamus (and earlier than the cortex). Others have successfully used ICA to isolate a range of 'resting state networks' (RSNs) (Beckmann et al., 2005;Damoiseaux et al., 2006;De et al., 2006) and examine their relative associations across a range of EEG power bands with interesting results (Mantini et al., 2007).

* * *

3. Chapter 3: Specific methodological issues

Despite much technical progress in acquiring simultaneous EEG and fMRI, EEG-correlated fMRI studies, inherit several problems from both modalities. EEG/fMRI is clinically most relevant to epilepsy, and in particular, in the study of IEDs for the presurgical evaluation of focal epilepsies. The modeling of BOLD activations in relation to spontaneous EEG activity however, is predicated upon a number of assumptions regarding both the generators of scalp EEG activity and the manner in which they might engender changes in BOLD. Here I will review some of the literature on this topic and explore both the theoretical and practical limitations of EEG/fMRI with specific emphasis on studying the generators of IEDs.

3.1 What defines fMRI activation

Conventionally, the detection of fMRI activation is achieved using classical statistics with the construction of voxel-based statistical parametric maps based on general linear models (Friston et al., 1995b). In event-related fMRI (Josephs and Henson, 1999), the temporal structure of a pattern of neural activity, predicted by a given paradigm, is modeled by a series of stick (delta) functions, convolved with an assumed time-invariant HRF - the convolution model (Bandettini et al., 1993) or an alternative set of basis functions (Josephs and Henson, 1999). Experimental confounds or effects of no interest may also be included as inference is ultimately based on the partitioning of variance and the ratio of the amount variance modeled by the effects of interest relative to the residual (unmodeled) component. The model hence embodies the null hypothesis to be tested such that its 'goodness of fit' - a signal to noise ratio (SNR) – both defines and determines 'activation'. It is therefore obvious that inferences in fMRI are far from unconditional measures of neural activity, but instead rely on the accuracy, validity and efficiency of pre-specified models/hypotheses. The 'goodness of fit' is usually expressed as a parametric statistic, such as a T or an F-statistic, conforming to a known distribution under the null hypothesis of no activation. In the context of neuroimaging experiments (unless one has an apriori interest in a single voxel), this 'mass univariate' approach gives rise to a multiple comparisons problem (for review see (Petersson et al., 1999a;Petersson et al., 1999b)). In the absence of a pre-specified ROIs therefore, and

when searching for areas of activation across the entire brain - as has virtually always been the case in paradigmless fMRI - it is necessary to threshold the results to account for the number of independent 'tests' carried out. The simplest approach to this - the Bonferroni correction - is generally too stringent, in view of the inherent spatial smoothness and its influence on the effective number of independent voxels/observations. The prevalent approach is based upon the application of Gaussian Random Field Theory(Friston et al., 1991). The use of 'uncorrected' images is seldom justified, and post-hoc definitions of regions of interest are contrary to the foremost assumptions of significance testing.

The construction of voxel-specific models of BOLD change for EEG phenomena is especially demanding. We will make a distinction between the incessant, waxing and waning patterns of rhythmic EEG activity and temporally discrete EEG events. For didactic purposes, we focus on the latter, specifically the most studied example of these: IEDs.

For discrete events, it is necessary to have (i) an efficient pattern of 'well-defined' (stereotyped) and 'well-detected' EEG events, and (ii) for these to share 'spatially consistent' generators so that responses may be effectively averaged*. Loosely speaking, 'a spike should be a spike and all spikes should be equal' but a degree of 'dedication'‡ is also demanded of the underlying generators if the residual (un-modeled) variance is to be minimized. So similarly, 'rest must be rest'.

3.1.1 Is rest, rest?

From an fMRI modeling perspective, the key issue here is the need to minimize residual BOLD variance. The BOLD signal essentially contains both experimentally-induced variance (in our case, signal change linked to the electrophysiological events of interest, whether detected entirely by EEG or not) and noise (i.e. all else). Within this context, unaccounted or incorrectly-modeled experimentally-induced variance will be adding directly, to the residuals (as neurogenic noise), from the explained component of variance, and thereby diminishing sensitivity. The same of course holds true for all sources of [unmodeled] noise, neurogenic and non-neurogenic. The latter includes physiological (e.g. cardiovascular, respiratory) noise, instrumental

* In the context of the general linear model, such averaging takes place by virtue of events featuring within the same regressor.

‡ We use the term 'dedication' in preference to 'functional specificity' as IED-generation is not a normal physiological brain function but an inconsistent feature of diseased tissue.

noise (e.g. Johnson/thermal noise, gradient drifts, changes in RF gain), and motion-related signal change (see below). In EEG/fMRI the concept of neurogenic noise is especially important and relates directly to the issue of dedication (i.e. functional specificity of pathophysiology).

Normal brain mapping experiments combine notions of functional specificity with optimal paradigm design and choice of baseline task, to minimize both neurogenic noise and the deleterious effects of residual variance. As we shall see, all of these considerations are less relevant in studies of spontaneous EEG activity. Starting with functional specificity, the targeted areas of potential activation (both generator and propagation sites) are: -

1) **Essentially unknown.** This is true both for the generators of spontaneous brain rhythms such as alpha (Nunez et al., 2001) and for interictal epileptiform discharges (i.e. in relation to 'the irritative zone')(Engel, Jr., 1993;Rosenow and Luders, 2001).

2) **Extensive.** Estimates of the cortical surface requirements for the generation of scalp-detectable IEDs range from 4-6 cm^2 (Cooper et al., 1965;Merlet and Gotman, 1999), though 10-20 cm^2 may be involved more commonly (Ebersole, 1997b;Tao et al., 2005), but again the importance of synchronization and dipole orientation over cortical amplitude has been noted repeatedly (Abraham and Ajmone-Marsan, 1958;Cooper et al., 1965;Gloor, 1985). Multiple simultaneously active regions can also be involved, overlapping in both space and time (Baumgartner et al., 1995) and spontaneous brain rhythms certainly exhibit global coherence and dynamics suggestive of distributed sources (see (Nunez et al., 2001) for review).

3) **Likely to encompass several functional areas.** Diffuse cortical areas frequently participate in IEDs (Alarcon et al., 1994;Merlet and Gotman, 1999) and these may also include eloquent cortices (Rosenow and Luders, 2001) so as to effect transient cognitive deficits (Hughes, 1989). Likewise, the generators of spontaneous brain rhythms are not functionally segregated, but rather involve multiple cortices. Examples include the associations of occipital alpha activity with visual areas (Lopes, 1991;Pfurtscheller and Aranibar, 1977), rolandic mu

(wicket) rhythm with primary somatosensory cortex (SI) (Tiihonen et al., 1989), and 'tau' rhythm with auditory cortex (Tiihonen et al., 1991).

The issue of paradigm optimality or efficiency is covered later but in spontaneous EEG/fMRI the choice of comparison or effective baseline task is restricted to periods devoid (or impoverished) of the relevant electrophysiological activity. There are two issues here. Firstly, the physical limitations of scalp EEG, as outlined above, dictate that substantial amounts of relevant activity* will not be visible on the scalp and studies with simultaneous scalp and invasive electrophysiological recordings fully support this conclusion (Ebersole, 1997a). IEDs may feature many times more frequently in invasive recordings (Alarcon et al., 1994;Devinsky et al., 1989;Niedermeyer and Rocca, 1972) and the surface attenuation of deeper voltages are severe (Cooper et al., 1965), though less so for the more extensive generators of cortical rhythms (Abraham and Ajmone-Marsan, 1958;Cooper et al., 1965). Consequently, IEDs involving smaller generators or deep mesial structures (potentially spherical dipoles) may remain completely undetectable (Ajmone-Marsan and Van Buren, 1958;Alarcon et al., 1994;Munari et al., 1994). An example, illustrating some of these points, is provided in Figure 3-1. In the context of scanner EEG, there are also added limitations: Sampling is often restricted and with fewer available EEG channels for example, there may be an additional sensitivity bias towards dipole orientation, where maximal scalp coverage is aimed for (Fuchs et al., 1998). Clearly, any 'missed' activity will be contributing directly to neurogenic noise, and hence residual variance

Secondly, the precarious nature of the 'resting state' concept has been long appreciated; human awareness being 'a stream of continuous mental experiences

Figure 3-1 Simultaneously recorded scalp and invasive EEG
Simultaneously recorded scalp and invasive EEG, from a patient with intractable focal epilepsy. A subdural grid (E), three subdural electrode strips (A-C) and 11 scalp electrodes (numbered O1-O11) are shown referenced to POz (positioning shown top left). Abundant interictal spiking is clearly evident over inferior and mesial temporal cortex, less so over the lateral surfaces, and yet little appears on the scalp. *Data courtesy of Dr M Merschhemke, Epilepsie-Zentrum Berlin-Brandenburg.*

* Relevant to modelling fully, the haemodynamic behaviour of the 'generator voxels' under search with fMRI.

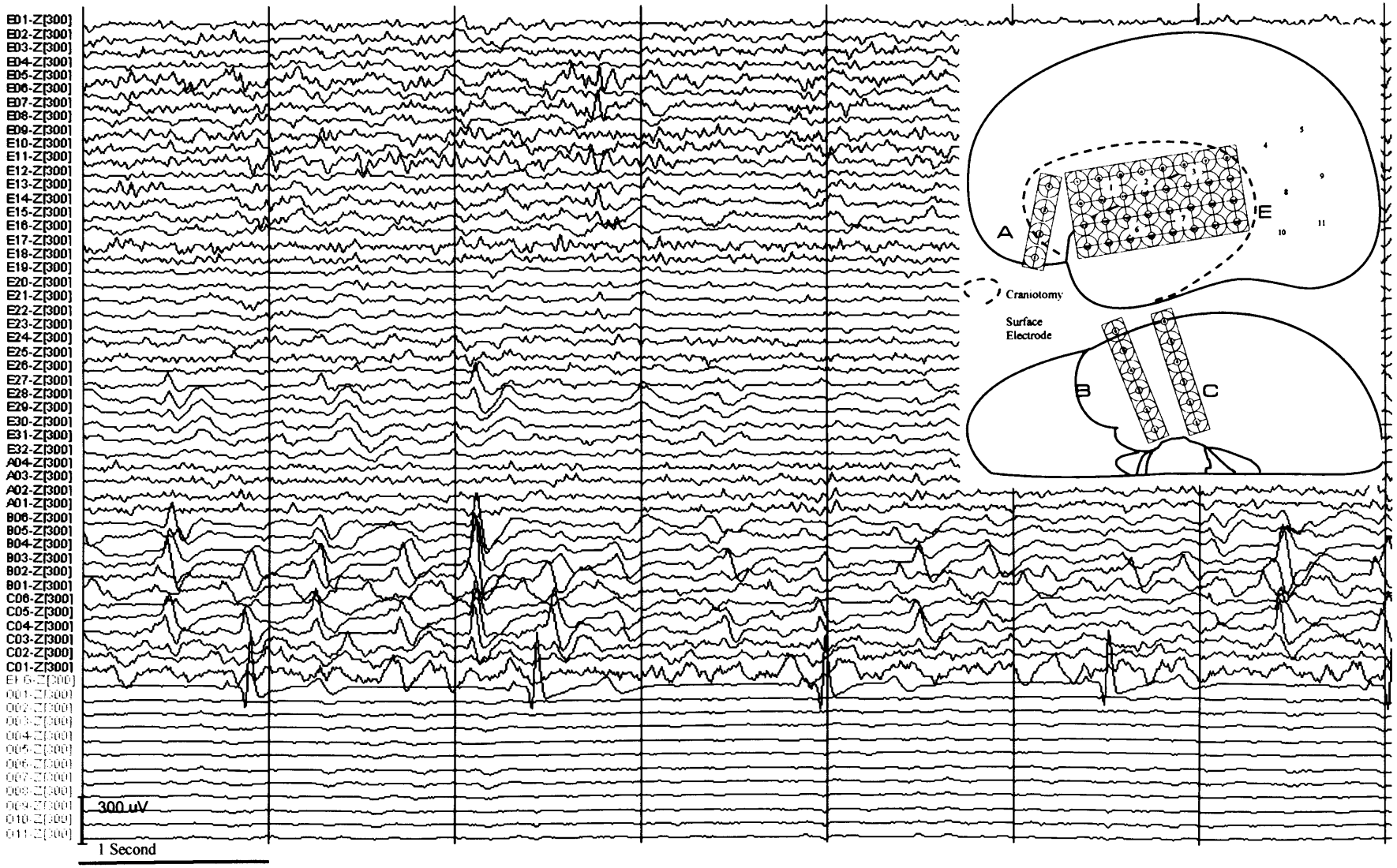
E01-Z[300]
E02-Z[300]
E03-Z[300]
E04-Z[300]
E05-Z[300]
E06-Z[300]
E07-Z[300]
E08-Z[300]
E09-Z[300]
E10-Z[300]
E11-Z[300]
E12-Z[300]
E13-Z[300]
E14-Z[300]
E15-Z[300]
E16-Z[300]
E17-Z[300]
E18-Z[300]
E19-Z[300]
E20-Z[300]
E21-Z[300]
E22-Z[300]
E23-Z[300]
E24-Z[300]
E25-Z[300]
E26-Z[300]
E27-Z[300]
E28-Z[300]
E29-Z[300]
E30-Z[300]
E31-Z[300]
E32-Z[300]
A04-Z[300]
A03-Z[300]
A02-Z[300]
A01-Z[300]
B06-Z[300]
B05-Z[300]
B04-Z[300]
B03-Z[300]
B02-Z[300]
B01-Z[300]
C06-Z[300]
C05-Z[300]
C04-Z[300]
C03-Z[300]
C02-Z[300]
C01-Z[300]
300 uV
1 Second
A
E
B
C
Craniotomy
Surface
Electrode

Figure 3-1

bearing no necessary relationship to external events' (James, 1890). Binder *et al.* for example, have addressed this issue explicitly using fMRI, to demonstrate compellingly, specific 'conceptual processing' networks more active during rest that 'deactivate' on stimulation (Binder et al., 1999). Indeed it is difficult to find a well-designed experiment that includes 'rest'. Instead, the paradoxes and difficulties of rest are normally resolved by considering only differential activity with respect to a control task. Clearly, it is necessary for IEDs or other EEG phenomena to induce differential haemodynamics, for rest to be considered as an appropriate baseline and this is especially true for the detection and localization of activation as opposed to studies of the signal dynamics. However, one way in which this difference may be obscured is if the haemodynamic response is already saturated by endogenous activity. Indeed, as the BOLD response to neural activity is non-linear and saturable (see below), were the very areas sought in EEG/fMRI of IEDs or other events, to be activated sufficiently during rest, it would clearly be to the detriment of eliciting additional activation in response to any effect/event of interest. Such background activity may well arise from changes in spontaneous brain rhythms such as alpha, for example, as linked to changes in arousal or sleep (unless imaging these were the actual objective); or second to mentation, were EEG generators to overlap the functionally relevant areas of cortex. Clearly, the larger the extent of the cortical networks being probed, the greater the chances of such functional overlap.

In paradigmless fMRI specifically, where there is no control over the reference condition, these considerations may be particularly relevant. For example, EEG/fMRI experiments performed in the eyes-closed-rest condition and lacking experimental stimulation are especially prone to confounding effects from changes in arousal or sleep, at either a local or global level. Also, in event-related fMRI of IEDs where paradigm efficiency may be low and SNR considerations paramount, the above considerations weigh more heavily. Fluctuations in brain rhythms, despite their more extensive generators, may prove more resilient to such effects by virtue of approaching the more efficient 'blocked' fMRI designs (see below). Likewise, simultaneous EEG recording may therefore ultimately be indicated during many fMRI experiments to better define the 'baseline'.

3.1.2 Are all spikes equal?

When events clearly occur in separate foci, as is often encountered in clinical EEG, the existence of multiple generators is seldom in doubt and so event classification and appropriate modeling proceeds accordingly. However, even where stereotyped IEDs occur repeatedly over the same focus, true source equivalency is never assured by virtue of the inverse problem (Plonsey, 1963). Indeed, that near identical scalp events may have spatially different intracranial appearances and vice versa, have both been demonstrated (Alarcon et al., 1994) and particularly in temporal lobe epilepsy, scalp discharges arising from widespread ECoG discharges have been shown to manifest very similarly (Fernandez Torre et al., 1999). The added limitations of scanner EEG (available number of channels, higher impedances, etc.) make this an especially significant concern as any misclassified events will contribute directly to neurogenic noise.

One should add that stable solutions do result from the application of source localization techniques based on equivalent current dipole estimation to averaged IEDs (Merlet and Gotman, 1999;Nakasato et al., 1994;Tseng et al., 1995;Wong, 1989), though individual dipole fits may vary (Nakasato et al., 1994;Tseng et al., 1995); and despite an accuracy of 10mm at best for EEG (Cohen et al., 1990;Cuffin et al., 1991) (and also MEG (Cohen et al., 1990;Mosher et al., 1993;Stefan et al., 1994)), results are often regarded as reflecting a 'centre of mass' with potential clinical value (Diekmann et al., 1998;Ebersole, 1994;Ebersole, 1997a;Ebersole and Wade, 1990;Nakasato et al., 1994). By analogy, as time-locked BOLD changes may, in principle, arise from both generator and propagation sites*, and as patterns of propagation may vary (Emerson et al., 1995), one might expect the 'average' fMRI activation to reflect the more 'consistent' areas and so similarly important information may be gained.

Another issue, concerning the need to include all 'relevant' activity within the statistical model, relates to the fact that efforts to localize epileptiform activity interictally, have largely concentrated upon the clearer, higher-SNR, spike/sharp wave discharges as opposed to focal slow waves or sharp transients for instance. This luxury, also afforded to an extent by EEG-triggered fMRI, is less applicable where one wishes to exploit the continuity and higher degrees of freedom offered by uninterrupted acquisitions. There is evidence to suggest that concomitant focal intermittent delta activity for example, may be very relevant (Huppertz et al.,

* Including functionally connected brain networks whose 'physiological' activity may have been influenced as a consequence of the epileptic discharge.

2001;Palmini et al., 1995) and even the sometimes-blurry morphological distinctions between spike and sharp wave, may prove significant. More extensive generators may encounter longer, more variable propagation times, and so give rise to less synchronized cortical spiking with more prolonged (blunter) scalp appearances i.e. preferentially giving rise to sharp and slow wave activity (Alarcon et al., 1994;Fernandez Torre et al., 1999). Clearly however, both may be equally relevant, haemodynamically, provided that the generators overlap. Although differences in IED amplitude may reflect different aspects of the generator (Abraham and Ajmone-Marsan, 1958), significant correlations have been reported between the amplitudes of evoked-potentials and BOLD changes for example (Arthurs et al., 2000), further questioning the validity of simple models which assume each IED to induce the same haemodynamic response. To summarize, theoretical considerations and experimental evidence indicate that the expression of neural activity as measured on the scalp is dependent on numerous physical and physiological factors. These must be taken into account, in the form of implicit or explicit models, in the interpretation and analysis of EEG/fMRI data.

Simultaneous fMRI and invasive electrophysiological recordings may help to clarify this issue, helping to further characterize the relationship between intracortical electrophysiological events and associated BOLD responses. Logothetis *et al.* (Logothetis et al., 2001) have already applied such techniques to primates but rigorous evaluation of the safety and feasibility of performing MRI with indwelling brain electrodes is currently lacking in man. However, anecdotal evidence suggests that they can be imaged safely using specific sequences, if precautions are taken (Davis et al., 1999;Rezai et al., 1999;Rezai et al., 2002;Tronnier et al., 1999). During pre-surgical evaluation for focal epilepsy, a proportion of patients undergo invasive investigations (e.g. implantation of depth or subdural electrodes) and so the application of such techniques to this population would be a natural way forward.

3.2 The neurovascular coupling in epilepsy

Successful EEG/fMRI requires an intact neurovascular coupling through which changes in metabolic demand are expressed, as changes in BOLD. This raises the question of whether scalp-detectable EEG phenomena should necessarily instigate 'normal' metabolic changes. Understanding the neuronal implications of scalp-recorded EEG activity and their potential metabolic consequences are clearly central

to establishing the link to BOLD. These issues are discussed next in relation to IEDs*.

3.2.1 What are the potentially relevant metabolic implications of IEDs?

The quintessential cellular correlates of IEDs are paroxysmal depolarization shifts (PDSs), comprising rapid bursts of action potentials riding on a slower wave of depolarization (Prince and Connors, 1986). Whilst bursting is a normal function of several neuronal populations (Llinas, 1988), in epilepsy, similar mechanisms involving specific intrinsic regenerative potentials, driven by subtypes of calcium and sodium currents, and independent of synaptic activity, are believed to generate the primary bursts initiating PDSs. Under conditions of hyperexcitability, these give rise to secondary discharges via recurrent synaptic feedback and once generated, synchronized population discharges ensue rapidly, promoting secondary bursting both through synaptic (glutamatergic and GABAergic) and non-synaptic entrainment (see (de Curtis and Avanzini, 2001) for full review). Extracellular potassium, in particular, rises significantly following ictal and interictal bursting (Jensen and Yaari, 1997) and ionic movements may provoke an additional chain of events further promoting depolarization and burst firing (de Curtis and Avanzini, 2001;Hochman et al., 1995). Hyperpolarizing after-potentials eventually terminate, follow and pace IEDs (de Curtis et al., 1998;de Curtis et al., 2001). These are mediated initially by both GABAa and GABAb receptors and later perhaps by a pH-dependent uncoupling of gap junction mediated currents (de Curtis et al., 1998).

3.2.2 Is the coupling affected?

Theoretically, anomalies in neurovascular coupling may arise, either as a consequence of the cumulative energy economics of epileptiform activity, as a consequence of an altered cellular environment, altered astrocytic function, regional [vascular] pathology, pharmacological intervention, or a mixture of all.

Glutamatergic transmission probably accounts for 80-90% of cortical glucose consumption (Sibson et al., 1998), over half of which may ultimately power the

* The haemodynamic and metabolic consequences of IEDs, seizures and generalised spike-wave activity are not similar. fMRI findings in relation to ictal electrographic activity and generalized spike-wave activity are discussed elsewhere{Salek-Haddadi, 2002 1 /id;Salek-Haddadi, 2003 164 /id}.

ouabain-sensitive Na+/K+ ATPase (Astrup et al., 1981), but the effects of concomitant inhibitory activity remain unclear. Inhibition is known to increase synaptic glucose uptake (Jueptner and Weiller, 1995), however, Waldvogel *et al.* were unable to demonstrate BOLD changes during an inhibitory task, arguing that a low ratio of inhibitory to excitatory synapses (1:6) together with a more strategic cytoarchitectural arrangement may render inhibition a more energy efficient process (Waldvogel et al., 2000). These issues together with the added uncertainties surrounding the relative contributions from changes in synchronicity versus changes in synaptic activity, leave much scope for speculation in relation to the overall energetics of IEDs.

The mediators of the neurovascular response are incompletely understood (Villringer and Dirnagl, 1995). The most prominent candidate is nitric oxide but others undoubtedly also play a part (Lindauer et al., 1999). Both potassium and hydrogen ions are known to alter arteriolar diameter (Kuschinsky et al., 1972;Kuschinsky and Wahl, 1978;McCulloch et al., 1982) and potassium in particular, has been repeatedly favored as a paracrine mediator of CBF (Dreier et al., 1995;McCarron and Halpern, 1990;Paulson and Newman, 1987). The relevance of this was pointed out above. Moreover, in addition to the direct involvement of several potentially important mediators of the neurovascular response, astrocytes themselves are intimately implicated in epileptogenesis and form the target of several antiepileptic drugs (Grisar et al., 1999). Astrocytes dominate several aspects of neuronal function, buffering the extracellular environment, and removing glutamate from the synaptic cleft. They may also play an important role in the neurovascular coupling (Bonvento et al., 2002;Harder et al., 2002), thereby offering another plausible mechanism through which it may be disturbed*.

Other defects may arise as a direct consequence of pathology, such as demonstrated in relation to Arteriovenous Malformations (AVM) (Duchene et al., 2001), or as a consequence of drugs. The anticonvulsants: Carbamazepine (Theodore et al., 1989), Phenytoin (Theodore et al., 1986a), Valproate (Leiderman et al., 1991), Barbiturates

* Magistretti & Pellerin have proposed an elegant but controversial theory whereby, the synaptic release of glutamate, electrogenic uptake by astrocytes, and conversion to glutamine prior to recycling might drive directly, the glycolytic conversion of glucose to lactate thereby providing a mechanism for 'sensing' neuronal activity, coupling blood flow with metabolism, and nourishing neurons through an 'astrocyte-neuron lactate shuttle' (Chih et al., 2001;Magistretti et al., 1999).

(Theodore et al., 1986b), and Benzodiazepines (de Wit et al., 1991) for example, are all known to reduce the regional Cerebral Metabolic Rate of Glucose (rCMRGlc). Acetazolamide, a vasodilating anticonvulsant, is also reported to impair BOLD contrast by way of enhancing resting-state signal (Bruhn et al., 1994;Kleinschmidt et al., 1995), as are Benzodiazepines (Kleinschmidt et al., 1999) which may, in addition, preferentially alter regional Cerebral Blood Flow (rCBF) (Forster et al., 1982;Matthew et al., 1995).

Despite much PET data on human interictal rCBF and rCMRGlc, relatively little is known about the acute changes following IEDs*. Interictal PET studies of human epileptogenic foci, generally reveal large areas of hypometabolism and hypoperfusion concordant with epileptogenic areas (Duncan, 1997b). A number of studies have specifically addressed coupling. Gaillard *et al.* studied 20 patients with temporal lobe epilepsy demonstrating disproportionate reductions in rCMRGlc vs rCBF (≈11% vs 3-6%) ipsilateral to the epileptogenic focus (Gaillard et al., 1995). Likewise, Fink *et al.* reporting on 13 similar patients, noted ipsilateral reductions in rCMRGlc otherwise unaccompanied by consistent reductions in rCBF within temporomesial structures (Fink et al., 1996). Both groups have interpreted their findings as evidence of interictal flow-metabolism uncoupling and this trend has been further confirmed by Breier *et al.* (Breier et al., 1997), who reported an association with the duration of epilepsy, and also by animal studies (Bruehl et al., 1998). Others however are not in agreement (Franck et al., 1989;Kuhl et al., 1980).

Interestingly, Bittar *et al.* reported focal rCBF and rCMRGlc increases (≈ 35% and ≈ 13%, respectively) comparing states of high versus low spiking, in patients with reflex epilepsy (Bittar et al., 1999) but in general, state-related studies provide unclear bearings for the sequelae of individual IEDs.

Certainly, concordant spike-triggered fMRI activations, in relation to IEDs, have been obtained by a number of centers and physiological event-related HRFs demonstrated in relation to IEDs (see Chapter 2.5.1). However, while such findings are reassuring, activations do not obtain in all cases, and so defects in neurovascular coupling may offer a partial explanation.

---

* The slow cerebral uptake and fixation of rates of ^{18}F-labeled 2-fluoro-2-deoxy-D-glucose (^{18}FDG) for example, severely impair the temporal resolution of FDG-PET measurements to effectively providing a weighted rCMRGlc average over some 40 minutes (Duncan, 1997b).

3.3 Modeling spontaneous EEG activity

Assuming a reliable transduction of the scalp EEG events into BOLD changes, both a sufficiently 'efficient' pattern of EEG activity and the specification of an appropriate statistical model and are central to the conjoint use of EEG and fMRI. These issues are considered next.

3.3.1 How efficient are spontaneous EEG paradigms (how may spikes constitute a study?)

An inability to influence experiments by way of altering 'stimulus' presentation, defines 'paradigmless fMRI' and represents perhaps the single most significant obstacle to the successful characterization of EEG/fMRI correlates. Simply speaking, fMRI is inherently blind to a whole range of neuronal signal frequencies. Scanner noise characteristics, roughly proportional to 1/frequency, are such that high-pass filtering becomes essential. In addition, the HRF functions as a low pass filter such that detection power is effectively limited to a narrow range of frequencies within which most conventional paradigms tend to operate (Josephs and Henson, 1999). For instance, in the case of rapid, continuous, and recurring patterns of focal neuronal activity, an HRF blanket (low-pass filter) would effectively create only a 'raised baseline' of BOLD such that, following mean correction and high-pass filtering, nothing would be detectable. On the other hand, with infrequent activity or stimuli, one clearly fails to capitalize on the maximum amount of experimental variance that could be induced in the BOLD signal.

Therefore, there must exist an 'ideal pattern' of signal change. This has been addressed theoretically (Friston et al., 1999b;Josephs and Henson, 1999) and a critical trade-off shown to exist between detection efficiency (i.e. the ability to detect activation) and estimation efficiency (i.e. the ability to accurately estimate the form of the HRF) such that conventional blocked designs optimize the former, and randomized short interstimulus event-related designs, the latter (Liu et al., 2001b). Theoretical estimates of efficiency are possible but rely on a number of assumptions regarding HRF-shape, non-linearities, and the temporal filtering employed. Moreover, the leap from estimates of efficiency to the chances of experimental success would require additional assumptions about noise. In short, while this remains a key consideration when designing and interpreting EEG/fMRI experiments, calculations serve only as a rough guide to the chances of success.

Attempts to 'optimize' spontaneous EEG activity, pharmacologically or physiologically are possible, but take us toward studies of evoked EEG activity. Manoeuvres such as eye-closure and relaxation are frequently used to elicit waxing and waning alpha activity and likewise, sleep deprivation to induce sleep. In general, where interventions are essentially uncorrelated with (orthogonal to) the effects of interest (e.g. the constant state of eyes closed or sleep deprived, versus the transient occurrences of alpha peaks or sleep spindles, respectively), the effects of interest should remain statistically discernable but experimental manipulations may introduce additional confounds (either region-specific or global) namely through task-by-condition or drug-by-condition interactions. Hyperventilation for example, is routinely used to elicit IEDs clinically, but in the fMRI context this risks introducing both global and region-specific confounds, through uncalibrated alterations in rCBF and BOLD contrast (Kastrup et al., 1999a;Rostrup et al., 2000). Photic-stimulation is another common means of eliciting IEDs (generalized spike-wave) in photosensitive individuals. It does so repetitively and through entrainment ('photic driving') at frequencies around 3Hz, but high correlation would be expected between the haemodynamic responses to the effects of interest (IEDs) and the nuisance covariate (i.e. the effects of visual stimulation), so that the individual effects are rendered inseparable.

Group comparisons with normal subjects, do offer a solution to this problem, but a less powerful one with fewer degrees of freedom and added [inter-subject] variability. This approach was used by Hill *et al.* (Hill et al., 1999) in an attempt to study [evoked] generalized spike-wave activity in photosensitive patients with a photoparoxysmal response through comparison with 'normal' patterns of visual activation in control subjects. The authors were unable to attribute any changes in BOLD to spike-wave activity *per se* but a compelling example, is provided by the work of Iannetti *et al.* (Iannetti et al., 2002)(see table 1). They performed EEG/fMRI on three patients with fixation-off sensitivity during epochs of eyes open and shut, demonstrating striking activation within extrastriate cortices in relation to induced occipital spiking during the eyes-closed condition. Although no formal group effects analysis was carried out, similar activation was not seen amongst age-matched controls and was therefore attributed to the interictal activity (see also (Krakow et al., 2000c)).

Specific forms of reflex epilepsy such as reading epilepsy offer another solution: IEDs amenable to provocation and yet in a manner orthogonal to the precipitating stimulus (see section 3.1, for example Archer *et al.* (Archer et al., 2003c)). Pharmacologically, Barbiturates such as Methohexital have also been used successfully to provoke IEDs (Diekmann et al., 1998) and likewise Benzodiazepines for suppression (Lazeyras et al., 2000a) but the potential for confounding effects has already been pointed out. Drug withdrawal is routinely used to facilitate seizure recordings in epileptic patients but the effects on interictal spike frequency are not pronounced (Gotman and Koffler, 1989;Gotman and Marciani, 1985).

3.3.2 What are the essential modeling requirements?

At its simplest, one might assume all events to evoke the same haemodynamic response, and assume linear summation over time. However, this is unlikely to be the case where trains of EEG events occur in close succession (e.g. runs of spikes, spike-wave or alpha waves). Studies using closely spaced physiological stimuli show substantial non-linear (saturation) effects, of increasing prominence at shorter interstimulus intervals, less than 1 and 4 seconds for auditory (Friston et al., 1998b) and visual (Vazquez and Noll, 1998) stimuli, respectively. Such non-linearities may enter at either the neuronal level (i.e. stimulus transduction into focal electrophysiological activity), or at the haemodynamic level (i.e. the translation to change in rCBF or BOLD).

Logically, EEG/fMRI experiments ought to concern the latter but in relation to normal brain function Friston *et al.* argue that synaptic activity and blood flow are linearly related (over normal ranges) such that non-linearities arise during translation of rCBF into BOLD (Friston et al., 2000c). This was reconciled successfully with current understanding of the transduction process in terms of the Balloon/Windkessel model (Buxton et al., 1998;Mandeville et al., 1999b). They investigated theoretically, a number of interacting factors including neuronal efficacy, referring to the potency of the underlying synaptic activity; signal decay, linked directly to the half-lives of the relevant mediators (e.g. 1 second for Nitric Oxide versus 5 seconds for Potassium (Paulson and Newman, 1987)); and resting oxygen extraction, a particularly important factor. However, these parameters might all be subject to transgression beyond physiological limits, during epileptic activity, with as yet undetermined

consequences for the coupling between electrophysiology and haemodynamics, as alluded to above.

Even assuming linearity, the HRF is subject to considerable variability. This variability can be inter-regional (Buckner et al., 1996;Buckner et al., 1998;Huettel and McCarthy, 2001;Kastrup et al., 1999a;Lee et al., 1995;Miezin et al., 2000;Robson et al., 1998;Rostrup et al., 2000;Schacter et al., 1997), inter-subject (Aguirre et al., 1998b), inter-sessional (McGonigle et al., 2000), age-related (D'Esposito et al., 1999), and sex-related (Kastrup et al., 1999b), leading some to advocate at least subject-specific HRFs in fMRI analysis (Postle et al., 2000). The prospects of additional pathophysiological variation are challenging indeed to studies of disease states.

More flexible models estimate the HRF not only for each subject, but also for each voxel. This is accomplished efficiently by convolving the cause of haemodynamic changes (i.e. stimulus or EEG changes) with a small basis set that spans all possible forms of the HRF. However, the more flexible and complex the model, the less straightforward the inference. The non-reproducible and inefficient nature of spontaneous EEG/fMRI 'paradigms', together with an inability to pre-specify regions of interest in the present context, renders the characterization of specific variants of the HRF a real challenge. Table 3-1 Summarizes the main issues.

3.4 How can one judge the validity of activations?

A valid measurement should be reliable and reproducible. However, spontaneous EEG/fMRI is, by nature, an instrument of varying sensitivity. The key point here is that, even if IEDs produce identical haemodynamic responses, the efficiency with which each IED is detected depends on their frequency and pattern of expression. It has been said that 'You cannot step into the same river twice'* and this applies to spontaneous EEG. Though stereotyped phenomena may be encountered individually, epochs of spontaneous activity that can be detected with the same efficiency are unlikely to recur. This is important to bear in mind, when comparing different analyses. Furthermore, even where results prove reliable, reliability itself is not sufficient for validity.

* Heraclitus of Ephesus (500BC).

Table 3-1 Essential conditions and assumptions in interictal EEG/fMRI.

Condition/Assumption Confounds/Issues
Focal changes in metabolic demand arise in relation to EEG events
Relative effects of Excitation vs. Inhibition
Changes in Synchrony vs. Changes in Firing
Misclassification of EEG events/Variable generators
Neurovascular transduction is intact
Effects of pathology
Influence of drugs
Consequences of epileptiform activity
Adequate EEG signal to noise
Imaging, pulse, and motion artefact
Safety resistors
EEG is 'fMRI-efficient'
Non-optimal EEG-event presentation
Adequate fMRI signal-to-noise
Field Strength
Choice of Head Coil
Choice of Sequence
Artefacts e.g. susceptibility
Influence of EEG setup e.g. RF noise
Head motion
No head motion
Lack of cooperation
Involuntary movement / Epilepsy
Discomfort / Noise / long experimental time
Sleep
Adequate modeling of expected BOLD change
Non-canonical HRF
Non-linear behavior
Unexpected interactions
Adequate control of Type I error
Inappropriate statistical model
Unaccounted Spatio-temporal autocorrelations

Clearly, the size of an activation, its shape, symmetry, whether it is restricted to grey matter or indeed the brain, and its anatomical emphasis (e.g. location of maximum) may lend results some degree of face validity, particularly where a discret focus is suspected or otherwise predetermined (e.g. by the presence of lesions or other corroborating data). The risks of type I errors (false positives) however, though controllable, are ever-present at every level. Furthermore, propagated activity may arguably underlie a proportion of cases, where activations prove more extensive that anticipated. Conversely, absence of evidence is not evidence of absence and a host of

seemingly less plausible activation patterns may in truth also represent genuine effects, eroded for instance by spatial inhomogeneities in noise or BOLD sensitivity. The wider issue here is that in functional neuroimaging, type II error control (against false negatives) is fettered by difficulties in the precise specification of alternate hypotheses (Zarahn and Slifstein, 2001).

Concurrent validity, present when a measure relates directly to another measure of the same thing, would require equivalent whole-brain high-spatial resolution imaging techniques for EEG activity, capable of imaging distributed networks. The hitherto unavailability of such techniques, explains the current lack of 'gold standards' in this field. Even in focal epilepsy, the use of invasive recordings as the gold standard for identifying epileptogenic regions is not without limitation (Gloor, 1985). Non-inferential or exploratory methods such as Principle Component Analysis (PCA) (Friston et al., 2000a), Cluster analysis (Baune et al., 1999), Independent Component Analysis (ICA) (McKeown et al., 1998) and variants (Stone et al., 2002), may hold promise in corroborating model based fMRI findings, but this approach is to some extent circular and the utility of data driven analysis techniques in this context, remains to be established.

Demonstrations of predictive validity are possible in the context of IEDs and epilepsy surgery, and although this aspect is by far of most interest clinically, efforts are hampered by the scarcity of suitable patients/lesion models. Ideally for example, pre and post-operative EEG/fMRI data would be combined with invasive electrophysiological recordings and surgical outcome, but there are problems. In our experience suitable candidates for EEG/fMRI are the exception rather than the rule in epilepsy, and these are not necessarily the best surgical candidates. The converse is also true, though the topic is gathering interest and larger efforts are bound to contribute more exciting data. The use of repetitive Transcranial Magnetic Stimulation (rTMS) as a non-invasive means of inducing transient functional lesions (Hallett, 2000) may be an alternative. More recently, fMRI and TMS have been successfully interleaved allowing for the detection, localization of TMS-induced BOLD responses (Baudewig et al., 2001b;Bohning et al., 2000) and so the potential for 'verifying' EEG-correlated activations through targeted functional lesioning is on the horizon.

In fMRI studies of normal brain function, demonstrations of reproducibility across subjects are an important aspect of validation. This principle may also extend to

fMRI studies of normal EEG activity (Burgess and Gruzelier, 1993), and possibly some forms of pathophysiological activity such as generalized spike-wave where the physiology may be universal (Snead, III, 1995). Focal IEDs however, do not share a common pathology but there are exceptions. The common syndrome of Benign childhood Epilepsy with Centro-Temporal Spikes (BECTS) presents an interesting opportunity. Comprising a familial idiopathic epilepsy, children with 'typical BECTS' display stereotyped, and well-detected focal IEDs with known and stable source estimates suggestive of a common functional epileptogenic focus within the sylvian fissure (Wong, 1991). EEG/fMRI studies of BECTS therefore, may yet provide important validative information with regards to reliability and reproducibility of activation across groups, if not also on the nature of the phenomenon itself (Archer et al., 2003b;Boor et al., 2003). Boor et al. (Boor et al., 2007) (extending the data presented in (Boor et al., 2003)) used an interleaved aperiodic acquisition in 11 children with BECTS to show concordant perisylvian activations in 4. Using multiple source (dipole) analysis they found the activations to co-localize in all but also include areas of propagation in 3 subjects.

3.5 Can interictal EEG/fMRI be used to study connectivity?

Functional connectivity is defined as *the correlation between spatially remote neurophysiological events.* It is not concerned with causality, unlike effective connectivity which refers to *the influence one neuronal system exerts on another* (Gerstein and Perkel, 1969). Two key points here are that (1) functional connectivity is not necessarily due to effective connectivity (e.g. areas A and B could share a common input from unknown C) and (2) where functional connectivity is due to effective connectivity, the influence may be indirect (e.g. A influencing unknown C influencing B). Several tools are available in functional imaging to study functional connectivity (see Human Brain Function (2004) for full discussion). These include eigenimage analysis/PCA, multidimensional scaling, partial least squares and generalized eigenimage analysis (principle co-ordinate analysis). The issue of functional connectivity however is generally less interesting given at any two brain areas are only separated by an average of 2.5-3 synapses (Sporns and Zwi, 2004) – the anatomical connectivity.

In contrast to the above, measures of effective connectivity are necessarily model based. They are not exploratory (*ergo* GIGO*). They use system identification (SI), defined as the use of observed data to estimate the parameters of mathematical models representing the physical system. These models fall into two categories, those that invoke hidden states (e.g. state space models (of which DCM is a special case), and hidden Markov models) and those that quantify the relationships between inputs and outputs by treating the system as a black box such as generalized convolution models and autoregressive models).

Such models also need to be dynamic (i.e. describe changes over time) and non-linear so as to be able to reproduce complex [biological] responses. As the later are mathematically intractable, a compromise is reached by making linear approximations such as in bilinear models which include non-linear components as interaction terms (Rao, 1992). This for example allows for the retention of a uniquely non-linear feature: input-dependent modulation of intrinsic dynamics. The inputs can then be divided into two classes: perturbing and contextual. For example, in creating a model of how area A influences B. On might account for the input to area A (contextual) and the influence of another area C (perturbing, such as 'attention'), on the connection between A and B. Time and input dependent changes in connectivity are a central feature of plasticity and the motivation for using bilinear state-space models.

Psychophysiological interaction (PPI) models are an example of *static* bilinear models which can be statistically framed and estimated within the GLM framework (for example (Buchel et al., 1996). A related but more sophisticated method is Structural Equation Modeling (SEM) or path analysis which can also be carried out within a modified GLM framework. SEM allows for several (nested) and constrained models of effective connectivity to be compared and tested, for example to establish whether an additional 'connection' is necessary for the model to explain the data (for example (Rowe et al., 2002). Some limitations of SEM are the ad hoc requirements of partitioning the data to create nested models, or pruning the coupling matrix to render the solution tractable. There is also the inability to capture temporal dependencies, that is that there is no way by which the history of input itself can embed prior knowledge into the model. That is to say that permuted data sets

* Garbage In, Garbage Out – A teaching mantra credited to George Fueschsel, an early IBM programmer.

produce identical path co-efficients. This is where dynamic models come in, with the promise of being more brain-like.

Dynamic models that do not refer to hidden states (i.e. non black box models) include Multivariate Autoregressive Models (MAR) and generalized convolution models for example of the type used to estimate the HRF. Examples of dynamic state-space models include the Kalman filter and DCM. Whereas static models provide snapshots of path co-efficient, dynamic models can reveal temporal fluctuations in coupling and connection strengths. The Kalman filter invokes an extra set of hidden variables to generate the data. The hidden states are estimated (the prediction step) using the current information, which is updated (the correction step). The process is therefore iterative. Dynamic causal modeling (Friston et al., 2003), employs a more plausible generative model of the measured brain response combining an anatomical model of interacting cortical regions or nodes, supplemented by a (more realistic and biologically plausible) forward model of how neuronal or synaptic activity is transformed into the measured responses. The model parameters reduce to three sets, those that (1) mediate the influence of extrinsic inputs on the states, (2) mediate intrinsic coupling among the states, (3) [bilinear] parameters that allow the inputs to modulate the coupling.

Again, all such models rely entirely on some form of *a priori* knowledge such as an anatomical model of how any regions of interest might be interconnected and whereas it may be possible to study the effects of IEDs on connectivity between A and B (i.e. during same unrelated cognitive task), to use IEDs themselves as both input and modulator is less meaningful. Furthermore, whereas scalp IEDs could feature as modulators, they only partly reflect the true neuronal input (e.g. intracranial EEG, LFP etc) engendering the observed changes in BOLD.

* * *

4. Chapter 4: Common Methods

4.1 Recruitment and ethics

Ethics approval for all work was obtained from the Joint Research Ethics Committee of the NHNN. Patients were recruited from within the department of clinical and experimental epilepsy at the NHNN, and the NSE. Patients for the generalized spike-wave study (chapter 10) were also recruited from the department of clinical neurophysiology and epilepsy at St Thomas's hospital in London and patients with reading epilepsy (chapter 11) were recruited from across the UK and also Germany.

All subjects gave written informed consent and all work was carried out in accordance with local* and national ethical guidelines[†‡].

For the main studies, patients were recruited according to the following criteria:

1. Frequent (>1/min) IEDs (focal or generalized) on recent interictal EEG
2. Able to tolerate MRI
3. Able to give informed consent

Most patients were therefore recruited or referred from patients undergoing inpatient assessment, pre-surgical evaluation, or outpatient EEG at the aforementioned centers.

4.2 Experimental set-up

4.2.1 EEG recording

Twelve gold disk electrodes (Figure 4-1) fitted with 10 kΩ safety resistors were applied to the scalp, at Fp2/Fp1, F8/F7, T4/T3, T6/T7, O2/O1, Fz (ground) and Pz according to the international 10-20 system. The scalp was prepared with abrasive cream (Nuprep, SLE diagnostics) and electrodes attached with collodion adhesive (SLE diagnostics). An MR compatible conductive electrode gel (Dracard, Crown graphic) was then applied under each electrode. The impedance across each electrode pair was measured and skin abrasion was used as necessary to achieve an impedance of <22kohms (i.e.<2kΩ for the scalp alone). ECG electrodes were attached either

---

* UCLH documentation on Research Governance, including Committees on the Ethics of Human Research for UCLH NHS Trust and UCL 2002; Consent and Security, A Data Protection Toolkit for Researches at UCLH 2002; and UCLH Research Governance Policies for the Conduct of Research Principle Investigators 2003 (www.uclh.org).

† MRC Ethics Series: Good Research Practice (www.mrc.ac.uk)

‡ Research: the Role and Responsibilities of Doctors (www.gmc_uk.org/standards/research.htm)

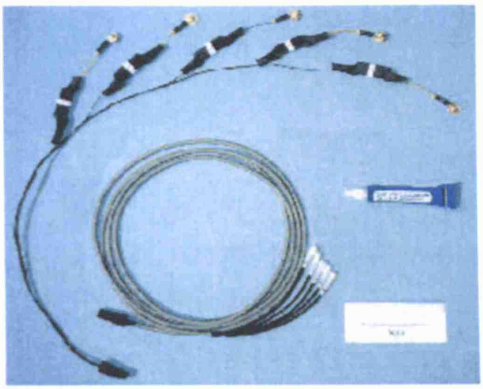

Figure 4-1 EEG Electrodes

Figure 4-2 EEG Transmitter

parasternally or over each clavicle depending on where the best signal could be obtained.

These together with a bipolar ECG channel, these were connected to a sixteen channel head box connected by ribbon cable to an MR-compatible battery powered digitizer-multiplexor-fibre optic transmitter (Figure 4-2). The fibre optic cable was passed through a wave guide and connected to a remote receiver in turn connected to a CED1401 (Cambridge Electronic Design) digitizer and Dell PC running Windows NT running in house EEG software (Figures 4-4 to 4-7). All components aside from the CED were made in-house by Mr Phillip Allen and his team, Medical Engineering, Department of Clinical Neurophysiology, NHNN.

Once in the scanner and with the patient seated on the table, the EEG was checked and then again after sliding the patient into the bore of the magnet. All cables were secured and routed under the mattress to minimize artefacts.

The ten EEG channels, referenced to Pz, and two channels of ECG were recorded as well was a timing signal derived from the scanner (5 kHz sampling, 33.3 mV range, 2μV resolution) with online pulse (Allen PJ et al., 1998) and imaging (Allen et al., 2000) artefact subtraction.

4.2.2 MRI acquisition

The patients were scanned on a 1.5 Tesla Horizon EchoSpeed MRI scanner (General Electric, Milwaukee, USA) using T2*-weighted single-shot gradient-echo echo-planar images (EPI; TE/TR 40/3000, flip angle: 90°, 21x5mm interleaved slices,

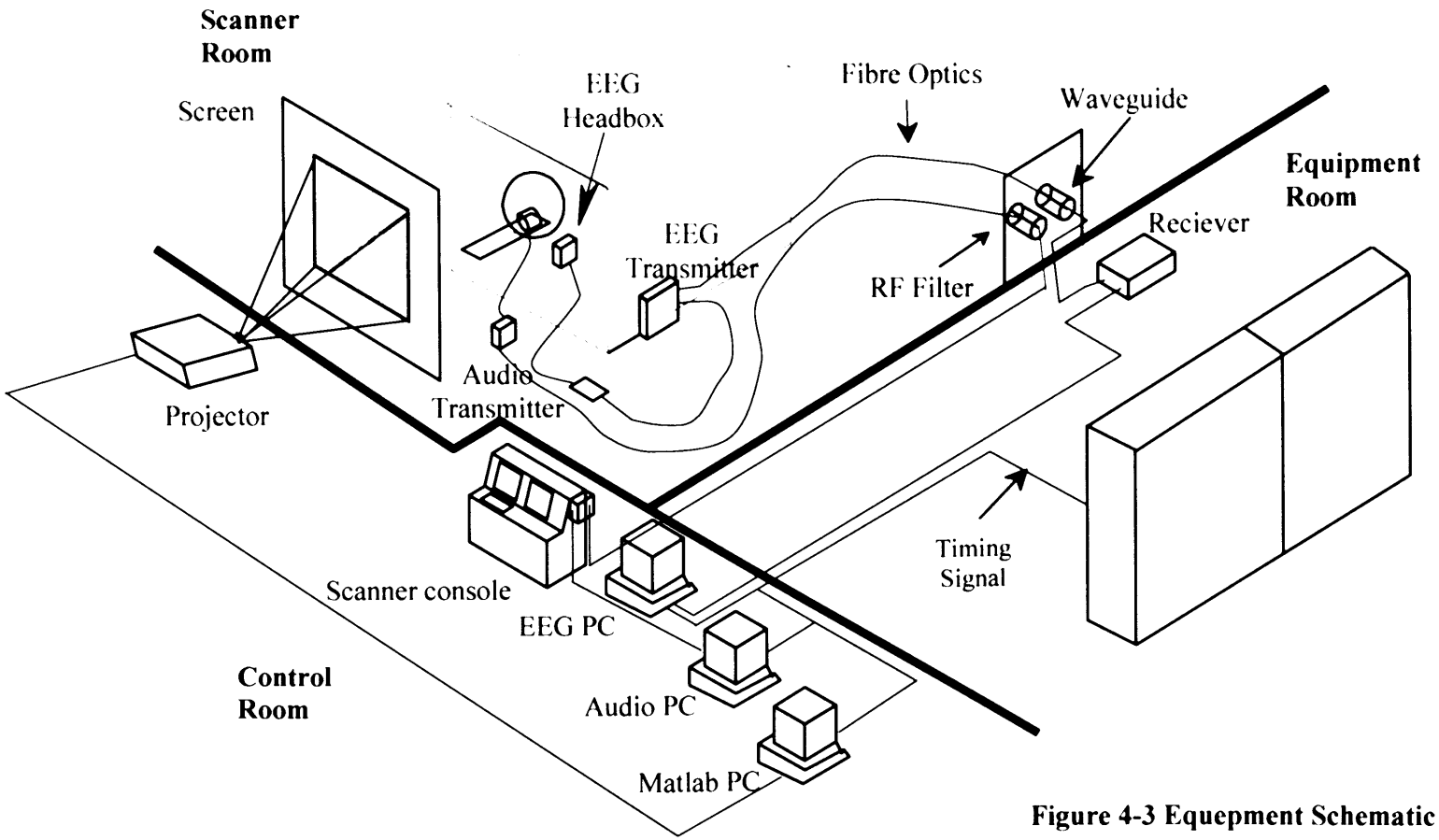

Figure 4-3 Equepment Schematic

Figure 4-3

Figure 4-4 Patient connected to headbox

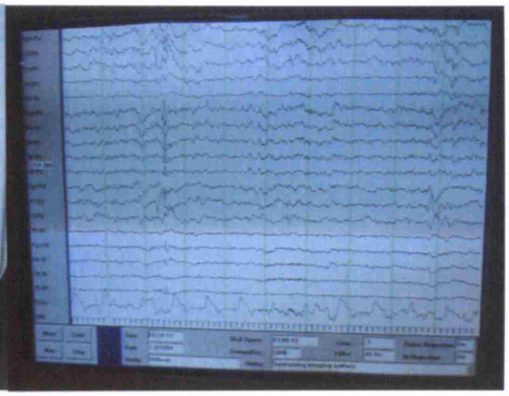

Figure 4-5 Online EEG Display

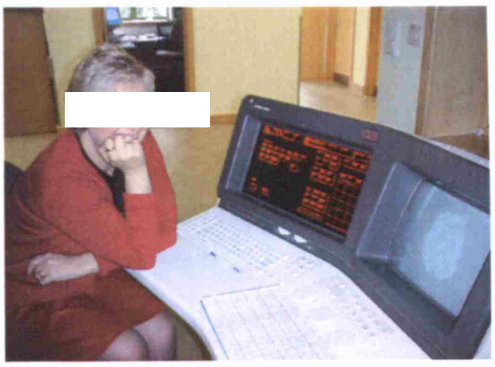

Figure 4-6 Scanner Console

Figure 4-7 Equipment Trolley

FOV=24 x 24cm, 64x64 matrix). 700 scans were acquired continuously over a 35-minute period following an initial 12 seconds of scanning to achieve steady state magnetization. For the duration of the functional scans, patients were asked to keep their heads still and to keep their eyes shut. Standard manufacturer-supplied cushions and plastic ear defenders (JSP, RS Components LTD, Northants, UK) were provided for comfort.

4.2.3 Pre-processing

All fMRI data were analyzed using the SPM (Statistical Parametric Mapping) software package [http://www.fil.ion.ucl.ac.uk/spm/spm2.html]. and Matlab® version 6.5 R13 (The Mathworks Inc.,USA) running on a Dell® PowerEdge 2650 under Red Hat Linux 9. Images were slice-time corrected (Henson et al., 1999), realigned (Friston et al., 1995a), and spatially smoothed using an isotropic Gaussian

kernel of 8mm FWHM. Scan realignment proceeds with an iterative estimation of the six rigid body motion parameters. An appropriate model (the design matrix) was then specified to allow further statistical analysis within the context and framework of the General Linear Model.

* * *

5. Chapter 5: Event-related EEG/fMRI

5.1 Summary

Using continuous EEG/fMRI recording for the first time, we were able to study a veteran patient with partial epilepsy, stereotyped left temporal spikes, and reproducible concordant BOLD activation on previous EEG-triggered fMRI (Lemieux et al., 2001a). Each spike was modeled flexibly using a Fourier set of basis functions and a conventional event-related analysis of the data was performed. Focal activation was once again seen within the left temporal lobe (concordant also with equivalent current dipoles), but in addition, it was possible to estimate the HRF directly. The stage was set for the work that followed.

5.2 Introduction

Electroencephalography (EEG) is the method of choice for the monitoring of certain aspects of the brain's normal activity, such as sleep stages and levels of consciousness, and for the assessment of a number of neurological conditions. EEG is characterized by an excellent temporal resolution but a limited spatial resolution.

Functional magnetic resonance imaging (fMRI) has proven to be a powerful tool for the localization of brain activity on a millimeter scale (Turner et al., 1998). In fMRI, knowledge of the brain's state throughout data acquisition is essential as the method relies on contrasts between images acquired in different brain states. In the standard so-called block design fMRI experiments this is accomplished by imposing a succession of stimulation and rest periods of fixed duration. More recently, the advent of event-related fMRI has allowed the analysis of events with variable or random presentation sequences (Josephs et al., 1997).

In epilepsy, the localization of the generators of interictal epileptiform events (spike or sharp wave) is important for clinical and basic science purposes. Although increasingly sophisticated electrophysiological measurement methods have been developed, e.g. EEG with up to 128 channels, the lack of an independent means of measuring the abnormal brain activity has limited the validation of source localization methods. The recent advent of safe and high-quality EEG recording inside the MRI scanner has given us the tools necessary to compare direct, namely blood-oxygenation level dependent (BOLD) image contrast, and EEG-derived

localization information (Allen PJ et al., 1998;Lemieux et al., 1997). EEG-triggered fMRI, where the fMRI data is acquired at a fixed interval following events of interest (e.g., spikes) and 'rest' periods, has already demonstrated the usefulness of EEG/fMRI in the investigation of epilepsy (Krakow et al., 1999b;Warach et al., 1996). However, it suffers from two main limitations, which are linked to the obliteration of the EEG during the image acquisition: First, the minimum time gap between successive image acquisitions must be of the order of 15 seconds (for 1.5T scanners) in order to avoid T1 effects, while the maximum duration of each image acquisition must be less than the expected duration of the BOLD response in order to ensure proper separation of the responses from events which may occur during image acquisition, and therefore be undetected. Conversely, the event rate must be at least the same as the minimum scanning interval to avoid invisible events but also short enough to allow acquisition of sufficient image data in a 45-minute period*. Second, it relies on an assumption about the hemodynamic response peak time. Given the difficulty of measuring the temporal characteristics of the spike HRF in these circumstances, there is uncertainty about the optimality of this model. Given these limitations, we have found BOLD activations associated with interictal spikes in approximately 50% of the patients studied (Krakow et al., 1999b).

Therefore, the possibility of undistorted EEG throughout the fMRI acquisition through removal of a well-characterized image acquisition artifact (Allen et al., 2000), should enable the identification of all EEG events and the use of a more sophisticated event-related fMRI approach by allowing the acquisition of images at random time-lags in relation to the EEG events of interest (Josephs et al., 1997). This can lead to improved sensitivity and efficiency of EEG/fMRI experiments by acquiring the maximum amount of data per unit time (Dale et al., 1999).

We report on our initial imaging findings from the first experiment with continuous EEG/fMRI and event-related analysis of epileptic events. Specifically, we demonstrate the potential ability of the method to provide spatio-temporal information on the brain activity underlying the generation of spontaneous EEG events.

5.3 Methods

5.3.1 Patient and data

* Patient discomfort and movement can become significant factors after 45-60 minutes.

The study was performed on a 50-year-old patient with chronic encephalitis of the left hemisphere and intractable partial and secondary generalized seizures. The standard 20-channel scalp EEG showed frequent spikes with a maximum over the left temporal region. Previous intraoperative electrocorticography had revealed spiking cortex in the pars opercularis of the left superior temporal gyrus and the adjacent perisylvian region. This patient was studied because previous spike-triggered fMRI studies had revealed consistent BOLD activations ((Krakow et al., 1999b): patient # 1) and 30% of the individual spikes resulted in a significant activation (Krakow et al., 2001c).

5.3.2 Continuous EEG/fMRI

Ten channels of common reference EEG and two ECG channels were recorded inside the MR scanner using a non-ferrous EEG head-box and a digital EEG recording system (sampling rate: 5000 Hz), developed in-house. Gold EEG electrodes fitted with 10 kOhm, 1 Watt current-limiting safety resistors were applied to Fp1, F7, T3, T5, O1 and the contralateral homologous channels; reference: Pz. On-line pulse and imaging artefact removal was used to monitor the EEG during the experiment. The image acquisition artifact method and its validation have been described previously (Allen et al., 2000). In summary, a scanner-supplied slice-acquisition pulse was recorded as a separate channel in the EEG and used to synchronize the calculation and subtraction of a running time-averaged artifact waveform; this is followed by adaptative noise cancellation. The slice pulse is also used to synchronize the EEG and image data acquisitions for the fMRI analysis.
This experiment was conducted on a 2T MRI scanner (Siemens Magnetom Vision; Siemens, Erlangen, Germany). 1200 volumes each consisting of 20 axial slices (1.8mm thick, 1.2mm gap; TE: 40ms; TR/slice: 76ms; FOV: 192mm; 64x64 image matrix) were acquired continuously over a period of 30 min 24 sec.

5.3.3 EEG source analysis

In a separate session, approximately 30 minutes of 64 channel EEG was recorded (reference: AFZ) using the Neuroscan QuickCap (Neuroscan, Sterling, Virginia, USA). Twenty two-second epochs each containing a typical spike were extracted from the recording and averaged. Source analysis was performed for the averaged waveform using the CURRY 3.0 software (Neuroscan). A realistically-shaped

boundary-element conduction model was derived from T1-weigthed volume scans by automatic segmentation (Wagner et al., 1995). The T1-weighted volume data had the following characteristics, devised to obtain high-resolution and full coverage of the head: fast IR-prepared SPGR (TI/TR/TE: 450/17.4/4.2 msec, flip angle: 20°), 280x210mm field of view, 256x192 matrix, 124 1.8 mm slices. A signal-to-noise ratio normalization was performed, followed by a principal components analysis to obtain dominating spatio-temporal field patterns(Fuchs et al., 1999). This allowed us to determine the probable number of generators needed to model the data; a model with three moving dipoles was thus used.

The BOLD echo-planar images were registered to the T1 volume using SPM99 for visualization purposes (Ashburner et al., 1997).

5.3.4 EEG and fMRI analysis

The EEG recording was examined retrospectively to identify spike and sharp wave complexes and record the corresponding fMRI slice number (from the slice pulse channel; range: 1 to 24000*).

The fMRI data were realigned, spatially normalized and smoothed (Gaussian kernel; full width at half-maximum: 6mm) using SPM99 (Ashburner and Friston, 1999;Friston et al., 1995b). The fMRI event slice number was then used as input for an event-related analysis of the time course of BOLD activation using a windowed Fourier expansion (8 sines, 8 cosines, plus constant term; window width = 64 sec) and the resulting SPM{F} was thresholded at $P<0.001$ (uncorrected) (Josephs et al., 1997).

5.4 Results

An asymmetric slow background was observed that was greater on the left. There were frequent interictal epileptiform discharges maximal over the left temporal region. Of these, high amplitude stereotyped sharp waves(>200μV) focal at T3 (left mid-temporal) were the most prominent feature. Thirty-seven of these were identified in the entire recording (mean inter-spike interval was 51 seconds), labeled and used for the fMRI analysis. Figure 5-1 illustrates an EEG segment recorded inside the scanner during fMRI and shows a typical spike and slow wave complex. The thresholded SPM{F} revealed an activation located in the left temporal region

* 24000 = 1200 volumes * 20 slices per volume

similar to the activation previously obtained using the spike-triggered method, as shown in Figure 5-2. The F ratio of the highlighted voxel is 5.23 ($P_{corrected}$ = 0.001). The 64-channel EEG recording showed a pattern of similar abnormal activity. Source analysis using the moving dipoles revealed two dominating generators, one located within and the other near the activation area, as shown in Figure 5-3.

The time course of the activation at the maximum activation voxel (highlighted in Figure 5-2 (b)) peaks at approximately 9 seconds post-spike (Figure 5-4).

Figure 5-1 EEG during fMRI

Ten-second segment of EEG recorded inside the MRI scanner during the fMRI acquisition, with pulse and image acquisition artifact suppression. The ten upper traces show a referential montage, followed by bi-temporal chains, the ECG (used for pulse artifact suppression) and the slice acquisition pulses (used for image acquisition artifact suppression and EEG/fMRI synchronization). There is an asymmetry of the background activity, with irregular slow activity on the left and epileptiform discharges at F7/T3 (indicated by the arrow).

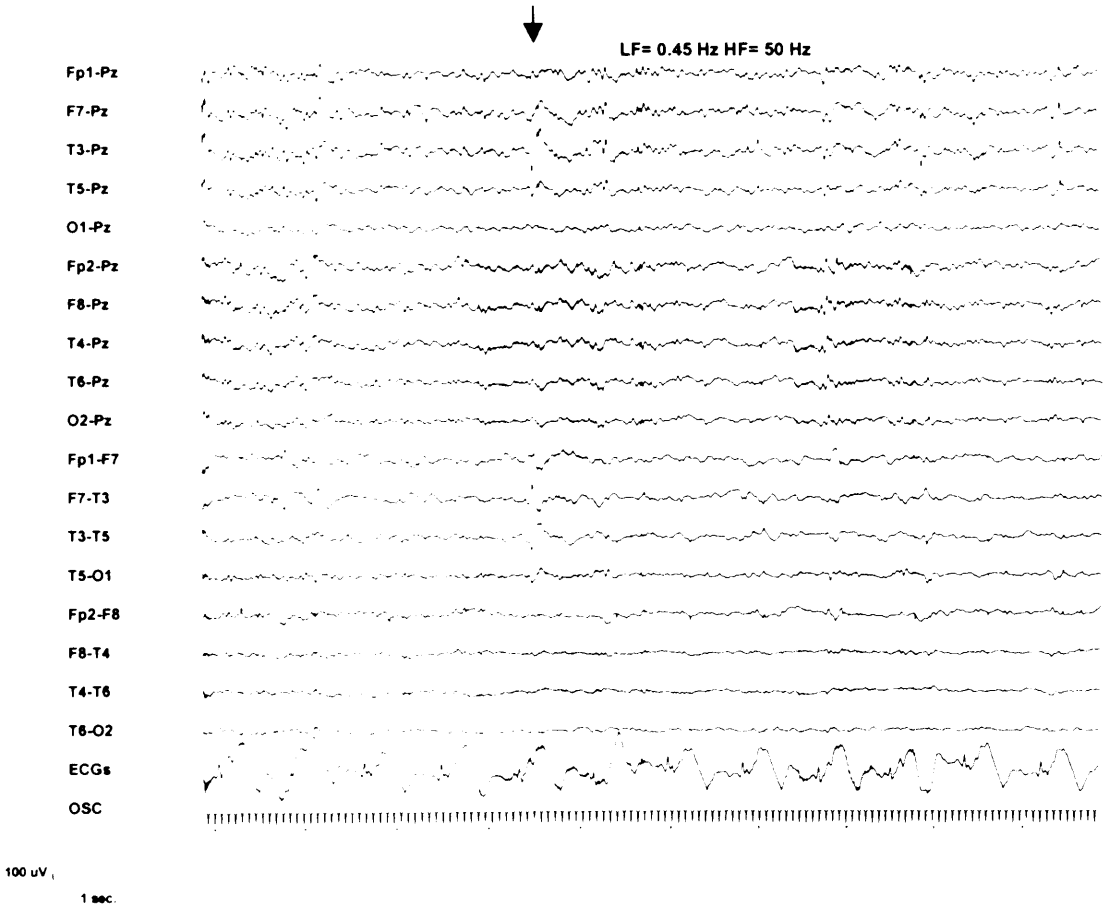

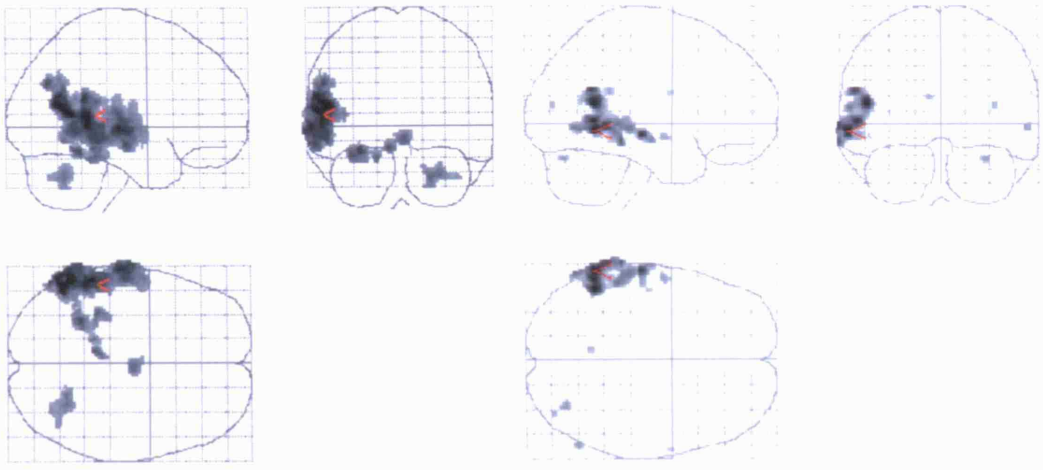

(a) (b)

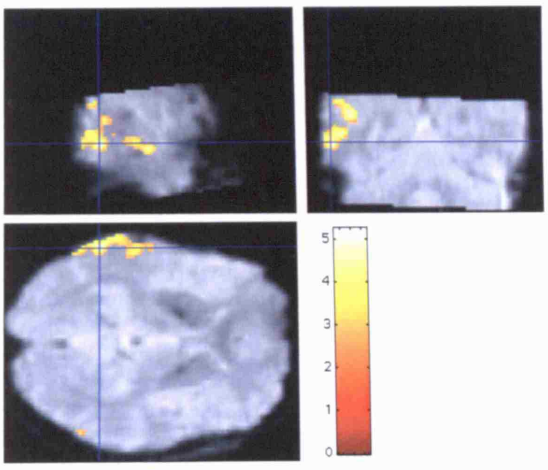

(c)

Figure 5-2 fMRI activation
(a) SPM{T} obtained in previous spike-triggered experiment represented on a graphical representation of the spatially normalized brain (so-called 'glass brain'). In this experiment, 43 spikes and 46 control epochs were sampled. (b) SPM{F} of the spike-related events in the continuous EEG-fMRI experiment. Height threshold: $P<0.001$ (uncorrected). (c) Highlighted cluster projected onto orthogonal slices of the mean EPI, showing activation localization in the left temporal region.

Figure 5-3 Dipoles vs BOLD
Model dipoles (light blue) at peak spike amplitude superimposed on T1-weighted anatomical volume scan (grey level) and co-registered BOLD activation ('hot metal' colours). The proportion of variance of the potential distribution explained by this model was 90%.

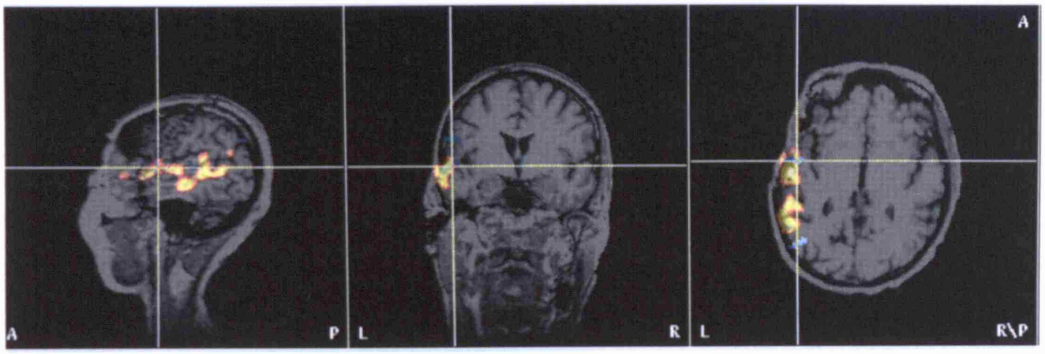

Figure 5-4 Timecourse
Timecourse of BOLD response at highlighted voxel (red arrow) in Figure 5-2b. The response is expressed as a % of the mean whole brain signal.

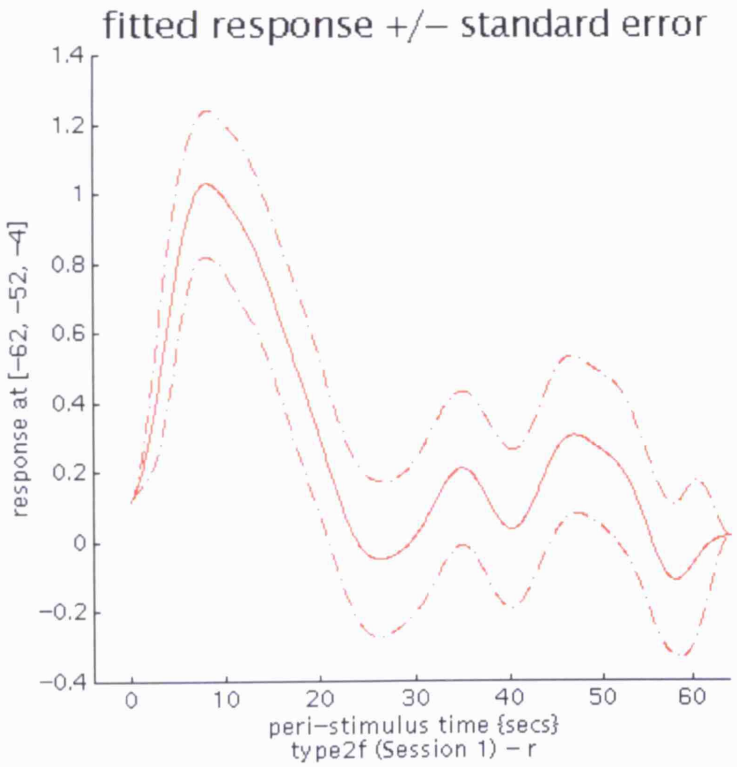

5.5 Discussion

We have demonstrated for the first time an event-related fMRI analysis of EEG events from continuous and simultaneous EEG/fMRI acquisition to obtain spatio-temporal patterns of activation.

The BOLD activation derived from these data was concordant with previous scalp and intracranial EEG findings, as well as results from previous fMRI studies obtained using spike-triggered EEG/fMRI. We have also shown good agreement between source localization and the BOLD results. At present, there is no model for the relationship between BOLD changes associated with spikes, and the underlying electrical generators. Furthermore, as mentioned previously, the validity of generator models for epileptic spikes remains a debated issue. Our approach may provide information useful to address this problem.

The time-course of the BOLD activation was consistent with the characteristic shape of the expected physiological hemodynamic response function (HRF) (Aguirre et al., 1998b). In particular, the observed response is consistent with a peak at 5-9 seconds latency followed by an under-shoot.

The recording of good quality EEG throughout the fMRI experiment, by recording all events, enables us for the first time to exploit the full power of both modalities. Therefore, the applicability of EEG/fMRI will also be enhanced by expanding the spectrum and frequency of events that can be acquired and analyzed.

The availability of continuous EEG and fMRI data will allow the study of the relationship between the BOLD response, spike morphology (amplitude, duration, etc) and the relative timing of EEG events (event interaction effects(Friston et al., 1998b)).

* * *

6. Chapter 6: EEG quality during EEG/fMRI

6.1 Summary

This chapter concerns the evaluation of the quality of interictal epileptiform EEG discharges recorded throughout simultaneous Echo Planar Imaging (EPI). BOLD (Blood Oxygen Level Dependent) functional MRI (fMRI) images were acquired continuously on a patient with intractable epilepsy. EEG was sampled simultaneously, during and after imaging, with removal of pulse and imaging artefacts by subtraction of channel-specific running averages. Contiguous EEG epochs recorded with and without fMRI (fMRI+ve vs fMRI-ve) were next randomized and presented to two blinded observers. Epileptiform discharges were identified retrospectively and comparison was made in terms of the number of identified events, their amplitude and spatio-temporal distribution. A Spectral analysis was also performed on the EEG. In the randomized comparison of EEG segments, 80 (fMRI+ve) vs. 69 (fMRI-ve) discharges were noted amongst both observers with good inter-observer agreement (69%). There were no significant differences in amplitude or spatio-temporal distribution. Comparison of the events detected and measured by two expert observers demonstrates that the IED characteristics are indistinguishable with and without scanning. We review briefly the existing literature on EEG recording quality for combined EEG/fMRI.

6.2 Introduction

Limited EEG monitoring within the MR scanner is possible (Ives et al., 1993;Warach et al., 1996) and has been applied to study a diverse range of EEG phenomena (Salek-Haddadi et al., 2002;Schomer et al., 2000). It is however, limited by three major issues: Patient safety, image quality and EEG quality. Current-limiting resistors and the fibre optic isolation of subjects within the scanner now provide good safety (Lemieux et al., 1997). Likewise the careful selection of conductors and RF-shielded equipment help minimize interference to the images (Bonmassar et al., 2001;Krakow et al., 2000b) so the remaining set of issues centre on EEG quality.

Experience has shown that EEG recorded inside an MR scanner, whether scanning is taking place or not, is degraded significantly unless several precautions are taken. Firstly, through the induction of voltages due to motion of the EEG wires in the

presence of the main (static) magnetic field, and secondly due to the effect of the time-varying magnetic fields (gradients and radio-frequency) acting through circuits formed by the EEG wires during scanning itself. Both these phenomena obey Faraday Induction Law (1831), which states that a change in magnetic flux (the product of the magnetic field and loop area, weighted by their relative angle) through a conducting loop is proportional to a current flowing in the loop. Blood flow in the presence of a strong magnetic field may also give rise to potential differences across blood vessels due to the field's action on the moving ions; the so called Hall effect (1879).

In this chapter, we briefly review the main literature on EEG quality as applied to simultaneous EEG-fMRI experiments, and present some new data of our own together with some imaging findings to illustrate the applicability.

Pulse-related artifact

In their seminal publication on recording of EEG during fMRI, Ives et al. (Ives et al., 1993) identified two types of artefact, cardiac pulse-related (which they labeled 'ballisto-cardiogram' and is often referred to as 'cardioballistogram'), and image acquisition-induced, in the EEG. They attributed their success to the careful arrangement of cabling and the elimination of all sources of RF and ferrous metals. They were able to 'obtain stable and readable EEG' by leaving sufficient gaps between image acquisitions and observed that the pulse-related artefact could be reduced by fixing the electrode wires to the subject's head.

Interleaved EEG and fMRI acquisition (i.e. with gaps in scanning) remained necessary to perform combined EEG-fMRI experiments (Krakow et al., 2001b;Lazeyras et al., 2000a;Warach et al., 1996) until techniques for the reduction of the imaging artifact became available (see below).

Huang-Hellinger et al. (Huang-Hellinger et al., 1995) tested the feasibility of a similar setup on 11 subjects, including 8 sleep studies. They used twisted wires, secured cables, current limiting safety resistors, and RF filters, which now form part of most setups. They noted significant increases in background activity inside the MRI scanner and identified several sources of vibration, but succeeded in recording alpha activity, eye movements, EMG, and sleep staging using an interleaved acquisition. A motion sensor was later described for differentiating pulse artefact and

the switch made to using fibre optics to transmit EEG out of the scanner room (Hill et al., 1995).

Allen et al. (Allen PJ et al., 1998) investigated the spatio-temporal characteristics of the pulse-related artefact and showed that these may be several times the scalp voltages with very sharp morphology making EEG interpretation impossible, particularly at higher field strengths. They observed considerable inter-subject variability in the amplitude and spatial distribution of the artefact with frontal predominance. To remediate the problem, they proposed a fully automated method that exploits the short-term consistency and time-locked nature of this phenomenon, by subtracting channel-specific pulse artefact templates. The templates are obtained by calculating running averages within time frames defined by detection of the QRS complex, from ECG recorded as a separate channel. The method was evaluated by comparing recordings made inside and outside the MRI scanner, and by superimposing separately recorded spikes onto the recordings. Spectral analysis revealed significant reductions in scanner-related EEG amplitude in all bands and significant improvements in spike detection accuracy. The method was implemented online and used in several subsequent EEG/fMRI studies. .

Muri et al. (Muri et al., 1998) made similar observations on the nature of the ECG-correlated artefact in EEG, in the context of visually evoked potentials (VEP), and at the same time the idea of pulse-triggered artefact subtraction was also presented independently by the Munich group (Jager et al., 1998).

The recording of EEG at 3T was first investigated by the Boston group, who proposed a spatial filter to reduce pulse-related artefacts based on signal and noise estimates derived from VEP's recorded outside the scanner (Bonmassar et al., 1999). Notably, this method does not require ECG recording and can account for motion but relies on the assumption of stationary noise (e.g. from outside to inside the scanner) and its applicability to spontaneous activity is questionable. Using a motion sensor the same group also developed a method based on adaptive ballistocardiogram and motion noise cancellation that can be implemented in real-time (Bonmassar et al., 2002). Spectral analysis showed good recovery of simulated alpha activity and visual comparison of EP's and field maps obtained outside and inside scanner showed good agreement following application of the filter. A cursory qualitative validation was also performed for epilepsy by adding a small number of simulated spikes for visual assessment.

Benar et al (Benar et al., 2003b) have recently explored pulse artefact reduction methods based on spatial filtering with principal (PCA) and independent components analysis (ICA) combined with visual selection of pulse-related components. In comparisons of data recorded in 10 patients with epilepsy, both methods resulted in reductions in pulse artefact amplitude of the order of 75% while preserving spike amplitude. However, no comparison was made with default averaging-subtraction methods.

Image acquisition artefact

Historically, scanning-induced (or 'imaging') artefacts in electrophysiological signals were first tackled for recording ECG. The problem was revisited by Felblinger et al. who proposed a method based on measuring the gradient induced impulse response for each of the three gradients and convolution with the digitized imaging gradient waveforms (Felblinger et al., 1999). Visually appealing results were obtained for ECG (and relatively small gradient slew rates) but the technique's applicability to EEG is uncertain.

A method based on the estimation and subtraction of average artefact power spectra was proposed and evaluated in rats (Felblinger et al., 1999;Sijbers et al., 1999). Quantitative evaluation from simulation (superposition of separately recorded artefacts over fMRI-free data) showed good results, although weak gradients and EEG loop dimensions considerations raise questions about the method's usefulness in humans.

Allen et al. proposed an imaging artefact reduction method conceptually similar to that of pulse-artefact removal (Allen et al., 2000). Using a timing signal generated by the scanner, running averages of the slice acquisition artefact are calculated for each channel and subtracted for each epoch, defined by the inter-slice scanning interval, followed by adaptive noise cancellation. The system requires at least 5 kHz sampling and exceptional dynamic range to capture the artefact accurately. Evaluation was performed on recordings in five subjects. Artefact amplitude was reduced from 9 mV to 8 μV. Frequency band power increases between fMRI-free and fMRI scanning with artefact reduction were in the range 10-18%, and spike detection (using simulated spikes) was drastically improved. The method was implemented in real time and allowed continuous and simultaneous EEG-fMRI (Lemieux et al., 2001b;Salek-Haddadi et al., 2002;Salek-Haddadi et al., 2003f).

Goldman et al. (Goldman et al., 2000), working at 3T, demonstrated a system based on dual-lead electrode bipolar chains and EEG 'blanking' during scanning to reduce the effect of the imaging-induced artefact. A method similar to Allen et al (Allen PJ et al., 1998) was used for pulse artefact subtraction and experiments in a phantom and a single subject showed significant pulse and imaging artefact reductions due to wire twisting and evidence of alpha power following processing (see (Goldman et al., 2002) for an example of the technique's application).

A radically different approach to imaging artefact reduction was proposed by Hoffmann et al. (Hoffmann et al., 2000) for the purpose of spike detection. Based on band-stop filtering in the time domain and spectral editing, spectra acquired prior to scanning are used to compare and identify artefact-specific frequencies in contaminated EEG. The values of these frequencies in the Fourier domain are set to zero and inverse Fourier transformed to get the corrected EEG. Visual evaluation was deemed satisfactory for detecting epileptiform spikes only, and the technique was not recommended for studying rhythmic activity.

An elegant and somewhat minimalist version of the running average subtraction method was proposed by Cohen et al. (Cohen et al., 2001) that relies on scanning-triggered EEG digitization. One should also note the work of Logothetis et al on simultaneous intra-cerebral recordings in monkeys during fMRI (4.7T) in which gradient-switching artefacts were reduced by performing PCA and eliminating gradient-correlated components, followed by signal reconstruction (Logothetis et al., 2001).

So far, artefact reduction assessment has been mostly based on simulations (e.g. added spikes) and spectral analysis. In this work we evaluate the effectiveness of the subtraction-based methods (Allen PJ et al., 1998;Allen et al., 2000) based on two experts' quantitative appraisal with emphasis on characterization of the temporal and amplitude distributions of the spikes.

6.3 Methods

A 48-year-old lady with intractable right-sided partial motor seizures, with secondary generalizations, was studied. She has biopsy confirmed left temporal lobe encephalitis and EEG was very abnormal, showing frequent large spike, sharp, and slow wave complexes centered over the F7 & T3 electrodes on a background of widespread polymorphic theta activity on the left. Electrocorticography had

previously demonstrated spiking cortex within the pars opercularis of the superior temporal gyrus and the adjacent perisylvian regions and this was concordant with previous spike-triggered fMRI findings (Krakow et al., 1999b) Patient #1.

EEG Acquisition

This was done as per Chapter 4. EEG was recorded continuously throughout imaging, and afterwards, to include an imaging-artefact free segment with pulse-artefact subtraction alone for comparison.

EEG Analysis

Thirty contiguous ten-second EEG epochs recorded with fMRI (fMRI+ve) and another 30 epochs recorded without (fMRI-ve), were randomized from the adjacent EEG segments. These 60 epochs were then examined by two blinded board-certified electroencephalographers in both referential (to Pz) and bipolar montages, on paper. An example is shown in Figure 6-1 (without OSC channel). Percentage inter-observer agreement was measured by the Jaccard coefficient of numerical taxonomy (Dunn and Everitt, 1982) as:

$$100 \times \frac{\text{Number of events indicated by both}}{\text{Number of events indicated by either or both}}.$$

Figure 6-1 EEG recorded during the experiment
Two bi-temporal chains are shown, referenced to Pz in the top ten channels, followed by a bipolar montage in the next eight. ECG and slice timing signals (OSC) are shown at the bottom. Segment A demonstrates obscuring of the EEG by image artefact during scanning, at the start of an experiment. Pulse and image artefact are removed at point E. Segment B is a ten second recording during scanning; an asymmetric slow background dominated by polymorphic theta activity is seen from which a focal spike wave complex arises at point F. Segment C contains the seamless transition point G from both pulse and image artefact to pulse artefact removal alone once acquisition is complete, leaving the EEG unaffected. Segment D is EEG recorded outside the scanner, pathologically as per B but for lack of flow artefact (large T waves) in the ECG. A discharge similar to F is marked at H.

Figure 6-1

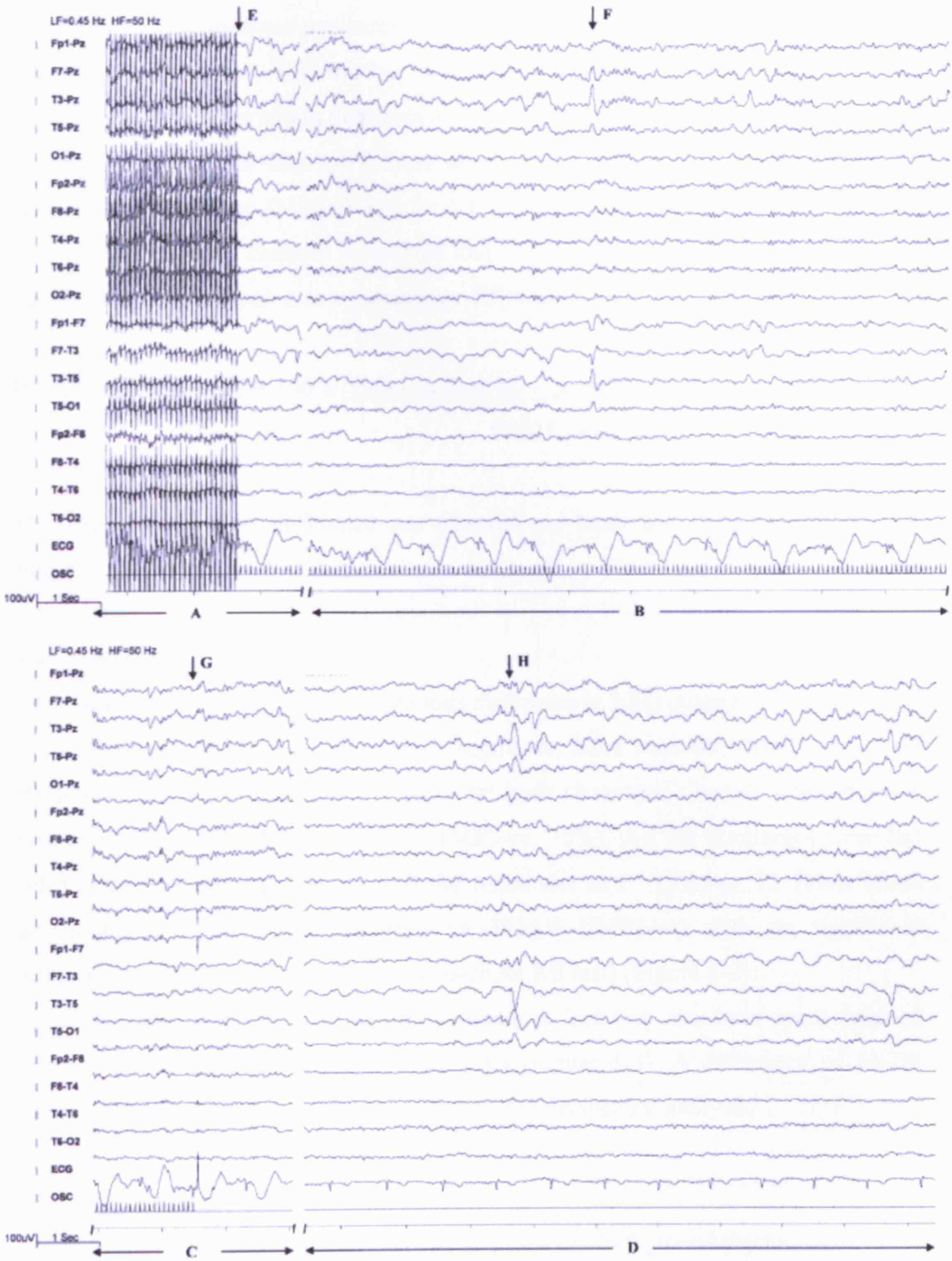
LF=0.45 Hz HF=50 Hz
E
F
Fp1-Pz
F7-Pz
T3-Pz
T5-Pz
O1-Pz
Fp2-Pz
F8-Pz
T4-Pz
T6-Pz
O2-Pz
Fp1-F7
F7-T3
T3-T5
T5-O1
Fp2-F8
F8-T4
T4-T6
T6-O2
ECG
OSC
100uV
1 Sec
A
B
LF=0.45 Hz HF=50 Hz
G
H
Fp1-Pz
F7-Pz
T3-Pz
T5-Pz
O1-Pz
Fp2-Pz
F8-Pz
T4-Pz
T6-Pz
O2-Pz
Fp1-F7
F7-T3
T3-T5
T5-O1
Fp2-F8
F8-T4
T4-T6
T6-O2
ECG
OSC
100uV
1 Sec
C
D

The numbers of discharges were next compared alongside the peak-to-peak amplitudes as measured on paper, the spatial locations judged by phase reversal and the temporal distributions measured through the inter-event intervals. Two-sample Kolmogorov-Smirnov (KS) testing was used where applicable, to check for significant differences within distributions.

Spectral analysis was also performed using in house software on 40 randomly selected fMRI+ve and fMRI-ve epochs (20 x 2.56 sec of each). The mean activity was derived for each channel in each of four frequency bands (0.8-4, 4-8, 8-12, and 12-24 Hz) and represented as a percentage difference:

$$\text{Percentage difference} = 100 \times \frac{\text{(fMRI-ve activity – corrected fMRI+ve activity)}}{\text{FMRI-ve activity}}$$

The mean percentage difference per channel per band was then expressed as a summary statistic.

6.4 Results

There was no visible distortion or obvious difference in EEG quality on inspection.

In the randomized comparison of EEG segments, there were 80 (fMRI+ve) vs. 69 (fMRI-ve) focal discharges noted amongst both observers. Overall inter-observer agreement was 69% (fMRI+ve: 63%, fMRI-ve: 75%). All the discharges were left sided with 96% maximal at T3 and the remainder at F7 (3%) or T5 (1%). Mean amplitudes were 365μV (fMRI+ve) vs 385μV (fMRI-ve) with no significant difference in distribution ($P<0.309$, two-sample KS test) (Figure 6-2).

Likewise there were no significant differences between the inter-event interval distributions ($P<0.617$, two-sample KS test) (Figure 6-3). A difference of 13.7% mean power per band per EEG channel was seen on spectral analysis.

6.5 Discussion

Spike detection is a probabilistic process in which the background rhythm plays an influential role (Wilson et al., 1996). This reflects well in the reported degrees of inter-observer (and intra-observer) agreement (Dumpelmann and Elger, 1999;Wilson et al., 1996) to which our findings are similar. Also, there is no absolute measure of

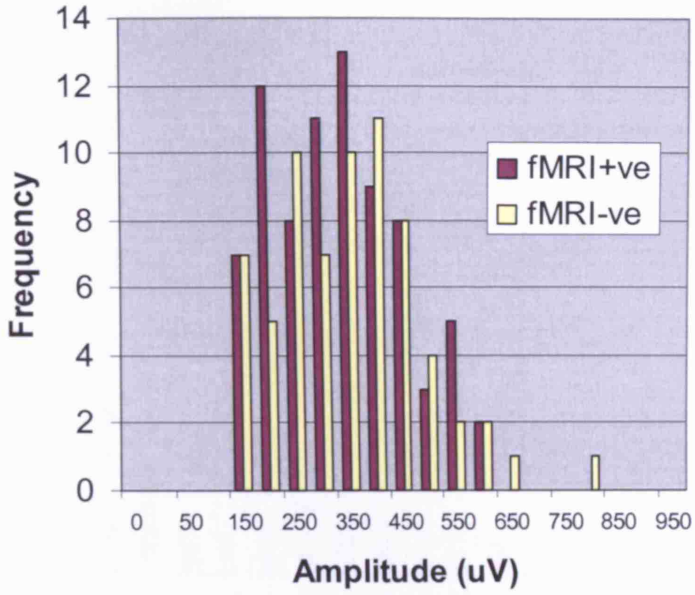

Figure 6-2 Amplitude distributions

the true number of underlying epileptiform events, regardless of EEG appearance so measures of reliability need be based on mutual agreement. Automated spike detection was not an option with short segments of abnormal EEG due to low specificity (Dumpelmann and Elger, 1998). The patient's EEG also lacked a well-defined background rhythm that might have further helped with comparison.

The inter-event intervals are of interest in that they would be expected to follow a negative exponential distribution if the events were memory-less (see figure 2a). It may therefore be argued that any significant differences in the interval distributions between the two samples could imply distortion of the EEG with scanning but this proved not to be an issue.

The interpretation of EEG power spectra is perhaps the most difficult. There is significant potential for distortion through artefacts and interpretation is further limited by intrinsic temporo-spatial autocorrelations within the time series. The approach opted for was therefore to avoid unwarranted multivariate statistics in favor of excluding a major difference and so a random sampling approach was taken in preference to selecting noise-free intervals. Comparison was also avoided with EEG recorded outside the scanner room where differences in recording system, wakefulness and lack of pulse artefact could not have been controlled for.

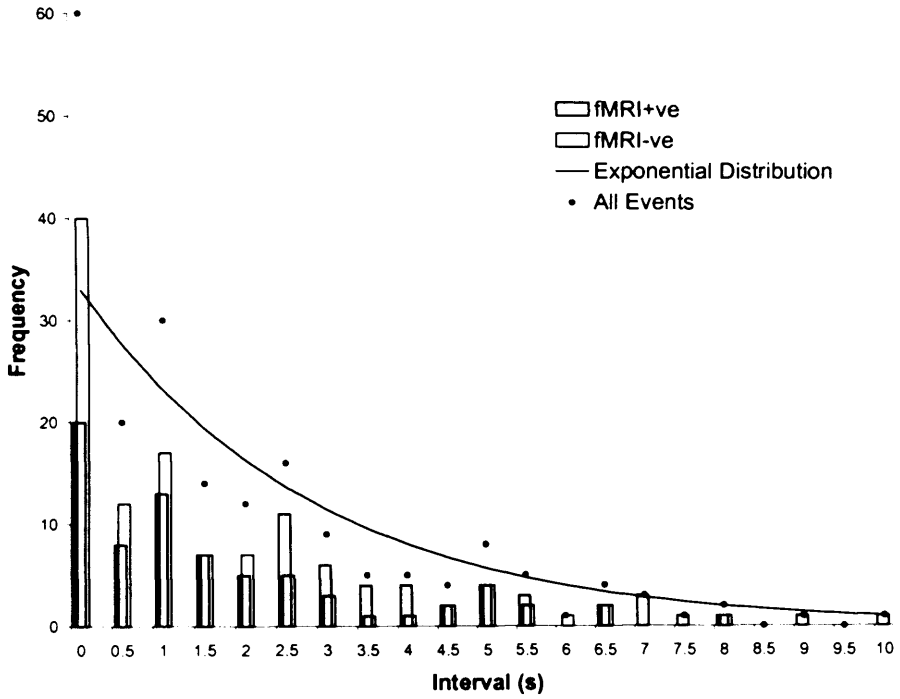

Figure 6-3 Inter-event interval distributions
The inter-event interval distributions of 80 and 69 events recorded with and without fMRI respectively. No significant difference was evident ($P<0.617$, two-sample KS test). The cumulative distributions of all events are also shown as dots alongside a negative exponential distribution of the form:

$$y = \frac{1}{\theta} e^{-x/\theta}$$

where θ is the mean inter-event interval (2.84 sec)

This distribution would be expected of randomly occurring events.

EEG quality was further supported indirectly, through event-related analysis of the functional data whereby concordant spike-related activations were seen in keeping with previous spike-triggered findings (Chapter 4).

In a recent paper, Benar et al. presented the first comprehensive study of EEG quality issues (Benar et al., 2003a). At the data acquisition level, they considered various wire immobilization schemes using sandbags, advocated wires extending from the top of the head to the back of the scanner, bandaging, and the use of vacuum cushions to further restrain the head. Using this setup, they found pulse artefact subtraction not always necessary to identify spikes. In our experience however, pulse artefact removal has proven sufficiently robust to obviate the need for such drastic measures.

The authors compared two imaging artefact reduction techniques: Hoffmann's Fourier transform method (Hoffmann et al., 2000) and a method related to Allen's subtraction technique (sampling at 1 kHz versus 5 kHz, and a different averaging mechanism). A single observer compared spikes recorded outside and inside the scanner, with imaging artefact removal by each of the two techniques. The Fourier method was noted to leave artefacts at frame boundaries such that they were unable to reproduce the quality of Hoffmann's results. For the same reason, 'blinding' of the observer may not have been possible, but the subtraction method was found to perform better than the Fourier filter in every case.

In conclusion, we provide further evidence that good quality EEG can be recorded continuously during imaging, enabling the identification of epileptiform events with good certainty. The data presented here focused on certain EEG characteristics, namely temporal and amplitude distribution, and inter-observer reliability that have been neglected, up to now, in the evaluation of intra-MRI EEG quality. The development of new artefact removal techniques is unlikely to cease, as interest in the technique's application gathers, new MR scanners are developed, and demands on EEG quality increase.

* * *

7. Chapter 7: Ictal EEG/fMRI

7.1 Summary

The ability to continuously acquire simultaneous EEG and fMRI data during seizures presents a formidable challenge both clinically and technically. Published ictal fMRI reports have so far been unable to benefit from simultaneous electrographic recordings and remain largely assumptive. Unique findings from a Continuous EEG-correlated fMRI experiment are presented in which a focal subclinical seizure was captured in its entirety. For the first time dynamic and biphasic Blood Oxygen Level Dependent (BOLD) signal changes are shown using statistical parametric mapping time-locked to the ictal EEG activity localizing seizure generation and propagation sites, with millimeter resolution, to electroclinically concordant grey matter structures. Though presently of limited clinical applicability, a new avenue is opened for further research.

7.2 Introduction

Intravoxel fluctuations in deoxyhaemoglobin influence the focal short-term changes in magnetic susceptibility to which Blood Oxygen Level Dependent (BOLD) fMRI is sensitive and these fluctuations appear to result from a complex interplay between blood flow, blood volume and oxygen metabolism as orchestrated by the neurovascular coupling (Buxton et al., 1998).There is a growing literature on EEG-correlated fMRI (Schomer et al., 2000) employing an interleaved method of data acquisition due to various technical limitations. EEG-triggered fMRI hence allows for the BOLD response to EEG events to be intermittently sampled at a number of discrete time points in order to detect areas of relative activation (Krakow et al., 2000a). In patients with partial epilepsy, spike-triggered fMRI has yielded promising results broadly consistent with electroclinical data (Krakow et al., 1998;Lazeyras et al., 2000a;Warach et al., 1996) but more recently we have been able to apply a technique to acquire good quality EEG/fMRI data continuously and simultaneously (Allen et al., 2000) to reveal the temporal characteristics of haemodynamic response to interictal events (chapter 5) (Lemieux et al., 2001b) and the potential exists to

investigate the extent and further characteristics of such changes in relation to different pathologies. Within this context, fMRI activations are felt to anatomically reflect areas involved in spike generation and propagation, the 'irritative zone'(Luders et al., 1993), the anatomical definition of which is an important part of the multidisciplinary presurgical evaluation of patients with medically refractory partial epilepsy.

By contrast ictal fMRI activation would be expected to reflect changes within the epileptogenic region itself (and propagation sites) but there have been no EEG-correlated ictal fMRI studies and otherwise few anecdotal reports of ictal fMRI, all in patients with an abnormal structural MRI and none employing statistical hypothesis testing. An outline of this literature is provided in Table 7-1 and reviewed below.

Jackson *et al* (Jackson et al., 1994) used a FLASH sequence to obtain susceptibility-weighted images from a 4 year old child experiencing partial motor seizures. Images were obtained every eight seconds from a single slice only. No motion correction was applied and analysis was by way of visual inspection only. Signal increases of up to 40% were depicted occurring over 4-5 minutes in positive areas, though not exclusively in association with clinically observable seizure activity.

Table 7-1 Summary of published ictal fMRI time series

Reference	Clinical data	Seizure detection	Functional MRI	Simultaneous EEG	Motion correction	Statistical Analysis
Jackson et al (1994)	4yr old male; right-sided partial motor seizures of body and face. **Diagnosis**: Rasmussen's encephalitis **MRI:** Thickened cortex with abnormal signal in left hemisphere grey matter. **Routine EEG** Interictal: Widespread slow and occasional L parietal spikes. Ictal: Irregular slow waves over anterior frontotemporal regions Preceding twitching by 8-20 seconds. **Sedation:** IV Diazepam	Facial movement	**Scanner :** 1.5T Siemens SP4000 **Sequence** Multishot FLASH (TE/TR 60/85ms, Matrix 64x128, FOV 230mm, flip angle 40) **Coverage:** Single 8mm slice **Time resolution**: 8 seconds	None	None	None. Visual inspection of subtraction images and time courses extracted from subsequently selected areas. Concordant activations with up to 40% signal increases reported.
Detre et al (1995 & 1996)	25yr old male; right-sided partial motor seizures of face. **Diagnosis**: Chronic gliosis **MRI:** Widespread left hemisphere atrophy **Routine EEG** Interictal: Increased theta during wakefulness. Ictal: No definite ictal findings **Sedation:** Phenytoin and Phenobarbitone with significant sedation.	None	**Scanner** 1.5T GE signa **Sequence** Single shot GE-EPI (TE/TR 50/4000 ms, 64x64 matrix, FOV 240mm.16x5mm slices no gap). **Coverage:** Whole brain **Time resolution:** 4 seconds	None	Yes	None Visual inspection of thresholded percentage change images and time courses extracted from selected cluster. Concordant areas with 3-4% signal increases reported
Krings et al (2000)	62yr old female; left-sided Jacksonian marches involving leg. **Diagnosis:** Glioblastoma multiforme **MRI** Right central space occupying lesion **Routine EEG** Ictal and interictal EEG normal. **Sedation:** Primidone 625mg daily.	Leg movement	**Scanner** 1.5T Phillips Gyroscan **Sequence** Multishot GE-EPI (TE/TR 35/2200ms, Voxel size 3x3x5mm flip angle 35) **Coverage:** Whole brain **Time resolution:** 2.2 seconds	None	Yes	None Visual inspection of thresholded percentage change images and time courses from interesting clusters. Concordant regions with either positive or negative signal changes of 3-4%.

Changes unaccompanied by observable seizure activity were attributed to sub-clinical seizure activity and other similar changes (delayed by 1.5 minutes) within the sagittal sinus and surrounding veins were attributed to venous drainage. Positive areas identified on subtraction images, appeared concordant with other investigations and it was concluded that 'functional MRI enables the time course, spatial distribution and spread of ictal activation to be observed during the seizure'.

Detre *et al* (Detre et al., 1995;Detre et al., 1996) described a patient with a history of partial motor seizures but with neither clinical nor electrographic evidence of seizure activity during fMRI. They nonetheless identified an area of signal change, concordant with ictal SPECT and intracranial EEG localizations of an epileptogenic focus, exhibiting a 3-4% signal increase and return to baseline over 100 seconds. These were assumed to represent subclinical seizure activity based mainly on temporal homology and spatial concordance but the degree of 'surprise' (Cover and Thomas, 1991) was not characterized statistically.

Krings *et al* (Krings et al., 2000) performed fMRI on a patient during a 33 second Jacksonian march involving the left leg with 'calf shaking'. They described three peri-lesional (glioma) regions of interest based on the visual inspection of subtraction images. These three areas each appeared to show variable (bi-directional) signal changes of +2.2%, -3.5% and +3.1% beginning 65 seconds, 30 seconds and 0 seconds prior to seizure onset, respectively. Initial changes were attributed to subclinical seizure activity and negative changes to a 'mismatch between oxygen consumption and delivery'. It was concluded that 'functional MRI allows for demonstrating seizure evolution and spread'.

Ictal fMRI is not routinely feasible for a number of reasons. BOLD-fMRI is not sensitive to detecting low frequency state-related changes due to large intersessional effects and scanner noise characteristics. Together with the sluggish haemodynamic response function (HRF), this limits detection power to the narrow frequency band within which most conventional fMRI paradigms operate and in the current context will tend to necessitate capturing both seizure onset and termination. Seizures however are generally short lasting, unpredictable and it may not be practical to keep patients in the scanner for long enough even where subclinical seizures are known to be occurring frequently, given the risks of seizure evolution and generalization within the scanner environment. Most ictal EEG phenomena are in addition associated with impairment of consciousness usually to a degree that the required

level of cooperation for an MRI scan cannot be achieved even where consent may have been obtained in advance. Any significant degree of head and body motion is also likely to render the imaging [and EEG] data uninterpretable and EEG-correlated studies, where appropriate facilities exist, are complicated further by the extra time involved in attaching electrodes, patient positioning and equipment set-up.

Despite these drawbacks however, EEG-correlated Ictal fMRI does offer the necessary spatiotemporal resolution theoretically required to study seizure generation and propagation in vivo and knowledge of ictal BOLD changes may contribute clinically both to seizure localization at an individual level and to an understanding of the generators of ictal EEG changes routinely recorded in other patients for example during video-EEG telemetry. There is also potential for scientific insights into the complex accompanying blood flow and metabolic changes to which this signal is sensitive (Buxton et al., 1998). We present here the first successful attempt at continuous and simultaneous EEG-correlated whole-head fMRI at short TR in a patient who fortuitously experienced an unequivocal subclinical electrographic seizure. Statistical parametric mapping (Friston et al., 1995b) was used to characterize the fMRI data, make systematic inferences and help protect against bias, type 1 error and motion related artefact.

7.3 Methods

Case Report

A 47-year-old right-handed gentleman with a 2-year history of intractable generalized tonic-clonic seizures underwent an EEG-correlated fMRI study. He also experienced frequent simple partial seizures characterized by cessation of activity and sitting still but without falls and did not report any auras. His past medical history was unremarkable and the aetiology of the epilepsy unknown. Structural MRI was normal* but interictal EEGs had consistently revealed focal left anterior temporal spikes, more pronounced in sleep. Neurological examination was unremarkable but the patient complained of poor memory and occasional word finding difficulties. Treatment was with Lamotrigine 400mg daily, and Gabapentin 1200mg daily. Written informed consent was obtained in accordance with local ethics committee

* Epilepsy protocol structural imaging included T1-weighted Coronal 3D IR-Prepared Spoiled GRASS, T2-weighted conventional dual spin echo and Fluid Attenuated Inversion Recovery sequences (Liu et al., 2001a).

approval with an initial study aim of establishing a spike-related activation through interictal EEG/fMRI.

Data Acquisition

Imaging was performed on a GE Horizon Echospeed 1.5 Tesla Scanner using a continuous BOLD-fMRI sequence (TE/TR 40/3000, 21x5mm interleaved slices, FOV=24 x 24cm, 64x64 matrix). 700 such scans were acquired over a 35-minute period. 11-channels of referential scalp EEG were recorded simultaneously with online and offline pulse (Allen PJ et al., 1998) and imaging (Allen et al., 2000) artefact subtraction using MR-compatible equipment.

Processing and Analysis

The SPM99 package [http://www.fil.ion.ucl.ac.uk/spm99] was used for all image pre-processing and voxel-based statistical analysis, within the context of the general linear model. A slice-timing correction (Henson et al., 1999) was performed prior to realignment (Friston et al., 1995a) to correct for the staggered order of slice acquisition. Spatial smoothing followed with an isotropic Gaussian kernel of 12mm FWHM to both boost signal* and conformity with the assumptions underlying Gaussian random field theory (see below) . The seizure event was initially modeled flexibly with a windowed Fourier set of basis functions (8 sines and 8 cosines) spanning 45 seconds (Josephs et al., 1997) making no assumptions about the shape of an underlying response, only that this period will likely explain a critical proportion of the overall variance encountered within the voxels being searched for. The six rigid-body motion correction parameters were included as confounding covariates within the design matrix (Friston et al., 1996) to regress out any possible motion-correlated signal change, regardless of the seizure. Both data and design matrix were high-pass filtered at 1/200 seconds cut-off, dictated by the noise characteristics of the scanner and the subsequent need to limit inferences to frequencies that may be reliably inferred about with fMRI. An AR(1) model was used to estimate the intrinsic autocorrelation structure of the data (Friston et al., 2000b) and derive the effective degrees of freedom. An F-contrast was specified to test for the additional variance explained by the subspace of the model embodying the 'effects of interest' (i.e. the

* The matched filter theorem states that optimal resolution of signal from noise will be achieved by matching the filter to the signal. The assumption here is that plausible seizure-related BOLD activations are unlikely to involve fewer than three neighbouring voxels (Cooper et al., 1965).

seizure) and the computed SPM{F} thresholded at P<0.05 using a correction for multiple comparisons based on Gaussian random field theory (Friston et al., 1991).

A second step was performed to ascertain the spatial extent specifically of the dominant temporal pattern. A volume of interest (VOI) was therefore defined by the entirety of the cluster containing the maximum of the SPM{F} and a time series accounting for the most variance (i.e. the first eigenvariate), filtered and adjusted for the above contrast, was extracted from this VOI. The seizure related signal change was well approximated by a sine wave cycle of 102 seconds, used for simplicity to model the seizure next as a single regressor (alongside the motion parameters). A T-contrast was specified as a unidirectional test of significance for the parameter estimate pertaining to this individual regressor, as orthogonalised with respect to all other covariates. The computed SPM{T} was thresholded as above. No cluster thresholds were applied and the result overlaid onto a high-resolution T1-weighted anatomical scan (Coronal 3D IR-Prepared Spoiled GRASS, TR/TE/TI 17/4.2/450, 124x1.5mm slices, FOV 240x180mm, matrix 256x192) for orientation. Co-registration was to the mean EPI image, using mutual information (Maes et al., 1997); part of the SPM99 package.

7.4 Results

The patient was visually observed and monitored throughout the experiment with good quality simultaneous and continuously acquired EEG (& ECG). Shortly into the experiment focal rhythmic delta activity was seen to emerge abruptly and unilaterally maximum over the F7/T3 electrodes (see). This activity was sustained for the next 15 seconds prior to evolving into a localized (F7/T3) 5Hz theta rhythm and decaying slowly over the next 26 seconds to constitute an electrographic seizure. Brief motion artefact was evident in the EEG five seconds into the seizure but there were no visible clinical accompaniments or subsequently reported symptoms. The rigid body motion correction parameters are given in Figure 7-3(b,c) for the entire session.

The SPM{F}, obtained from the initial analysis step, reveals a principal cluster of 917 voxels as displaying significant amounts of time-locked variance (Figure 7-2), the dominant temporal nature of which was captured by the first eigenvariate shown in figure 3a. The SPM{T} obtained from the next step (Figure 7-2), is in excellent agreement with the SPM{F} and further reveals those particular voxels to share the

same pattern and direction of signal change (described by the sine wave). Figure 7-3a, illustrates the rise in signal (approx. 2.5% mean) peaking at around six seconds into the seizure followed later by a prolonged undershoot. The greatest signal rise (approx 5.5%) is also shown.

The anatomy of the seizure related activation is clear from Figure 7-4. The principal cluster extends posteroinferiorly from the left insular grey matter, through the temporal lobe insula, along the superior and middle temporal gyri to the left fusiform gyrus; anteriorly to the left inferior frontal gyrus; and superiorly up to the left inferior parietal lobule. A smaller cluster (18 voxels) is also evident within the grey matter of the ipsilateral cingulate gyrus. The statistical maximum ($P<1x10^{-13}$) overlies the left inferior parietal lobule but the maximum of the parameter estimate (beta) images, representing signal as opposed to signal: noise, falls within the anterior segment of the middle temporal gyrus.

Figure 7-1 EEG recorded during the experiment.
Two bi-temporal chains are shown, referenced to Pz in the top ten channels, followed by a bipolar montage in the next eight. ECG and slice timing signals (OSC) are shown at the bottom. fMRI was carried out continuously throughout the recording as indicated by the timing signals. Pulse and imaging artifact were subtracted online. Focal seizure activity begins at point A. Brief movement artifact is evident at point B.

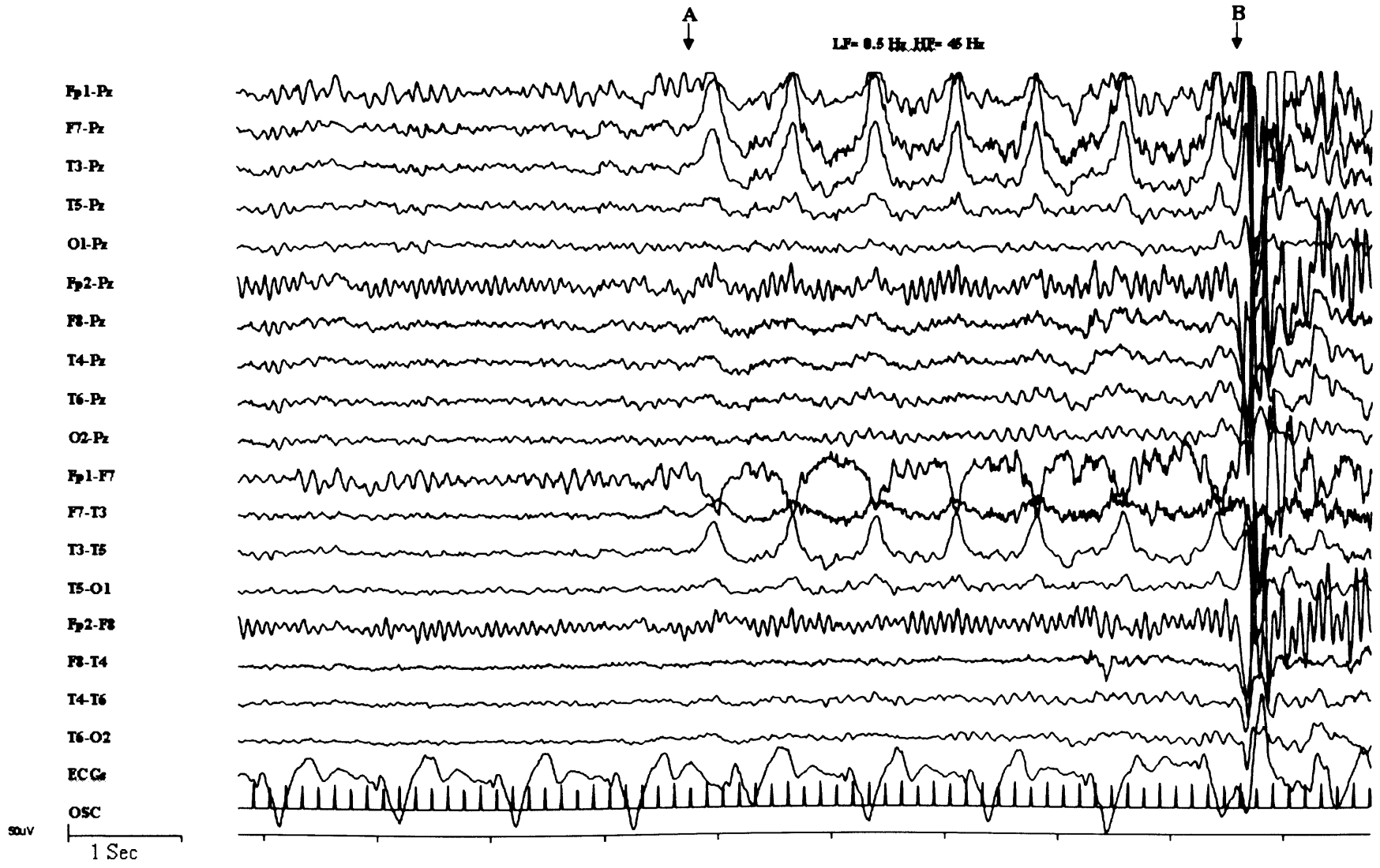
A
B
LF= 0.5 Hz HF= 45 Hz
Fp1-Pz
F7-Pz
T3-Pz
T5-Pz
O1-Pz
Fp2-Pz
F8-Pz
T4-Pz
T6-Pz
O2-Pz
Fp1-F7
F7-T3
T3-T5
T5-O1
Fp2-F8
F8-T4
T4-T6
T6-O2
ECG
OSC
50uV
1 Sec

Figure 7-1

a) b)

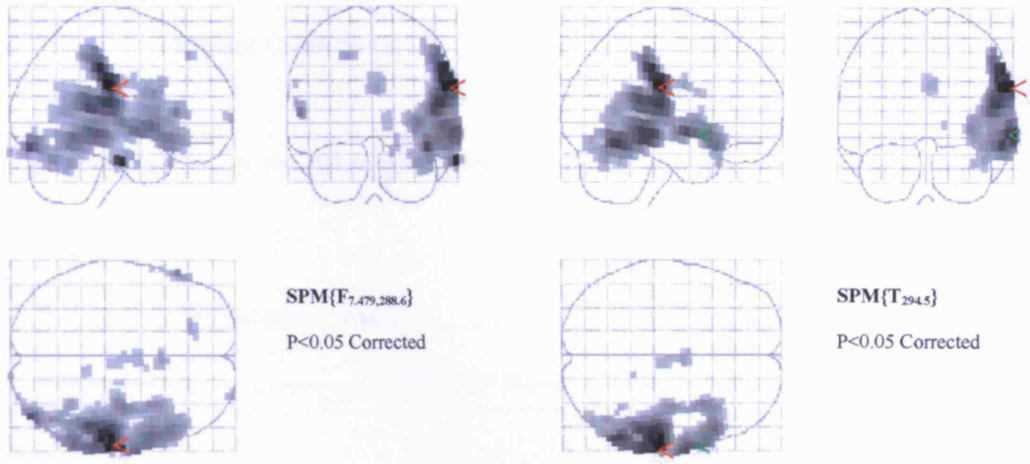

Figure 7-2 SPM
Figure 7-2 - SPM{F} These results were obtained using a Fourier set of basis functions spanning the seizure event. Realignment parameters were included as confounds. The statistical maximum is shown in red. Figure 7-2 – SPM{T} These results were obtained using a single sine wave regressor spanning the seizure (see text). Realignment parameters were included as confounds. The statistical maximum is shown in red but the maximum parameter estimate for the regressor of interest (the beta image maximum) is shown in green.

7.5 Discussion

The physiological impact of seizure activity on cerebral blood flow has been appreciated for some time (Gibbs et al., 1934;Penfield et al., 1939), indeed ictal SPECT has proved a useful technique for the clinical localization of epileptogenic areas as a consequence (Cascino, 2001;Duncan, 1997b). In brief, ictal SPECT studies using ^{99m}Tc-HMPAO (technetium 99m hexamethylene propylene amine oxime) demonstrate sustained hyperperfusion within seizure foci surrounded by a rim of hypoperfusion, followed later by a return through baseline to a period of sustained hypoperfusion (Duncan, 1997b). A transition from increased regional cerebral blood flow (rCBF) to decreased rCBF is suggested to take place at around 90 seconds after seizure onset, independently of offset (Avery et al., 1999;Avery et al., 2000), but return to baseline may occur more rapidly for shorter durations of seizure activity (Zubal et al., 1999). Such findings are in good keeping with the general time course of the BOLD changes demonstrated here.

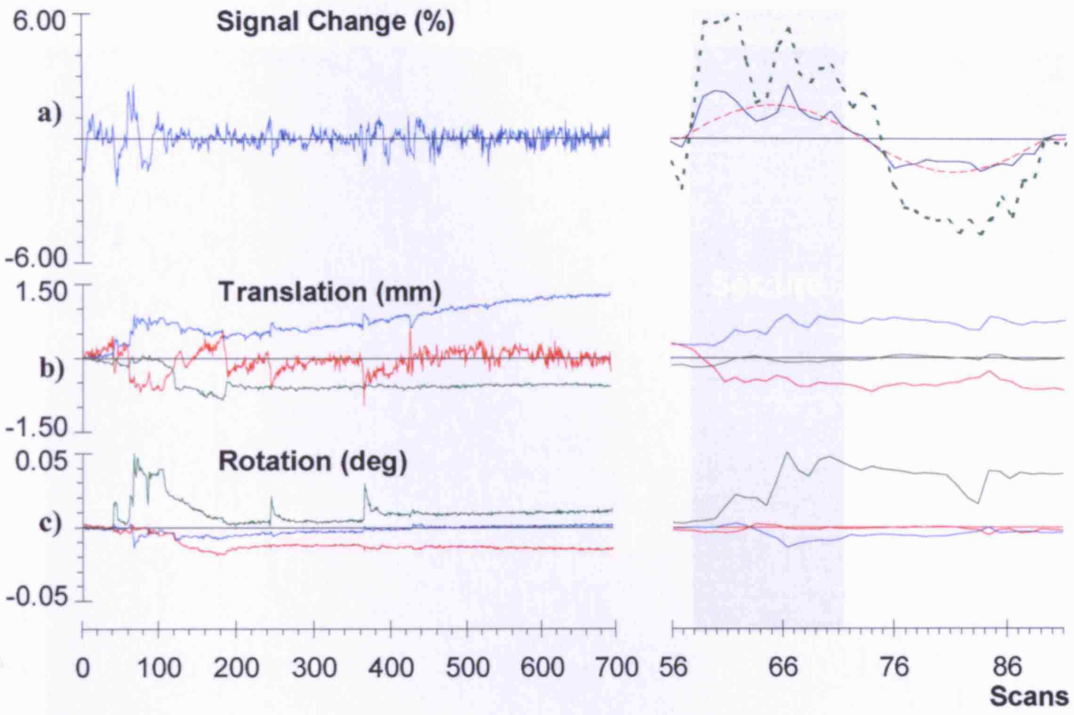

Figure 7-3 Regional timeseries and realignment parameters
Figure 7-3 (a) – Regional Time series. The first eigenvariate is shown as extracted from the principal cluster of the SPM{F}. The seizure period is appropriately scaled on the right and the signal change approximated by the single sine wave regressor shown in red. The maximum signal change is shown in green. Percentage signal changes are with respect to the grand session mean. (b,c) – Realignment Parameters. The X, Y, and Z translations in units of millimeters are shown in red, green and blue respectively, and the corresponding rotations given underneath in degrees. The seizure interval is shaded in gray.

In regard to magnitude, BOLD changes in isolation are difficult to quantify directly in terms of physiological variables and a more intricate knowledge of the underlying physiology is essential. Though quantitative PET measurements of ictal rCBF are difficult to obtain (Duncan, 1997b), increases of around 150-200% are suggested (Theodore et al., 1996) but whilst cerebral blood flow and metabolism are closely coupled under physiological conditions (Siesjo, 1978) the influence of seizure activity is far less clear.

Figure 7-4 Anatomical Overlay

The seizure related activation obtaining from Figure 7-2b is shown overlaid onto consecutive slices of a co-registered T1-weighted scan.

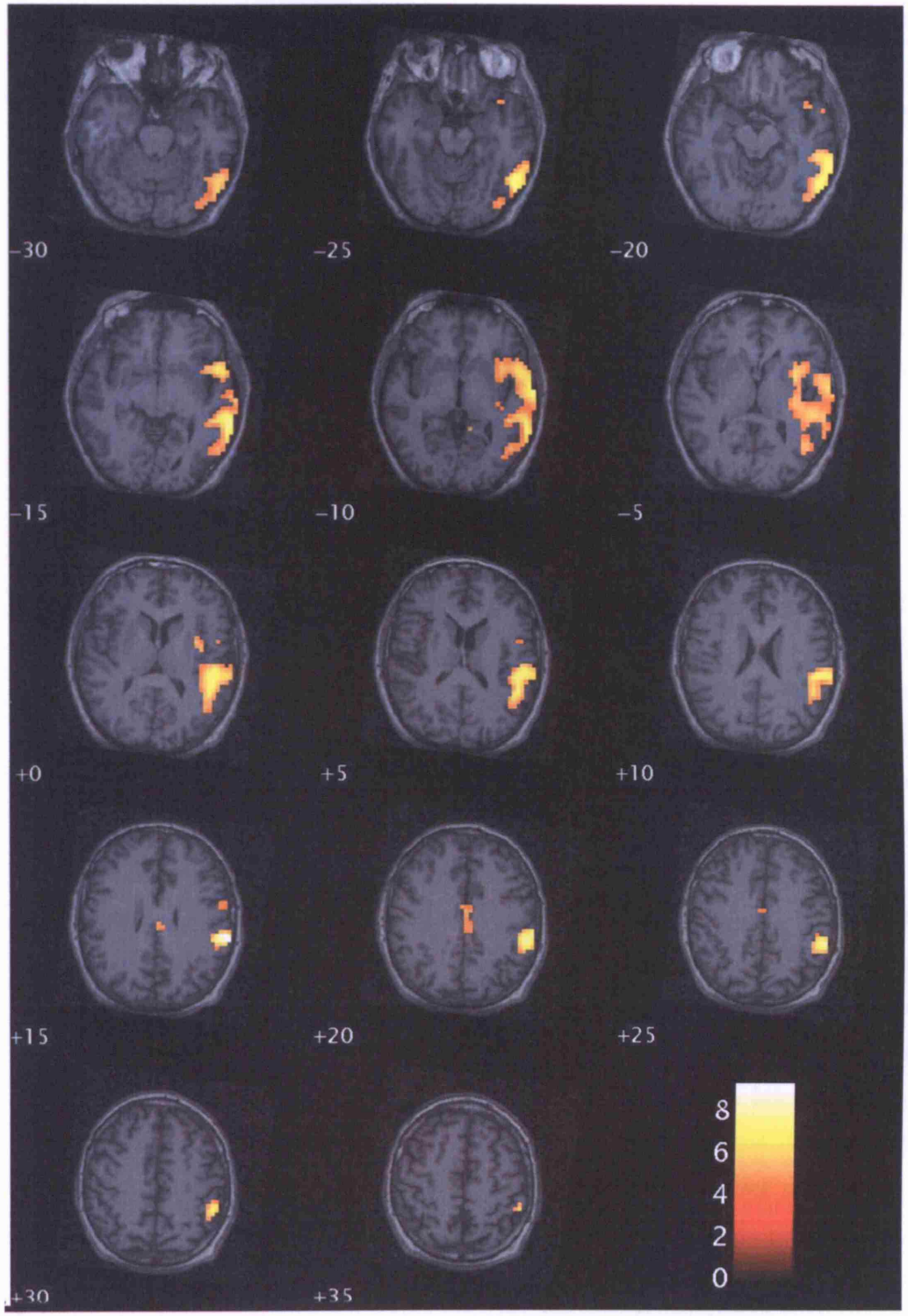

Interictally, there is evidence for both unmatched reductions in the regional metabolic rate of glucose (rCMRGlc) as compared to rCBF within human epileptic foci (Duncan, 1997b;Fink et al., 1996;Gaillard et al., 1995) and similar uncoupling in animal models (Bruehl et al., 1998).

Ictally, Kuhl *et al* (Kuhl et al., 1980) report rCMRGlc increases of 82-130% using ^{18}FDG-PET in association with smaller flow changes but Engel *et al* (Engel, Jr. et al., 1982) found rCMRGlc increases of an order 2-6 times the measured interictal values for homotopic regions. Franck *et al* (Franck et al., 1986) have described disproportionate increases in CBF compared to $CMRO_2$ in five patients one of whom underwent ^{18}FDG-PET but with an unchanged glucose extraction ratio. They conclude that the supply of oxygen by blood flow was sufficient to meet local metabolic demands in status epilepticus and that glucose utilization is more important that oxygen consumption in determining rCBF but Buxton & Frank have since provided a widely embraced explanation for such data compatible with an intact neurovascular coupling (Buxton and Frank, 1997).

The 'oxygen limitation model' of Buxton & Frank (1997) suggests blood flow and metabolism to be coupled in a non-linear fashion such that relatively small increments in the cerebral metabolic rate of oxygen ($CMRO_2$) necessitate disproportionately large increases in rCBF. Quantitative theoretical relationships between BOLD and rCBF were provided (Buxton and Frank, 1997) within which context the rCBF changes implied by our data are found to be broadly compatible with the PET literature (assuming true underlying rCBF increases of 100-200%).

An unexpected feature of the seizure-related BOLD change seen in the patient we report lies in its temporal relationship to the EEG. The BOLD changes shown in figure 3(a) might appear to precede the EEG changes by several seconds (as also suggested by others (Krings et al., 2000)) but this cannot be reliably shown in relation to a single event and with the necessitated high-pass filter. Interestingly, a post stimulus undershoot is seen more markedly than would be predicted through conventional models of sustained neural activity (e.g. the convolution of a boxcar function with a canonical Haemodynamic Response Function (Aguirre et al., 1998b)). Assuming an underlying temporal mismatch between flow and volume (Mandeville et al., 1999a), a very sharp initial increase in flow (Buxton et al., 1998)

presumably second to a particularly potent BOLD-inducing aspect of the seizure activity might thereby be suspected.

Anatomically, our results demonstrate a large and highly significant grey matter signal change centered over the left temporal and insular cortices, starting at seizure onset. The electrographic seizure focus (F_7-T_3), concordant with previous interictal spike foci (left anterior temporal), was also concordant with the fMRI activation and even more so perhaps with the area of maximal signal change as demonstrated in Figure 7-2 (b).

In this respect, the ictal rCMRGlc changes observed by Engel *et al* (Engel, Jr. et al., 1982) did not always correspond to areas of maximal interictal hypoperfusion and were not confined to (though included) EEG sites of ictal onset and spread. There were also extensive differences across subjects ranging from activation of an entire left hemisphere with seizures generalizing from the left parietal area, to more selective activation of the left perisylvian area with seizures confined electrographically to the left temporal and central electrodes. Interestingly in one case, seizures involving the right temporal lobe were also associated with increased activity in limbic projection sites (hippocampus and cingulate cortex). Chugani *et al* (Chugani et al., 1994) distinguished between three dominant ictal rCMRGlc patterns in 18 children including 'hypermetabolism restricted to cerebral cortex' and taken together with such observations, the BOLD activation patterns presented are extremely plausible both anatomically and neurobiologically as well as being in keeping with the patients clinical picture and provide further support for similar activation patterns arising from subclinical and clinical seizure activity (Alfonso et al., 1998;Handforth et al., 1994).

The rigorous data analysis and use of stringent thresholds were motivated by a desire to minimize the risks of false positives and motion-related effects to every possible extent and indeed the spatial characteristics of our activation are quite distinct from 'edge effects' traditionally associated with stimulus-correlated motion in fMRI (Hajnal et al., 1994). It also differs markedly in spatial extent from those attributed to focal seizure activity by other groups (see Table 7-1) and further studies are clearly essential to resolving such disparities in terms of patient characteristics, seizure activity, scanner characteristics and data acquisition and analyses techniques.

Our decision to model the EEG activity as a single neural event was primarily motivated by the theoretical signal to noise considerations. Sampling of an inherently

noisy fMRI time series at low temporal resolution concealing a single relatively brief, undefined and sluggish BOLD fluctuation would not permit inferences regarding the spatiotemporal cascade. Similarly the relative length of an HRF in relation to the ictus prohibits any meaningful subdivision of the epoch for modeling as other than a single event without prior knowledge of subtle interactions and non-linearities for instance. Moreover, even were sequential activation to be evincible, any extrapolation of temporal relationships to the underlying neural activity would be hampered by interregional variability within the HRF (Buckner et al., 1996;Buckner et al., 1998;Kastrup et al., 1999a;Lee et al., 1995;Miezin et al., 2000;Robson et al., 1998;Schacter et al., 1997). To the best of our knowledge therefore sequential activation and propagation effects have never been convincingly demonstrated through fMRI in relation to a seizure.

In summary, we have demonstrated the ability to detect electrographic seizure activity during continuously acquired fMRI and the potential for EEG-correlated ictal fMRI to illuminate the spatial extent of the neural networks underlying a unilateral sub-clinical seizure. Whilst not routinely feasible, this technique allows for the 'BOLD signatures' of EEG phenomena to be established, providing unique perspectives into the complex perfusion and metabolic changes that accompany seizure activity with localizing information of immediate clinical interest.

* * *

8. Chapter 8: EEG/fMRI of human absence seizures

8.1 Summary

We studied a patient with idiopathic generalized epilepsy (IGE) and frequent absences, using EEG-correlated fMRI. Four prolonged runs of generalized spike-wave discharge occurred during a 35-minute experiment. Time-locked activation was observed bilaterally within the thalami in conjunction with widespread but symmetrical cortical deactivation with a frontal maximum. We demonstrate for the first time, the reciprocal participation of focal thalamic and widespread cortical networks during human absence seizures and suggest reductions in cortical blood flow, in response to synchronized EEG activity.

8.2 Introduction

The electrophysiological correlates of human absence seizures were first characterized by Gibbs *et al* (1935) who described a strikingly stereotyped EEG feature, the 3Hz generalized spike-wave discharge (GSWD), which occurs bilaterally, synchronously and symmetrically with paroxysmal onset and termination (Avoli et al., 1990). Later, work in several animal models led Gloor and associates to propose the 'corticoreticular hypothesis' attributing essential roles to both thalamus and cortex in GSWD generation and current concepts of GSWD revolve around 'a thalamocortical circuit' whereby a thalamic oscillator may bring about cyclical changes in cortical excitability and synchronization through intracortical and callosal connections to generate GSWD (Avoli et al., 1990). Similar mechanisms are thought to underlie other physiological brain rhythms such as sleep spindle generation (Kostopoulos, 2000). However, beyond scalp EEG and clinical observations, a very limited number of invasive electrophysiological recordings exist in humans (Hayne et al., 1949;Niedermeyer et al., 1969;spiegel et al., 1951;Williams, 1953) variably implicating cortex, hypothalamus and thalamus in GSWD generation. Higher spatial sampling *in vivo* imaging techniques are crucial to establishing the relevance of basic work to humans but have, thus far, lacked temporal resolution. The advent of simultaneous and continuous EEG-Correlated fMRI provides an unprecedented opportunity to identify and study the neural correlates of such EEG phenomena and we describe the first such study.

8.3 Methods

Case report. We studied a 36-year old right-handed lady with intractable juvenile absence epilepsy, a subtype of IGE. Birth and early development were normal. There were no learning disabilities. Habitual seizure onset was at age 14 years with frequent typical absences (1-4/day) and no myoclonic jerks. She also experienced occasional generalized tonic-clonic seizures. Several clinical EEG recordings had shown frequent runs of frontally predominant, symmetrical, and bilaterally synchronous 3Hz GSWD. These were more marked on hyperventilation, always associated with unresponsiveness, and not always recalled by the patient. There was no family history. Neurological examination and high-resolution structural imaging were normal. A number of agents including Valproate, Lamotrigine, and Clonazepam had been previously tried and discontinued due to lack of effect and side-effects. At the time of study she was experiencing frequent unprovoked absences on Topiramate 150mg daily.

Data Acquisition. Imaging was performed on a 1.5 Tesla GE signa system (General Electric, Milwaukee, WN) using a standard head coil. 700 BOLD sensitive scans were acquired continuously using a T2*-weighted gradient-echo echo planar imaging (EPI) sequence (TE/TR 40/3000, 21x5mm interleaved slices, FOV = 24x24cm, 64x64 matrix) over 35-minutes. 11-channels of referential scalp EEG were recorded simultaneously using MR-compatible equipment with online and offline pulse and imaging artefact subtraction (Allen et al., 2000). A single precordial ECG channel was also recorded.

EEG analysis. Digital EEG recordings were displayed on-screen in referential and bipolar montage using in house software to allow visual identification of GSWD onset and offset by consensus in relation to slice acquisitions (Figure 8-1). A running power spectral density measurement at 3Hz (Figure 8-2b,c) was also obtained by averaging discrete Fourier transforms of consecutive 3-second Hann-windowed epochs from all EEG channels within MATLAB (MathWorks, USA).

Figure 8-1 EEG from the experiment.
Two bi-temporal chains are shown, referenced to Pz in the top ten channels, followed by a bipolar montage in the next eight. ECG and slice timing signals (OSC) are shown at the bottom. fMRI was carried out continuously throughout the recording as indicated by the timing signals. Pulse and imaging artefact were subtracted online. An arrow marks the beginning of 3Hz gSWD.

Figure 8-2 Experimental parameters.
EEG recorded during fMRI (fronto-polar electrodes referenced to Pz) is shown in (a) covering the first seizure. The small arrows mark GSWD onset and offset with the base of the large arrow indicating the temporal position of this 40-second epoch within the 35-minute experiment. All other data (below) are plotted in parallel against time (scans) over the entire experiment. A running power spectral density measurement over 0-20 Hz is shown in (b) with the 3Hz band plotted underneath in (c) where red asterisks mark GSWD onsets and offsets. Band-pass filtered BOLD time-series are shown next from the maximally activated (d) and deactivated (e) voxels (indicated in figures 3a,b) showing percentage change with respect to the grand session mean. Lastly the six rigid-body motion parameters, XYZ translations in millimeters (f) and rotations in degrees (g), are given in red, green, and blue respectively, to show they cannot explain the observed responses.

fMRI analysis. The SPM99 package [http://www.fil.ion.ucl.ac.uk/spm99] was used for all pre-processing and voxel-based statistical analysis, carried out in the context of the general linear model. A slice-timing correction was performed prior to realignment and spatial smoothing by an isotropic Gaussian kernel of 8-mm full width half maximum. To further protect against motion-related artefact, all design matrices included the six rigid-body motion correction parameters, $R_{i\ (i=1,\ldots,6)}(t)$ as shown in Figure 8-2 (f) and (g), plus $R_i(t-1)$, $R_i(t)^2$ and $R_i(t-1)^2$. These can be regarded as confounding covariates corresponding to the first few terms of a Volterra series spanning the subspace of linear and non-linear motion-related effects (Friston et al., 1996).

Two statistical models were compared to test for seizure-related BOLD changes: (1) GSWD were modeled as a series of boxcars (1 for present and 0 for absent) convolved with a canonical HRF plus the temporal derivative as a second regressor (modeling additional onset variability). (2) 3Hz activity was modeled as a single regressor by convolving the 3Hz power spectral density derived as above with a canonical HRF.

Figure 8-1

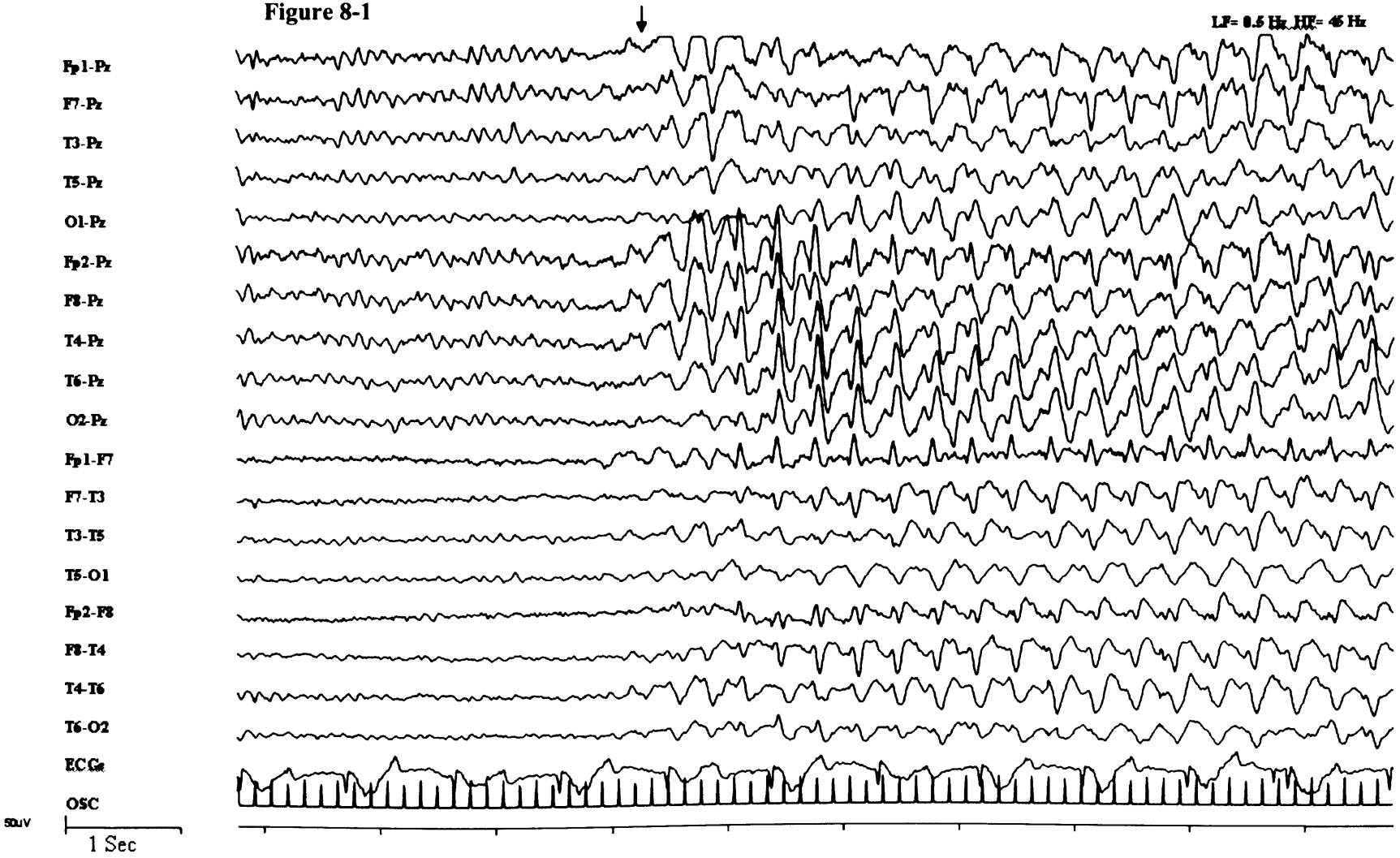

Figure 8-1

Figure 8-2

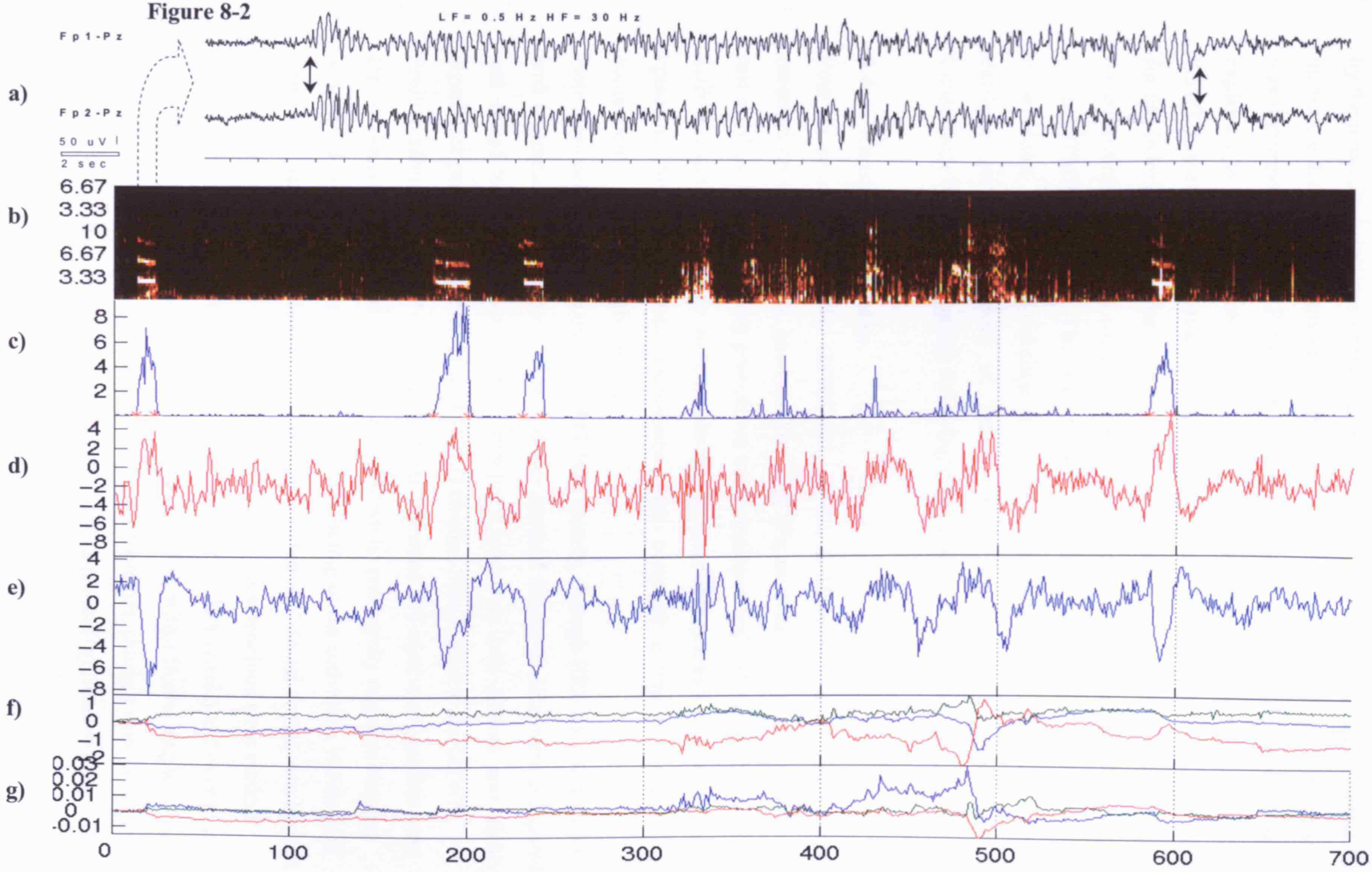
a)
b)
c)
d)
e)
f)
g)
Fp1-Pz
Fp2-Pz
50 uV
2 sec
LF= 0.5 Hz HF= 30 Hz
6.67
3.33
10
6.67
3.33
0
100
200
300
400
500
600
700

Data and design matrices were high-pass filtered at 1/200 seconds cut-off, dictated by the noise characteristics of the scanner. An AR(1) model was used to estimate the intrinsic autocorrelation structure of the data. No global scaling/global normalization was performed. In (1) an F-contrast was specified to test for the additional variance explained by the subspace of the model embodying the 'effects of interest' (i.e. GSWD) otherwise a T-contrast was specified as a unidirectional test of significance for the individual parameter estimates. All SPMs were thresholded at $P<0.05$ using the correction for multiple comparisons based on Gaussian random field theory (part of the SPM99 package). The results were overlaid onto the mean EPI scan for presentation. Anatomical labeling was performed using the 'Talairach demon' database server (University of Texas Health Sciences Centre, International Consortium for Brain Mapping) following stereotactic normalization.

8.4 Results & Discussion

Four prolonged runs of 3Hz GSWD (31, 60, 32, & 35 seconds, respectively) were recorded on uninterrupted, good quality EEG (Figure 8-2a) during the eyes-closed rest condition. No activating procedures were employed and only spontaneous EEG activity was studied. There were no changes in heart or respiratory rate during these episodes. No other seizure-phenomena were observed during the study, nor subsequently reported by the patient.

Both approaches to integrating the EEG data, namely, through HRF convolution both with a representative boxcar and with power spectral density at 3Hz, were compared and found to yield almost identical results. There were two distinct and highly significant patterns of seizure-related BOLD change, time-locked to the GSWD.

Positive changes (Figure 8-3a) or activations of around 3% relative to baseline were seen exclusively within the thalami bilaterally whilst profoundly negative changes were noted outside (Figure 8-3b). Anatomical labeling of the activation, although in terms of ventral posterior lateral, ventral lateral and medial dorsal nuclei, was limited by spatial resolution, normalization, and smoothing. Deactivations were evident symmetrically (left cerebrum = 2005, right cerebrum = 1888 voxels) and over large areas of cortical grey matter as illustrated in Figure 8-4, with a frontal emphasis and maximum of around –8% relative to baseline. Furthermore, changes were consistent across the individual seizures as shown in Figure 8-2 (d) and (e) (inter-regional HRF

variability limits further inferences in relation to temporal structure and relative onsets across voxels).

Figure 8-3 Statistical parametric maps.
Activations (a) and deactivations (b) in relation to GSWD activity are illustrated. SPM{T}s are shown thresholded at the P<0.05 level, corrected for the search volume.

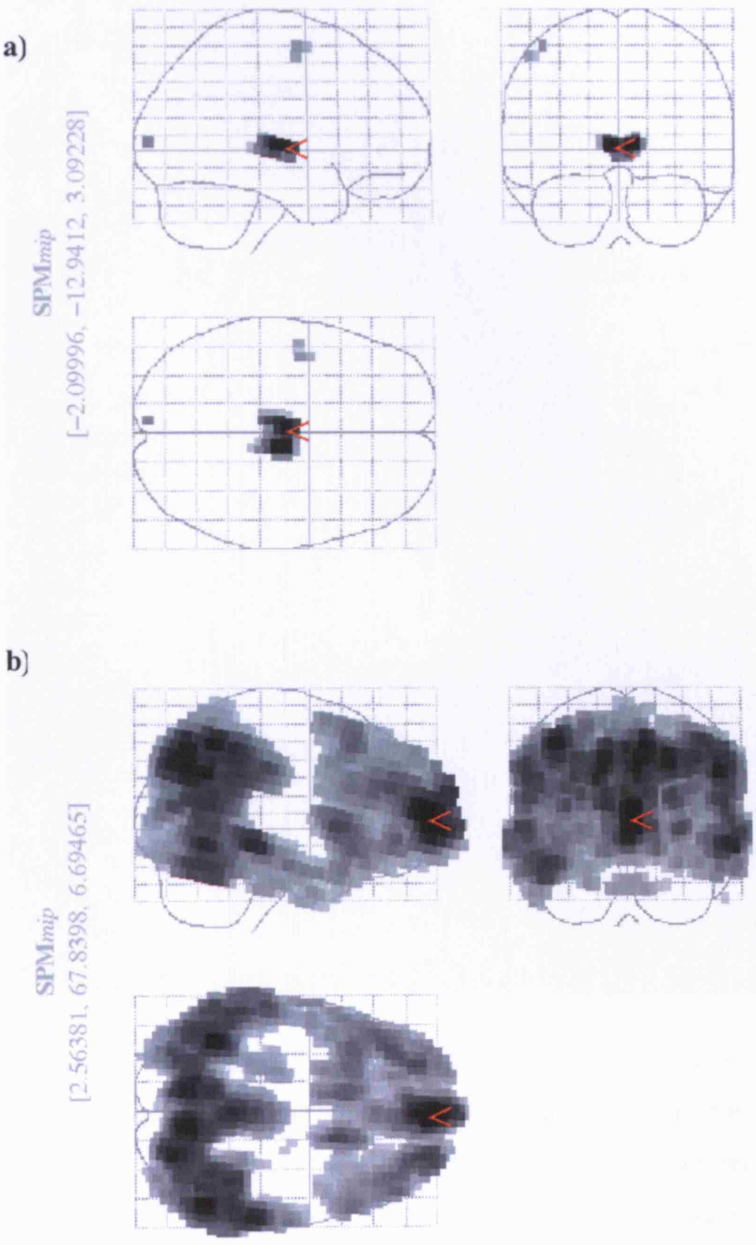

Figure 8-4 Anatomical overlay
Activations (red-yellow) and deactivations (cyan-pink) are shown using separate colour-scales overlaid onto the mean EPI image.

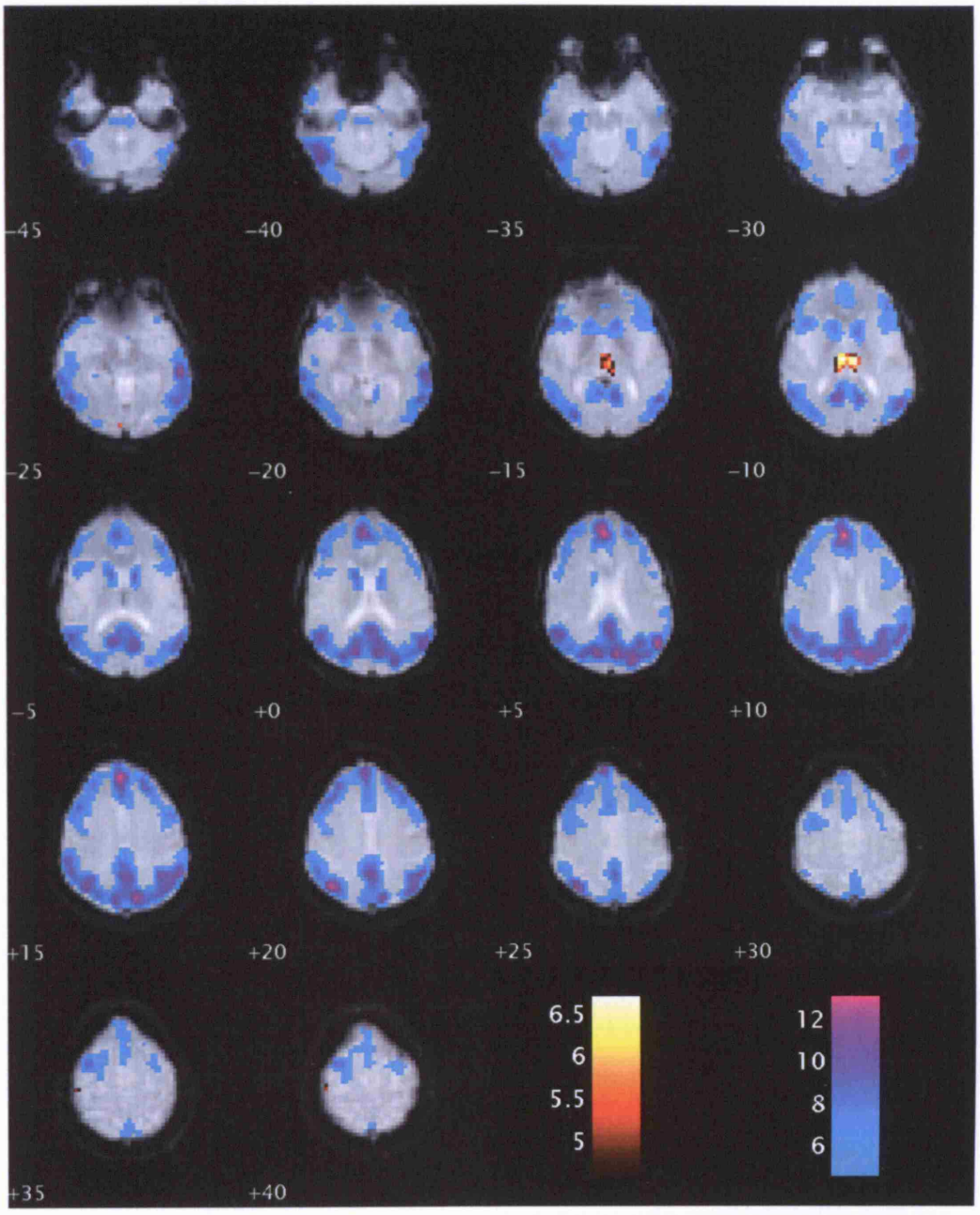

Current density source reconstruction using high resolution EEG has revealed two principle centers of gravity underlying GSWD, near frontal and occipital poles (Rodin, 1999) and maximal frontal lobe involvement has been repeatedly suggested (Pavone and Niedermeyer, 2000). Such observations are very consistent with our data.

PET studies of cerebral glucose metabolism (CMRGlu) during GSWD are fundamentally limited by tracer uptake and can never pertain to individual electrographic events. Instead, such observations represent a weighted amalgam of pre-ictal, ictal, and post-ictal states, further confounded by intersessional differences, hyperventilation effects, and patient selection criteria. Not surprisingly therefore, CMRGlu changes appear inconsistent across studies (Engel, Jr. et al., 1985;Ochs et al., 1987) though reductions have been reported in at least one patient with absence status (Theodore et al., 1985). Likewise, EEG-correlated transcranial Doppler (Diehl et al., 1998;Nehlig et al., 1996) studies of cerebral blood flow (CBF) have failed to reach unanimity, although cortical decreases in CBF have been noted and are particularly well supported by animal data (Nehlig et al., 1996). Interestingly, thalamic hyper-perfusion was previously described by the only CBF study using H_2O^{15}-PET (Prevett et al., 1995).

Transient changes in BOLD may arise from a number of interlinked physiological parameters including changes in CBF, cerebral blood volume (CBV) and the cerebral metabolic rate of oxygen ($CMRO_2$) (Heeger and Ress, 2002). However, as the BOLD changes reported here were both pronounced and sustained, to relate them to anything other than CBF change would necessarily imply significant failure of the neurovascular coupling during GSWD, and we are not aware of evidence to support this. Early measurements using Near Infrared Spectroscopy (NIRS) also appear to indicate reductions in cortical oxyhaemoglobin, increases in deoxy-haemoglobin, with unchanged total haemoglobin (i.e. blood volume) during human GSWD (A.Villringer, personal communication).

Recent work has demonstrated, directly, the relationship between BOLD and synaptic activity (or more precisely, local field potential)(Logothetis et al., 2001). This would suggest that GSWD represents a relatively inactive cortical state with low mean synaptic activity, whereas EEG 'desynchronization' phenomena have been indicated to signal cortical activation (Pfurtscheller and Lopes da Silva, 1999) and in keeping with this, similar patterns of cortical deactivation with thalamic activation have recently been linked to alpha (8-13Hz) activity using EEG/fMRI (Goldman et al., 2002).

It is intriguing that opposite cortical and thalamic BOLD responses are observed in response to the same pattern of synchronized electrophysiological activity and this implies differing pathophysiological processed in these sites. Certainly, the overall

metabolic demands of GSWD may differ between these structures, and the relative contributions of excitatory versus inhibitory synaptic activity to BOLD remains subject to controversy (Heeger and Ress, 2002).

This study is important for a number of reasons. 1) Evidence is provided for a reduction in cortical activity during human absence seizures, time-locked directly to the ictal GSWD activity itself. 2) A key role for the thalamus is suggested. 3) It speaks to the existence of thalamocortical mechanisms in humans. 4) The anatomy and spatial dynamics of BOLD changes during human GSWD activity are revealed for the first time.

* * *

9. Chapter 9: Interictal EEG/fMRI in focal epilepsy

9.1 Summary

Using continuous EEG-correlated fMRI we investigated the BOLD correlates of interictal epileptic discharges (IEDs) in 63 consecutively recruited patients with focal epilepsy. Semi-automated spike detection and advanced modeling strategies were introduced to account for different EEG event types, and to minimize false activations from uncontrolled motion. Our results show that: (1) significant hemodynamic correlates were detectable in over 68% of patients in whom discharges were captured and were highly, but not entirely, concordant with site(s) of presumed seizure generation where known; (2) deactivations were less concordant and may non-specifically reflect the consequential effects of IEDs on brain activity; (3) a striking pattern of retrosplenial deactivation was observed in 7 cases mainly with focal discharges; (4) the basic hemodynamic response to IEDs is physiological; (5) incorporating information about different types of IEDs, their durations and saturation effects resulted in more powerful models for the detection of fMRI correlates; (6) focal activations were more likely when there was good electroclinical localization, frequent stereotyped spikes, less head motion and less background EEG abnormality but were also seen in patients in whom the electroclinical focus localization was uncertain. These findings provide important new information on the optimal use and interpretation of EEG-fMRI in focal epilepsy, and suggest a possible role for EEG-fMRI to provide new targets for invasive EEG monitoring.

9.2 Introduction

The accurate spatial localization of epileptiform EEG activity remains central in both the diagnosis and treatment of the epilepsies (Fish, 2003). In patients with focal epilepsy, successful surgery relates directly to the confidence with which the 'epileptogenic zone' - theoretically defined as the minimum volume of tissue whose resection is both necessary and sufficient for seizure ablation (Luders et al., 1993) – can be identified. Despite well over a century of epilepsy surgery (Horsely, 1886), a non-invasive gold standard technique for prospectively mapping the epileptogenic zone is still lacking (Rosenow and Luders, 2001). The irritative zone, the source of interictal epileptic activity recorded on the EEG, is typically related closely to the

epileptogenic zone but remains anatomically difficult to define using EEG alone (Engel, Jr., 1993;Luders et al., 1993). This is principally due to the inverse problem (Plonsey, 1963).

EEG-correlated fMRI (EEG-fMRI) can be used to map Blood Oxygen Level Dependent (BOLD) signal changes linked to spontaneous EEG activity non-invasively and has attracted a great deal of interest as both a scientific and clinical tool (Salek-Haddadi et al., 2003a;Schomer et al., 2000). A number of groups have previously reported BOLD activations in relation to IEDs using a variety of methods (Al-Asmi et al., 2003;Jager et al., 2002;Krakow et al., 1999b;Krakow et al., 2001a;Lazeyras et al., 2000a;Patel et al., 1999;Seeck et al., 1998;Symms et al., 1999;Warach et al., 1996). Consensus however is still lacking on several key issues such as which EEG characteristics lend themselves best to EEG/fMRI? What comprises a biologically meaningful activation? What are the range of BOLD responses to IEDs? What influences these responses and how can these be best modeled and characterized experimentally? How should any anatomical information be used clinically? What is clear is that these studies remain difficult to perform for several reasons. Firstly, patient selection, generally based on a high rate of stereotyped IEDs, is limiting. IEDs themselves may be sparse and difficult to discern. Secondly, by nature, studies of spontaneous EEG activity are not as powerful or efficient as studies allowing experimental manipulations via a paradigm. This may explain why only half of experiments in patients with focal epilepsy and in whom IEDs are recorded tend to yield significant activations; thirdly, there is little consensus or comparison on how data should be analyzed. The available data does however suggest that there is good test-retest reproducibility where activations are observed and most, but by no means all, positive cases show at least one activation concordant with conventional localization.

Using continuous EEG-fMRI, we aimed to establish the range of activation patterns linked to IEDs across different epilepsy syndromes and pathologies; to evaluate the relative proportion of focal epilepsy patients showing BOLD activations using EEG/fMRI; to explore the clinical relevance of any fMRI findings; and to identify patients for whom the technique may hold greatest promise. Our primary focus was on mapping IEDs and to this end, our study included both patients with and without electroclinically well-defined epileptogenic foci in the hope that information obtained with regards to anatomical concordance between the fMRI activation and

the epileptogenic focus in the former, would in turn help validate fMRI findings in the latter group. We also aimed to characterize the hemodynamic responses to focal IEDs specifically in this group to avoid doubts as to the biological significance of the areas interrogated.

Methodologically, we aimed to explore different ways of maximizing information from the EEG (both manual and semi-automated), of minimizing the deleterious effects of patient head motion, of constructing better models of the EEG data for fMRI analysis. In particular, we used statistical tests to elucidate the importance of modeling runs of IEDs compared to individual events, and of taking into account non-linearity of the BOLD response in cases with very frequent discharges. The results should provide guidance on the best analytical strategy for IED-correlated fMRI data. Finally we aimed to identify qualitatively and retrospectively, any experimental factors linked to the likelihood of activation.

9.3 Methods

9.3.1 Patients

63 patients (25 male) who were attending the epilepsy clinics at either the National Hospital for Neurology and Neurosurgery, Queen Square, London, UK, or the National Society for Epilepsy (UK) with focal epilepsies were studied over a three year period. These patients were selected if they had frequent IEDs (spikes, polyspikes, and sharp waves) on a recent EEG.

In all patients the seizure focus was first classified on the basis of the clinical, EEG, video-EEG telemetry and structural MRI as being localized, lateralized or bifocal (e.g. bi-temporal), diffuse, multifocal or uncertain, by two of the authors (ASH & DRF) blind to the fMRI analysis.

9.3.2 Data acquisition

The patients were scanned on a 1.5 Tesla Horizon EchoSpeed MRI scanner (General Electric, Milwaukee, USA) using T2*-weighted single-shot gradient-echo echo-planar images (EPI; TE/TR 40/3000, flip angle: 90°, 21x5mm interleaved slices, FOV=24 x 24cm, 64x64 matrix). 700 scans were acquired continuously over a 35-minute period following an initial 12 seconds of scanning to achieve steady state magnetization. For the duration of the functional scans, patients were asked to keep

their heads still and to keep their eyes shut. Standard manufacturer-supplied cushions, ear plugs and plastic ear defenders were used.

Twelve gold disk electrodes fitted with 10 kOhm safety resistors were applied to the scalp, at Fp2/Fp1, F8/F7, T4/T3, T6/T7, O2/O1, Fz (ground) and Pz according to the international 10-20 system. Ten channels of EEG referenced to Pz and two channels of ECG were recorded as well was a timing signal derived from the scanner (5 kHz sampling, 33.3 mV range, 2μV resolution) with online pulse(Allen PJ et al., 1998) and imaging (Allen et al., 2000) artefact subtraction using MR-compatible equipment (Lemieux et al., 1997), providing good quality EEG display throughout the fMRI acquisition (see Figure 9-1).

9.3.3 Pre-processing

All fMRI data were analyzed using the SPM (Statistical Parametric Mapping) software package [http://www.fil.ion.ucl.ac.uk/spm/spm2.html]. and Matlab® version 6.5 R13 (The Mathworks Inc.,USA) running on a Dell® PowerEdge 2650 under Red Hat Linux 9. Images were slice-time corrected (Henson et al., 1999), realigned (Friston et al., 1995a), and spatially smoothed using an isotropic Gaussian kernel of 8mm FWHM. Scan realignment proceeds with an iterative estimation of the six rigid body motion parameters. In order to summarize the degree of head motion in each session, we estimated the absolute magnitude of the net displacement vector, d, using Pythagoras' theorem. The scan-to-scan displacement was calculated by estimating the absolute magnitude of the first derivative of d, $|d'|$. Individual head jerks were defined by $|d'| > 0.2$ mm/scan. These were counted automatically and incorporated into the fMRI model.

Figure 9-1 EEG recorded during fMRI from patient #25
EEG recorded during fMRI from patient #25 showing left anterior temporal spikes. Pulse and imaging artefact have been removed. Two bi-temporal chains are shown, referenced to Pz in the top ten channels, followed by a bipolar montage in the next eight. ECG and slice timing signals (OSC) are shown at the bottom.

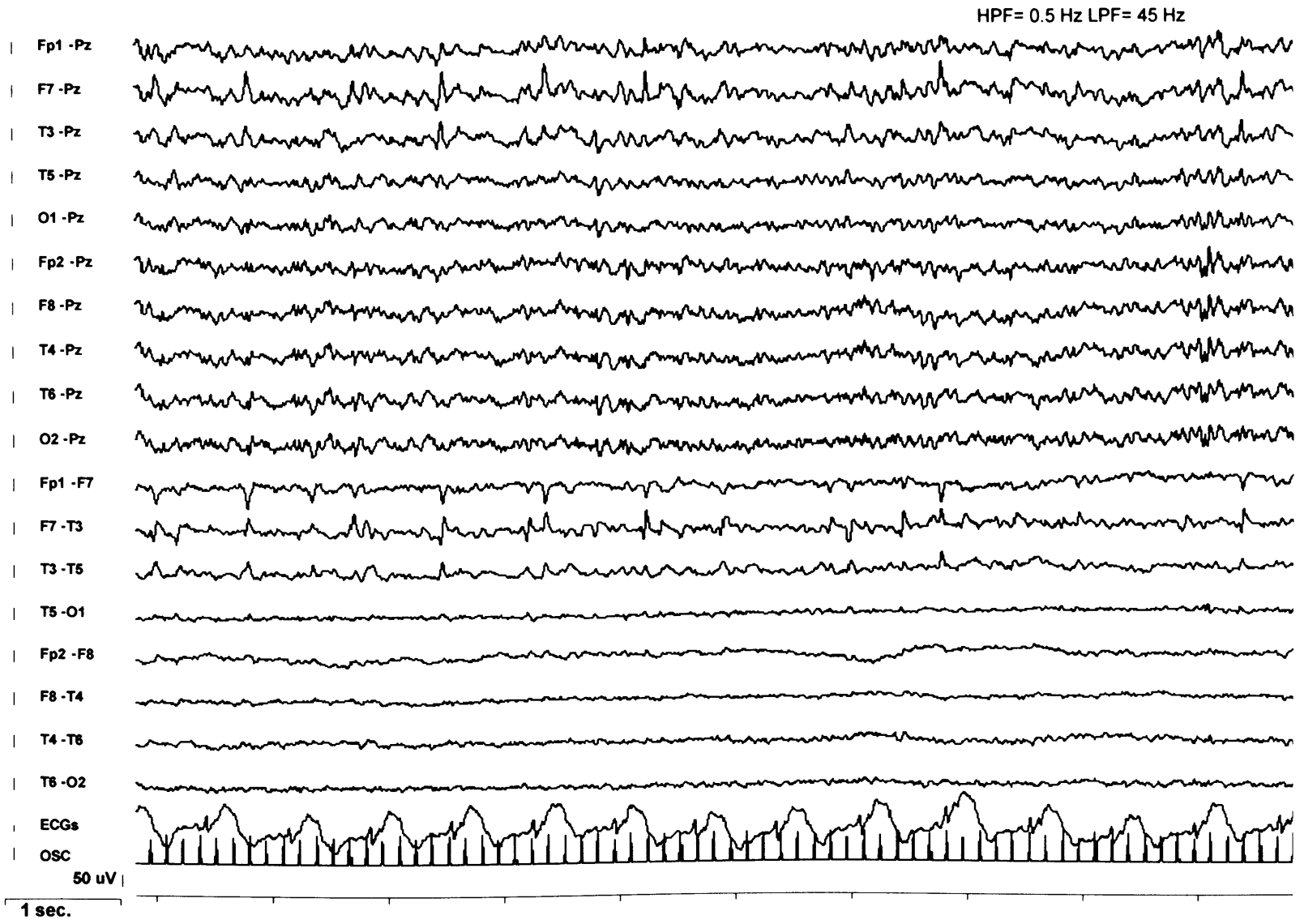
HPF= 0.5 Hz LPF= 45 Hz
Fp1 -Pz
F7 -Pz
T3 -Pz
T5 -Pz
O1 -Pz
Fp2 -Pz
F8 -Pz
T4 -Pz
T6 -Pz
O2 -Pz
Fp1 -F7
F7 -T3
T3 -T5
T5 -O1
Fp2 -F8
F8 -T4
T4 -T6
T6 -O2
ECGs
OSC
50 uV
1 sec.

Figure 9-1

9.3.4 EEG analysis

Online EEG and ECG were used to monitor epileptiform activity, head motion, arousal level and eye movements. Offline EEG analysis and classification was carried out by 2 expert observers (ASH & BD or MM). EEG data were displayed in both referential and bipolar montages using in-house software. The classification objectives were: (1) to estimate the numbers and types of IED based on amplitude, spatial distribution and morphology; (2) to group events and onset times into different categories based on whether or not they were likely to share the same generators. Each event was marked manually using a mouse-driven time cursor to create a software-generated list of onset times, in relation to the fMRI data using scanner generated slice-timing information (Allen et al., 2000).

In five cases (#20, #25b, #29, #36, #39), a semi-automatic spike-detection method was used based on a threshold crossing algorithm. These were cases where unambiguous large-amplitude discharges were seen clearly against the background, with distinct phase reversal across 2 or more bipolar channels. But critically, occurring with such frequency so as to render manual identification impracticable (Salek-Haddadi et al., 2003a). Firstly, any ambiguous or artefact contaminated segments of EEG were marked and excluded. A single compound EEG channel was then created by summing the two or more bipolar channels over which phase reversal takes place resulting in spikes being represented as large amplitude deflections. A threshold of two standard deviations was applied to the compound channel and all transition points, positive and negative, marked in time, along with the maximum amplitude of the detection channel between the transition points. A histogram of amplitude distribution was generated and the individual events at either extreme were recursively checked by visual inspection of the EEG and removed until the remaining band was free from artefacts. To exclude multiple events as part of the same IED complex, all events within one third of a second from the previous were removed.

9.3.5 fMRI analysis

For each patient, the analysis proceeded as follows:

9.3.5.1 - Step 1: Are there areas that display a conventional hemodynamic response to IEDs?

To answer these, a mass-univariate approach was taken using the SPM2 implementation of the general linear model (GLM), to generate statistical parametric of the likelihood of an effect at each and every voxel (Friston et al., 1995b).

Design matrices (DMs) were assembled using sets of regressors spanning both the effects of interest and confounds. To protect against motion-related artefact, all design matrices included the six rigid-body motion correction parameters, $R_{i\ (i=1,\ldots,6)}(t)$, plus $R_i(t-1)$, $R_i(t)^2$ and $R_i(t-1)^2$. These can be regarded as confounding covariates corresponding to the first few terms of a Volterra series spanning the subspace of linear and non-linear motion-related effects (Friston et al., 1996). In addition, a number of scans were effectively removed from each session by modeling them explicitly within the DM as a single delta function. For every head jerk detected automatically (see above), a total of 4 scans were removed spanning a 12 second interval beginning with the jerk-scan. No subjects were therefore excluded specifically, due to poor head motion. Both data and DM were high-pass filtered (1/200 seconds cutoff) and pre-whitened to remove slow drifts and correct for temporal non-sphericity (Friston et al., 2000b).

IEDs were modeled through convolution of a series of delta functions specifying the EEG-derived onsets, with a canonical hemodynamic response function. A temporal derivative (orthogonal) was also included to account for small systematic differences in hemodynamic latency, as per the Taylor approximation (Friston et al., 1998a). A plain T-contrast, either positive or negative, was then used to test the relevant parameter estimate for statistical significance in relation to its standard error.

All results were thresholded at the $P<0.05$ level, corrected for multiple comparisons using Gaussian field theory (Friston et al., 1991). No cluster thresholds were applied and they were presented as Statistical Parametric Maps (SPMs), using the familiar glass-brain format to allow visualization of the entire activation pattern.

9.3.5.2 - Step 2: Are there areas that display any time-locked activity linked to IED, other than the above?

The approach outlined in step 1 is potentially powerful but relies on the assumption that IED event-related responses are well approximated by a canonical HRF. We therefore looked for event-related responses of any form, when step 1 did not reveal

activations. We used an event-locked Fourier basis set (8 sines and 8 cosines modulated with a Hanning filter) spanning a 45 second window to model the event-related response in an unconstrained fashion and tested for an effect using an F-test (Josephs et al., 1997).

9.3.5.3 - Step 3: Are the activated areas concordant with seizure focus?

Where possible, we made categorical judgments regarding the fMRI concordance with the independently-determined focus. Activation patterns were classified as either Concordant, where the entire activation was concordant with the electroclinical localization; Concordant plus where maximum was concordant but additional, discordant clusters were seen; Discordant or Nil for no activation. This was done for both positive and negative BOLD responses.

9.3.5.4 - Step 4: What is the hemodynamic response to IEDs?

Steps 4 & 5 were applied to patients with positive Concordant and Concordant Plus activations only. Event-related responses were estimated using SPM2 for both the most significant voxel and the most significant cluster as a whole. This was done by fitting a finite impulse response set (32 x 1 second bins) to the extracted timeseries and an eigentimeseries derived from singular value decomposition across the entire cluster, following filtering and adjustment for the effects of no interest. Each result was displayed as a peristimulus time histogram and summarized as a set of parameters (time to peak, time to undershoot, peak percentage change, and peak to undershoot ratio). The duration of each response was estimated visually.

9.3.5.5 - Step 5: Do IED characteristics influence the BOLD response?

A. Cases with multiple IED types

In patients in whom more than one event type was recorded (#6, #25, #31, #35), we addressed two questions: firstly, which event types needed to be included in the model and secondly, whether any distinction among these event types was warranted. We used the principle of 'backward elimination' to select among a hierarchy of models (Draper and Smith, 1981). For example, where there were three event types corresponding to different IED amplitudes (#31 & #35), we compared three models representing different combinations of events: we began by combining all three as a

single set of events: '1+2+3' (i.e. representing the assumption that all event types share the same generator) and tested for activations. The two other models were created and tested for activation by adding two different combinations of events: '1+2' (types 1 and 2 share the same generator) and '1' (type 1 events have their own generator). The same principle was used for the cases with 2 event types, giving: '1+2', '2'. Note that in our scheme, event types are ordered by presumed importance, i.e. type 1 represents the dominant IEDs, and other types represent types of decreasing importance. The differences in contribution of the various event types on the BOLD activation were assessed using F-tests.

B. Cases with runs of IED

In cases where runs/bursts of IEDs events were modeled using a single onset vector (#3, #7a, #13, #23a, & #23b), we explored the influence of the duration of the EEG run on the BOLD response. This was done using the concept of parametric modulation, to look for an effect on the amplitude of the BOLD (Buchel et al., 1998). We tested for additional variance explained using F-test.

C. Cases with very frequent IED

In cases with very frequent discharges (number > 100 per 35-minute scan, excluding runs) we looked for non-linear effects in the BOLD response, such as saturation (#6, #7b, #8, #9, #11, #12, #31, and #39. We used a Volterra expansion of the basis functions(Friston et al., 1998b). Here, we were only concerned with the presence or absence of such effects, for the global maxima.

Further details of the models used for parts A,B & C are given in Web Table 1.

9.3.5.6- Step 6: What are the factors that influence the likelihood of activation?

We examined quantitatively the link between activation and runs of IED versus single spikes, and the degree of abnormality of background rhythms (mild theta, moderate theta/delta, severe delta, and loss of alpha or of other normal rhythms). The EEG background abnormalities were ranked visually as mild, moderate or severe for this purpose and the significance was assessed using the Chi-square statistic. We also looked for the effect of head motion as expressed by the mean and maximum scan-to-scan displacement and total number of spikes using two-sample t-tests to look for

significant differences between the means in all patients with BOLD changes versus those without (BOLD vs non-BOLD cases).

9.4 Results

Four of the 63 patients who underwent EEG-fMRI were excluded from further analysis: One due to the presence of post-operative MR artefacts, 2 due to excessive head motion that rendered the EPI data un-interpretable and in one, the scan was terminated because of a spontaneous convulsive seizure.

None of the patients reported any discomfort or adverse effects from EEG-fMRI, and EEG quality readily allowed the identification of IEDs. In 25 patients (42%), no IED was observed. These patients were not clinically distinguishable from those in whom IEDs were captured. One patient was studied on three occasions with a sub-clinical electrographic seizure recorded during one of these and was presented in Chapter 7. Repeat data were acquired in 5 cases in which IEDs were captured (#7, #23, #25, #27 and #38).

We recorded IEDs in 34 patients (16 male, mean age 32 years, range 20-63) the clinical details of whom are provided in Table 9-1. The mean number of events captured during each 35-minute recording session was 286 (range: 12-1710). 25 patients had 1 event type only, 7 had 2 event types and 2 had 3 event types (Table 9-2 & Table 9-3).

Table 9-1 Electroclinical data

Case	Onset Age (y)	Aetiology	Seizure type	Structural MRI	Ictal EEG	Interictal EEG	Localization
1	0	Post left temporal lobectomy for DNET, plus R-HS	CPS, SGTCS	Extensive left temporal lobectomy with considerable amount of altered brain surrounding cavity.	Subdural electrodes: Left frontal or possibly contralateral seizure onset, outside of the resected areas	Intermittent and widespread theta. Frequent temporal sharp waves and spikes with shifting lateralization, predominantly left mid temporal.	Uncertain
2	7	MCD	FMS	Diffuse cortical thickening right hemisphere, within parietal and occipital lobes, extending to frontal region.	Right temporal spikes	Widespread, right-sided spikes, sharp waves, and sharp and slow waves maximal frontocentral and centrotemporally.	R Lateralized
3	7	MCD	CPS, SGTCS	Widespread band and subcortical nodular heterotopia, predominantly posterior.	No clear changes	Bilateral, posterior temporal/occipital sharp and slow wave complexes with some left-sided spikes.	Bilateral
4	3	DNET	CPS, SGTCS (non-localising/lateralising)	Focal lesion expanding left middle temporal gyrus. Left temporal lobe is smaller than the right.	No clear lateralization.	Left-sided slowing, bursts of bilateral spike and wave/polyspikes, left temporal spikes.	Diffuse
5	0	MCD	CPS, SGTCS	Extensive MCD involving both hemispheres.	-	Left-sided spikes, sharp waves and slow waves, some bilaterally synchronous and occasionally right-sided.	Diffuse
6	40	Chronic encephalitis	FMS, CPS, SGTCS	Mild atrophy of left cerebral hemisphere.	Widespread over left hemisphere	Left midtemporal spikes and slow waves.	L Cent-Temp
7	15	Low-grade astrocytoma (post surgery and radiotherapy)	SPS, CPS	Focal scarring of left middle frontal gyrus.	Widespread over left hemisphere	Left frontal spikes.	L Front
8	5	Post-traumatic	SGTCS	MRI negative	-	Left temporal slowing with frequent left anterior temporal spikes.	L Lateralized
9	1	L-HS	SPS, CPS.	Severe diffuse L-HS	No lateralization	Left anterior temporal spikes.	L Temp
10	4	L-HS	CPS, SGTCS	L-HS	Left lateralization	Bursts of left-sided frontotemporal spikes. Sometimes occurring bilaterally.	L Lateralized
11	0	Perinatal subarachnoid haemorrhage	CPS, SGTCS	Left cystic encephalomalacia plus L-HS	-	Left-sided slowing with left posterior temporal spikes.	L Lateralized
12	1	Unknown (Family history, post-vaccine seizures ,	MJ, SPS, CPS, SGTCS	L-HS	No lateralization	Left anterior temporal spikes and sharp waves.	L Temp

Case	Onset Age (y)	Aetiology	Seizure type	Structural MRI	Ictal EEG	Interictal EEG	Localization
		and L-HS);					
13	18	L-HS	CPS	L-HS	Left hemisphere	Left temporal slow and sharp waves.	L Temp
14	3	Cryptogenic	SPS, CPS, SGTCS	MRI negative	No clear lateralization	Bifrontal spike-wave discharges with right-sided emphasis.	Uncertain
15	5	Cryptogenic Occipital lobe epilepsy	SPS (Visual phenomena R>>L)	MRI negative	-	Left posterior temporal/occipital spikes and sharp waves.	L Occ/Temp
16	5	Cryptogenic	CPS (frontal semiology), SGTCS	MRI negative	-	Spikes over right hemisphere with wide field, maximal temporally.	Uncertain
17	3	Grade II left parietal astrocytoma resected at age 11	SPS, SGTCS	Large temporoparietal resection.	Widespread over left hemisphere	Left posterior temporo-parietal spikes.	L Lateralized
18	19	Cryptogenic	CPS, SGTCS	MRI negative	Multifocal onset	Left temporal slow waves and spikes plus right temporal spikes during sleep.	Diffuse
19	7	Cryptogenic	CPS (extra-temporal semiology), SGTCS	MRI negative	Bilateral onset	Left temporal sharp waves and spikes with bilateral frontal sharp waves.	Uncertain
20	3	HS	CPS,SGTCS	L-HS	Widespread over left hemisphere	Spikes and sharp waves intermixed with slow activity over left anterior to mid temporal regions.	L Lateralized
21	4	MCD	SPS, FMS, SGTCS.	Right parietal open leptoschizencephaly.	-	Bursts of spike-wave activity over central region bilaterally.	R Frontal
22	5	DNET	SPS, SGTCS	Right temporal lobe lesion involving amygdale and uncus but not hippocampus.	No clear lateralization*	Right-sided anterior temporal spikes with some independent left-sided spikes.	Diffuse
23	9	Post- traumatic	CPS,SGTCS	Right middle frontal gyrus cortical scar.	-	Right-sided polyspike and slow wave discharges, single and in bursts, maximal centro-temporally.	R Frontal
25	1	Neoplasm	CPS, SGTCS	Mass in left temporal lobe involving amygdala, hippocampus and parahippocampal gyrus associated with irregular cystic cavity.	No clear change	Left anterior temporal spikes.	L Temp
26	4	FCD	CPS, SGTCS	Focal signal change in left middle	-	Independent left and right mid-temporal spikes and	Uncertain*

* #22: Two distinct seizure types were recorded during video telemetry. One type would begin with a peculiar feeling around the head, followed by head slumping to the right, unresponsiveness and post-ictal dysphasia lasting minutes. Here, ictal changes were seen bilaterally but greater on the left. The second type began with the same aura followed by clasping together of the hands, rocking movements of the arms, followed by fidgeting and secondary generalisation into a tonic-clonic seizure. This attack began with right fronto-temporal fast activity.

Case	Onset Age (y)	Aetiology	Seizure type	Structural MRI	Ictal EEG	Interictal EEG	Localization
				frontal gyrus consistent with focal cortical dysplasia.		slow-waves. L>>R.	
27	7	MCD	CPS, SGTCS	Marked malformation affecting both hemispheres, mainly the right. The right hemisphere is smaller and the fronto parietal regions are most affected.	-	Spikes, sharp-waves, and slow-waves widespread over the right.	R Lateralized
29	3	MCD	SPS (simple visual hallucinations)	Extensive MCD affecting the left cerebral hemisphere, particularly the posterior part. Does not affect the frontal lobe.	-	Bilaterally synchronous spikes over occipital and posterior temporal areas.	L Occ
30	8	Cryptogenic	CPS, SGTCS	MRI negative	Widespread over left hemisphere	L fronto-temporal bursts of spikes, sharp waves, and spike and slow-waves.	L Lateralized
31	0	MCD	SPS, CPS, SGTCS	Two large heterotopic nodules: Frontoparietocentral and medial parietal.	-	Frequent right centro-parietal spikes.	R Frontoparietal
35	<10	MCD	SPS, CPS, SGTCS	Left hemisphere atrophy with parietal polymicrogyria and L-HS.	Widespread over left hemisphere	Left anterior-mid temporal spikes.	L Lateralized
36	3	FCD	SPS	Thickened cortex in the left antero-inferior parietal region just extending into the inferior frontal gyrus.	No change	Continuous Left parietal spikes.	L Parietal
37	14	L-HS	CPS (temporal semiology)	Severe diffuse L-HS.	Independent right and left seizure onsets with temporal lobe-type automatisms. Psychometry non-lateralizing.	Left anterior-mid temporal spikes and slow waves.	Temp, uncertain laterality.
38	5	Cryptogenic	CPS, SGTCS	MRI negative	-	Right-sided mid-anterior temporal sharp waves plus rare independent left-sided sharp waves.	Diffuse
39	7	L-HS	CPS, SGTCS	L-HS	Left temporal onset	Left anterior temporal spikes.	L Temp

Abbreviations: Bil = Bilateral; CPS = Complex partial seizure; DNET= Dysembryoplastic neuroepithelial tumor; FCD= Focal cortical dysplasia; FMS = Focal Motor Seizures; HS = Hippocampal sclerosis; MCD= Malformation of cortical development; MJ=Myoclonic jerk; Post = Posterior; SGTCS = Secondary generalized tonic-clonic seizure; SPS = Simple partial seizure.

* #26: Frontal lesion, seizure semiology non-localising and non-lateralising, bitemporal spiking, no ictal recording.

Table 9-2 fMRI results for basic model

Case	Description of IEDs	fMRI Maximum		Clinical Localization	Activation				Deactivation				Figure 9-7
		Activation	Deactivation		C	C+	D	Ø	C	C+	D	Ø	
1	L Temp IED		R Front	Uncertain				•			•		W1
2	R Temp IED	R Front + R Par + L Occ		R Lateralized		•						•	W2
3	Runs of Bil Post-Temp/Occ IED	L Post + R Post		Bilateral	•							•	W3
4	Bursts of Bil (R>L) polyspikes	L Front/Par + Bil Occ		Diffuse		•						•	W4
5	Frequent Bil synchronous spikes			Diffuse				•				•	
6	L Temp IED<250uV L Temp IED>250uV	L Temp	L Temp/Par	L Cent-Temp	•						•		W5
7a	Runs of bifrontal IED	Bil Mid Front + Bil Front	R Temp + Mid Occ + Bil Par	L Front		•					•		W6
7b	Bifrontal IED	Bil Mid Front + Bil Front + Bil Occ	Mid Occ + Bil Par										
8	L Temp IED R Temp IED	L Temp + more widespread and some contralat	Bil Mid Occ/Par	L Lateralized		•					•		W7
9	L Temp IED	L Temp	R Temp + L Temp + Cereb	L Temp	•						•		W8
10	Bil spike-wave	Cereb + Widespread	Occ	L Lateralized			•				•		W9
11	L Post Temp IED	L Temp		L Lateralized	•							•	W10
12	L Ant Temp IED	L Temp	L Temp + Mid Occ + R Temp + Bil Par	L Temp	•					•			W11
13	Runs of L Ant Temp IED	L Temp		L Temp	•							•	9-3
14	Runs of R Front generalized spike-wave.	R Front + R Par		Uncertain		•						•	W12
15	L Post Temp/Occ IED	L Occ		L Occ/Temp	•							•	W13
16	L Temp IED R Temp IED			Uncertain				•				•	
17	L Temp IED			L Lateralized				•				•	
18	Runs of L Temp IED		Mid Occ + Mid Par + Mid Front	Diffuse				•		•			W14
19	L-sided IED			Uncertain				•				•	
20	L Temp IED (Auto)			L Lateralized				•				•	
21	R-sided IED			R Frontal				•				•	
22	R Ant Temp IED			Diffuse				•				•	
23a	Runs of Bil polyspike-wave	R Front + R Par + L Cereb + R Temp	Bilat Par +Bil Occ + L Front	R Frontal		•					•		9-4
23b	Runs of Bil polyspike-wave	R Front + R Par + L Cereb + R Temp	Bilat Par +Bil Occ										

Case	Description of IEDs	fMRI Maximum		Clinical Localization	Activation				Deactivation				Figure 9-7
		Activation	Deactivation		C	C+	D	Ø	C	C+	D	Ø	
25a	L Front-temp IED L Temp IED	L Temp	Mid Occ	L Temp	•						•		9-5
25b	L Front-temp IED (Auto) L Temp IED	L Temp	Mid-frontal + Mid Occ/Par + L Front										
26	R-sided IED L-sided IED			Uncertain				•				•	
27a	R Temp IED			R Lateralized				•				•	
27b	R Temp IED												
29	L Occ IED (Auto)		L Occ + L Par + Bil Front	L Occ				•		•			W15
30	L-sided IED			L Lateralized				•				•	
31	R Cent IED <160uV R Cent IED >160uV R Cent slow	R Front/Par		R Frontoparietal	•							•	W16
35	L Front-temp spike <50uV L Front-temp spike 50-100uV L Front-temp spike >100uV	L Temp		L Lateralized	•							•	W17
36	L Cent spike (Auto)	Mid Front		L Parietal			•					•	W18
37	L Temp spike		L Temp + R Temp	Temp, uncertain laterality				•		•			W19
38a	L-sided IED			Diffuse				•				•	
38b	R-sided IED												
39	L Front-temp spike (Auto)	L Temp + Bil Occ + Bil Par	R Cereb + L Cereb	L Temp		•					•		W20

Legend: IED = Interictal epileptiform discharge; Auto = automated event detection; Temp = temporal; Par = parietal; Occ = occipital; Front = frontal; Cereb = cerebellum; R= right; L = left; Bil = bilateral; Mid = midline; C = concordant; C+ = concordant plus; D = discordant; Ø = nil.

Table 9-3 fMRI models and statistics

Case	Scanner EEG		Motion (mm)			fMRI models		Results	
	EEG Events Type: n	Description of IEDs (Background EEG)	Mean $\|d'\|$	Max $\|d'\|$	Jerk	Basis function	Regressor(s)	Contrast Matrix	$Z_{max}(k_E)$
1	1: 45	L Temp spike (Severe)	0.03	0.36	5	HRFt	1	F[1] T[1] T[-1]	5.56 (14) Nil 6.02(29)
2	1: 82	R Temp spike (Moderate)	0.05	0.86	20	HRFt	1	F[1] T[1] T[-1]	5.55(34) 5.91(60) Nil
3	1: 50	Runs of Bil Post-Temp/Occ spike (Mild)	0.03	0.49	4	HRFt HRFt+PM	1 1	F[1] T[1] T[-1] F[0 1]	5.97(13) 6.37(34) Nil Nil
4	1: 166	Bursts of Bil (R>L) polyspikes (Severe)	0.12	3.18	71	HRFt	1	F[1] T[1] T[-1]	5.21(6) 5.53(11) Nil
5	1:422	Frequent Bil synchronous spike (Mild)	0.05	1.59	34	HRFt	1	F[1] T[1] T[-1]	Nil Nil Nil
6	1: 233 2: 250	L Temp spike<250uV L Temp spike>250uV (Severe)	0.02	0.19	0	HRFt HRFt HRFt HRFt+Volt	2+1 2+1,1 2,1 2	F[1] T[1] T[-1] F[0 1] T[1] F[0 1]	7.69(145) 7.14(58) 6.26(29) 4.76(35) 8.08(124) 3.38(2)
7a	1: 371	Runs of bifrontal spike (Moderate)	0.08	14.16	14	HRFt HRFt+PM HRFt	1 1 1	F[1] T[1] T[-1] F[0 1] F[1] T[1]	7.65(300) 6.3(88) 6.76(36) 8.04(2898) 8.04(3135) 8.04(4196)
7b	1: 300	Bifrontal spike	0.02	0.23	1				

Case	Scanner EEG		Motion (mm)			fMRI models		Results	
	EEG Events Type: n	Description of IEDs (Background EEG)	Mean $\|d'\|$	Max $\|d'\|$	Jerk	Basis function	Regressor(s)	Contrast Matrix	$Z_{max}(k_E)$
		(Moderate)				HRFt+Volt	1	T[-1] F[0 1]	7.71(114) 5.94(276)
8	1: 178 2: 12	L Temp spike R Temp spike (Mild)	0.04	0.29	3	HRFt HRFt+Volt	1,2 1	F[1;0 1] F[0 1] T[1] T[-1] F[0 1]	8.04(1623) Nil 8.04(454) 6.99(128) 5.07(855)
9	1: 404	L Temp spike (Mild)	0.03	0.38	1	HRFt HRFt+Volt	1 1	F[1] T[1] T[-1] F[0 1]	7.68(59) 4.51(1) 6.96(40) 4(13)
10	1: 59	Bil spike-wave (Mild)	0.04	0.27	5	HRFt	1	F[1] T[1] T[-1]	8.04(4939) 8.04(2828) 6.56(12)
11	1: 230	L Post Temp spike (Mild)	0.03	0.17	0	HRFt HRFt+Volt	1 1	F[1] T[1] T[-1] F[0 1]	Nil 4.57(1) Nil Nil
12	1: 638	L Ant Temp spike (Mild)	0.03	0.39	6	HRFt HRFt+Volt	1 1	F[1] T[1] T[-1] F[0 1]	7.57(31) 7.43(33) 6.57(66) 3.73(3)
13	1: 79	Runs of L Ant Temp spike (Mild)	0.05	1.12	30	HRFt HRFt+PM	1 1	F[1] T[1] T[-1] F[0 1]	Nil 5.01(3) Nil 6.73(74)

Case	Scanner EEG		Motion (mm)			fMRI models		Results	
	EEG Events Type: n	Description of IEDs (Background EEG)	Mean $\|d'\|$	Max $\|d'\|$	Jerk	Basis function	Regressor(s)	Contrast Matrix	$Z_{max}(k_E)$
14	1: 92	Runs of R Front generalised spike-wave. (Mild)	0.16	26.19	66	HRFt HRFt+PM HRFt (blck)	1 1 1	F[1] T[1] T[-1] F[0 1] F[0 1]	4.99(4) 5.47(8) Nil 5.91(99) 7.69(563)
15	1: 12	L Post Temp/Occ spike (Mild)	0.05	0.61	18	HRFt	1	F[1] T[1] T[-1]	Nil 4.50(1) Nil
16	1: 25 2: 20	L Temp spike R Temp spike (Severe)	0.18	37.20	60	HRFt	1,2	F[1;0 1]	Nil
17	1: 38	L Temp spike (Moderate)	0.08	1.16	45	HRFt	1	F[1] T[1] T[-1]	Nil Nil Nil
18	1: 58	Runs of L Temp spike (Moderate)	0.04	1.89	9	HRFt HRFt+PM HRFt (blck)	1 1 1	F[1] T[1] T[-1] F[0 1] F[0 1]	6.3(271) Nil 6.47(293) Nil 6.09(111)
19	1: 103	L-sided spike (Moderate)	0.07	1.45	39	HRFt	1	F[1] T[1] T[-1]	Nil Nil Nil
20	1: 971 (Auto)	L Temp spike (Mild)	0.06	0.25	3	HRFt	1	F[1] T[1] T[-1]	5.15(5) Nil Nil
21	1:73	R-sided spike (Moderate)	0.11	14.12	20	HRFt	1	F[1] T[1] T[-1]	Nil Nil Nil
22	1: 28	R Ant Temp spike (Severe)	0.06	1.75	27	HRFt	1	F[1] T[1]	5.54(5) Nil

Case	Scanner EEG		Motion (mm)			fMRI models		Results	
	EEG Events Type: n	Description of IEDs (Background EEG)	Mean $\lvert d' \rvert$	Max $\lvert d' \rvert$	Jerk	Basis function	Regressor(s)	Contrast Matrix	$Z_{max}(k_E)$
								T[-1]	Nil
23a	1: 198	Runs of Bil polyspike-wave discharge (Mild)	0.06	3.63	5	HRFt	1	F[1]	8.04(141)
								T[1]	8.04(63)
								T[-1]	8.04(924)
23b						HRFt+PM	1	F[0 1]	8.04(943)
	1: 236	Runs of Bil polyspike-wave discharge (Mild)	0.03	0.17	0	HRFt	1	F[1]	8.04(66)
								T[1]	8.04(88) 8.04(658)
								T[-1]	8.04(1062)
						HRFt+PM	1	F[0 1]	
25a	1: 219	L Front-temp spike	0.03	0.29	2	HRFt	1+2	F[1]	8.04(35)
	2: 411	L Temp spike (Mild)						T[1]	8.04(11) 8.04(188)
								T[-1]	3.26(2)
						HRFt	1+2,2	F[0 1]	
						HRFt	1,2		
25b						HRFt+Volt	1+2	F[0 1]	
	1: 1294	L Front-temp spike	0.04	2.39	24	HRFt	1+2	F[1]	8.04(33)
	2: 1416	L Temp spike						T[1]	8.04(37) 4.74(2)
	(Auto)	(Mild)						T[-1]	Nil
						HRFt	1+2,2	F[0 1]	
						HRFt	1,2		
26	1: 27	R-sided spike	0.19	1.45	235	HRFt	1,2	F[1;0 1]	Nil
	2: 30	L-sided spike (Severe)							
27a	1: 37	R Temp spike (Moderate)	0.12	3.90	87	HRFt	1	F[1]	5.81(29)
								T[1]	Nil
27b								T[-1]	Nil
	1: 12	R Temp spike (Severe)	0.14	2.44	118	HRFt	1	F[1]	Nil
								T[1]	Nil
								T[-1]	Nil

Case	Scanner EEG		Motion (mm)			fMRI models		Results	
	EEG Events Type: n	Description of IEDs (Background EEG)	Mean $\|d'\|$	Max $\|d'\|$	Jerk	Basis function	Regressor(s)	Contrast Matrix	$Z_{max}(k_E)$
29	1: 1472 (Auto)	L Occ spike (Mild)	0.05	0.55	37	HRFt	1	F[1] T[1] T[-1]	8.04(247) Nil 8.04(258)
30	1: 30	L-sided spike (Severe)	0.03	0.43	8	HRFt	1	F[1] T[1] T[-1]	Nil Nil Nil
31	1: 270 2: 51 3: 126	R Cent spike <160uV R Cent spike >160uV R Cent slow (Mild)	0.03	1.57	14	HRFt HRFt+Volt	1+2+3 1+2+3,1+3 1+2+3,1+3,3 1+2+3	F[1] T[1] T[-1] F[1;0 1] F[0 1] F[0 0 1] F[0 1]	7.46(54) 7.71(91) Nil 7.56(62) Nil Nil Nil
35	1: 36 2: 59 3: 17	L Front-temp spike <50uV L Front-temp spike 50-100uV L Front-temp spike >100uV (Mild)	0.05	0.50	5	HRFt HRFt HRFt HRFt	1+2+3 1+2+3,1+2 1+2+3,1+2,1 1,2,3	F[1] T[1] T[-1] F[0 1] F[0 0 1] F[1;0 1;0 0 1]	4.71(2) 5.06(6) Nil Nil Nil
36	1: 477 Auto	L Cent spike (Mild)	0.02	1.42	7	HRFt	1	F[1] T[1] T[-1]	Nil 4.52(1) Nil
37	1: 72	L Temp spike (Mild)	0.13	2.32	135	HRFt	1	F[1] T[1] T[-1]	5.82(16) Nil 6.16(41)
38a	1: 11 2: 36	L-sided spike R-sided spike (Severe)	0.05	1.64	8	HRFt	1,2	F[1;0 1]	Nil
38b	1: 26 2: 31	L-sided spike R-sided spike	0.06	0.57	30	HRFt	1,2	F[1;0 1]	Nil

Case	Scanner EEG		Motion (mm)			fMRI models		Results	
	EEG Events Type: n	Description of IEDs (Background EEG)	Mean $\|d'\|$	Max $\|d'\|$	Jerk	Basis function	Regressor(s)	Contrast Matrix	$Z_{max}(k_E)$
		(Severe)							
39	1: 622 (Auto)	L Front-temp spike (Mild)	0.02	0.51	4	HRFt	1	F[1] T[1] T[-1]	8.04(339) 8.04(360) 6.37(17) 4.39(85)
						HRFt+Volt	1	F[0 1]	

Legend: R: Right, L: Left; Ant: anterior, Post: posterior, Bil: bilateral, Front: frontal, Temp: temporal, Cent: central, Occ: occipital; Jrk: events defined based on inter-scan motion exceeding 0.2mm; HRFt: Canonical HRF and its time derivative; Volt: Volterra expansion of basis functions added; PM: Event duration used as parametric modulator; '1,2': events of type 1 and 2 represented as separate regressors (hypothesizing different generators), '1+2': events of type 1 and 2 merged into a single regressor (hypothesizing a common generator), '1+2+3, 1+2, 1': three regressors in case of EEG with 3 event types: one with all event types merged, one with events of type 1 and 2 merged, and events of type alone, respectively; F[1]: F-test across regressor(s) representing events of type 1, F[1;0 1]: F-test across regressor(s) representing events of type 2, T[1]: t-test on canonical HRF for regressor 1, T[-1]: t-test on inverted canonical HRF for regressor 1; PM: parametric modulation to test for effects of duration; Nil: no significant activation.

The overall findings in terms of yield, sign and concordance of the significant BOLD activations are summarized in Figure 9-2.

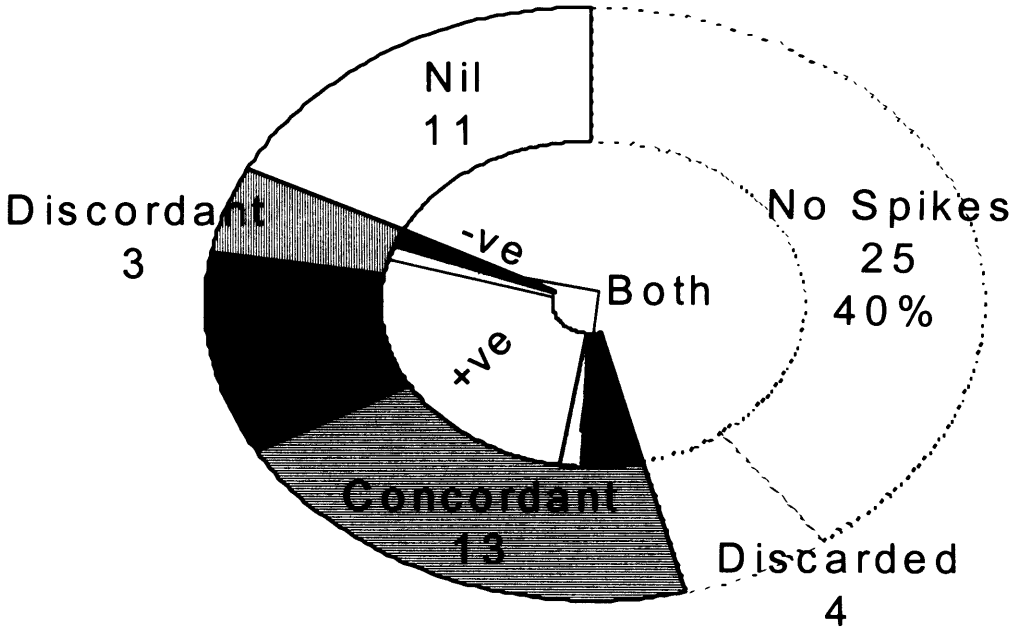

Figure 9-2 Summary of scanning and activation findings for basic model
In Figure 9-3 to Figure 9-6 we present more detailed results from 3 patients to illustrate different types of activation patterns, degrees of concordance and diagnoses. All other results are provided together as subparts of Figure 9-7.

Figure 9-3 *Concordant* activation and *Discordant* deactivation
Effect of event duration. Patient #13 had left hippocampal sclerosis and left-temporal IEDs. EEG/fMRI revealed a highly concordant cluster of left temporal activation (overall maximum indicated by red arrow in glass brain and cross-hair on EPI) with smaller clusters in the occipital region (a); more pronounced when discharge duration was taken into account (b); EPI overlay and hemodynamic response shown in (c) and (d), respectively. Incorporating duration into the model also resulted in a retrosplenial deactivation pattern, shown in (e-f), with the fitted hemodynamic response in (g).

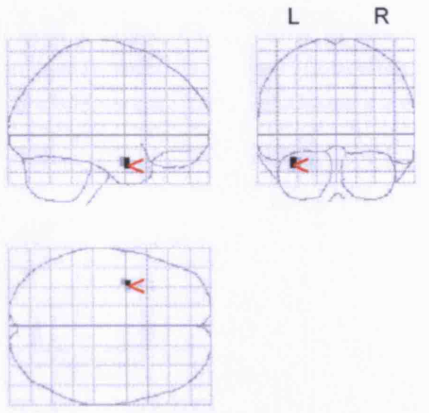
L
R

(a)

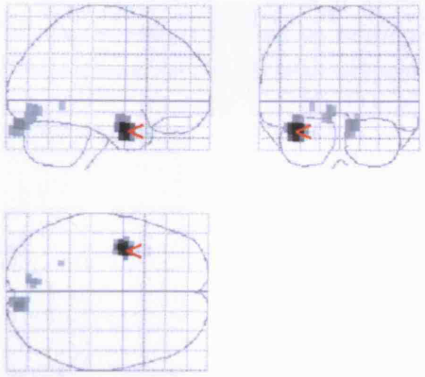

(b)

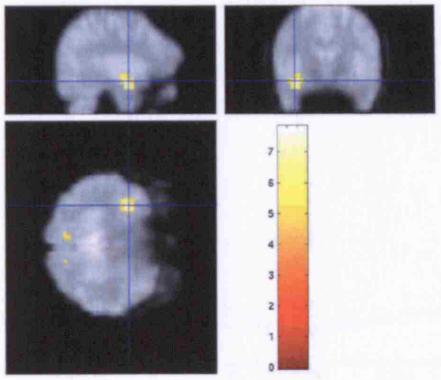

(c)

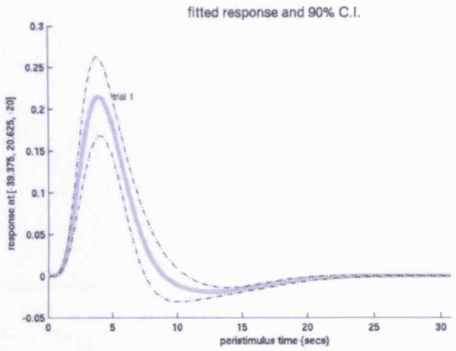
fitted response and 90% C.I.
trial 1
response at [-39.375, 20.625, -20]
peristimulus time (secs)

(d)

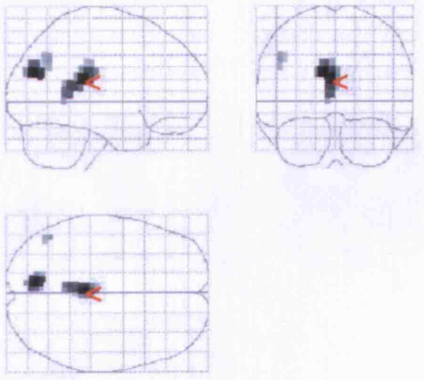

(e)

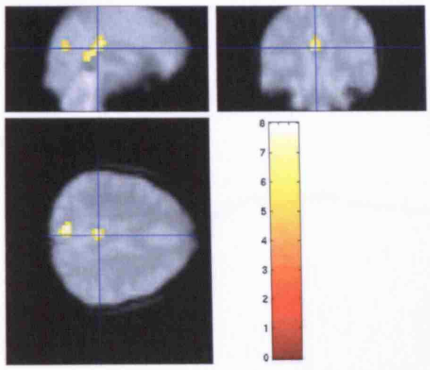

(f)

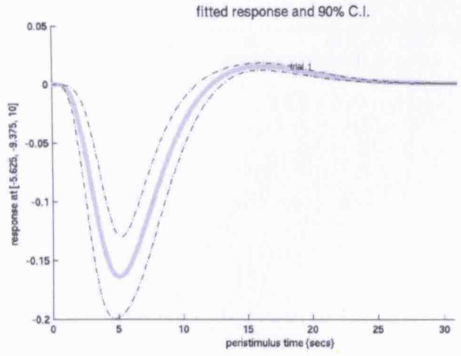
fitted response and 90% C.I.
trial 1
response at [-5.625, -9.375, 10]
peristimulus time (secs)

(g)

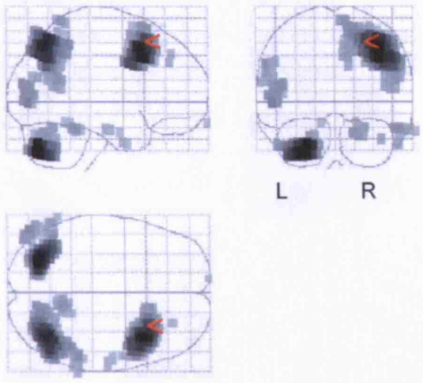
L
R

(a)

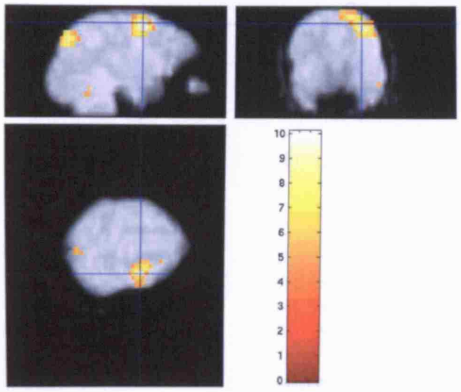
10
9
8
7
6
5
4
3
2
1
0

(b)

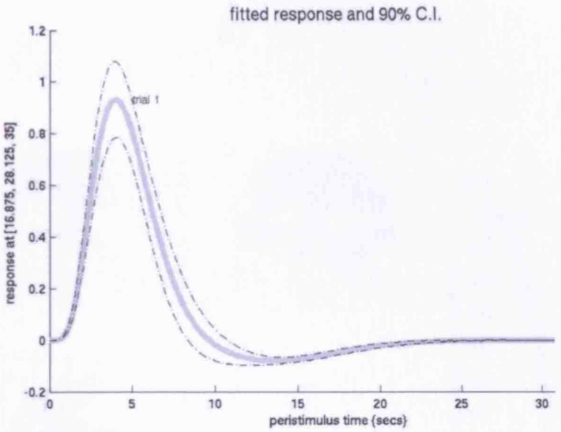
fitted response and 90% C.I.
response at [16.875, 28.125, 35]
trial 1
1.2
1
0.8
0.6
0.4
0.2
0
-0.2
0
5
10
15
20
25
30
peristimulus time (secs)

(c)

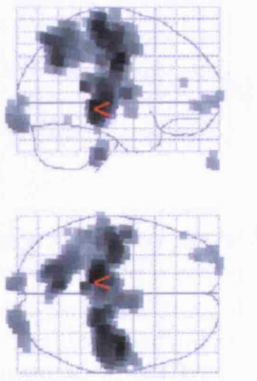

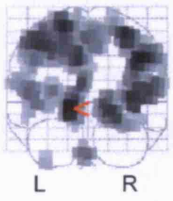
L
R

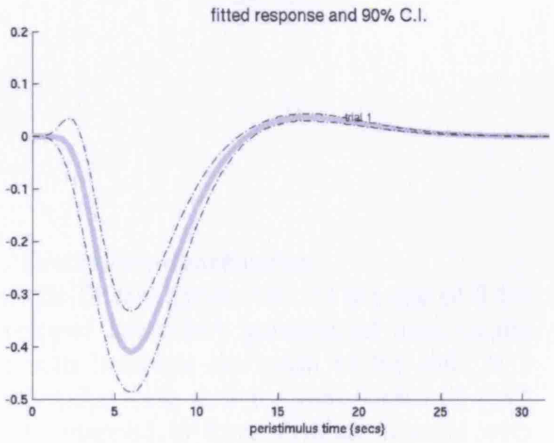
fitted response and 90% C.I.
trial 1
0.2
0.1
0
-0.1
-0.2
-0.3
-0.4
-0.5
0
5
10
15
20
25
30
peristimulus time (secs)

(d) (e)

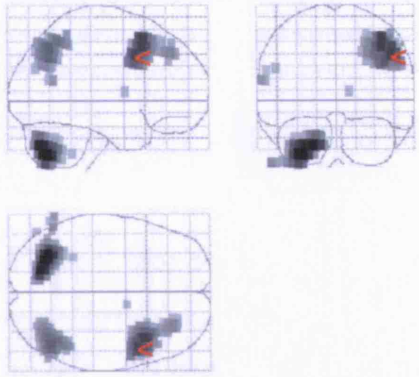

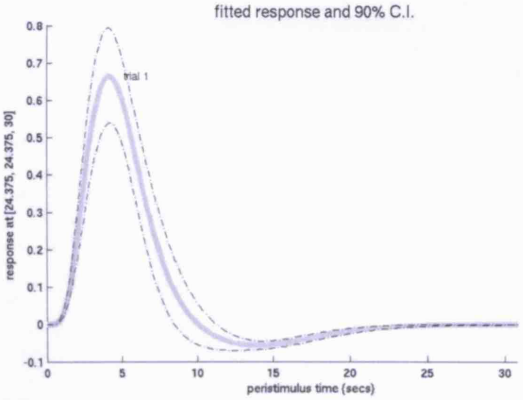

(f) (g)

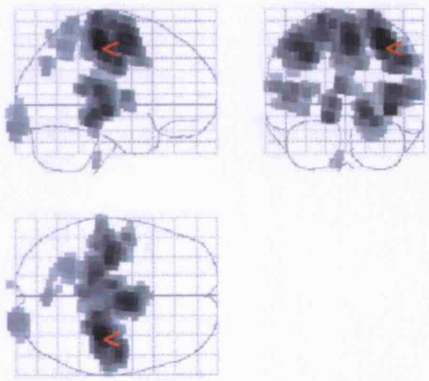

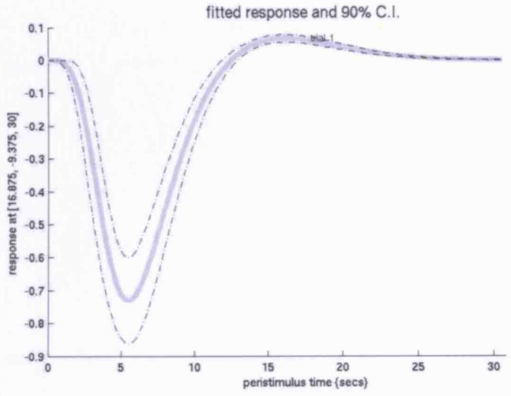

(h) (i)

Figure 9-4 *Concordant Plus* activation / *Discordant* deactivation
Patient #23 had a post-traumatic right middle frontal gyrus scar. At the age of 8 the patient suffered a head injury, and developed secondary generalized tonic-clonic seizures and partial seizures, beginning with head/eye deviation to the left. In 2 separate EEG-fMRI sessions, runs of polyspike-wave activity were captured (198 and 236 in each session respectively) and mapped to three distinct clusters with excellent reproducibility. A diffuse pattern of activation with a concordant maximum from the first session is shown in (a), overlaid onto the mean EPI in (b), with hemodynamic response shown in (c). There were also areas of deactivation (d) with the signal change shown in (e). The same results are also shown for the second session in (f-i).

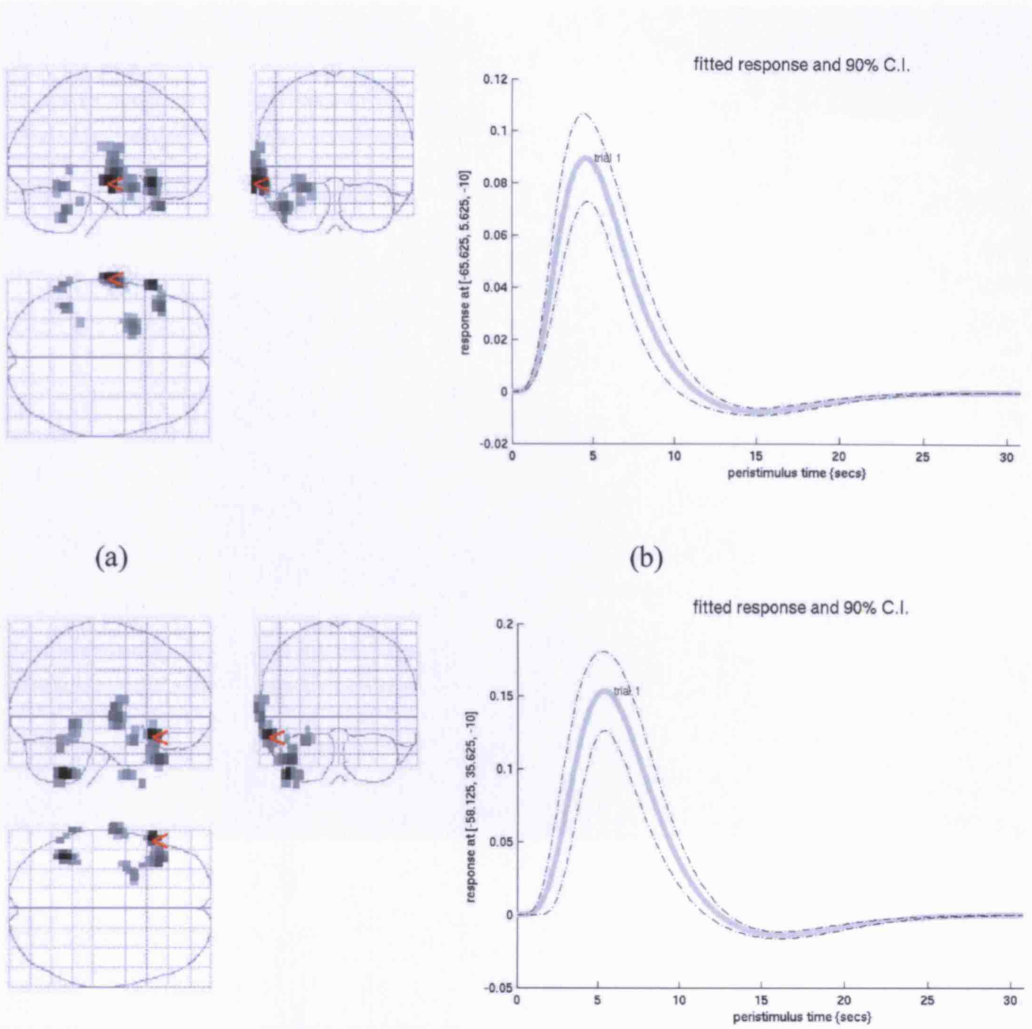

Figure 9-5 *Concordant* activation / *Discordant* deactivation
Patient #25 had left temporal lobe mass, probably neoplastic. During EEG/fMRI there was continuous left anterior temporal spiking. Results are shown from two separate sessions, the first analyzed using a semi-automated spike-detection technique (a-b) and the second, conventionally (c-d). Spike-linked activation was exclusively seen around the cavity (a,c). The anatomical relationships are seen more clearly on the EPI (e) and T1 (f) overlays. There was minimal deactivation in the first session (g,h). During the second session, the patient was asked to open and close her eyes periodically, as it was discovered that the rate of spiking could be altered by doing so. The eyes closed/open condition was modeled separately as a confound. Spike-linked deactivations were marked during this session (j), (k).

(e)

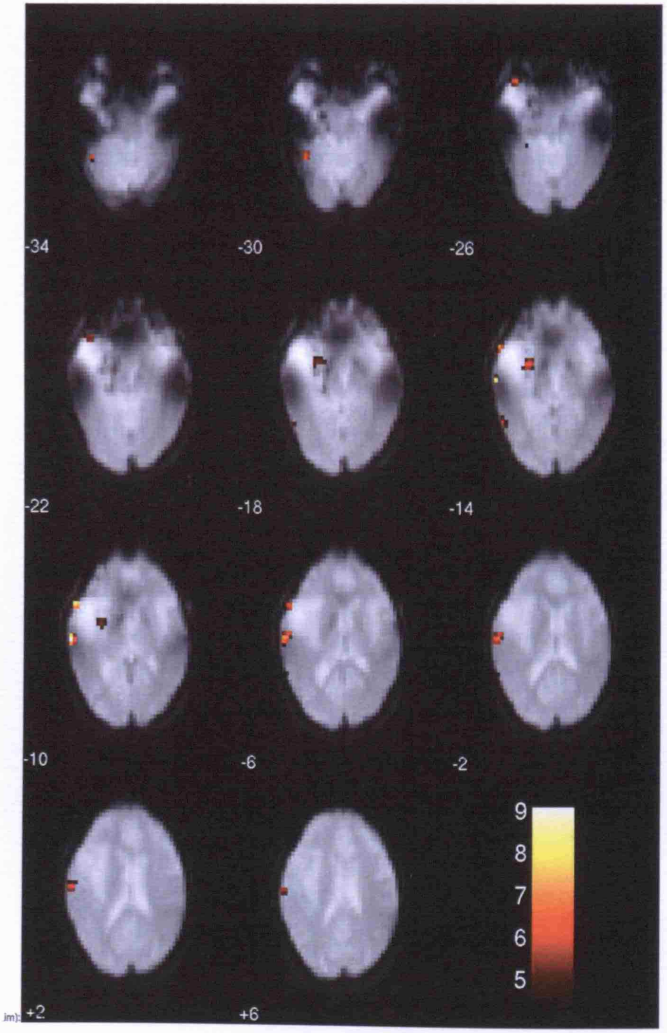

(f)

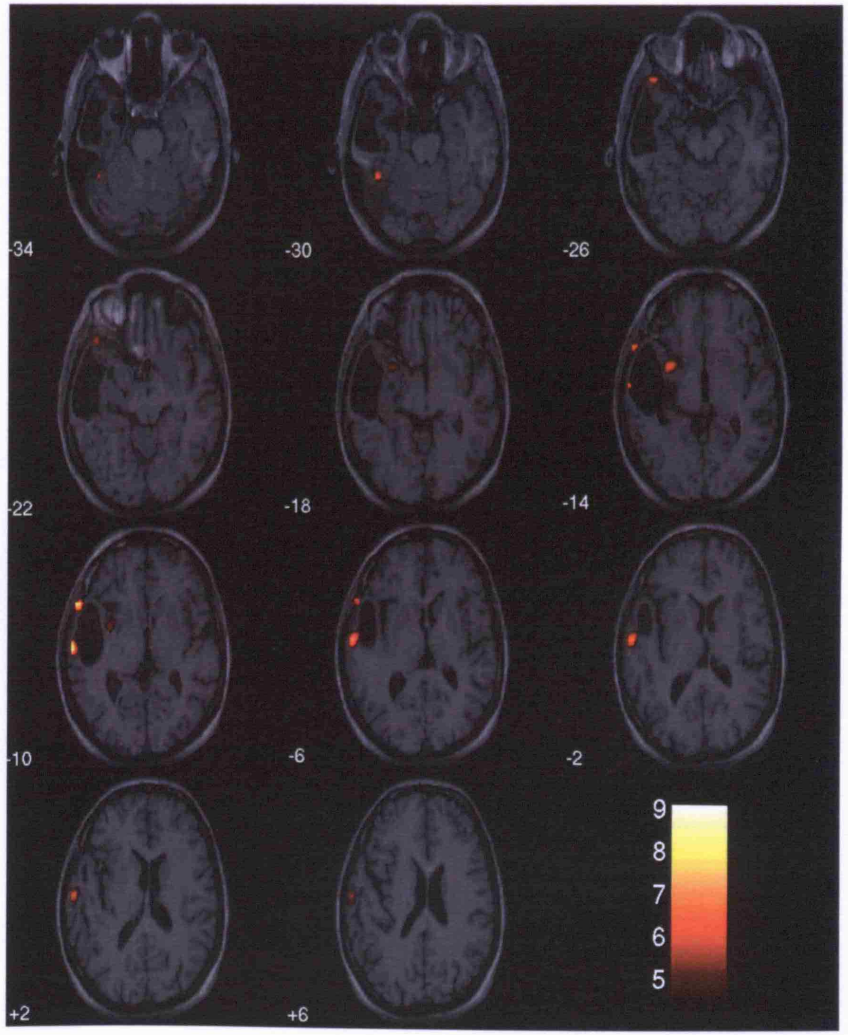

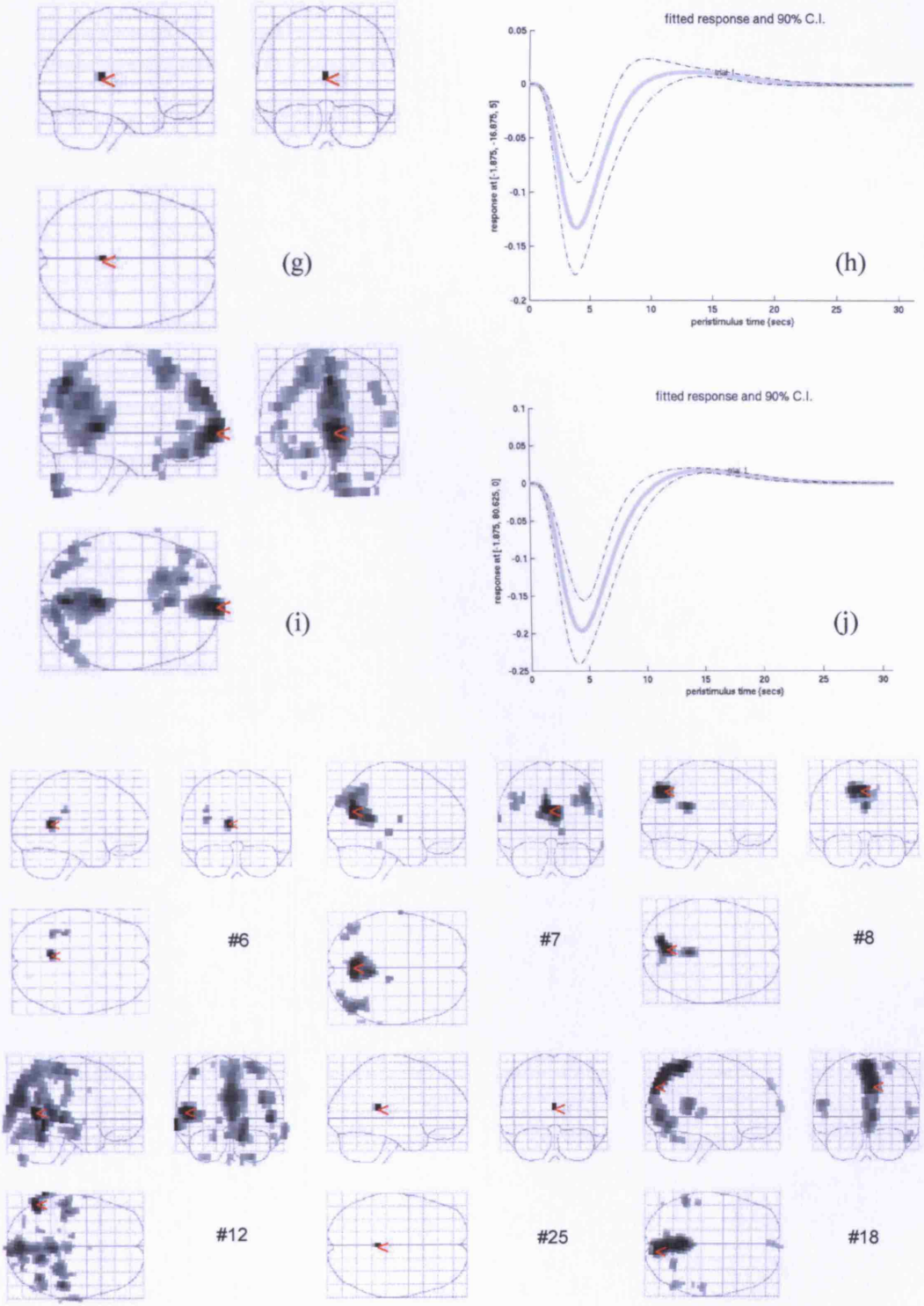

Figure 9-6 Bilateral precuneus deactivation
Pattern of bilateral medial occipital (precuneus) deactivation observed in 6 patients. SPM{-T} for negative HRFs, with the maximum indicated by red arrows. In case #12, the maximum is in the left parietal region, while in case #18 the maximum is in the posterior occipital region (sagittal sinus). See Figure 9-3 for case #13.

Figure 9-7 Other EEG/fMRI activations

W1 – Patient #1 was a 35 year-old lady who had previously undergone an extensive partial left temporal lobectomy for a neuroglial malformation at the age of 24. She had had lifelong seizures prior to surgery which took the form of absences, drop attacks and tonic-clonic seizures. Following surgery, there was resolution of her partial seizures but she continued to have tonic-clonic attacks. She underwent further implantation of subdural mats over the remaining hippocampus and temporal stump three years later but it was concluded that seizures were arising outside of the margins of the electrode array, most probably over left frontal mesial frontal or even contralateral frontal. On recent MRI the resection was seen to include the temporal pole, most of the amygdale and the hippocampus at least to the posterior margin of the brain stem, with a considerable amount of altered brain surrounding the cavity. She also has right hippocampal sclerosis.
EEG/fMRI reveals an area of right frontal deactivation with a smaller parietal cluster. The electroclinical seizure localization in this case was uncertain, although the possibility of a right frontal focus had been raised.

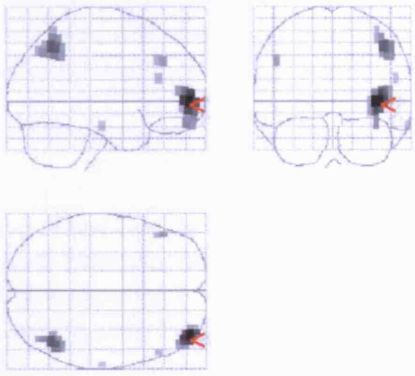

W2. Example of diffuse activation pattern: *Concordant Plus* activation / No deactivation. Patient #2 had an extensive malformation of cortical development in the right hemisphere, involving predominantly the parietal lobe but extending to the occipital and frontal lobes, plus focal atrophy of the left parietal lobe. Frequent widespread right-sided (fronto-central, posterior-temporal, and centro-temporal) spikes were observed on several routine EEGs. Seizure semiology was of brief episodes of outstretching of both arms with no post ictal confusion. EEG-fMRI revealed a concordant area of right frontal activation linked to right temporal IEDs.

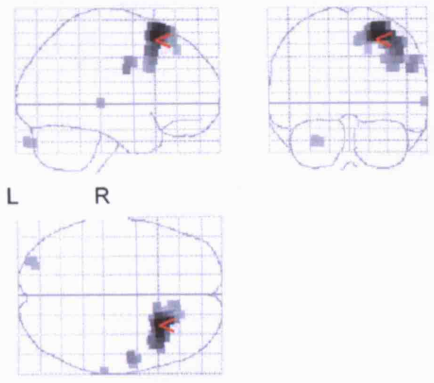

W3. Patient #3 had widespread predominantly posterior band and nodular heterotopia and bursts of posterior temporal/occipital discharges with left-sided emphasis. Seizure onset was at the age of 7 with blank staring, lip-smacking, vocalization and fiddling followed by post-ictal confusion and often secondary generalization. EEG-fMRI revealed clusters of bilateral posterior-temporal/occipital activation with left sided emphasis highly concordant with structural MRI and interictal EEG.

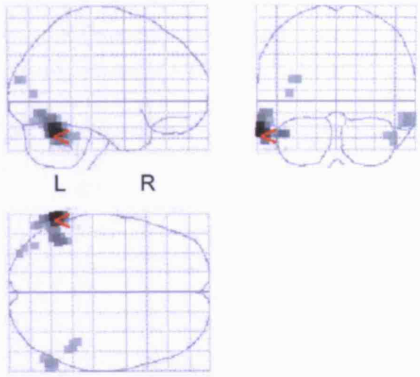

W4 – Patient #4 with a focal lesion within the left middle temporal gyrus. Electroclinical seizure onset however was diffuse. During EEG/fMRI there were several bursts of bilateral (R>L) polyspikes with several small widespread clusters of activation. We cannot be certain as to the biological significance of this result.

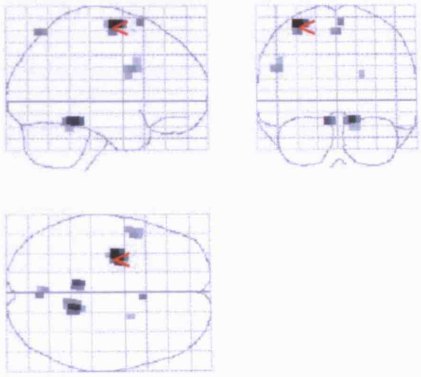

W5. Patient #6 had left hemisphere chronic encephalitis of adult onset(Krakow et al., 2001c;Lemieux et al., 2001b). Left temporal activation was again seen in response to high-amplitude left-temporal sharp-wave discharges with excellent reproducibility between these studies The concordant area of BOLD activation shown in (a) was linked to 250 high-amplitude left-temporal sharp-wave discharges. The maximum deactivation was in the posterior cingulate and there were also small islands of deactivation near the main cluster of activation (b).

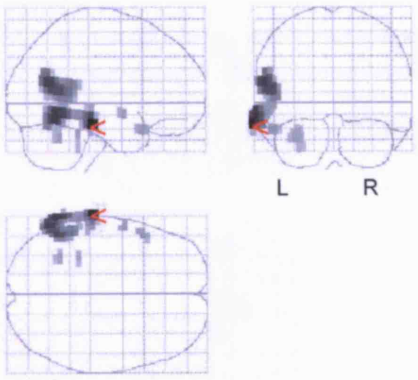

(a)

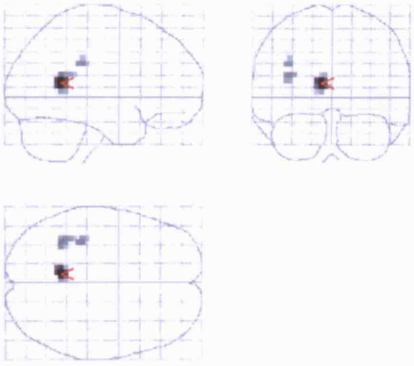

(b)

W6. Patient #7 was a 31 year-old patient with DNET of the left middle frontal gyrus. The patient had previously undergone a partial resection of the lesion with radiotherapy on the assumption that it was a low-grade astrocytoma. EEG/fMRI revealed a large area of midline frontal activation (a) linked to several hundred runs of bifrontal IEDs with more posteriorly placed clusters of deactivation also (b). (c) and (d) show corresponding results from a model taking run duration into account. Results from a separate session are shown in (e) and (f). The patient was later implanted with a subdural grid and underwent further resective surgery.

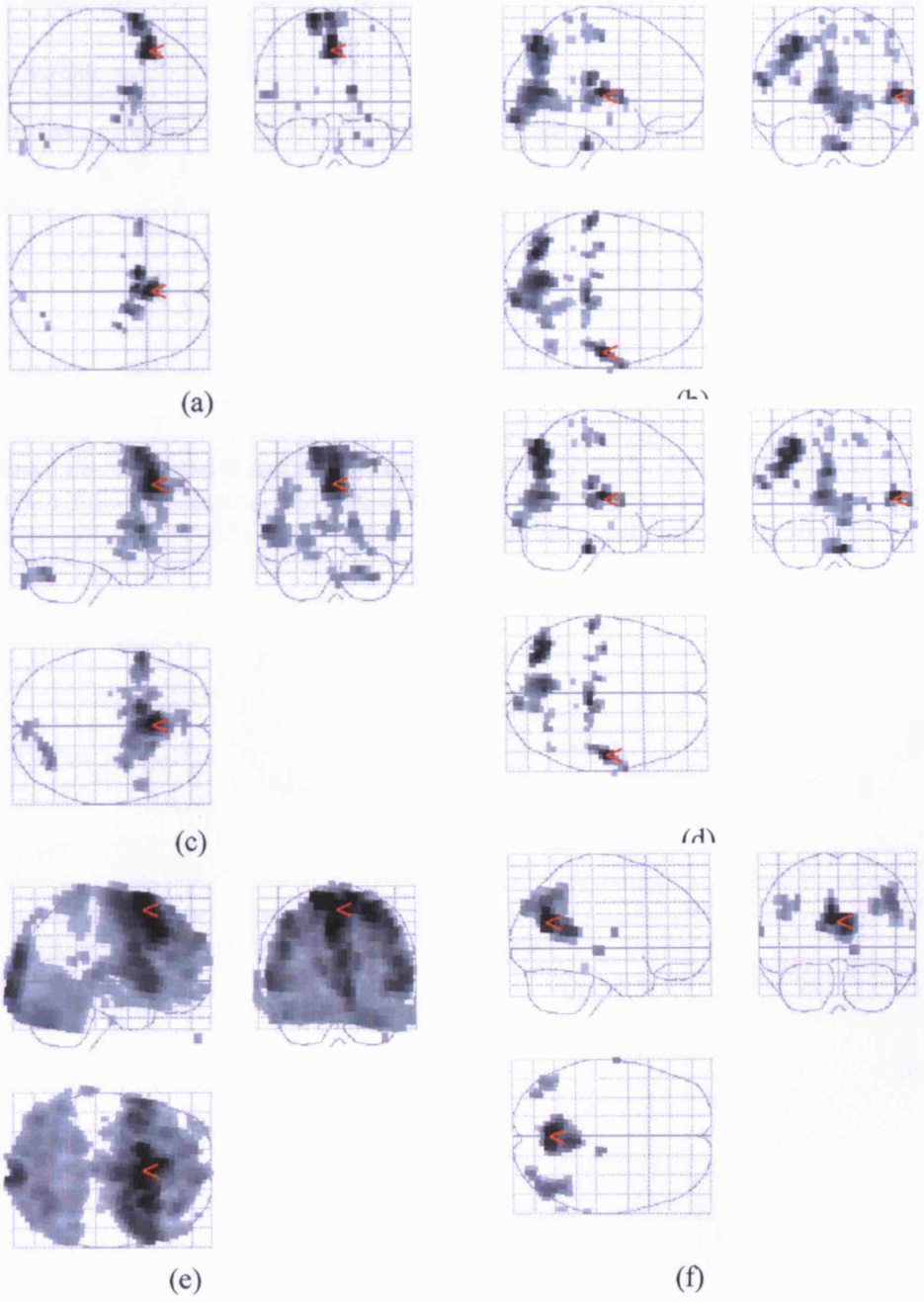

W7. Patient #8 had post-traumatic epilepsy of left hemisphere origin. Areas of activation linked to left temporal IEDs are show in (a). In addition, areas of deactivation are shown in (b).

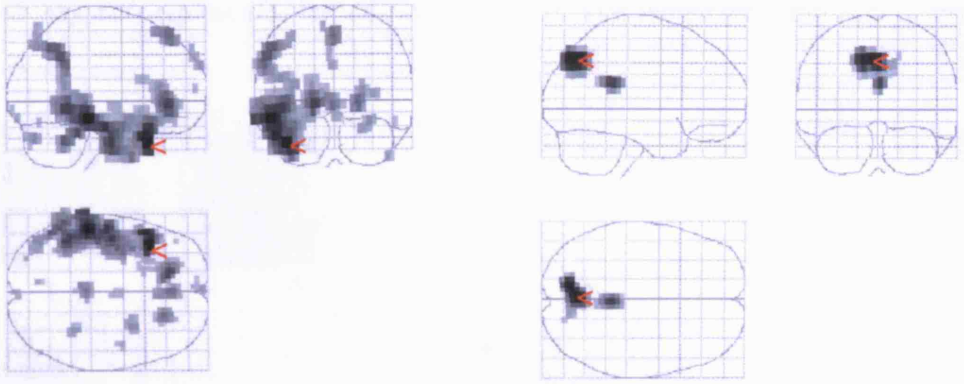

(a) (b)

W8. Patient #9 with severe diffuse left hippocampal sclerosis. 404 left temporal (F7) spikes were linked to a small cluster of ipsilateral anterior temporal activation (a). There were also clusters of deactivation more posteriorly and contra-laterally (b).

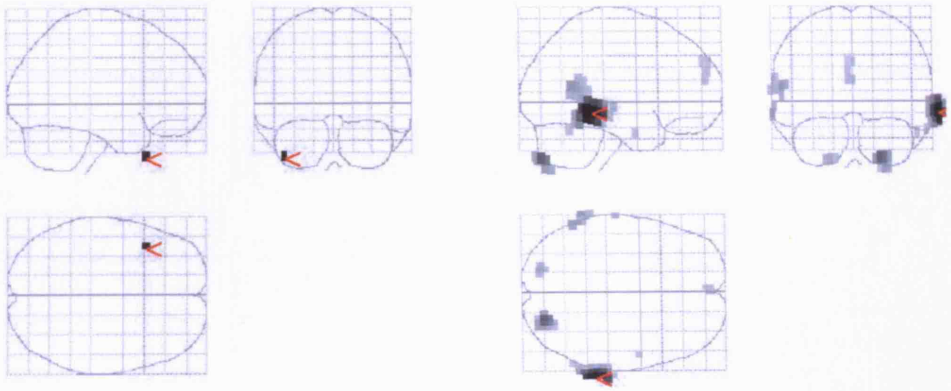

(a) (b)

W9. Patient #10 had left hippocampal sclerosis, a history of early febrile convulsions at 11 months, blank spells from the age of three, developing into complex partial seizures. The SPM{T} revealed large areas of activation (a) and SPM{-T} diffuse deactivation pattern (b) associated with several bilaterally synchronous bursts of spike-wave discharges. The EEG abnormality from which these fMRI changes were derived may have represented an additional generalized epileptic tendency.

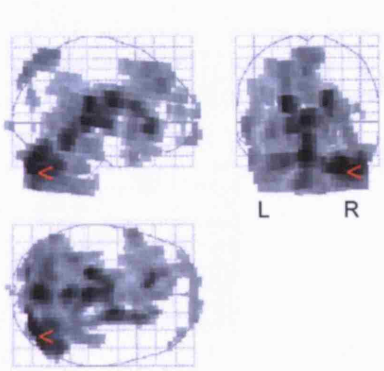

(a)

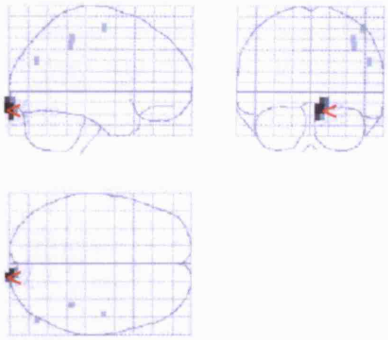

(b)

W10. Patient #11 with left temporal cystic encephalomalacia second to a neonatal subarachnoid haemorrhage, and left hippocampal sclerosis. EEG/fMRI revealed a small but highly concordant cluster of activation more posteriorly within the left mesial temporal lobe, linked to left posterior temporal IEDs.

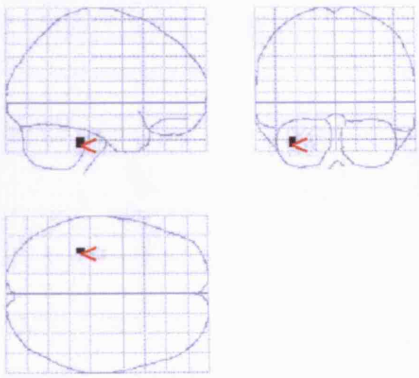

W11. Patient #12 with left hippocampal sclerosis and left anterior temporal spikes. EEG/fMRI revealed a highly concordant cluster of lateral temporal lobe activation (a). In addition there was deactivation more posteriorly and symmetrically (b).

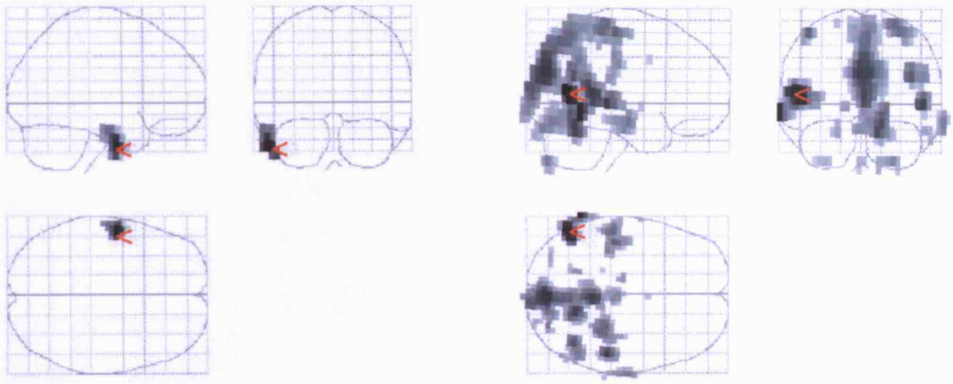

(a) (b)

W12. Patient #14 had cryptogenic refractory complex partial seizures (suspected frontal lobe semiology). The patient's first generalized tonic-clonic seizure occurred at 3 years of age with regular attacks since the age of 11 including simple and complex partial seizures beginning with an uncomfortable sensation in the stomach, facial twitching and lip smacking. Imaging was normal but interictal EEG showed bilaterally synchronous runs of generalized interictal polyspike-wave activity. 92 runs of polyspike-wave activity were modeled as single events; Focal activation was clearly visible within the right frontal lobe with weaker activations parietally. The activation was remarkably unilateral, in contrast to the IEDs.

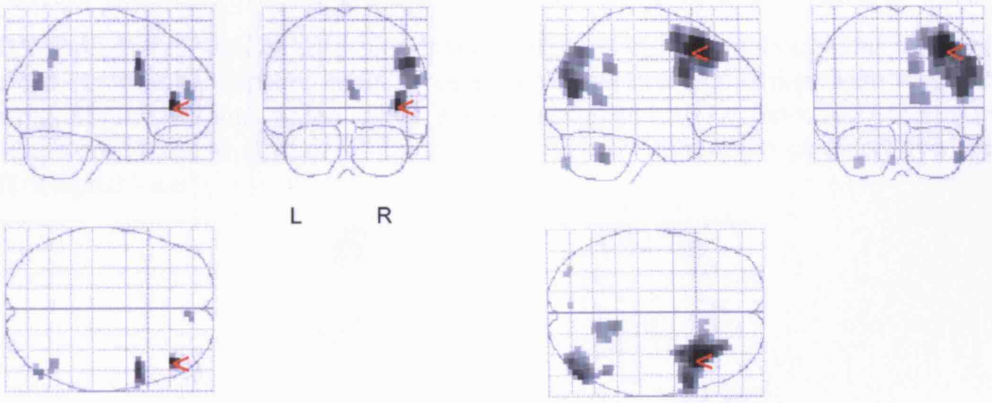

(a) (b)

W13. Patient #15 with cryptogenic occipital lobe epilepsy and left posterior temporal/occipital spikes. EEG/fMRI revealed a small but highly concordant area of activation.

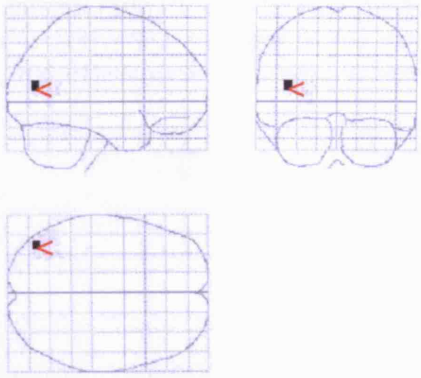

W14. Patient #18 with cryptogenic refractory complex partial seizures of bilateral diffuse multifocal onset. EEG/fMRI of left temporal IEDs revealed several clusters of deactivation predominantly along the superior sagittal sinus. We are uncertain as to the biological significance of the result.

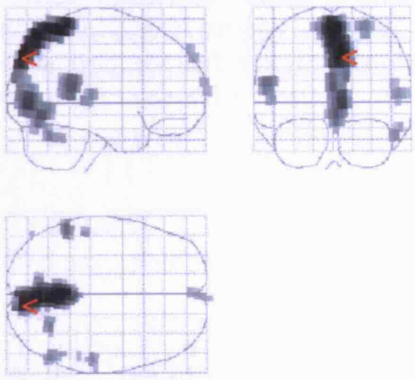

W15. Patient #29 with an extensive malformation of cortical development affecting the left cerebral hemisphere, mainly posteriorly. Left occipital spikes were recorded during EEG/fMRI and coded using a semi-automated spike detection technique. These were linked to clusters of deactivation, with the maximum centered over the left occipital lobe.

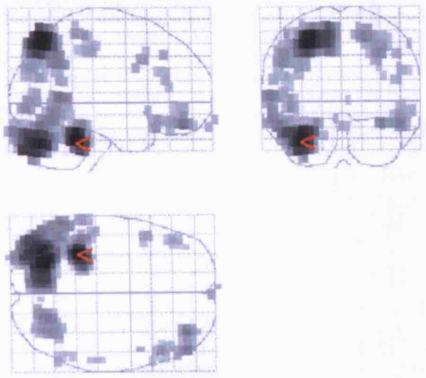

W16. Patient #31 with a malformation of cortical development comprising two large heterotopic nodules, frontoparietocentral and medial parietal. During EEG/fMRI there were frequent right-central spikes or varying amplitudes plus slow-waves. Clear spike-linked activation was observed exclusively within the larger of the nodules (a). In this case, incorporating focal slow waves into the model resulted in stronger and more extensive activation adjacent to the suspected symptomatogenic zone (b) (see (Diehl et al., 2003;Krakow et al., 1999a;Wieshmann et al., 2001)).

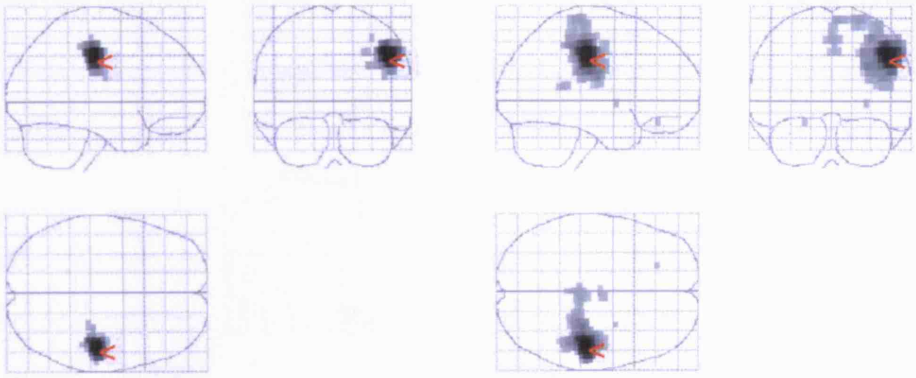

(a) (b)

W17. Patient #35 with a malformation of cortical development comprising left parietal polymicrogyria, left hemisphere atrophy and left hippocampal sclerosis. During EEG/fMRI there were frequent left anterior temporal spikes which were linked to a concordant cluster of left temporal activation.

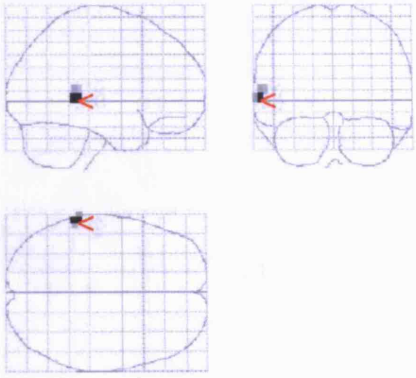

W18. Patient #36 with a focal left frontoparietal cortical dysplasia. During EEG/fMRI there was continuous left centroparietal spiking which was linked to a small midline frontal cluster.

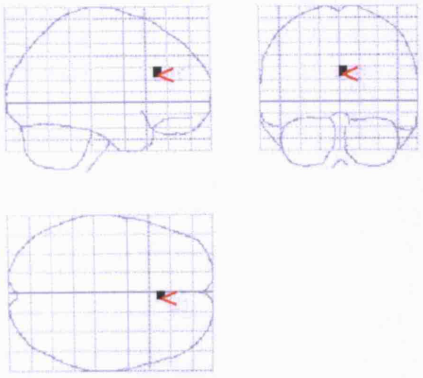

W19. Patient #37 with diffuse left-sided hippocampal sclerosis but temporal lobe seizures but of uncertain laterality. During EEG/fMRI, frequent left-sided mid-temporal IEDs were captured. These were associated predominantly with an ipsilateral cluster of deactivation within the left temporal lobe.

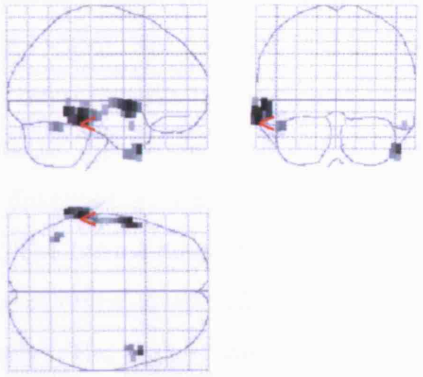

W20. Patient #39 with left hippocampal sclerosis. During EEG/fMRI there were left anterior temporal spikes which were linked to extensive clusters of activation, maximal within the left temporal lobe but also extending into occipital and parietal lobes (a). There were clusters of deactivation more inferiorly within the cerebellar hemispheres (b).

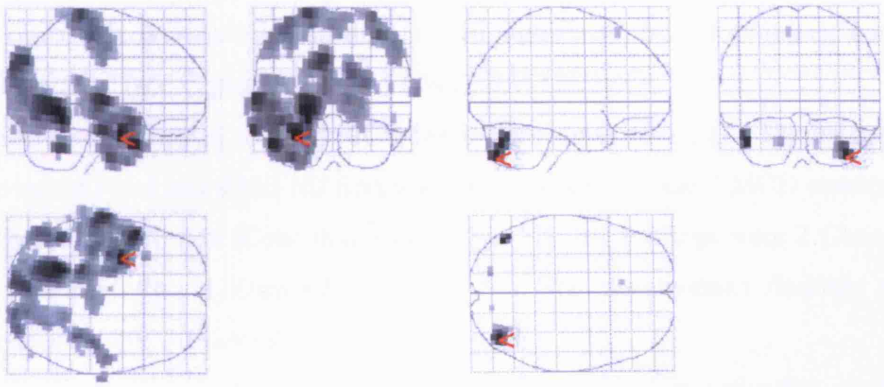

(a) (b)

9.4.1 fMRI activation and concordance

The clinical fMRI results for all patients, in whom IED were captured, are presented in Table 9-2. The full description of the fMRI models and statistics are provided in Table 9-3.

10 of 34 patients (29%) had significant positive BOLD changes only, 4 (12%) had negative changes only, 9 (26%) patients had both and 11 (32%) had no significant change. The mean number of discharges observed per experiment in cases with significant activation or deactivation was 355, and 148 for the cases with no activation or deactivation. The lowest number of discharges recorded in a case with activation or deactivation was revealed was 12 (case #15) but the activation was tiny (1 suprathreshold voxel only). The highest number of discharges captured in a case with no activation was 971 (case #20).

Significant IED-linked BOLD changes were seen in 23 of the 34 patients with discharges during fMRI acquisition. Considering positive and negative BOLD changes together, where available there was concordance with electro-clinical data in 17 patients, comprising 7 *Concordant* and 10 *Concordant Plus, Discordant* in 2 patients and *Nil* findings in 5. Activations were *Concordant* in 10 patients, *Concordant Plus* in 5, *Discordant* in 2. Deactivations were *Concordant* in 1 patient, *Concordant Plus* in 2 patients, and *Discordant* in 7. In the ten remaining patients with diffuse or uncertain localization, 4 had significant BOLD changes, 2 positive and 2 negative (see Figure 9-7: W1,W4,W12 &W18).

In terms of aetiology, 4 of the 8 MCD cases were Concordant, (3 *Concordant*, and 1 *Concordant Plus)* and 4 had *Nil* findings. Only one case of the 7 MCD cases showed significant deactivation (Concordant Plus). For HS, the findings were 2 *Concordant*, 1 *Concordant Plus* 1 *Discordant* and 1 *Nil*. The deactivation findings were 1 *Concordant Plus*, 3 *Discordant* and 2 *Nil*.

The maximum deactivation was remote from the concordant activation in all cases except #12. For example, deactivations were found in the central structures or retrosplenial (including bilateral medial occipital) in 8 cases (5 with lateralized or focal activations, 1 with midline activation (#7) and 2 without activation (#29 & #18)).

Of the five patients with no activation and a localized/lateralized seizure focus (#17, #20, #21, #27, #30), two (#17 & #30) showed few scattered specs on uncorrected SPMs but the others nothing. In these cases, analysis using a flexible set of basis

functions also failed to reveal any concordant foci. In #17 there was a single voxel in the brainstem, In #20 event onsets were automatically detected. There were scattered voxels throughout but no concordant foci. In #21 & #27 there was nothing and in #30 there was a very small right frontal cluster of uncertain significance.

9.4.2 The hemodynamic response to IEDs

The mean peak amplitude for activations (N=15) was 0.46% (range: 0.07-1.70) and −0.52% for deactivations (N=2; −0.16 and −0.88). The mean time to peak was 5.3s seconds (range: 2.5-9.5s) and the mean time to undershoot 21.2 seconds (range: 10.5-31.5s) for the positive responses, and mean time to (negative) peak 9s (6.5-11.5) and overshoot 24s (range: 21.5-26.5s) for negative responses. The mean undershoot to peak ratio was 0.54 (range: 0.02-1.21) for the positive responses and the mean overshoot to negative peak ratio was 0.91 (range: 0.88-0.94) for the negative responses. The data is provided in Table 9-4.

9.4.3 IED characteristics and the BOLD response

a. Cases with multiple IED types

Of the four cases with multiple IED types, the distinction was in terms of IED amplitude in 3 (#6, #31, #35), and field distribution in the other (#25). In summary: in patient #6 the smaller IEDs contributed very little to the activation such that failing to distinguish between the events would be detrimental to sensitivity. In case #25a, we were able to demonstrate a statistically significant difference in activation linked to the F7 versus T3 spikes with a relatively greater contribution of the former to the anterior segments of the activation in the first session. In the second session (#25b), this difference could not be seen. In case #31, the largest responses were linked to the large spikes followed in order by the smaller spikes and finally the slow waves but the difference in response was not statistically significant enough to warrant accounting for within the model. In case #35, there was a statistically significant difference between responses to the three event types (see Table 9-3 for detailed results).

Table 9-4 Hemodynamic response characteristics.
Concordant and *Concordant Plus* cases only, from global maximum cluster.

Case	IED		Hemodynamic response characteristics				
	N	Mean Interval (s)	Peak amplitude (%) (95% CI)	Peak Time (s)	Undershoot amplitude (%) (95% CI)	Under shoot Time (s)	Under shoot /Peak Ratio
A2	82	15.57	0.92 (0.48)	4.5	-0.26 (0.37)	12.5	0.28
A3	50	40.6	0.78 (0.34)	5.5	-0.63 (0.49)	25.5	0.8
A6	483	3.98	0.3 (0.09)	4.5	-0.08 (0.08)	30.5	0.27
A7a	371	5.66	0.42 (0.17)	4.5	-0.36 (0.15)	17.5	0.84
A7b	300	6.89	0.34 (0.1)	5.5	-0.25 (0.1)	19.5	0.73
A8	178	11.82	0.57 (0.1)	4.5	-0.2 (0.09)	13.5	0.36
A9	404	5.03	0.18 (0.08)	4.5	-0.08 (0.08)	30.5	0.46
A11	230	9.01	0.23 (0.12)	4.5	-0.07 (0.11)	19.5	0.3
A12	638	3.28	0.2 (0.08)	5.5	-0.11 (0.08)	10.5	0.54
A13	79	25.83	0.54 (0.24)	6.5	-0.41 (0.2)	28.5	0.75
A15	12	85.92	1.7 (0.81)	6.5	-0.63 (0.59)	14.5	0.37
A23a	167	12.63	0.48 (0.22)	2.5	-0.44 (0.18)	15.5	0.93
A23b	236	8.14	0.44 (0.18)	6.5	-0.29 (0.17)	18.5	0.66
A25a	630	3.23	0.12 (0.07)	6.5	-0.14 (0.07)	27.5	1.21
A25b	2710	0.77	0.07 (0.03)	4.5	-0.03 (0.03)	21.5	0.45
A29	1472	1.43	-0.16 (0.06)	6.5	0.14 (0.06)	26.5	0.88
A31	447	4.69	0.31 (0.11)	5.5	-0.1 (0.1)	28.5	0.33
A35	109	19.07	0.37 (0.21)	9.5	-0.15 (0.2)	15.5	0.41
A37	72	28.15	-0.88 (0.53)	11.5	0.83 (0.43)	21.5	0.94
A39	622	3.38	0.22 (0.06)	3.5	-0.01 (0.05)	31.5	0.02

b. Cases with runs of IEDs

In case #3 there was no significant effect over the additional regressors, indicating that event duration was not a factor. In #7a, #13, #23a and #23b however, a significant proportion of variance was attributable to event duration (see Figure 9-4). Interestingly, in #13, there was retrosplenial deactivation in addition with the more complex model (see Figure 9-3).

c. Cases with very frequent IEDs

Significant non-linear effects were demonstrated in #6, #7b, #8, #9, #12, #39, but not #31 & #11. Notably, in #6, #7, #8, #12 & #39 the second-order Volterra kernels were negative indicating a saturation effect of the BOLD response to frequent events. In case #9 non-linear positive effects were observed most significantly within the ipsilateral cluster but also within the contralateral cluster.

9.4.4 Factors influencing activation

On average all motion parameters were larger in the non-BOLD cases with the difference reaching statistical significance for the mean scan-to-scan displacement, |d'|. The mean number of spikes was larger in the BOLD group but this did not reach significance. However, cases with runs of IEDs were significantly over-represented compared to cases with individual IEDs. Abnormalities in the background EEG were also a significant factor for activation. The results of these analyses are shown in Table 9-5.

Table 9-5 Experimental factors and presence of fMRI activation.

Experimental Factor	**BOLD Present** (n=23)	**BOLD Absent** (n=11)	**Statistic**
Head Motion (Mean ± Std)	0.05 ± 0.04	0.09 ± 0.055	P<0.005* (T)
Mean $\|d'\|$ (mm)	2.47 ± 5.57	23 ± 10.3	P<0.28 (T)
Max $\|d'\|$ (mm)			
Jerks	18.7 ± 30.2	54.9± 63.2	P<0.02 (T)
IED Characteristics			
Number (Mean ± Std)	355.2 ± 415.5	147.7± 269.1	P<0.12 (T)
Runs/ Spikes (n=8/ 31)	8/ 18	0/ 13	P<0.03* (χ^2)
EEG Background			
Mild/ Moderate/ Severe (n=20/ 9/ 10)	18/ 5/ 3	2/ 4/ 7	P<0.004* (χ^2)

9.5 Discussion

The application of continuous EEG-correlated fMRI in focal epilepsy has allowed us to show a wide range of activation patterns linked to IEDs and address a number of important questions on the relationship between the characteristics of the EEG record and regional hemodynamic changes. Our approach is based on a novel modeling framework capable of accounting for various important EEG features and minimize the impact of undesirable effects such as motion.

9.5.1 Methodological Aspects

9.5.1.1 Choice of Subjects and EEG recording

We chose to study a wide range of subjects from the outset, motivated by the need to establish the full range of fMRI correlates for interictal EEG events, irrespective of pathology. Our patient population was heterogenous providing a good base from which to explore methodological issues but with less scope for clinicopathological correlation. The choice of fMRI acquisition sequence was motivated primarily by the desire to obtain whole brain coverage with good SNR and hence investigate IED-related changes throughout the brain. Whilst the benefits of recording a greater number of EEG channels are obvious, EEG here was used primarily for spike detection where localization was already known. The simultaneous use of high-density EEG could allow for more in depth studies of individual events or classes of events, as well as dipole modeling, all of which are the subject of ongoing efforts (Liston et al., 2006).

9.5.1.2 EEG Classification & Automatic spike detection

The manual interrogation of EEG data (EEG coding) is perhaps the most crucial part of analyzing continuously-acquired EEG-fMRI data. For the purposes of modeling the entire fMRI time-series fully, one would need to account for every possible event or feature that may influence the BOLD (Blood Oxygen Level Dependent) response of the voxels under investigation. Our strategy was therefore to 'over-code' the EEG both in terms of the number of events that may be epileptiform in origin and the sub-grouping of events so that the most information is extracted from each recording. We used a consensus of opinion. This is an important step up from how EEG information was used in spike-triggered fMRI studies, whereby scanning was restricted to events with pre-determined features (Krakow et al., 1999b).

We were able to show the benefits of using automated event detection to identify IEDs where visual assessment was technically difficult due to large numbers of IED. For example, in case #25 we demonstrate the activations derived using automated event detection compare extremely well with those derived conventionally from a separate session. In patients #29 and #39 we were able to demonstrate concordant BOLD changes using this method also. To our knowledge automatic event detection has never been applied to EEG-fMRI.

9.5.1.3 Motion & Modeling implications

Due to the noisy nature of the fMRI signal, the ability to infer effects rests on careful hypothesis testing. Devising realistic models based on the EEG events of interest is therefore crucial and remains one of the technique's main challenges. Our results show that the IED-related BOLD responses could be captured effectively using the canonical HRF (plus its time derivative). Previously, the application of the Fourier expansion set, a model capable of accommodating very varied shapes of the BOLD response, allowed us to confirm the physiological nature of concordant IED-related BOLD responses in specific cases (Diehl et al., 2003;Lemieux et al., 2001b). In the patients studied here, this more flexible modeling approach resulted in no increase of concordant activations. This suggests that the approach adopted, based on the canonical HRF and its time derivative, is sufficiently capable of capturing the variability in BOLD response but there are several intermediate strategies (e.g. the sequential application of multiple HRFs followed by correction for multiple tests (Bagshaw et al., 2004b)). The optimal choice of basis functions remains an open question; however higher degrees of modeling flexibility generally translate into lower sensitivity and specificity.

Bagshaw et al (Bagshaw et al., 2005) suggested that event duration should be considered when modeling IED-related BOLD. They looked at the effect of IED duration on the positive BOLD response in selected mixture of patients with both idiopathic generalized and focal epilepsy but did not statistically assess the significance of any extra contribution. We were able to demonstrate that significantly improved models could be obtained by accounting for different EEG event topographies and durations. For example, the results for case #6 demonstrate that failing to distinguish between the two event types within the model would reduce sensitivity since the small spikes do not contribute significantly to the

activation. For runs of IEDs, we were able to demonstrate significantly improved models in three cases. Together, these findings show that in cases with different types of IED, a decision ought to be made concerning whether or not the different types are likely to share the same anatomical generators. Where this is not the case then separate regressors ought to be used and tested individually. In cases where different types of IED are presumed to share a unique generator nested models should be used to determine the best strategy. Moreover, consideration ought to be given to including both duration and saturation effects in the modeling in cases featuring runs or very frequent IED, with significant effects demonstrated in some cases in our series.

Motion remains an important concern in the analysis of fMRI data, even with the best immobilization measures (Lund et al., 2005) and particularly in patient populations.. In cases where the motion bears no relationship to the experimental variables (i.e. non-stimulus correlated) activations linked to the effects of interest may be 'drowned out' by the consequent increase in noise. However, in cases where the head motion is stimulus correlated (i.e. coincident with events of interest), the result can be artifactual areas of false activation or a decrease in specificity. The effects are complex and unpredictable and we do not feel that this point has received due consideration in the epilepsy literature so far (Salek-Haddadi et al., 2003a). We address this by incorporating motion into the fMRI model, reducing the likelihood that any given activation is the result of motion alone, partly trading sensitivity for specificity.

9.5.1.4 The assessment of concordance

There are two important choices that have to be made in assessing concordance, the first is what to judge against and the second is how. Like previous studies, we chose to assess concordance by comparing EEG/fMRI against the best available indicators to the epileptogenic zone. The inclusion of patients with diffuse or uncertain electroclinical localization was motivated by the need to study more patients in order to test the technique at a time when no other continuous EEG/fMRI studies were available. Both ourselves (Lemieux et al., 2001b) and others however have since established some basic principles (Al-Asmi et al., 2003;Bagshaw et al., 2004a;Benar et al., 2002). Despite the lack of surgical data in our series, we avoided judging

fMRI localization against scalp EEG alone as we felt this would be of less clinical interest and prevent comparison with other EEG/fMRI studies.

How to judge concordance is not a new problem in EEG/fMRI (Salek-Haddadi et al., 2003a). fMRI maps generally contain multiple activations that are strongly threshold dependent. In contrast to other, even more recent studies (Federico et al., 2005;Kobayashi et al., 2005c), we have chosen to use a conventional and fixed thresholding method across the board to avoid bias and facilitate comparison. There are obvious difficulties in translating imagery as complex as fMRI maps into words and lobes especially given that neither fMRI activations nor pathological lesions respect the traditional anatomical boundaries between lobes or quadrants. This is however necessary to compare against 'electroclinical localization' as derived from a range of different sources. The distinction between Concordant and Concordant Plus is also important in that more distant or diffuse activations are either indicative of remote effects or represent false positive activations (e.g. stimulus correlated motion) both of which are important to recognize. Several previous studies have potentially ignored such effects, reporting only on activation within a region of interest (Archer et al., 2003b) or lesion (Kobayashi et al., 2005c). We feel the reporting of activations in their entirety is important and the publication of activation maps using the glass brain rather than single slices should be encouraged (Salek-Haddadi et al., 2003a).

9.5.2 Clinical and neurobiological aspects

9.5.2.1 Yield, localization and clinical relevance

Overall, BOLD changes were revealed in 67% of patients in whom IEDs were detected during scanning and this is in line with previous studies (Al-Asmi et al., 2003;Krakow et al., 2001b). There was a tendency for more spikes, less motion, more runs of IEDs and less EEG background abnormality in cases with activation, which has not been shown before. A similar analysis for the negative responses revealed that the BOLD cases had three times the number of events as the non-BOLD cases ($p<0.011$) and a significantly lower degree of head motion. The activation/deactivation patterns were mostly diffuse, involving more than one lobe. Reproducibility, assessed in five cases was good, and included two cases with no activation on both occasions. The relationship between extent of EEG abnormality and fMRI activation pattern was varied, bilateral activation patterns being sometimes linked to bilateral IEDs (e.g. cases #3 and #7), while in some cases unilateral cerebral

activations were found with bilateral IEDs (e.g. #23, figure 4, & #14) and vice versa (#2, #37, #39).

All but two patients with localized/lateralized or bifocal electroclinical findings in whom there was activation showed some degree of concordance (#10, #36). The BOLD changes were often much more extensive than expected from the focal nature of the electroclinical findings, and often included discordant areas. This is similar to the findings from other functional interictal studies in partial epilepsy such as ^{18}FDG PET, which typically reveal much larger areas of metabolic change than the epileptogenic zone, possibly reflecting areas of functional deficit (see (Mauguiere and Ryvlin, 2004)) .

Temporal spikes generally resulted in concordant (lateral) activations with the single discordant finding linked with bilateral fronto-central spikes. Deactivations were common in temporal lobe epilepsy, and often remote. The general picture for activations in MCD is very similar to that in TLE, with good concordance and activations often localized within the structural abnormality (e.g. case #2).

In general, positive changes tended to be highly concordant at least for the lobe of presumed seizure localization, while negative changes appeared to be much less in agreement with the electroclinical findings and were more critically dependent on the number of IEDs, possibly reflecting a smaller or more variable effect for individual IEDs compared to the positive BOLD changes. A pattern of deactivation in the retrosplenial region (precuneus and posterior cingulate) was revealed in 7 patients including #13, mainly with focal or unilateral IEDs, corresponding to a notably higher proportion of cases than previously reported (Kobayashi et al., 2005a). No case of clear activation in the same region was found. The majority of these cases had very frequent IEDs or runs. The significance of this pattern is uncertain. The retrosplenial region has been implicated in fluctuations of cognition level (Gusnard et al., 2001) and shows changes in activity in relation to both the EEG alpha band (Laufs et al., 2003b) and generalized spike-wave (Hamandi et al., 2005b). Deactivation here may reflect downstream state changes linked to consciousness (Kobayashi et al., 2005b).

9.5.2.2 The Hemodynamic response to IEDs

A high degree of variability in the shape of the HRF has been reported in normal subjects (Aguirre et al., 1998b). Based on our results, and from the data available to

far (Benar et al., 2002;Krakow et al., 2001b;Lemieux et al., 2001b), it would appear that in general IEDs observed on the scalp are associated with physiological hemodynamic responses. Our data also suggests that negative responses tend to differ from the mirror image of the canonical (positive) HRF. Frequent events resulted in very small peak BOLD changes and in saturation (non-linear effects). The data is shown in Table 9-4.

9.5.2.3 Clinical relevance

The clinical relevance of EEG-fMRI rests on its ability to provide novel localizing information non-invasively and objectively in a good proportion of patients. This study indicates the technique's capability in patients with focal epilepsy and frequent IEDs.

In patients in whom electroclinical data already provides a likely generator, EEG-fMRI may provide some degree of confirmation. The finding of localized activation in patients with poor electroclinical localization (#1, #4, #14, #18) is at least tantalizing in so far as indicating a potential role for EEG-fMRI to provide new hypotheses for testing, for example as part of an implantation strategy for invasive EEG studies. A true interdisciplinary approach however remains essential to successfully carrying out such work in the clinical setting.

9.5.3 Future work

Higher density EEG allowing source modeling could enable the study of more subtle differences in IEDs and associated BOLD responses, especially at higher field strengths. Physiological noise (cardiac, respiratory and background EEG rhythms) modeling also holds promise is this regard (Liston et al., 2005).

Clinically, future investigation need focus on correlation/ validation with invasive monitoring and surgical/pathological findings in specific syndromes to allow the direct testing of localization hypotheses derived from fMRI. Important insights into the neuronal basis of the fMRI signal have been gleaned from combining fMRI with simultaneous invasive electrophysiological recordings in monkeys (Logothetis and Pfeuffer, 2004). Similar studies in epilepsy surgery patients (Arnold et al., 2002) could go some way toward establishing the link between scalp EEG events are the corresponding EEG/fMRI activations.

10. Chapter 10: Interictal EEG/fMRI of idiopathic & secondarily generalized epilepsies

10.1 Summary

We used simultaneous EEG and functional MRI (EEG–fMRI) to study generalized spike wave activity (GSW) in idiopathic and secondary generalized epilepsy (SGE). Recent studies have demonstrated thalamic and cortical fMRI signal changes in association with GSW in idiopathic generalized epilepsy (IGE). We report on a large cohort of patients that included both IGE and SGE, and give a functional interpretation of our findings. Forty-six patients with GSW were studied with EEG–fMRI; 30 with IGE and 16 with SGE. GSW-related BOLD signal changes were seen in 25 of 36 individual patients who had GSW during EEG–fMRI. This was seen in thalamus (60%) and symmetrically in frontal cortex (92%), parietal cortex (76%), and posterior cingulate cortex/precuneus (80%). Thalamic BOLD changes were predominantly positive and cortical changes predominantly negative. Group analysis showed a negative BOLD response in the cortex in the IGE group and to a lesser extent a positive response in thalamus. Thalamic activation was consistent with its known role in GSW, and its detection in individual cases with EEG–fMRI may in part be related to the number and duration of GSW epochs recorded. The spatial distribution of the cortical fMRI response to GSW in both IGE and SGE involved areas of association cortex that are most active during conscious rest. Reduction of activity in these regions during GSW is consistent with the clinical manifestation of absence seizures.

10.2 Introduction

Generalized spike wave (GSW) activity, is the electroencephalographic (EEG) hallmark of idiopathic generalized epilepsy (IGE), occurring in runs of 2.5-4 Hz spike and slow wave activity, typically arising from a normal background EEG (Duncan, 1997a). GSW is also seen in symptomatic generalized epilepsies where it is usually associated with an abnormal background EEG, and clinical evidence of other neurological dysfunction (Holmes et al., 1987).

The pathophysiological substrate of GSW remains enigmatic. The debate between a sub-cortical origin "the centrencephalic hypothesis" (Jasper and Droogleever-Fortuyn, 1947) versus a cortical origin (Marcus and Watson, 1968) was reconciled to an extent by the corticoreticular hypothesis (Gloor, 1968). This proposed a role for

both cortex and subcortical structures, with aberrant oscillatory rhythms in reciprocally connected thalamocortical loops normally involved in the generation of sleep spindles (Gloor, 1968), leading to GSW. The primary neuroanatomical and neurochemical abnormality in IGE remains undetermined with evidence and arguments for onset in either cortex or thalamus (Avoli et al., 2001;Timofeev and Steriade, 2004).

Much of the evidence pertaining to the pathophysiology of GSW comes from invasive electrophysiological and neurochemical recordings in animals (Avoli et al., 2001). A small number of intracranial studies have been reported in man in which spike wave activity was recorded in both thalamus and cortex (Niedermeyer et al., 1969;Velasco et al., 1989;Williams, 1953). The spatial sampling of depth studies is limited to the immediate vicinity of the implanted electrodes, and their invasiveness, in the absence of clinical benefit precludes their current use in IGE.

Combining EEG recording with fMRI (EEG-fMRI) enables the non-invasive mapping of haemodynamic correlates of specific EEG events or rhythms (Salek-Haddadi et al., 2003a), by means of the blood oxygen level dependent (BOLD) contrast (Ogawa et al., 1990). Studies in patients with focal epilepsy have demonstrated spatially concordant BOLD activations in relation to focal epileptiform discharges (IED), evidence that EEG-fMRI can provide localizing information on generators of these discharges (Krakow et al., 1999b;Warach et al., 1996) (Al-Asmi et al., 2003;Jager et al., 2002;Lemieux et al., 2001b;Salek-Haddadi et al., 2006;Seeck et al., 1998). Whether EEG-fMRI is able to shed further light on the pathophysiology of GSW, by localizing generators of these discharges remains to be seen.

In Chapter 8 (Salek-Haddadi et al., 2003g) we described using continuous EEG-fMRI at 1.5T, described bilateral thalamic BOLD signal increase, and widespread cortical decrease in a patient with juvenile absence epilepsy (JAE). Aghakhani et al. (Aghakhani et al., 2004) with continuous EEG-fMRI at 1.5T found thalamic haemodynamic signal change, predominantly activation, in 12 of 15 patients who had GSW during scanning, in addition to symmetrical cortical activation or deactivation associated with GSW. Archer et al. (Archer et al., 2003a) found posterior cingulate cortex (PCC) deactivation in association with GSW in four of five IGE patients studied with EEG-triggered fMRI at 3 T. Laufs et al. (Laufs et al., 2006b) noted thalamic activation and widespread cortical deactivation in a patient studied on two occasions, and emphasized the distribution of the cortical deactivation; being

cerebral areas thought to be most active during the conscious resting state, the "default mode" hypotheses (Raichle et al., 2001).

We report on a large consecutive series of patients with GSW, including patients with different subtypes of IGE as well as SGE. We hypothesized that population specific BOLD effects to GSW could be identified using EEG-fMRI and a random effects group analysis in a large group of patients.

10.3 Methods

10.3.1 Patients

Forty six patients, 30 with IGE and 16 with SGE, and frequent GSW discharges on recent interictal EEG were recruited from the epilepsy clinics at the National Hospital for Neurology and Neurosurgery, London, the National Society for Epilepsy, Chalfont St Peter and St Thomas' Hospital, London.

Patients were grouped according to the ILAE (1989) classification scheme. These were IGE and its sub classifications - juvenile myoclonic epilepsy (JME), juvenile absence epilepsy (JAE), childhood absence epilepsy (CAE), and epilepsy with generalized tonic clonic seizures only (IGE-GTCS) - and secondary generalized epilepsy (SGE). The latter group had one or more of the following: atypical absences, an abnormal background EEG, and irregular GSW. In one patient there was electrographic evidence of a unilateral frontal focus (patient 43, see Table 10-1 and Table 10-2B) . All patients had a normal structural MRI.

10.3.2 Data acquisition

See Chapters 4 and 9. Two successive 35 minute scan sessions at the same sitting were acquired in 13 patients, giving 59 sessions in 46 patients.

Table 10-1 Clinical Details

Clinical details of patients studied based on ILAE diagnostic categories, showing seizure type and frequency, age at onset, medication at time of study and frequency of GSW. Structural MRI in all patients was normal. The sub classification of IGE is often a source of debate, with a degree of overlap between syndromes, and some would therefore argue they represent a continuum rather than specific disease entities. For example patient #10, whilst the age of onset 7 years might suggest CAE, we prefer to classify as JAE on the basis of GTCS occurring with the onset of epilepsy, similarly patient #32 whilst the age of onset of 10 might suggest JAE has never had a GTCS, this would be unusual for JAE, hence we include them in CAE (Panayiotopoulos, 2002).

ID no	Age	Seizure type frequency (onset/yrs)		Antiepileptic Drugs	GSW (Hz)
JAE					
1	19	Abs daily (11)	GTCS 5/yr (15)	LEV, LTG	2.5–3
2*	24	Abs 15 d (10)	GTCS 4/yr (13)	CBZ, ESM, LTG, TPM	3
3*	18	Abs (10)	GTCS 2/mth (14)	LTG	3-4
4	43	Abs 2/wk (9)	GTCS 5/yr (9)	CBZ, LTG	3
5*	43	Abs daily (8)	GTCS 4 /yr (13)	CLB, LTG, VPA	3
6*	22	Abs 4-5 wk (9)	GTCS 6/yr (16)	LTG, VPA	4
7	22	Abs 2-3 day (8)	GTCS 2/mth (19)	ESM, LTG, TPM	3-4
8	54	Abs 1/mth (19)	GTCS none for 10yrs (19)	CBZ, PHT, PB, VPA	3-4
9*	18	Abs weekly (15)		Nil	2.5-3
10	19	Abs daily (7)	GTCS <1 yr (7)	CBZ, VPA	2.5-3
11	33	Abs daily (teens)		LTG, VPA	3
12 †	33	Abs 10/day (10)	GTCS 5/yr (14)	LTG, VPA	3
13 †	37	Abs 1/mth (4)	GTCS 2/yr (11)	LTG, OXC, PB, VPA	3
14*†	36	Abs weekly (3)	GTCS 3 in total (6)	LTG	3
Age range: 18-54 yrs, mean 30, median 28.5. sex ratio M:F - 4:3.					
JME					
15	55	Abs resolved (13) MJ 2-3/wk (teens)	GTCS 1-2/yr (13)	CLB, LEV, LTG	3
16‡	20	Abs daily (13) MJ daily (18),	GTCS 2/mth (13)	CLN, TPM, VPA	2-3
17*	59	MJ several/wk(10)	GTCS 1/wk (5)	CBZ, PB, VPA	4
18	20	Abs 3/d (<10) MJ resolved (14)	GTCS 1/mth (13)	LEV	3
19	41	Abs nil MJ resolved (15)	GTCS 1/mth (15)	CLB, LTG, PHT, VPA	3
20*	18	Abs 2-3/wk (15) MJ daily(15)	GTCS<1/yr(16)	LEV, LMT, VPA	4-5
21*	37	Abs 10 d (7) MJ (teens),	GTCS 2/yr (12)	CLB, GBP, VPA	2-3
22	18	Abs nil MJ resolved (14)	GTCS 1/yr (14)	VPA	3
23*†	20	Abs 3 wk (19), MJ daily (18),	GTCS 1/yr (18)	CLN, LTG	2-3
Age range 18-59 yrs, mean 34, median 33. M:F - 5:4					

IGE-GTCS					
24	33		GTCS free 2 yrs (11)	LTG	4
25*	34		GTCS 3 in total (12)	CBZ	3
26	32		GTCS 4 in total (22)	CBZ, CLN	3-4
27†	21		GTCS 1/mth (1)	CLB, LTG, VPA	2.5 - 3
28†	48		GTCS 1<10yrs (7)	VPA	2-3
29*†	24		GTCS 1 in total	Nil	2-3
Age range 21-48, mean 32, median 32. M:F 2:1					
CAE					
30	23	Abs 10/d (4)	GTCS 1/mth (12)	LEV	3
31‡	26	Abs 15/d (8)		Nil	3
32‡	53	Abs several/day (10)		DZP	4
Age range 26-53 yrs, mean 34, median 26. M:F 8:5					
SGE					
33	29	Abs daily (20)	GTCS <1 yr (23)	LTG, VPA	2-3 abn bkgd
34	29	Abs 3/d (16)	GTCS <1 yr (14)	ACE, CBZ, VPA	1.5-2
35	21	Abs daily (10) tonic sz 1/wk (10)	GTCS <1 yr (10)	ACE, CBZ, CLN	2-3
36	19	Abs 6-8/ d (7)	GTCS 6/yr (7)	LEV, LTG, TGB	3 abn bkgd
37	22	Abs 2/wk (8) MJ 2/wk	GTCS resolved (9)	CLN, LTG, OXC, VPA	2-3
38	26	drop attacks 6/yr (26)	GTCS 2-3/yr (14)	LTG, TPM	2-3
39	26	Abs 2-3/wk (9) atonic sz 1/wk (10)	GTCS <1/yr (12)	CLN, LTG, OXC	2 abn bkgd
40	74	Abs daily (teens)	GTCS 2/mth(14)	PHT, TPM	2.5-3
41	22		GTCS 6/mth (11)	CBZ, TPM	3
42	38	Abs 10-20/d (7)	GTCS -4/mth (11)	CBZ, LEV	2 -3
43	21	Abs 8/mth (13)	GTCS 4/yr (18)	CBZ, LEV, VPA	2 L>R, max F3
44†	40	Abs 1-2/mth, (11)	GTCS 2/yr, (11)	CBZ, PHT, TGB	3
45†	19		GTCS 2/mth (2)	LTG, TPM	2-3 abn bkgd
46*†	47	Abs 15/d (2)	GTCS 3/mth (4)	PHT	3-4
Age range 19-74 yrs, mean 31, median 26. M:F 4:3					

JAE, Juvenile absence epilepsy; JME, Juvenile Myoclonic Epilepsy; IGE-GTC, idiopathic generalized epilepsy with generalized tonic clonic seizures only; SGE. secondary generalized epilepsy; abs, absence seizures; MJ, myoclonic jerks; GTCS, generalized tonic clonic seizures; ACE, acetazolamide; CBZ, carbamazepine; CLB, clobazam; CLN, clonazepam; DZP, diazepam; ESM, ethosuximide; GBP, gabapentin; LEV, levetiracetam; LTG, lamotrigine; OXC, oxcarbazepine; PB, phenobarbitone; PHT, phenytoin; TGB, tiagabine; TPM, topiramate; VPA, sodium valproate; M, male; F, female; abn, abnormal; bkgd, background; F3, left frontal electrode; d, day; wk, week; mth, month; yr, year; sz, seizure. * patients studied in two successive sessions, † patients in whom no GSW was seen during scanning, ‡ patients excluded due to correlated motion.

10.3.3 Data Analyses

The SPM2 software package (www.fil.ion.ucl.ac.uk/spm/) was used for all image pre-processing and voxel based statistical analyses. Images were slice-time corrected to the middle slice and spatially realigned to the first scan of the series, and then spatially normalized to the MNI template supplied by SPM. Finally images were spatially smoothed using an isotropic Gaussian kernel (10 mm full width at half maximum).

The artifact corrected EEG was reviewed off-line and the onset and offset of GSW epochs were identified relative to the fMRI time series. These were used to construct a boxcar model of the active (GSW) versus rest (background) EEG state. This model was convolved with the canonical haemodynamic response function (HRF), as supplied by SPM2 (peak at 6 seconds relative to inset, delay of undershoot 16 seconds and length of kernel 32 seconds), its time and dispersion derivatives, to form regressors testing for GSW-related BOLD changes. The temporal derivative (TD) and dispersion derivative (DD) were used to accommodate variations in the canonical HRF (Henson et al., 2002). Spatial realignment parameters and their first order expansion were included as effects of no interest to model the linear and non-linear effects of motion (Friston et al., 1996). Data and design matrices were high pass filtered at 128 seconds cutoff. An auto regression (AR(1)) model was used to estimate the intrinsic autocorrelation of the data (Friston et al., 2000b). No global scaling or normalization was performed, to preclude introducing apparent deactivations in the analysis that would be artifactual.

An F-contrast was used to assess the variance at each voxel explained by GSW. The resulting SPMs were thresholded at $p<0.05$ using the correction for multiple comparisons based on random field theory (Friston et al., 1991). The contrast estimate pertaining to the canonical HRF was used to ascertain the direction of the BOLD response at the global maxima and at the local maxima of frontal, posterior superior parietal, and posterior cingulate cortices.

A random effects group analysis was performed on each of the groups IGE, and SGE using the following two stage procedure to infer the average pattern at a population level (Friston et al., 1999a). The contrast estimates pertaining to HRF, TD and DD, were taken to a second level random effects group analysis using a one-way analysis of variance. The inter-session variability in the number of EEG events requires particular consideration for group analyses due to the risk of unbalanced designs

(Friston et al., 2005). We therefore selected patient sessions in which the number of GSW events fell within one order of magnitude of each other (see Table 10-2, sessions marked *), giving 18 IGE cases and 10 SGE cases for the group analyses. An F contrast at the second (i.e. the between subject) level was used to test for the variance explained by GSW across the group. We had insufficient patient numbers (Desmond and Glover, 2002) with GSW during scanning for group analysis in JME and JAE.

10.4 Results

10.4.1 Clinical features

See Table 10-1 for the patients' clinical features. Good quality EEG was obtained following pulse and gradient artifact subtraction, allowing identification of epileptiform discharges. In 16 sessions (10 patients, marked † in Table 10-1) no GSW was seen; these sessions were not considered further. Three further patients were excluded due to correlation between head motion and GSW events (marked ‡ in Table 10-1). The rate of occurrence of GSW events in the remaining 40 sessions (in 33 patients) varied between 1 and 189 per 35-minute scan session (mean 28, median 11).

10.4.2 Single subject results

Significant BOLD signal changes were seen in 25 patients, (29 sessions, and 73% of sessions containing GSW): in thalamus (15 patients), frontal cortex (FC) (23 patients), posterior parietal cortex (PPC) (19 patients) and PCC / precuneus (20 patients), with one or typically more of these areas involved in each case (Table 10-2). In addition, BOLD change was also seen, to a variable extent in some patients in basal ganglia, cerebellum, brainstem, the sagittal sinus, or all lobes.

Figure 10-1 shows examples of BOLD response patterns in 3 patients with the different IGE syndromes JME, IGE-GTCS, JAE, and figure 3 in one case with SGE, illustrating the similarities of the cortical pattern in these distinct syndromes. Negative cortical changes predominated, although positive, and biphasic changes, were also seen (Table 10-2). BOLD decreases in FC were seen in 14 sessions (8 IGE, 6 SGE), increases in 10 (5 IGE, 5 SGE), and biphasic changes in 2 (IGE), PPC decreases were seen in 17 (11 IGE, 6 SGE), increases in 3 (1 IGE, 2 SGE), and biphasic changes in 1 (SGE), and PCC / precuneus decreases in 15 (8 IGE, 7 SGE),

increases in 6 (3 IGE, 3 SGE) and biphasic changes in 1. The signal change in the thalamus was positive in 9 sessions, biphasic in 4 and negative in 3 sessions. In patient 43, with SGE and EEG evidence of left frontal epileptogenicity a small area of frontal activation was seen in addition to a more widespread fronto-parietal cortical negative response (Figure 10-2).

Table 10-2 Summary of results

Summary of results for all sessions during which GSW activity occurred, detailing number and duration of GSW epochs, and regions of significant BOLD signal change labeled in accordance with direction of HRF loading. All SPMs corrected for multiple comparisons using random field theory ($p<0.05$).

Diagnostic category	Id No.	No. of GSW Events	Duration of GSW events. Median (range) (seconds)	Regions of significant fMRI signal change				
				Thalamus	Frontal	Parietal	Posterior cingulate / precuneus	Other
JAE	1*	9	2.1 (1.6-8.1)	-	↑ B (L **m**)	↓ B	↑B	↑ ss, cereb, temp
	2a	3	7.3 (4.4-7.7)	-	↑ B (L **m**)	↓ B	-	↑ L temp
	2b	1	5.9	-	↑ R **m**	-	-	↑ B temp
	3*	7	1.3 (0.9-3.3)	↓ R	↕ B	-	-	↕ B head caudate (R **m**)
	4*	4	2.6 (1.0-3.0)	-	-	-	-	-
	5a	18	0.6 (0.4-3.6)	↑ B	↑ B	-	↑ B	↑ ss, cereb (R **m**), B occ
	5b*	16	0.7 (0.4-1.7)	-	-	-	↕ B	↑ cereb (L **m**), B occ
	6a	4	1.9 (1.3-3.0)	-	-	-	-	-
	6b*	17	1.3 (0.4-4.3)	-	-	-	-	↓ L inf occ **m**
	7	2	4.3 (3.4-5.3)	↑ B	↑ B (L **m**)	↑ R	-	↑ ss
	8*	8	2.1 (1.0-5.3)	-	↓ B (L **m**)	↓ B.	↓ B	-
	9a*	8	1.9 (0.7-3.6)	-	↕ B	↓ B	↓ B	↑ ss **m**
	9b	2	0.6 (0.6-0.7)	-	-	-	-	-
	10*	11	1.3 (0.9-2.6)	-	-	-	-	-
	11	189	1.6 (0.3-73.9)	↕ B	↓ B (L **m**)	↓ B	↓ B	↓ ss, cereb
JME	15*	17	0.7 (0.4-5.3)	-	-	-	-	↓ occ **m**,↕ R BS
	17a*	7	1.4 (1.1-1.6)	-	-	-	-	-
	17b	1	1.4	-	-	-	-	-
	18*	25	1.3 (0.4-3.4)	↑ B (L **m**)	↑ B	-	↑ B	↑ occ, B temp
	19*	4	0.6 (0.6-0.9)	-	-	-	-	-
	20*	7	1.6 (0.7-1.7)	-	-	-	-	-
	21a	60	1.4 (0.4-8.4)	↓ B (L **m**)	↓ B	↓ B	↓ B	↓ BS
	21b	89	1.0 (0.3-5.4)	↑ B	↓ B	↓ R	↓ B	↑ BS **m**
	22*	11	9 (2.4-15.7)	-	↓ B	↓ B (L **m**)	↓ B	-

Diagnostic category	Id No.	No. of GSW Events	Duration of GSW events. Median (range) (seconds)	Regions of significant fMRI signal change				
				Thalamus	Frontal	Parietal	Posterior cingulate / precuneus	Other
IGE-GTCS	24*	6	1.1 (0.9-1.7)	-	-	-	-	-
	25a	33	1.6 (0.6-3.9)	-	↓ B	↓ B (L **m**)	↓ B	-
	25b*	24	1.4 (0.6-4.1)	-	↓ B	↓ B (L **m**)	-	-
	26*	5	1.1 (0.7-1.4)	-	-	-	-	-
CAE	32*	17	2.1	↑ B	↓ B	↓ B	↓ B	↑ cereb **m**
SGE	33*	25	1.1 (0.3-2.0)	↕ R	↓ B	↓ B (R **m**)	↓ B	-
	34*	55	13.7 (1.0-82.4)	↑ B	↓ B	↕ B	↓ B (R **m**)	↓ all lobes, cereb, BS, BG
	35*	32	10.9 (1.3-82.4)	↓ B	↓ B (L **m**)	↓ B	↓ B	↓ ss, cereb., temp, BS
	36*	9	7.1 (5.0-12.6)	-	↑ B (R **m**)	↓ B	↓ B	↑ ss, ↓ BS
	37*	78	2.6 (0.6-15.0)	↕ B	↑ B	-	↑ B (L **m**)	↕ occ
	38*	43	5.7 (0.7-12.3)	↑ B (R **m**)	↑ B	↑ B	↑ B	↑ ss, cereb, ↕ BS
	39*	68	6.6 (0.4-39)	↑ B (R **m**)	↑ B	↑ B	↑ B	↑ cereb, temp, BS, BG
	40	3	6.9 (1.9-8.6)	-	-	-	-	-
	41*	46	0.7 (0.3-12.9)	↕ B	↓ B midline (L **m**)	↓ B	↓ B	↓ cereb, ↑ BS, temp, occ
	42*	57	4.1 (1.1-24.6)	-	↓ B	↓ B (R **m**)	↓ B	↓ temp
	43*	46	5.2 (1.1-29.3)	↑ L	↓ B + area of L ↑	↓ B (R **m**)	↓ B	↓ BS

Id no – identification number, corresponds to that in table 1. (a) and (b) are given for those studied with two sessions.
↑ - increase, ↓ - decrease, ↕ - biphasic. B - bilateral, L - left, R - right, m - global maxima, BG - basal ganglia, BS - brainstem, BG - basal ganglia, cereb – cerebellum, temp - temporal lobes, occ - occipital lobes, ss - sagittal sinus (draining vein).
*indicates sessions included in second level group analysis.

Figure 10-1 (below) Cortical signal change with GSW
Examples of maximum intensity projections from single subject SPM analyses showing cortical signal change with GSW involving symmetrical bi-frontal, bi-parietal, posterior cingulate/precuneus in three patients with different diagnostic syndromes a) patient #10, JAE, b) patient #22 JME c) patient #25 IGE-GTCS. The fitted response for each global maximum (marked with red arrow on the SPM) is plotted on the right indicating the peristimulus time course and percent signal change. (SPMs corrected, $p < 0.05$).

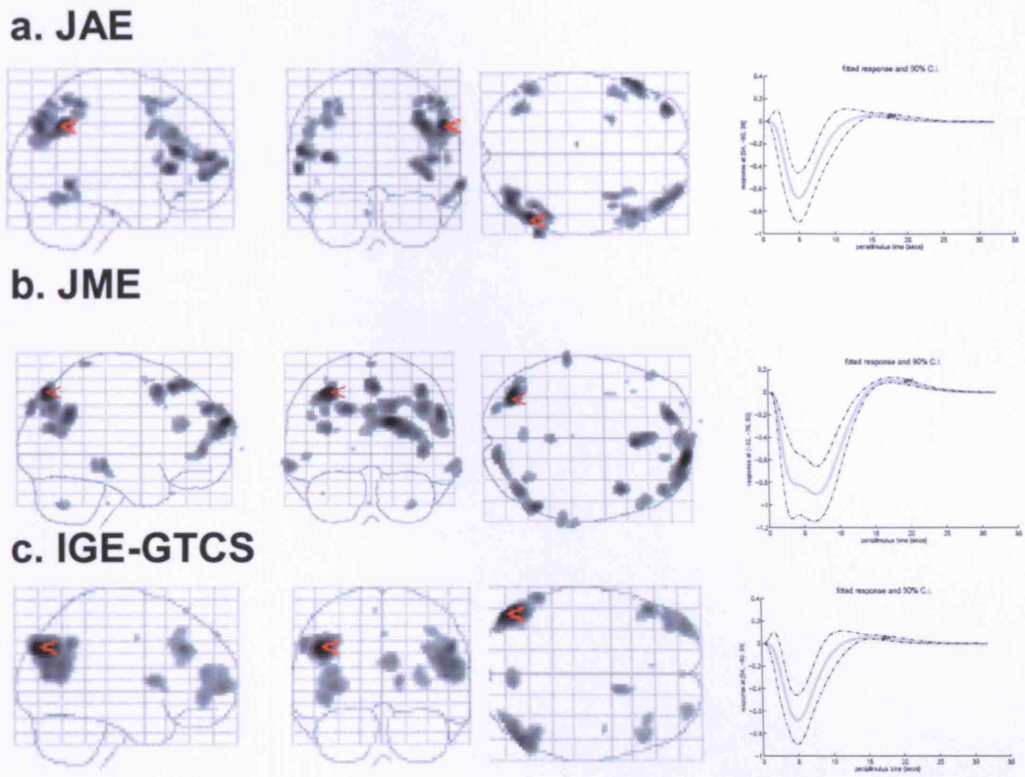

Figure 10-2 (overleaf) Examples from 2 patients with SGE
Examples of mean intensity projections SPM{F} from 2 patients with SGE. A color coded overlay of SPM{T}(red-activation and green deactivation) onto the surface render is shown for display purposes and a plot of the weighting on the contrast estimates also shown to indicate the direction of the signal change, both show a similar distribution on negative BOLD to the IGE cases shown on Figure 10-1, although to a greater extent due to the higher number of events during the scan session.. A) Patient #35 shows widespread cortical deactivation sparing primary cortical areas. B) Patient #43 is also shown as this illustrates in addition to the negative BOLD changes a small area of left frontal activation concordant with the EEG abnormality.

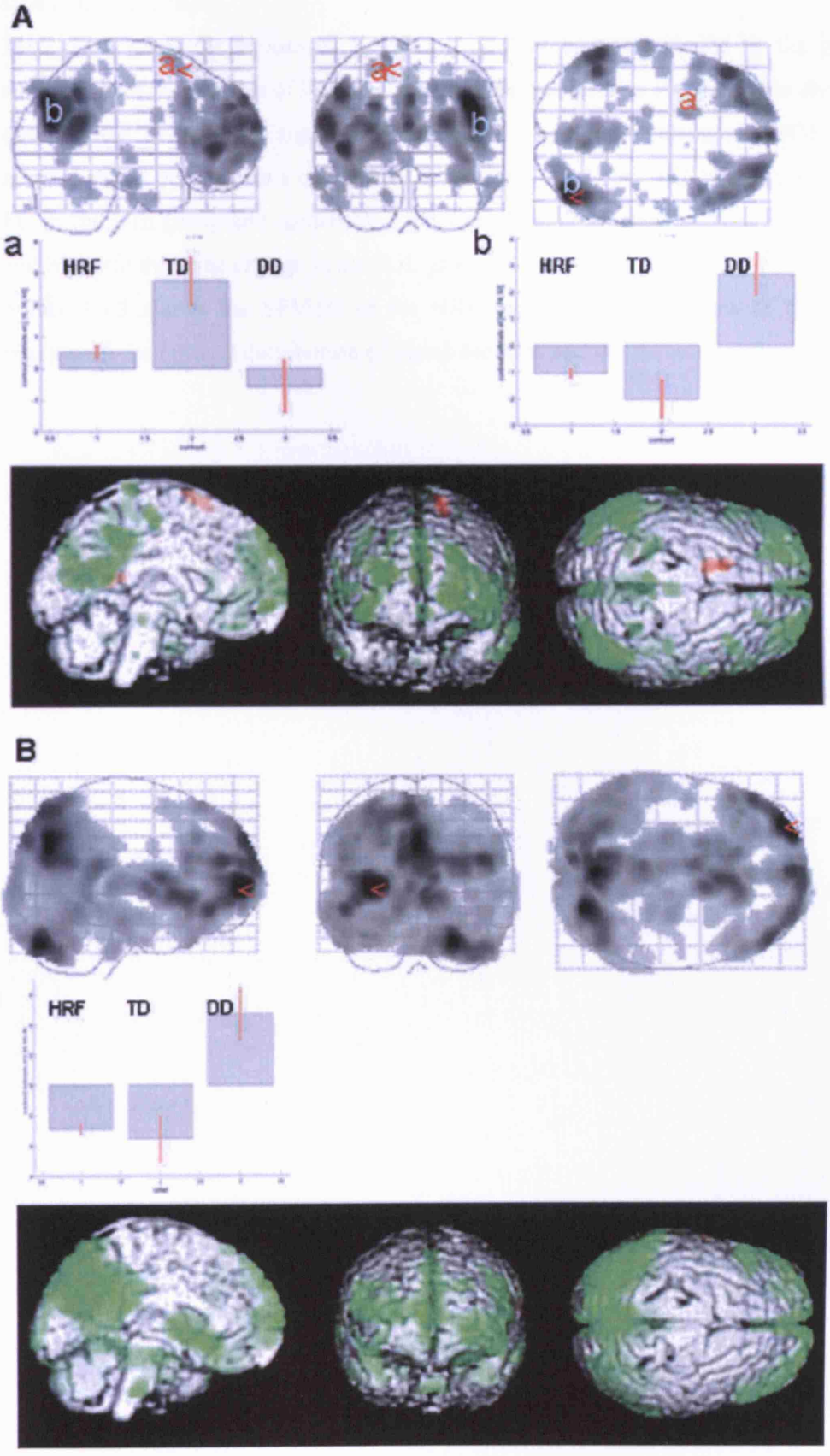
A
a
b
a
b
a
b
a
HRF
TD
DD
b
HRF
TD
DD
B
HRF
TD
DD

10.4.3 Group results

Table 10-3 gives the regions of significant BOLD changes revealed by the group analysis, with coordinates of local maxima and their respective Z score. This shows a group effect of thalamic signal increase in IGE, a biphasic change in SGE, and cortical signal decrease in a characteristic distribution of PPC, PCC / precuneus and FC in the IGE group and medial FC / anterior cingulate increase in the SGE group and biphasic thalamic change in the SGE group.

Figure 10-3 shows the SPM{t} of the HRF for the group analyses of the IGE, illustrating the cortical distribution of signal decrease and the thalamic activation.

Table 10-3 Group Analysis
Brain regions that showed significant change on the group analysis. A: IGE cases and B: SGE cases. The weighting on the contrast is given to show the direction of BOLD signal change.

A. IGE group analysis

Region		*x,y,z*	Peak Z score	Weighting on estimate
Parietal				
L	Angular Gyrus	-44, -62, 34	5.96	↓
R	Supramarginal Gyrus	46, -51, 32	5.86	↓
R	Posterior Cingulate	6, -48, 17	5.23	↓
Frontal				
L	Inferior Frontal Gyrus	-51, 16, 16	4.75	↓
L	Inferior Frontal Gyrus	-50, 26, -15	4.11	↓
R	Inferior Frontal Gyrus	53, 35, 7	3.86	↕
L	Inferior Frontal Gyrus	-38, 49, 1	3.82	↓
R	Middle Frontal Gyrus	53, 23, 23	5.47	↓
L	Superior Frontal Gyrus	-12, 61, 23	3.76	↓
R	Superior Frontal Gyrus	18, 48, 29	3.59	↓
Temporal				
L	Fusiform Gyrus	-51, -34, -20	4.21	↓
R	Middle Temporal Gyrus	67, -28, -12	4.51	↓
L	Middle Temporal Gyrus	-46, -52, 3	3.78	↕
L	Parahippocampal Gyrus	-16, -10, -13	3.98	↕
Subcortical				
L	Caudate	-14, 10, 5	4.68	↓
R	Caudate	10, 8, 5	4.13	↓
R	Thalamus	12, -11, 4	3.67	↑

B. SGE group analysis

Region	*x,y,x*	Peak Z score	Weighting on estimate
Frontal			
L Cingulate Gyrus	-8, 10, 42	5.56	↑
L Anterior Cingulate	-8, 33, 2	3.94	↕
L Inferior Frontal Gyrus	-50, 5, 27	3.98	↕
R Cingulate Gyrus	10, 9, 33	3.89	↕
Subcortical			
L Thalamus	-14, -15, 4	4.15	↕
R Thalamus	10, -15, 3	3.92	↕

L, left; R, right; hrf, canonical haemodynamic response; td, temporal derivative

Figure 10-3 IGE group analysis
SPM{t} overlaid onto canonical brain of positive HRF (red) and negative HRF (green) (uncorrected $p<0.001$) illustrating the thalamic and cortical distribution of BOLD changes to GSW in the IGE group analysis. This shows bilateral parietal [46 -51 32] and [-44 -62 34] and posterior cingulate / precuneus deactivation and [6 -48 17] thalamic activation [12 -11 4], the activation around the ventricles, we suspect is due to modeled changes in CSF pulsation as a result of the widespread haemodynamic changes occurring during GSW.

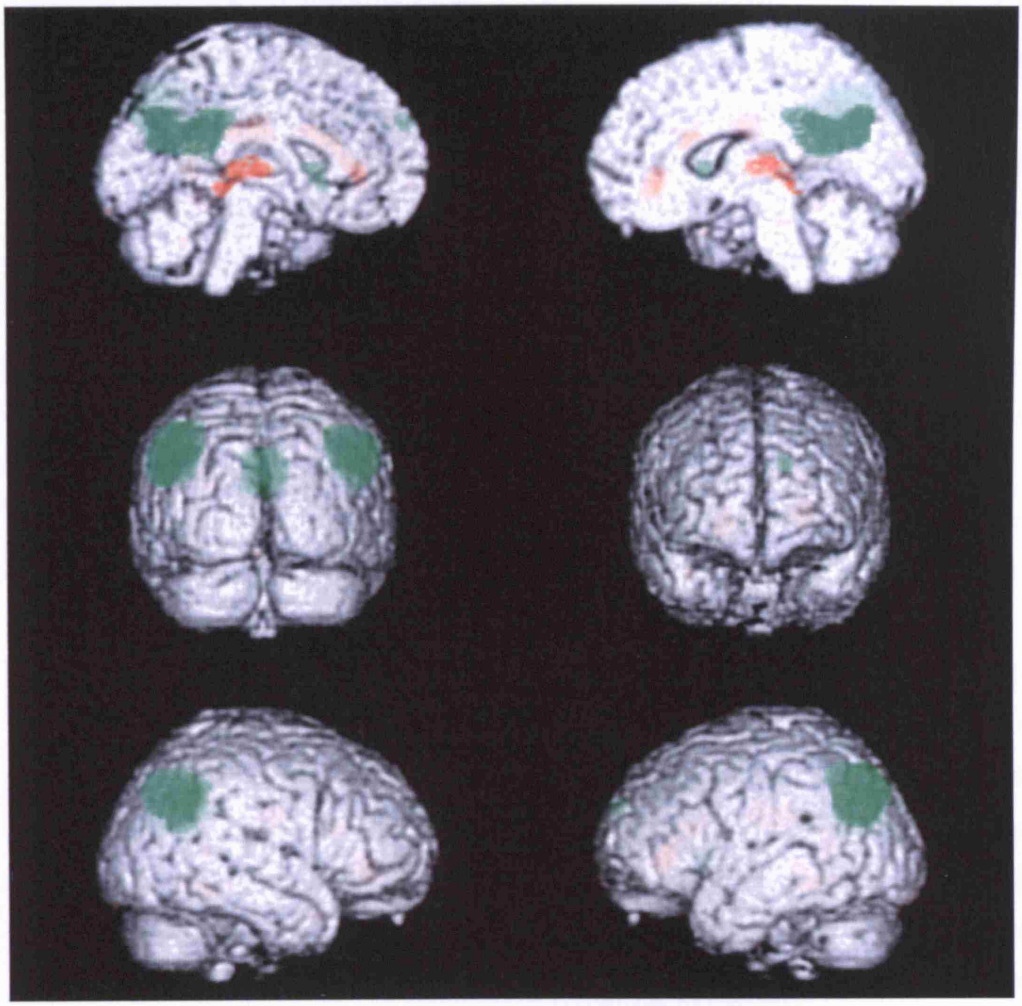

10.5 Discussion

BOLD signal changes were detected in 73% of sessions, a yield comparable to that previously reported (Aghakhani et al., 2004). Those with no BOLD response had 7 events or less, all of which were of less than 2 seconds duration (Table 10-2). The most striking feature of our results is the lack of changes in the primary cortices, except in a few cases, the primary visual cortex. Aghakhani et al (2004) similarly, found the cortical BOLD changes predominantly in a frontal and posterior

distribution, similar to those seen here. They highlighted the symmetrical nature of their findings as well as the predominance of negative changes in cortex as seen here. We used a second level random effects group analysis to look for population specific BOLD effects to GSW. Sub threshold signal changes that are not seen at the individual level will become significant if they are present across subjects. Similarly if there is a high degree of variance at a particular voxel then activations that are seen on the individual level will not reach significance at the group level. We chose to show the results for both the individual analyses and the random effects group analysis to demonstrate 1) the degree of intersubject similarity, in different syndromes and variability within the same syndrome, at the individual level, that, at this present time preclude the use of EEG-fMRI as a clinical tool, and 2) population specific effects that allow inferences to be made about neuronal activity during GSW.

The selection of patients for this study was necessarily biased to those at the severe end of the spectrum often referred for optimization of medical treatment. Rarely were patients on no medication. Carbamazepine (CBZ) and gabapentin (GBP) are known to increase the amount of GSW in patients with IGE (Kochen et al., 2002), however they are used if the initial diagnosis is incorrect, or if some improvements in generalized seizures are seen despite the relative contraindication. It is notable that 7 of 34 of our IGE patients with frequent discharges were taking CBZ or GBP at the time of the study. In the other EEG-fMRI studies 4 of 15 were taking CBZ in (Aghakhani et al., 2004) and 4 of 5 in (Archer et al., 2003a). The effect of anti epileptic medication on the neurovascular response is not known, although any effect is lessened by the fact that comparisons made here are within sessions. Even with optimal patient selection, the unpredictability and in cases paucity of GSW during scan sessions remains a limitation of EEG-fMRI. Activating procedures such as hyperventilation could be employed but are likely to introduce confounds due to variable effects on cerebral circulation and the BOLD response (Kemna and Posse, 2001), whilst photic stimulation, sleep deprivation or drug withdrawal would run the risk of provoking generalized tonic clonic seizures.

The predominant finding in individual subject and group analyses was of thalamic activation and cortical BOLD negative response, consistent with recent EEG-fMRI reports (Aghakhani et al., 2004;Archer et al., 2003a;Laufs et al., 2006b;Salek-Haddadi et al., 2003c). Thalamic signal change was seen in less than half of patients

with IGE and almost all patients with SGE. This may be due to the greater occurrence of GSW in SGE cases compared to IGE (median SGE 44.5 versus IGE 8), and tended to be seen in those individual IGE cases with a higher number or longer duration of GSW. Primary cortical areas were spared, with changes occurring in frontal, parietal and temporal association areas. At the single subject level similar BOLD responses were seen across IGE syndromes and in SGE, suggesting that the predominant BOLD findings represent generic changes associated with GSW per se rather than syndrome specific patterns. This is unlikely due to syndrome misclassification (Berkovic et al., 1987) given the similarity of our findings in cases with very clear syndromic differences (Figure 10-1 and Figure 10-2).

It is not possible to infer causality of the BOLD changes relative to our modeled covariate, GSW; they may represent areas generating GSW, or alternatively reflect areas secondarily affected by GSW. This difficulty in inferring causality is in contrast to paradigm driven fMRI where it is generally safe to assume a primary association between the task or stimulus and the observed fMRI changes; in addition a prior hypothesis about a relatively well defined location of expected neural activity usually exits. In GSW however we have little prior anatomical hypotheses regarding the spatial extent of BOLD changes. We propose that thalamic activation seen here represents subcortical activity necessary for the maintenance of GSW(Avoli et al., 2001). The absence of thalamic activation in a number of our cases may reflect low sensitivity of our model at 1.5T (Laufs et al., 2006b). The left frontal cortical activation in case 43 (Figure 10-2B) requires further validation but likely represent an area of initiation of GSW, given its concordance with the left frontal EEG onset of GSW.

The cortical distribution of signal change, FC, PPC and PCC / precuneus, comprises areas of association cortex that are hypothesized, at rest, to be involved in an organized, baseline level of activity, a "default mode" of brain function (Raichle et al., 2001). The default mode concept came from observations of consistent deactivations in meta analyses of different task related paradigms in fMRI, in addition to independent PET measurements of increased blood flow to these areas during awake conscious rest (Raichle et al., 2001). Activity in these areas as measured by PET is also altered during sleep, coma and anesthesia (Laureys et al., 2004). Default mode areas likely represent part of a neural network subserving human awareness (Laureys et al., 2004). Our study, and others (Aghakhani et al.,

2004;Archer et al., 2003a;Laufs et al., 2006b), shows alteration of activity in these regions during GSW, which would be consistent with the clinical manifestation of absence seizures. These findings are also consistent with PET findings of opioid release in association neocortex, most marked in parietal cortex and posterior cingulate, following absence seizures (Bartenstein et al., 1993).

The majority of cortical BOLD responses were negative (Table 10-2), in keeping with other fMRI (Aghakhani et al., 2004;Archer et al., 2003a;Laufs et al., 2006b) as well as transcranial Doppler (TCD) (Bode, 1992;De Simone et al., 1998;Diehl et al., 1998;Klingelhofer et al., 1991;Nehlig et al., 1996;Sanada et al., 1988) and near infrared spectroscopy studies (Buchheim et al., 2004;Haginoya et al., 2002). A number of lines of evidence suggest that BOLD negative responses represent a reduction in neural activity. In visual cortex, a reduction of BOLD signal, elicited by stimulating part of the visual field is due, primarily, to a reduction of neuronal activity (Shmuel et al., 2002). A decrease in BOLD signal is seen in the occipital cortex during auditory induced saccades (Wenzel et al., 2000), a manipulation known to suppress neuronal activity (Duffy and Burchfiel, 1975). BOLD decreases have also been observed in the context of neuronal synchronization, modulated by sub-cortical structures (Parkes et al., 2004). Visual stimulation during sleep leads to occipital BOLD negative responses, confirmed as a decrease in rCBF with H215O PET (Born et al., 2002). Similarly auditory BOLD negative responses occur on auditory stimulation during sleep, the amplitude and extent of which correlate positively with measures of EEG synchronization in sleep (Czisch et al., 2004).

Although the majority of our cases showed cortical negative response a number of cases showed activation or biphasic time courses in the same areas. These did not differ significantly (2-sample t-tests, all $p > 0.8$) from those with negative response in terms of the frequency of GSW, the number of events, their median duration or total duration during the scan session. Nevertheless activations were seen in a greater proportion of SGE than IGE patients. This would explain the absence of widespread cortical change in the SGE group analysis, where positive signal changes in some subjects and negative in others in the same region lead to a loss of this effect at the group level.

Our cases of cortical activation are compatible with the findings of others; cortical increases were seen in some cases with fMRI (Aghakhani et al., 2004) and in TCD an initial increase was seen prior to the more prolonged decrease (De Simone et al.,

1998;Diehl et al., 1998). Similarly, SPECT and PET showed increases as well as decreases in cortical activity to spike wave (Engel, Jr. et al., 1985) (Ochs et al., 1987;Prevett et al., 1995;Theodore et al., 1985;Yeni et al., 2000). The terms "activation" and "deactivation" are operational terms that reflect measured vascular or metabolic responses from which inferences about neuronal activity are made, we have preferred to use the term negative BOLD response rather than deactivation as the neural correlates of these responses aren't yet clear. The terms have their origins in the field of PET (Friston et al., 1990), in which measures are quantitative and more direct. In fMRI the modeling of signal changes is relative, i.e. a comparison between two states (Bandettini et al., 1992). Given that 1) we, and others (Aghakhani et al., 2004;Salek-Haddadi et al., 2003b) model GSW against an implicit baseline, i.e. active (GSW) against rest (background resting state activity), and 2) we detect changes in areas of association cortex, then the level of arousal or sleep reflecting resting state activity in these regions may affect the direction of detected BOLD signal changes. A negative response is therefore seen where there is a decrease or interruption of awake resting state activity; if however the patient is drowsy or asleep activity in these areas may be lower than that engendered by GSW thus giving rise to activations. Future studies of GSW with EEG-fMRI need to take this into account, by modeling the background EEG in more detail or presenting the subject with a low grade task designed to maintain and monitor a constant level of vigilance.

In conclusion, we have shown that the main BOLD fMRI correlates of GSW consist of widespread cortical negative response in areas associated with normal brain activity during conscious rest. These likely reflect a decrease in neural activity, as a result of either synchronization or inhibition of cortical activity due to thalamo-cortical interactions. This is in keeping with the clinical features of absence seizures, i.e. a brief alteration of consciousness with minimal somatosensory or motor manifestations.

* * *

11. Chapter 11: Ictal fMRI in primary reading epilepsy

11.1 Summary

The aim was to characterize the spatial relationship between activations related to language-induced seizure activity, language processing and motor control in patients with reading epilepsy.

We recorded and simultaneously monitored several physiological parameters (voice-recording, EMG, ECG, EEG) during blood oxygen level dependent (BOLD) functional magnetic resonance imaging in nine patients with reading epilepsy. Individually tailored language paradigms were used to induce and record habitual seizures inside the MRI scanner. Voxel based morphometry (VBM) was used for structural brain analysis.

Reading induced seizures occurred in six out of nine patients. One patient experienced abundant orofacial reflex myocloni during silent reading in association with bilateral frontal or generalized epileptiform discharges. In a further five patients, symptoms were only elicited whilst reading aloud with self-indicated events. Consistent activation patterns in response to reading induced myoclonic seizures were observed within left motor and pre-motor areas in five of these six patients, in the left striatum (n=4), in mesio-temporal/limbic areas (n=4), in Brodmann area 47 (n=3) and thalamus (n=2). These BOLD activations were overlapping or adjacent to areas physiologically activated during language and facial motor tasks. No subtle structural abnormalities common to all patients were identified using VBM, but one patient had a left temporal ischemic lesion.

Based on the findings, we hypothesize that reflex seizures occur in reading epilepsy when a critical mass of neurons are activated through a provoking stimulus within cortico-reticular and cortico-cortical circuitry subserving normal functions.

11.2 Introduction

Reading epilepsy is a relatively rare, but underdiagnosed age-related reflex epilepsy syndrome (Koutroumanidis et al., 1998;Radhakrishnan et al., 1995;Wolf, 1992;Wolf et al., 1998). Whilst originally classified as an idiopathic localization-related epilepsy syndrome (ILAE, 1989), more recent classifications have been less dichotomous on this issue (Engel, Jr., 2001). Reading epilepsy comprises partial seizures, or orofacial

reflex myocloni (ORM), triggered by reading, or language-related activities, without spontaneous seizures.

Reflex epilepsies, such as reading epilepsy, provide an ideal model for studying functional changes occurring at or around the time of seizures, in a sense that seizures may be elicited 'on demand'. In addition, functional imaging in reflex epilepsies may help identify neuronal and cognitive re-organization. This should increase our understanding of both the pathophysiology and spatial distribution of networks underlying seizure activity, and the relationship between seizure activity and cognition.

The neuroanatomical and biochemical basis of reading epilepsy is largely unknown; structural neuroimaging is usually normal, and functional neuroimaging has had until now a limited impact on our understanding of the pathophysiological and neurochemical abnormalities underlying reading epilepsy with few reports in the literature (Archer et al., 2003c;Koepp et al., 1998a;Koutroumanidis et al., 1998;Miyamoto et al., 1995). Debate continues as to precisely which cognitive step or component of the reading process is epileptogenic, but it is clear from the available literature that there is significant variability amongst patients in this regard, for example with eye movements, comprehension, emotional content, speech production, and proprioceptive feedback all proposed at one point or another (see Wolf (1992) for review). Previously, we found evidence for the release of endogenous opioids during and following reading-induced partial seizures (Koepp et al., 1998b) in areas of brain involved in normal reading (Noppeney and Price, 2004). This led to the hypothesis that there are networks of cortical areas concurrently subserving both cognitive functions and epileptic activity.

A recent case-report showed spike-triggered blood oxygen level dependent (BOLD) activation in the left posterior middle frontal gyrus, bilateral inferior central sulcus and bilateral globus pallidus during reading (Archer et al., 2003c). The authors hypothesized on the basis of a subtle structural difference that the spikes of reading epilepsy spread from working memory areas into adjacent motor cortex, activating a cortical-subcortical circuit.

In the present study, we investigated the neuronal systems that underlie the specific seizure-provoking trigger, i.e. reading, and its relationship to seizure output, i.e. ORM, and normal oro-facial movement. We performed simultaneous EEG, EMG, fMRI and audio recordings in nine patients with language-induced epilepsy. In a

separate fMRI session, motor (hand, mouth, jaw) and language mapping was performed.

In view of the recently described anatomical variant observed in a few reading epilepsy patients, we aimed in a second experiment to relate functional changes to any subtle morphometric changes as detected by voxel-based morphometry of structural MRI.

11.3 Methods

11.3.1 Subjects

A total of 34 patients were invited to participate in the study: seven from those previously known to the National Hospital for Neurology and Neurosurgery and the National Society for Epilepsy, three from the Bethel Epilepsy Centre, Bielefeld, Germany and a further 24 were referred from across the UK via the British Neurological Surveillance Unit. Of these patients, 20 declined to participate (eight because they were driving), three were found not to have reading epilepsy, and two were asymptomatic. Nine patients therefore entered the study (5 female; median age: 27 years; range: 20 –50 years). Eight of the nine patients were on antiepileptic medication, which was reduced where possible on the day.

11.3.2 Pre- assessment

Prior to fMRI scanning, all subjects were assessed clinically and with prolonged video EEG during spontaneous speech, overt reading and covert reading, including both native language and foreign texts, in order to design the best paradigm for eliciting reading induced seizures. Continuous EEG was only performed in patients with ictal EEG correlates.

11.3.3 Experiment design

For every patient, the following experiments were carried out:

- Session 1: Mapping of motor cortex for finger tapping and jaw movements (blocked design)
- Session 2: Mapping of language areas (blocked design)
- Session 3: Mapping of seizure-related activity during continuous reading (event-related design)

11.3.4 Data acquisition

The fMRI acquisition is described in Chapter 4.

Motor mapping. This was first carried out for the hands with a simple block-design paradigm running over 5 minutes and alternating 20 second blocks of a right versus left-sided self-paced finger-tapping. During a second trial subjects performed gentle chewing movements using the jaw, tongue and lips, so as to avoid any head displacement, in blocks of 20 seconds versus rest.

Language mapping. This was achieved using a visual stimulus presentation system, comprising a screen and back-projector driven by a PC running Matlab scripts based on Cogent 2000 [http://www.vislab.ucl.ac.uk/Cogent/]. Again, a simple block-design paradigm was used alternating 20 second blocks of covert reading versus "false fonts" (Greek symbols of same text – none of the subjects was able to read Greek). Sentences and false fonts were presented centrally, one word at a time, at a fixed rate every 300ms. This serial presentation mode was used to control for visual input and eye movements. Short blocks of reading were chosen to minimize the risk of reading-induced seizures during this part of the experiment. In the activation condition, subjects silently read text covering a range of different syntactic structures and semantic content. In the baseline condition, subjects attentively viewed the same text transformed into false fonts. This baseline controlled for visual input but not lexical, semantic or syntactic content. The paradigm therefore maximized our chances of seeing reading related activation at any level of the reading system.

11.3.5 Simultaneous EEG/EMG recording during fMRI

Where necessary, 11-channels of referential scalp EEG were recorded as described in Chapter 4. The in-house EEG system provided for recording an additional 6 bipolar channels. One of these was used to record slice-timing information from the scanner, and another to record the parasternal ECG. Of the remainder, one was fitted with a higher (250Hz) low pass filter suited to recording surface EMG. The others were used to record motor responses from the patient via a hand-held piezoelectric button-press switch.

11.3.6 Simultaneous voice recording and communication during fMRI

Online voice monitoring was achieved using a dedicated system developed in-house and running in parallel to the EEG/EMG acquisition. Voice was recorded via a small condenser microphone attached to the headcoil assembly. The signal was led out of the scanner room through RF filters to a small battery powered amplifier and then digitized (together with the scanner-sourced slice-timing signal) on a Dell Optiplex PC running Linux SuSE 7.3 fitted with an E-series NI Multifunction DAQ card plus BNC-2110 desktop adapter (National Instruments Corp., Texas, USA). A real-time adaptive noise cancellation algorithm, written in C, was used. The digitized slice trigger was signal fed into a 'tapped delay line' digital filter and the filter tap weights adapted after every sample to mimic the interference caused by the scanner. The output of the filter was subtracted from the microphone signal to cancel the interference, allowing for the faintest of whispers to be heard with clarity (Featherstone and Josephs, 2001). Where necessary, communication with the patient was achieved using a commercially available MR compatible audio system (Silent ScanTM 3000 series, Avotec Inc, Florida, USA).

11.3.7 Ictal EEG-fMRI acquisition

Various texts were identified as seizure-provoking outside the fMRI scanner in each individual subject. These texts were presented one word at a time at an individually-fixed rate between 300-900ms. Subjects either:

- showed clear reading-induced seizure activity on the on-line continuous EEG recording
- showed clear seizure-related EMG activity on online EMG recordings from the submental muscles.
- had audible seizure activity (brief interruption during loud reading) on on-line audio recordings
- signaled their own seizures via button-press using the non-dominant hand

We took care to avoid a secondary generalized seizure by switching to false font, if more than 2 seizures occurred within 30 seconds, and modeling the effect separately.

11.3.8 fMRI analysis

All fMRI data were analyzed using the SPM2 (Statistical Parametric Mapping) software package [http://www.fil.ion.ucl.ac.uk/spm/spm2.html] and Matlab® version 6.5 R13 (The Mathworks Inc.,USA) running on a Dell® PowerEdge 2650 under Red

Hat Linux 9. Images were slice-time corrected, realigned, and spatially smoothed using an isotropic Gaussian kernel of 8mm FWHM (Friston et al., 1995b).

Ictal EEG-fMRI runs were analyzed by modeling the visually-identified spikes or button presses as stick functions convolved with a canonical hemodynamic response and its first temporal derivative in an event-related design. Language and motor mapping runs were modeled using a boxcar convolved with the HRF plus temporal derivative, contrasting the active condition versus rest. Spatial realignment parameters were included as nuisance covariates to protect against motion induced artifact. Both data and design matrices were high-pass filtered (1/200 seconds cutoff) and pre-whitened to remove slow drifts and correct for temporal non-sphericity. Condition-specific effects for each subject were estimated according to the general linear model (Friston et al., 1995b) using an F-contrast to assess the additional variance at each voxel explained by the effects of interest relative to residual variance.

The resulting statistical parametric maps (SPMs) were thresholded at $p<0.05$ using the correction for multiple comparisons based on random field theory. In those patients who self-indicated ORM using button-press, the ictal SPMs were masked by the motor SPMs.

11.3.9 VBM

Thirty neurologically normal control subjects (18 female, median age 30 years, range 16 to 46 years) were scanned for comparison. An optimized method of VBM was used, as described elsewhere (Ashburner and Friston, 2000;Good et al., 2001). All image processing and statistical analyses were performed in SPM2 (Wellcome Department of Imaging Neuroscience, London, UK). The images were pre-processed according to the optimized VBM protocol (Good et al., 2001). This involved initial affine registration and segmentation. The structural images were then spatially normalized into standard MNI space using normalization parameters that were estimated by matching the gray (or white) matter images of each individual to a gray (or white) matter template. Each normalized anatomical scan was segmented (i.e. partitioned into different tissue classes such as gray matter, white matter and CSF) using mixture model cluster analysis techniques. However, warping images to match a template inevitably introduces volumetric differences into the images. For instance, if a subject's brain region has half of the volume of that of the template, then its

volume (i.e. voxels labeled as gray matter) will be doubled during spatial normalization. To remove this confound, the ensuing gray (or white) matter images were multiplied by the Jacobian determinants of the deformation fields defined during normalization (Ashburner and Friston, 2000). In other words, the spatially normalized gray (or white) matter image intensities were scaled by the amount of contraction and expansion applied during spatial normalization. This adjustment procedure allowed us to compare the absolute amount of gray matter in a particular region rather than its relative concentration. Finally, the images were smoothed using a 12 mm isotropic Gaussian kernel to enable parametric statistics with individual subjects.

The smoothed data were analyzed using SPM2. Regionally specific structural differences were assessed statistically using a F-test, testing for changes (i.e. increases or decreases) in gray matter. Significance levels were set at $p<0.05$, corrected for multiple comparisons.

11.4 Results

11.4.1 Clinical features

The patient details are provided in Table 11-1.

11.4.2 Motor and language mapping

All patients showed strong bilateral activations to the oral motor paradigm within the somatomotor and somatosensory face representations and expected (contralateral motor cortex and ipsilateral cerebellum) activations to finger tapping. The language paradigm generated strong dominant hemisphere activations centered around Wernicke's area, the angular gyrus, and the frontal premotor areas.

Table 11-1 Clinical demographics in nine patients with reading epilepsy

N	Age sex	Age of onset	Seizure types & triggering factors	Last treatment (Daily dose)	Ictal EEG	MRI
1	24 M	14	ORM, 2nd GTCS during reading aloud, conversation	LTG 200mg	Bilateral/generalized spike-wave maximum frontally.	Normal
2	23 F	15	ORM during reading aloud, conversation	GBP 0.9g	ORM with sharp or spike and slow wave discharge (phase reversal at F3).	Normal
3	29 F	13 MJ 18 ORM	Jaw (and body) jerks during reading aloud, conversation	LTG LEV	Occasional ORM during reading. No EEG changes.	Normal
4	47 M	15	ORM during reading aloud, conversation	None	Frequent ORM during reading. No EEG changes.	Normal
5	44 M	14	ORM, 2nd GTCS during reading aloud, conversation	CBZ VPA	Bilateral sharp / wave complexes maximum around vertex.	Left temp damage
6	20 F	12	ORM, 2nd GTCS during reading aloud and silently	CLB 10mg VPA 1g	Occasional ORM during reading. No EEG changes.	Normal
7	50 F	18	ORM, 2nd GTCS during reading aloud, conversation	CBZ 200mg	Occasional ORM during reading. No EEG changes.	Normal
8	27 M	14	ORM during reading aloud, conversation	VPA 1g CNZ 2mg	Occasional ORM during reading. No EEG changes.	Normal
9	25 F	17	ORM, 2nd GTCS during reading aloud	VPA 1g	Occasional ORM during reading. No EEG changes.	Normal

Abbreviations: 2nd GTCS = Secondary Generalized Tonic-Clonic Seizure; AED = Antiepileptic Drug treatment; CBZ = Carbamazepine; CLB = Clobazam; CNZ = Clonazepam; GBP = Gabapentin; JME = Juvenile Myoclonic Epilepsy; LEV = Levetiracetam; LTG = Lamotrigine; MJ = Myoclonic Jerk; ORM = Orofacial Reflex Myoclonus; OXC = Oxcarbazepine; PB = Phenobarbitone; PHT = Phenytoin; R/L = handedness right/left; VPA = Sodium Valproate.

11.4.3 Ictal fMRI

No seizures could be elicited in three patients despite up to 35 minutes of continuous reading during repeated EEG-fMRI sessions. The remaining six patients required a warm up period of reading aloud before seizures could be induced. Seizures consisted typically of brief orofacial reflex myocloni. Identification of seizures on covert reading was only possible in patient #1 who showed frequent reading-induced seizures during both his fMRI sessions (Figure 11-1). In five patients, seizures could only be elicited through reading aloud. Here a combination of audio recording, EMG recording and button presses was used to identify seizure activity. In one patient (#3) with a coexisting diagnosis of juvenile myoclonic epilepsy (JME), ORM could also be induced through interactive conversation which was done online, eliciting the same seizure phenomenology as with reading-induced seizures.

In patient #1, consistent seizure-associated BOLD responses were observed in the left lateral premotor cortex ($p < 0.05$ corr). This area of seizure-correlated BOLD response was found to be in close proximity to both hand and face areas of the motor cortex as identified through mapping of finger tapping and jaw opening (see Figure 11-2).

In two patients (#2,#3) who indicated ORM using a button press with their non-dominant hand, significant BOLD increases were observed bilaterally in the hand and face motor areas. The remaining three patients (#4-#6) showed unilateral activation in the hand area of the motor cortex, contralateral to the hand used for button press.

In addition, we detected significant ORM-related increases in BOLD response in mesio-temporal/limbic areas in four patients (left hippocampus in 2 patients, bilateral amygdala and left insula) and in the ventral (orbital) frontal cortex (BA 47) in three patients (see Figure 11-3).

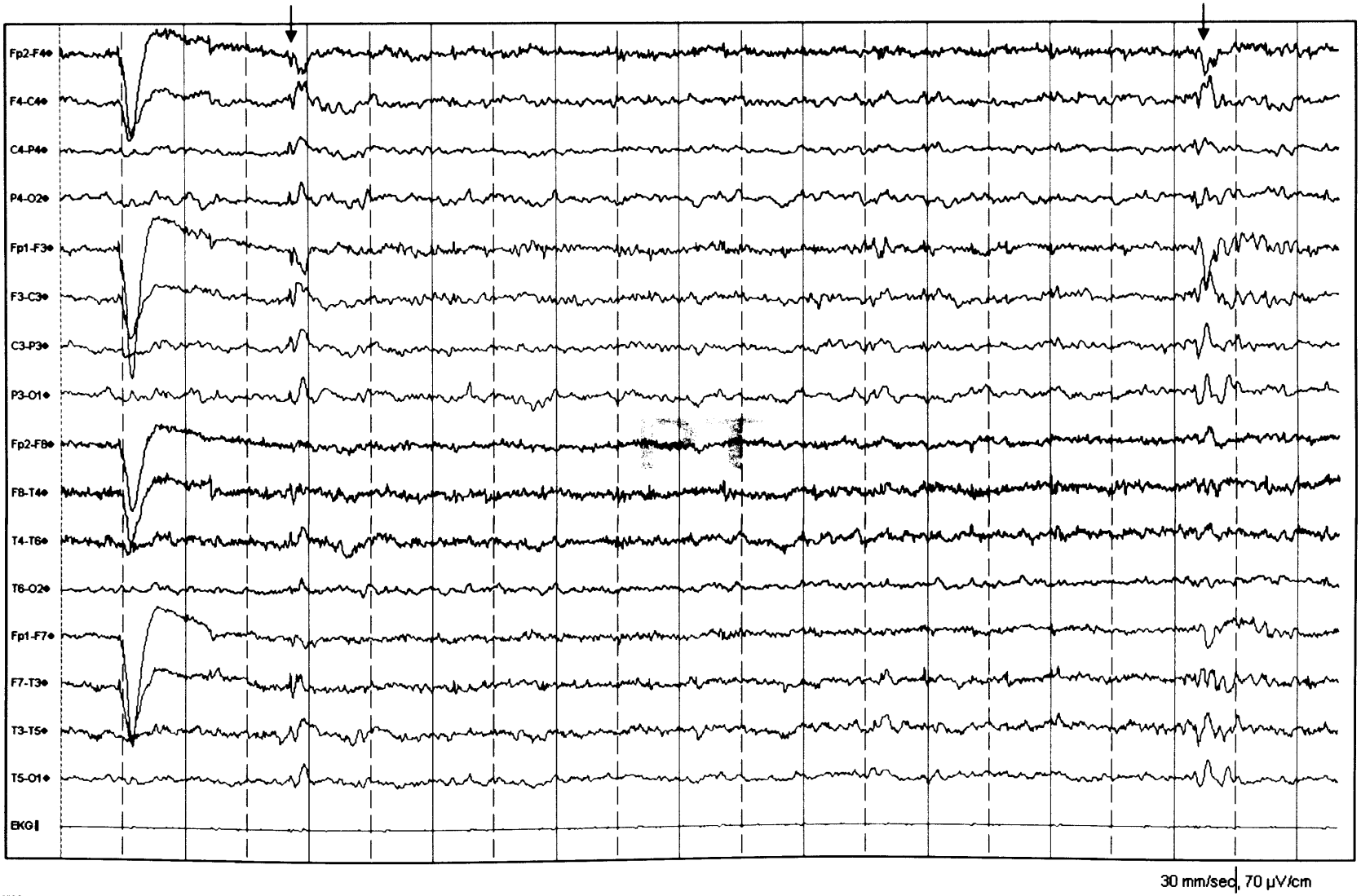

Figure 11-1 EEG in reading epilepsy

EEG from patient #1 showing generalized spike-wave discharges (arrows) during reading-elicited orofacial reflex myocloni.

Figure 11-2 fMRI activation during reading induced seizures
Surface rendering of significant fMRI activations in patient #1. Reading-induced seizures (green), language activations (blue) and motor mapping of mouth/jaw (red) are shown ($P < 0.05$, corr).

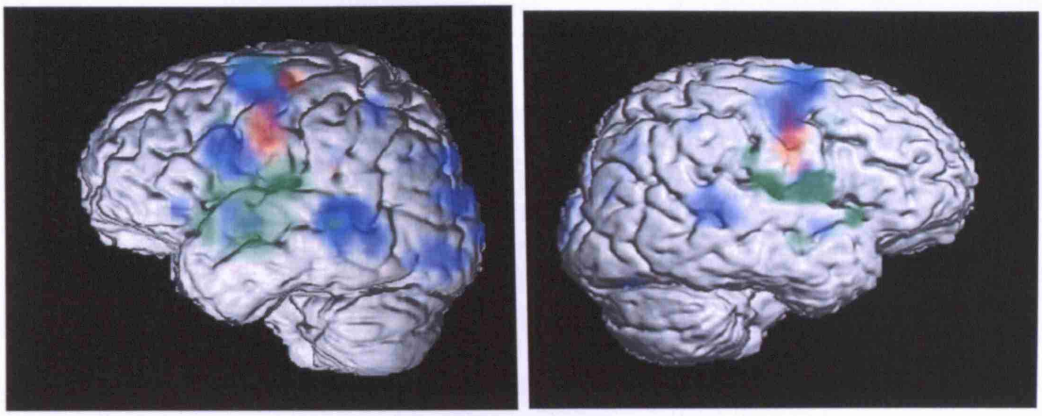

Subcortical BOLD increases were found in the thalamus in two patients (Figure 11-3: pat #3,) and in the left pallidum/putamen in three patients (Figure 11-4: pat #1,). One patient showed significant de-activations in the putamen bilaterally.

11.4.4 Voxel-based-morphometry

No significant differences in gray matter density, neither increases nor decreases, were detected when comparing all nine reading epilepsy patients with a group of 30 normal control subjects with a similar age range and gender distribution. Close radiological review also failed to reveal any abnormalities except for one patient (#5) who had had a left temporal perinatal ischaemic event.

Table 11-2 EEG-fMRI results

No	Study Design	Events	BOLD-fMRI response
1	EEG + EMG 35min study (2 x) Covert reading	> 100 myoclonic seizures associated with generalized spike-wave activity, maximal frontally	L motor jaw/hand area R cerebellum L thalamus R Brodmann Area 47 L putamen/pallidum, Caudate Bilat amygdala L>R
2	EMG 35min reading aloud (2x)	>50 myoclonic seizures self-indicated during reading with sharp, spike and slow wave discharge (phase reversal at F3)	Bilat motor hand/jaw area R>L L putamen/pallidum L insula
3	EMG 10 min reading silently 20 min conversation	>50 myoclonic seizures during conversation >30 myoclonic seizures during reading No localized EEG change	Bilat motor hand/jaw area R>L Bilat thalamus R>L Brodmann Area 47 L putamen/pallidum L Hippocampus
4	EMG 35 min reading aloud	> 40 myoclonic seizures self-indicated during reading aloud No localized EEG change	L motor hand area, R cerebellum L>R putamen deactivation
5	EMG 20 min reading aloud (2x)	>20 myoclonic seizures self-indicated during reading aloud background suppression only, no localized EEG change	L motor hand area, R cerebellum L hippocampus
6	EMG 35 min reading aloud	>100 myoclonic seizures self-indicated during reading aloud No localized EEG change	R motor hand area, L cerebellum L Brodmann Area 47
7	2 x 35 min reading aloud	No seizures	No analysis possible
8	2 x 35 min reading aloud	No seizures	No analysis possible
9	2 x 35 min reading aloud	No seizures	No analysis possible

Abbreviations: L = left, R = right, Bilat = bilateral, ORM = oro-facial reflex myoclonus.

Figure 11-3 Activations during conversation induced seizures
Statistical parametric maps (SPM{F}) superimposed on the mean-EPI image demonstrating significant activations ($P < 0.05$, corr) in a patient with conversation-induced seizures (patient #3). Note activations in the thalamus, BA 47left > right and in the left hippocampus.

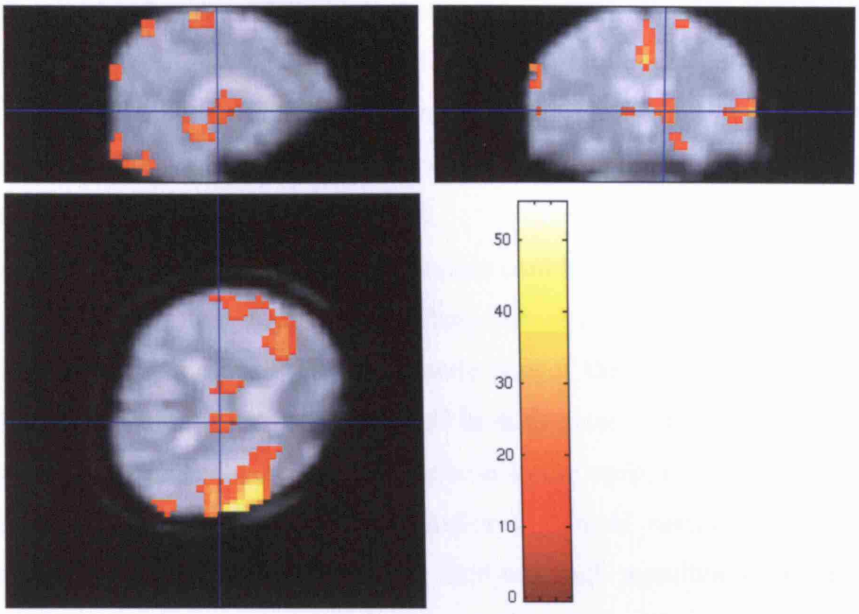

Figure 11-4 Subcortical activations with reading induced seizures
Statistical parametric maps (SPM{F}) showing significant ($P < 0.05$, corr) subcortical activations associated with reading-induced seizures on covert reading superimposed on coronal view (patient #1). Glass brain representations show all activations, but note that fMRI data was not normalized to fit into MNI space.

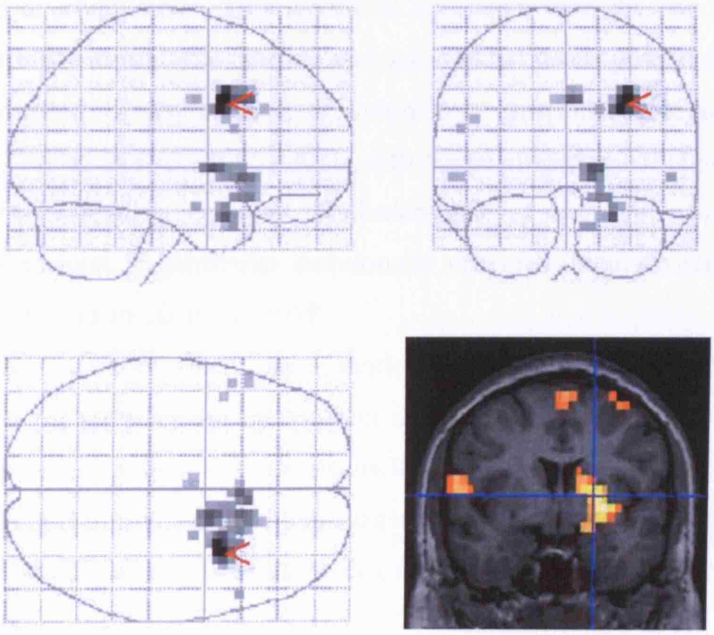

11.5 Discussion

We performed simultaneous EEG, EMG, and functional MRI in nine patients with reading epilepsy. Ictal fMRI revealed patterns of BOLD activations within cortical and subcortical areas during reading induced seizures: three patients showed activations within language dominant motor cortex for hand and face; three patients showed additional BOLD increases in BA 47; five patients showed subcortical BOLD responses either within the striatum (n=4), or the thalami (n=2). Most of the ictal cortical areas were either in close proximity to or directly overlapping areas activated by cognitive and motor functions.

Our findings of subcortical ictal BOLD changes corroborate a previous case report of reading epilepsy (Archer et al., 2003c). These subcortical areas may closely link to areas of hyperexcitable cortex that constitute part of the normal reading or motor networks. Recruitment of a "critical mass" in such areas with synchronization and subsequent spreading of excitation in response to the epileptogenic stimulus could precipitate epileptiform EEG activity and/or a clinical seizure. Increasing the complexity of epileptogenic stimuli may facilitate such recruitment (Koepp et al., 1998b). This recruitment may involve the participation and interaction of several cortical and sub-cortical structures activated by reading (BOLD activation in BA 47) or the emotional content of the reading material (mesiotemporal/amygdale/limbic structures). It may rely on both existing and re-organized functional links between brain regions and need not be confined to physically contiguous brain sites or established neuronal links. This would be consistent with the concept of variable hyperexcitability at multiple cortical and sub-cortical levels potentially allowing for any combination of asymmetric or symmetric, generalized, regional and focal discharges (Ferlazzo et al., 2005). Also, with the heterogeneity of clinical phenomena encountered in reading epilepsy (Radhakrishnan et al., 1995) and the variable efficacy of various, in particular emotionally charged, linguistic stimuli as seizure triggers (Koutroumanidis et al., 1998).

Our ictal fMRI data provides further evidence for the involvement of the putamen, caudate and pallidum in the modulation of seizure activity. The area of maximal BOLD response in patient #1 is functionally connected to a network of cortical and subcortical regions involved in the propagation and modulation of seizure activity as previously established in animals (Piredda and Gale, 1985) and humans (Blumenfeld et al., 2004).

We observed bilateral BOLD increases in the hand area of the patient with JME. In this case, primary motor areas are presumably part of the hyperexcitable cortex providing a functional link for the often seen association of reading epilepsy and JME in the same individual, and the recently reported observation of seizures triggered by reading in JME (Mayer et al., 2006).

The relationship of supposedly "generalized" discharges to the regional expression of bilateral or unilateral clinical symptoms remains controversial (Wolf et al., 1998). The thalamus and a complex reciprocal thalamo-cortical network are thought to be critically important in generalized seizures (Norden and Blumenfeld, 2002). More recently, specific cortical-subcortical circuits were also found to sustain and propagate focal cortical seizure activity (Blumenfeld et al., 2004). In view of the extensive thalamocortical and corticothalamic connections, and the wide range of motor, sensory and higher order functions subserved by the thalamus, it is reasonable to assume that widespread thalamic connections may be crucial to seizure propagation in reading epilepsy: abnormal [increased] activity in some areas of the brain (language areas) can lead to functional inhibition (speech arrest) or disinhibition (ORM) in remote structures, presumably through transsynaptic mechanisms, akin to the phenomenon of diaschisis following stroke. We suggest that the observed ORM are neither focal nor generalized seizures, but thalamocortical network seizures, supporting the views expressed by the ILEA Classification Core Group on the inadequacies of current seizure classification and the classification of reading epilepsy as a 'Special epilepsy condition' (Engel, Jr., 2006).

Most of the structures activated in association with reading-induced ORM are known to be relevant to language function. Activation in BA 47 is sometime observed specifically in relation to semantic tasks (Noppeney and Price, 2004). It was originally found in the pioneering studies of (Petersen et al., 1990), to be active when word reading was contrasted with viewing meaningless symbols, as in our experiment. Other studies however, have failed to replicate these findings (Poldrack et al., 1999;Rumsey et al., 1997).

Interestingly, (Gabrieli et al., 1998) have proposed that left inferior frontal activation during semantic tasks depends on the amount, duration and selection demands on semantic knowledge held in working memory. Archer and colleagues in their patient showed spike-triggered fMRI BOLD activation in the left posterior middle frontal

gyrus and bilateral inferior central sulcus, areas also thought to be recruited during working memory cognitive tasks (Archer et al., 2003c).

11.5.1 Methodological considerations & limitations

Subject selection and seizure detection: In spite of launching the largest recruitment effort in the UK for patients with reading epilepsy, the number of subjects from whom useful data could be acquired was low for the reasons above (see methods). It was decided not to stop medication for ethical reasons. The artificial scanner environment can have profound effects on cognitive activity, levels of concentration, arousal, and anxiety. Reading epilepsy patients appear to require a warm up period of reading before ORM would appear (Koepp et al., 1998a), it was notable that this warm up was longer inside the scanner. Some patients did experience ORM during the assessment process but not inside the scanner, others only on reading aloud inside the scanner. Studying this group was particularly difficult. In spite of voice monitoring, it was often difficult to distinguish the normal pauses and breaks that occur during overt reading from any stutters or disruptions symptomatic of reading epilepsy. We therefore had to rely on self-reporting in the majority of cases and accept this as a confound. As expected, button presses in our particular subjects were associated with BOLD increases in contralateral motor cortex and possibly SMA. Unilateral button press therefore, was unlikely to explain the ipsilateral motor cortex activations seen in two patients during seizures. Furthermore, patient #1 with EEG spikes during silent reading, showed BOLD increases in the motor cortex of the language dominant hemisphere despite there being no voluntary limb movements.

Experimental setup & motion artifacts: We adjusted the projection rate to simulate natural reading as far as possible, but reading single projected words is clearly different to reading standard text on paper. A combination of altered arousal and differences in reading might explain why three of our patients did not experience any seizures in the scanner.

It is possible for ORMs to generate stimulus-correlated motion and false activations so we took great efforts to minimize the possibility of such effects occurring in our study. Firstly, the subjects were immobilized in so far as possible. The volumes were movement-corrected by image registration, and the movement parameters were included as covariates of no interest in the design thereby trading a degree of

sensitivity for the additional specificity (Friston et al., 1996). Finally, the whole-brain protocol helped maintain a uniform steady state of T1-relaxation.

Effect of disease on performance: We often assume that the processes engaged by a chosen cognitive or motor task are similarly manipulable in normal and disease states. Matched behavioral performance, however, does not ensure matched cognitive processing, e.g. having "reading epilepsy" profoundly effects the way in which the seizure-provoking activity is carried out, in terms of the attentional resources allocated, the behavioral strategies adopted and, ultimately, task performance. Yet, if we wish to infer an attenuation or augmentation of regional task-related activation directly due to the epileptic condition, an assumption that the explanatory variable ("reading") is directly comparable across the two settings must be made. Even though we attempted to minimize the chance of seizure induction during the language mapping studies by using short periods of reading, we cannot exclude the possibility of sub-clinical epileptiform activity or different reading strategies in patients. Thus, the direct comparison of language mapping between reading epilepsy patients and healthy volunteers might not be meaningful.

In summary, we detected a network of cortical and subcortical areas of significant BOLD changes time-locked with seizure activity in five patients. These areas of potential cortical hyperexcitability were in close proximity or overlapping with functional areas relevant for language and motor functions. There were no gross abnormalities in cognitive or motor organization. We conclude that a network of cortical areas involved in normal language and motor function, together with their associated subcortical structures, subserve ictogenesis in reading-epilepsy.

* * *

12. Chapter 12: Discussion

12.1 Summary of findings

Chapter 5 (Event-related EEG/fMRI):

- The simultaneous and continuous acquisition of EEG during fMRI allows for an event-related fMRI analysis of EEG events.*
- The results of such analyses, in terms of localization as applied to focal IEDs, are in general agreement with those of previous spike-triggered fMRI studies.
- Continuous recording allows the study and comparison of BOLD responses across a range of different EEG events and therefore the construction of potentially more accurate and sophisticated models.

Chapter 6 (EEG Quality):

- The simultaneous acquisition methods employed in this work provide EEG recordings during fMRI scanning, virtually indistinguishable (both visually and spectrographically) from EEG acquired without scanning.
- There is good interobserver agreement in detecting focal epileptiform discharges on scanner EEG.

Chapter 7 (Ictal fMRI):

- Using simultaneous EEG/fMRI, dynamic and biphasic signal changes can be shown and localized during focal subclinical seizures.*

Chapter 8 (fMRI of absences):

- fMRI during human absence seizures reveals the reciprocal participation of focal thalamic and widespread cortical networks, supporting the corticoreticular hypothesis of Gloor.*
- There is widespread cortical deactivation suggestive of reductions in cortical blood flow and metabolism in response to synchronized EEG activity.*

Chapter 9 (EEG/fMRI in focal epilepsy):

---

* Novel findings, demostrated and published for the first time.

- Significant activations were detectible in over 68% of patients in whom IEDs were captured.
- Activations were highly concordant with sites of presumed seizure generation where known.
- Deactivations were less concordant but a striking pattern of retrosplenial deactivation was observed in 7 patients.*
- The basic HRF to IEDs is physiological.
- Focal activations are more likely when there is:
    - Good electroclinical localization
    - Frequent and stereotyped IEDs
    - Minimal head motion
    - A normal background EEG
- Incorporating information about different types of IEDs, their durations and saturation effects results in more powerful models for detecting activation.*

Chapter 10 (EEG/fMRI in generalized epilepsy):

- The changes observed were predominantly, but not exclusively, of thalamic BOLD signal increase with a decrease in cortical association areas, in keeping with the clinical manifestation of GSW.
- There were no significant syndrome-specific differences in activation patterns between IGE and SGE or the different IGE subtypes.*

Chapter 11 (EEG/fMRI in reading epilepsy):

- BOLD activations during orofacial myoclonus were adjacent to or overlapping cortical areas physiologically activated during language and facial motor tasks supporting the notion that seizures arise when a critical mass of neurons are activated through a provoking stimulus within cortico-reticular and cortico-cortical circuitry subserving normal functions.*

12.2 Further work

12.2.1 EEG/fMRI in paediatric epiliepsies

Several studies now have shown similar interictal findings in children with partial (De, X et al., 2007b;Jacobs et al., 2007), and generalized epilepsy (Labate et al.,

2005a) and also ictally (De, X et al., 2007b;De, X et al., 2007a). These particular studies are important because (1) there is a significant need for early surgery in children with refractory partial epilepsy, (2) the threshold for surgery and intracranial EEG is higher and hence the need for non-invasive localization greater, (3) structural MRI is less powerful where myelination is incomplete (Cross, 2002).

Moeller et al. (Moeller et al., 2008b) studied 10 children with drug naive absence seizures and confirmed the same pattern of consistent thalamic signal increase with a cortical decrease in BOLD, what has since proved to be the common metabolic signature of human GSW activity. There was no difference therefore between findings in this group and in those of adults, on drug treatment, and with chronic epilepsy. Differences in age, medication and disease duration were therefore felt not to have any substantial impact on the fMRI findings in contrast to other reports (Marcar et al., 2004;Richter and Richter, 2003).

12.2.2 GSW, deactivations & the default mode hypothesis

Hamandi et al. (Hamandi et al., 2008a)(also (Carmichael et al., 2008)) further studied the physiological basis of deactivation in generalized spike and wave by means of simultaneous EEG correlated BOLD fMRI and perfusion imaging at 3 Tesla in a group of 4 patients, 2 with IGE and 2 with SGE.. The main finding was of a normal neurovascular coupling evidenced by a reduction in CBF with BOLD deactivation. There was also good reproducibility in one patient studied also at 1.5 Tesla.

Having linked 'default mode areas' to EEG power in the 17-23 Hz range (Laufs et al., 2003b) (also see Chapter 2.6.2), Laufs et al. (Laufs et al., 2006b) put forward an interesting interpretation for deactivations during GSW, one championed by others (Gotman et al., 2005) that has subsequenltly gained popularity (Gotman, 2008).

Debate continues as to the significance of these observations. According to the 'default mode network hypothesis', the cortical areas of BOLD decrease are those that are active at rest and maintain consciousness (Raichle et al., 2001;Raichle and Mintun, 2006). Are we simply observing the consequence (Aghakhani et al., 2004;Gotman et al., 2005;Hamandi et al., 2006) of impaired consciousness or the cause (Salek-Haddadi et al., 2003e)? The distinction is subtle but the question remains unanswered. It is also unclear (and arguably not possible) from the current

fMRI studies to establish whether discharge initiation is subcortical or cortical as the animal evidence now suggests*.

In (Laufs et al., 2007a) we set out to further test 'the default mode hypothesis' as an explanation for deactivations by way of performing a group analysis on our TLE and exta-temproal lobe epilepsy data. We showed common decreases of resting state activity in 9 patients with TLE but not in 10 with extra-TLE. This suggests that the functional consequences, in terms of influence on background activity, of TLE IEDs may be different to extra-TLE. Group-level activations were detected in the ipsilateral hippocampus in TLE and in subthalamic, bilateral superior temporal and medial frontal brain regions in extra-TLE, possibly reflecting differences in propagation patterns.

12.2.3 EEG/fMRI & neurobiology

Several other reports have confirmed various aspects of our findings both interictally (Bagshaw et al., 2006;Briellmann et al., 2006;Di et al., 2006;Kobayashi et al., 2007;Labate et al., 2005b;Lengler et al., 2007;Liu et al., 2008) and ictally (Archer et al., 2006;Kobayashi et al., 2006c), without adding much new information (See appendix II).

At least two studies (Laufs et al., 2006a;Manganotti et al., 2008) have found focal slow wave activity in selected patients to be associated with concordant BOLD activation re-iterating the fact that voltage and morphology are less important than IED focality and frequency.

Leal et al. (Leal et al., 2007) (an ICA study) reported on a child with idiopathic occipital lobe epilepsy (Panayiotopolous syndrome) postulating seizure origin in lateral occipital areas followed by symptomatic propagation to temporal pole and lateral temporal cortex. The same group reported previously on 3 patients with OLE studied with both EEG source analysis and EEG/fMRI (Leal et al., 2006). Two children had late-onset OLE and another photosensitive idiopathic OLE. In neither condition are the exact sources known but interestingly the observed EEG/fMRI activations were better placed to explain the symptomatology than the results of EEG source localization. It is worth noting that the occipital lobes are particularly well amenable to EPI.

---

* Recent studies in GAERS rats have suggested a cortical onset within layer 5/6 neurons of the facial somatosensory cortex (Meeren et al., 2005;Polack et al., 2007).

Other studies have tried to look further at HRF variability and better ways of modeling the response to IEDs. Jacobs et al. (Jacobs et al., 2008a) studied a group of 37 children ages from 3 months to 18 years with different epilepsy syndromes including idiopathic generalized epilepsy (details not given). Patients were sedated using different doses and medications and grouped into various arbitrary age bands for comparison. In younger subjects a relative delay in HRF peak was reported with evidence of saturation effects at higher spike frequencies (see Apprendix II) but there were too many variables for meaningful interpretation of the findings.

In another study the same group (Jacobs et al., 2008b) looked at 5 children with tuberous sclerosis and several lesions and IED types. In four patients, at least one tuber in the assumed lobe of seizure onset showed a BOLD response, mostly positive but some negative. In all patients more than one tuber was implicated in generating the response. Some activations or deactivations were distant and within 'normal' brain tissue. In other cases, responses extending outward from tubers into surrounding brain. Conversely, different IED types in one patient often linked to activation/deactivation in the same network of tubers. Unfortunately, some results are given for sessions rather than patients and in four patients more than one seizure onset zone was known to exist but the relationship between the ictal onset and the irritative zones for each patient was not fully declared. There was no surgical data but this study is at least noteworthy as a proof of principle for the sorts of questions that could be answered with EEG/fMRI in complex multilesional or multifocal cases.

12.2.4 EEG/fMRI vs Intracranial EEG

Whilst here have been odd reports of interictal EEG/fMRI in patient who later had intracranial EEG (Al-Asmi et al., 2003;De, X et al., 2007b;Laufs et al., 2006a;Seeck et al., 1998), the most systematic study looking at this has been the work of Benar et al. (Benar et al., 2006) who studied 5 patients with EEG/fMRI, high density EEG source localization and intracranial EEG. They showed that where there was an intracranial electrode within 20-40mm of an EEG or fMRI peak (either positive or negative), there was at least 1 active contact, but within 20mm, fMRI concordance was greater. This might have been due to limitations of the dipole model (c.f. distributes source models). EEG dipoles and fMRI maxima were generally in less agreement together than either of the two were separately with intracranial EEG, re-enforcing the notion that given their individual limitations, the two modalities

provide complimentary rather than confirmatory information with respect to localizing the irritative zone. Ultimately this was a non simultaneous study with respect to the fMRI and intracranial EEG, but there did seem to be some correlation between deactivation and lower low-frequency content on intracranial recordings, lending weight to the notion that slow wave (inhibitory) activity may be reducing the regional metabolic activity (Stefanovic et al., 2005).

12.2.5 EEG/fMRI in epilepsy surgery

Zijlmans et al. (Zijlmans et al., 2007) used EEG/fMRI to study a selected* group of 29 patients (13 MRI negative), previously rejected for epilepsy surgery because of either an unclear focus or presumed multifocality. A significant BOLD response (either positive or negative) was found in 15/29 patients. 11/15 were considered to have a 'robust' positive BOLD response and in 8/11 it was considered topographically correlated to the EEG. These patients were put forward for clinical consideration.

Of these 8 patients, 3 had been previously rejected for surgery because of an unclear focus, 2 because of multifocality and 3 on both accounts. EEG-fMRI improved localization in 4 out of 6 patients with unclear localization:

- In patient #29 (left hippocampal sclerosis but suspected FLE) – a left frontal focus was found with both right and left sided IEDs. This patient was offered intracranial EEG but then improved.
- In patient #1 (MRI negative) - a parasagittal EEG focus was found to activate the medial postcentral gyri but surgery was considered too risky (too close to leg area).
- In patient #3 (MRI negative, ictal EEG unclear) – a left basofrontal EEG-fMRI focus was found and confirmed as the ictal onset zone on intracranial EEG but surgery was not performed due to overlap with Broca's area.

In the multifocal group, multifocality was confirmed in 4/5 and a single focus was advocated in the remaining patient (patient #10), which was considered to have previously been rejected on both accounts.

- In patient #10 (left temporal low grade glioma but with both right frontal and left temporal ictal onset and IEDs) - EEG-fMRI of the dominant left

* Patients were recruited by post. Other critieria included no contra-indications to MRI and >10 IEDs on 40mins of previous EEG.

frontotemporal focus revealed a concordant activation (interestingly with a discordant right frontal deactivation) which on acute electrocorticography was confirmed to co-localize with the ictal onset zone. After resection and anterior temporal lobectomy, the patient had an Engel II outcome*.

In 4 patients therefore, new surgical prospects were opened up and in 2, intracranial EEG recordings were in agreement with EEG-fMRI. This study was important because the application of EEG-fMRI to this particular population probably represents its toughest challenge to date. In five patients the study was repeated for various reasons and the 'technically best' measurements were used for analysis. The main factor contributing to low yield was lack of IEDs. In 3 patients the study was discontinued due to patient discomfort and in 9 patients the study was done over multiple sessions. Still, EEG-fMRI was clearly shown to be a valuable tool in pre-surgical evaluation by way of either corroborating a focus or supporting a negative decision.

12.2.6 Early BOLD responses

Hawco et al. (Hawco et al., 2007) reported 'early' BOLD changes preceding scalp discharges in a group of 15 patients selected out of a database of 130. They found 7 datasets where the models used indicated an HRF that peaked 1 second after the IED which they concluded was indicative of an 'event' that must have preceded the IED. A long discussion then follows as to the significance but there are several methodological problems:

1) Their group included a difficult to interpret mixture of patients with focal and generalized epilepsy, the later including both IGE and SGE.
2) The methodology was primitive. Rather than using 7 separate models, the authors should have used use a single flexible model such as a finite impulse response model and looked at the corresponding parameter estimates.
3) Activations were considered concordant if within the same lobe as the electroclinical localization, but further information should have been provided as to whether the early responses were concordant with the classical responses reported in their original studies on the same patients. Also, GSW activations were considered concordant if non-focal, but this is at odds with their application of an arbitrary cluster threshold to their results.

* Sporadic seizures only at 6 months follow-up.

4) There was considerable circularity in the choice of methods and inferences drawn. For each patient, 7 analyses were performed using a time shifted gamma function in each case. If an activation was found to pass the concordance criteria (437 clusters of activation in total), another HRF was fitted to each significant activation by deconvolution. Only HRFs with a signal to noise ratio of >3 (another arbitrary cut-off) were then taken (330 in total) and from each of these a time-to-peak was derived. In one data set, none of the HRFs passed their criterion which is rather surprising. 5/7 non-burst data sets and 2/9 burst data sets [not surprisingly] had at least 1 early-peaking HRF. Of these 7 datasets, 4 had either a maximum t-statistic or volume statistic early gamma function map. They conclude that when an early activation is present, it most often represents the main activation but even accepting the various shortcomings, the number of patients reported with early responses were 4, that is 4 out of 15 (or 130 patients overall) and with all kinds of pathologies.

It is also unclear why deactivations were ignored. The findings may have been equally informative (or uninformative). The reasons stated were:

a. HRFs tend to be noisier - but good statistics ought to take care of that.
b. The neurophysiological origins are less well understood - but surely no better than those of 'early responses'.
c. Their localization tends to be less well correlated - but it is unclear how the inclusion of GSW patients could have helped in this respect.

Moeller et al (Moeller et al., 2008a) reported 'early' BOLD changes preceding GWS in 6 patients with IGE. They reported thalamic changes up to 6 seconds prior to discharges with cortical deactivations 3-6 seconds prior again. A large discussion follows are to the biological significance but like many previous studies there are again several methodological caveats:

1) The patients reportedly had irregular generalized poly spike and wave discharges of 0.5 to 3 seconds duration. From the single EEG example provided (without ECG) it is not possible to be certain as to what the recorded events actually were. In focusing on poly spike-wave activity, the authors may have denied themselves the diagnostic certainty associated with observing runs of stereotypes discharges which are virtually unmistakable in

morphology on scanner EEG*. It is interesting to note in this regard that when the same group later studied patients with childhood absence seizures, no early changes were found (Moeller et al., 2008b).

2) No information is provided on head motion and what extra pre-cautions were taken during the analysis. This would have been especially important given the diagnostic uncertainty on EEG.
3) The methodology was taken from (Hawco et al., 2007) so again, rather than using 5 separate models, the authors should have used use a single flexible model such as a finite impulse response model and looked at the corresponding parameter estimates. (They seem to have missed the fact that when generating SPMs, the regressors are effectively orthogonalised such that they would not need to run separate analysis and resort to Bonferroni corrections.)
4) In applying the high-pass filter, to the model and the data, the authors may have introduced a 'time leak', i.e. artifactual undulations in the timeseries whereby power evoked by one event could have inadvertently leaked into a region of time modeled by another (Josephs and Henson, 1999).

12.2.7 Data Driven Analysis Techniques (TCA & ICA)

Several data driven analysis methods have been put forward as potentially capable of detecting epileptiform activity within fMRI timeseries alone (i.e. without simultaneous EEG). These include temporal cluster analysis (Morgan et al., 2004;Morgan et al., 2007) and ICA (McKeown et al., 1998). We investigated the former using a similar subgroup of TLE fMRI data but found several problems related to the confounding effects of head motion, physiological noise and problems with validation of results (Hamandi et al., 2005a). Using the later, we further analyzed the data presented in Chapter 8 and found several independent spatial components to be active during generalized spike-wave (Salek-Haddadi et al., 2004)(see Appendix 1), hinting at the entrainment of multiple separate networks, some of which in retrospect correspond to known RSNs. A mechanism was therefore provided whereby changes in 'the blend' could potentially account for differences in observations across the literature (Aghakhani et al., 2004;Archer et al., 2003a;Hamandi et al., 2006;Salek-Haddadi et al., 2003e).

* The authors state that subjects with longer discharges were excluded because analysis for early effects would not have been possible but their reasoning is unclear.

Rodionov et al. (Rodionov et al., 2007) were able to further analyze with ICA a subset of the focal epilepsy data presented in Chapter 9 (Salek-Haddadi et al., 2006). They selected eight of the most clear cur and concordant results and performed a spatial ICA on the fMRI timeseries using the Brain Voyager QX Software. The ICs were then classified automatically (De et al., 2007), according to training datasets acquired from healthy volunteers, into BOLD and non-BOLD such as motion artefact, susceptibility artefact, physiological noise etc. The individual BOLD ICs and their timecourses were then cross checked against the GLM-derived results looking for *both* spatial overlap (>10%) and temporal correlation ($P<0.01$) to select the most relevant. In 6 cases one and in 1 case two of the candidate ICs met the criteria. In one case no ICs were found to match, but on later inspection one of the non-BOLD ICs did suggesting contamination by motion. Several of the ICs found corresponded to resting state networks (Damoiseaux et al., 2006) and a further 50% still of the BOLD-ICs were confirmed to be noise on visual inspection. Conversely in one patient, one of the noise-ICs was also found to be relevant. Amongst the rejected BOLD-ICs, some were found to have a temporally correlated timecourse and is was felt that they could be describing some part of the 'true' epileptogenic network. In 5/7 cases, 'time-lagged' components ranging from -1 to 2 TRs were found, in some cases suggesting delayed changes contralaterally and adding to the potential 'added value' of ICA.

There is clearly some middle ground to be achieved between the rigid GLM analyses and the more flexible but less-specific and less objective data driven techniques. One long recommended approach to combining the two is using ICA to denoise fMRI timeseries prior to GLM analysis (McKeown et al., 2005). This approach would seem particularly suited to patient studies but remains to be fully explored.

12.2.8 Functional connectivity & DCM

Hamandi et al. (Hamandi et al., 2008b) studied a patient with TLE using both EEG/fMRI and probabilistic tractography. Activations were found in left parahippocampal, middle temporal and superior temporal gyri together with bilateral activations in parietal and occipital areas including the lingual gyrus. Tractography demonstrated anatomical connections from the left temporal to ipsilateral occipital and orbitofrontal areas. Two dynamic causal models were next constructed using the parahippocampal and lingual activations as regions of interest or nodes with

reciprocal connectivity, one in which the IED was modeled as input to the former and another, as input to the later in order to assess the impact of IEDs on the connections strengths within the model. DCM showed stronger connectivity from lingual to parahippocampal than vice versa in both cases but there was stronger evidence for the IED acting on the later. This study serves as a demonstration of combining EEG/fMRI data with tractography but also highlights the difficulties in using interictal EEG/fMRI data to infer propagation or connectivity (see Chapter 3.5).

12.3 Future work & conclusions

The multifaceted technological challenge of acquiring simultaneous EEG-correlated fMRI data has been met and the potential exists for mapping electrophysiological activity with unprecedented spatio-temporal resolution. A PubMed search reveals over 254 separate publications on the topic of simultaneous EEG/fMRI*, 125 in epilepsy and 19 in this year alone, all dating back to the seminal work of John Ives (Ives et al., 1993). The last few years have seen the emergence of ever more novel ways of acquiring EEG/fMRI data (Anami et al., 2003;Hanson et al., 2007), at ever increasing field strengths (Mullinger et al., 2008b;Mullinger et al., 2008a) and with newer materials (Negishi et al., 2008).

At least for the time being, the transformation of EEG data into linear models suitable for voxel-based statistical hypothesis testing is central to the endeavor. This in turn is predicated upon a number of assumptions regarding the manner in which the generators of EEG phenomena may engender changes in Blood Oxygen Level Dependent (BOLD) signal. I anticipate that further characterization of the BOLD correlates of spontaneous EEG activity and the development of ever more sophisticated fMRI models will constitute an important effort over the next few years, aided by data from both animal and human simultaneous intracranial EEG and fMRI.

EEG-correlated fMRI remains a developing technique with significant scientific and clinical potential but also important theoretical, methodological and practical limitations. Future clinical roles in epilepsy, such as in seizure disorder classification (e.g. in conjunction with EEG) or the localization of epileptogenic cortex during pre-surgical evaluation, will depend on the accumulation of further EEG/fMRI data and

* Serach terms 'EEG' 'fMRI and 'Simultaneous'.

specifically, in combination with other markers of the epileptogenic zone and surgical outcome data. Clinical value need ultimately be dictated by considerations of sensitivity, specificity, and diagnostic yield versus practicality, applicability and limitations.

Debate continues as to whether MRI could ultimately be used to detect neuronal electrical activity directly (Konn et al., 2003;Konn et al., 2004;Petridou et al., 2006), but continuing developments in parallel imaging techniques (Sodickson and McKenzie, 2001) at least promise to increase temporal resolution to where this might become achievable (Lin et al., 2006). In the meantime a new generation of physiologically-sensitive contrast agents could go someway toward realizing this (Bowtell, 2008).

* * *

13. Appendices

13.1 Appendix I - Previous EEG/fMRI studies in epilepsy

Reference & Citation	N/I	Scanner & Sequence Parameters	Acquisition Mode & EEG System	IA PA	CR	fMRI Analysis		
						Method & Software	Multiple Comparisons correction	Threshold
(Warach et al., 1996)	2 1	1 5 Tesla, Siemens Vision TE 51 - 60ms 96 - 128 x 128 matrix 10-14 x 7mm slices	EEG-triggered fMRI Optilink, Neuroscan	No No	No	Thresholded % change images with *AFS* software (**Conclusions**: Bilateral activation where EEG suggested left temporal localization and anterior cingulate activation in relation to generalized epileptiform activity ' we cannot make conclusions about the source of the discharge from the present data ')	None	Arbitrary
(Seeck et al., 1998)	1 1	1 5 Tesla, Picker Edge TE/TR 35 560 ms 128 x 64 matrix (multishot) 6 x 6mm slices, 1mm gap	EEG-triggered fMRI Optilink, Neuroscan	No No	Yes	Cross-correlation (**Conclusions**: Multiple areas of signal enhancement on fMRI Confirmed on 3D-EEG source localization with evidence of a focal onset Focus later confirmed on subdural recordings)	Bonferroni & CT 10 voxels	P< 0 005
(Symms et al., 1999)	1 1	1 5 Tesla, GE Horizon TE/TR 40 3500-4500 ms 96x96 or 64x64 matrix 10-20 x 5mm slices	EEG-triggered fMRI In House	No No	Yes	Two-tailed t-test using *Stimulate* software (**Conclusions**: Reproducible and concordant activation across 4 sessions)	Limited Monte Carlo simulations	P< 0 05
(Patel et al., 1999)	20 1	1 5 Tesla, Siemens Vision TE/TR 64 2000ms 128x128 matrix 8-11 x 5-8mm sections	EEG-triggered fMRI Optilink, Neuroscan	No No	No	Based on comparison of individual spike images with rest using *AFS* software (**Conclusions**: 9 10 overall reported as showing 'activation corresponding to the EEG focus')	None	Arbitrary
(Krakow et al., 1999b)	10 2	1 5 Tesla, GE Horizon TE/TR 40ms 4500 ms 64 x 64 matrix 20 x 5mm slices (plus other)	EEG-triggered fMRI In House	No Yes	Yes	Two-tailed t-test using *Stimulate* software (**Conclusions**: Reproducible activations (same lobe and overlapping) obtained in 6 10 patients in close spatial relation to EEG focus)	Limited & CT - 3-voxels 2-slices	P<0 05
(Krakow et al., 1999a)	1 1	1 5 Tesla, GE Horizon TE/TR - 40ms 4500 ms 64 x 64 matrix 20 x 5mm slices	EEG-triggered fMRI In House	No Yes	Yes	GLM analysis using *SPM96* software (**Conclusions**: Focal activation within a large malformation of cortical development in response to focal epileptiform discharges)	GFT	P<0 05
(Lazeyras et al., 2000a)	11 4	1 5 Tesla, Marconi Eclipse TE/TR - 40 979 11-15 x 5mm slices (plus other)	EEG-triggered fMRI Optilink, Neuroscan	No No	Yes	Cross-correlation using *Interactive Data Language* (**Conclusions**: Activation confirmed clinical diagnosis in 7 11 In 5 6 intracranial EEG confirmed result)	Bonferroni	Variable
(Lazeyras et al., 2000b)	1 1	1 5 Tesla, Marconi Eclipse TE/TR - 40 979 11 x 5mm slices	EEG-triggered fMRI Optilink, Neuroscan	No No	Yes	Cross-correlation using *Interactive Data Language* (**Conclusions**: Area of signal enhancement concordant with hyperintensity seen on ictal FLAIR images in a patient with non-lesional partial epilepsy)	Bonferroni	P<0 05
(Krakow et al., 2001c)	1 1	1 5 Tesla, GE Horizon TE/TR - 40ms 4500 ms 64 x 64 matrix 20 x 5mm slices	EEG-triggered fMRI In House	No Yes	Yes	Individual spike images compared to mean of rest using t-test using *SPM99b* software (**Conclusions**: Focal concordant activation within encephalitic cortex also obtained in relation to 15 43 individual spikes 'Single event-related fMRI of interictal spikes in feasible in selected patients ')	GFT	P<0 05
(Baudewig et al., 2001a)	1 1	2 Tesla, Siemens Vision TE/TR - 53 2000 ms 2x 4 x 4mm sections	Continuous EEG fMRI (Interleaved) EMR32, Schwarzer	No No	Yes	Cross-correlation with shifted boxcar (**Conclusions**: Unilateral insular activation shown in relation to generalized epileptiform discharges ' strategy resulted in robust BOLD MRI responses to epileptic activity that resemble the same characteristics as are commonly observed for functional challenges ')	None	Unspecified
(Krakow et al., 2001b)	24 0	1 5 Tesla, GE Horizon TE/TR - 40ms 4500 ms 64 x 64 matrix 20 x 5mm slices (plus other)	EEG-triggered fMRI In House	No Yes	Yes	GLM analysis using *SPM96* software (**Conclusions**: 12 24 patients showed activations concordant with EEG focus, 7 12 of which also had concordant structural lesions 2 24 were discordant and 10 24 showed no significant activation 64-channel EEG dipole solutions were later concordant in 6 6 (Lemieux et al., 2001a))	GFT	P<0 05
(Lemieux et al., 2001b)	1 1	2 Tesla, Siemens Vision TE/TR 40 1520 ms 64 x 64 matrix 20x1 8mm slices, 1 2mm gap	Continuous EEG fMRI In House	Yes Yes	Yes	GLM analysis using *SPM99* software (**Conclusions**: Localization of BOLD activation was consistent with previous findings and EEG source modeling Timecourse of activation was comparable to physiological HRF)	None	P< 0 001

Reference & Citation	N/I	Scanner & Sequence Parameters	Acquisition Mode & EEG System	IA	PA	CR	fMRI Analysis		
							Method & Software	Multiple Comparisons correction	Threshold
(Jager et al., 2002)	10/1	1.5 Tesla, Siemens Vision Te/TR = 64/1630 ms 128 x 64 matrix 10 x 5mm slices	EEG-triggered fMRI (Burst mode) EMR32, Schwarzer	Yes	Yes	Yes	Cross-correlation (**Conclusions**: Focal activation in 5/5 patients, concordant with EEG amplitude mapping. Mean signal increase was 15±9%. Spike amplitude correlated with volume of activation.)	None	P<0.001
(Iannetti et al., 2002)	3/3	1.5 Tesla, Philips Gyroscan TE/TR = 50ms/3000 ms 64 x 64 matrix 25 x 4mm slices	Continuous EEG/fMRI In House	Yes	Yes	Yes	GLM analysis using *SPM99b* software (**Conclusions**: Activation within extrastriate visual cortices in all three patients with fixation-off sensitivity, linked to paroxysmal EEG activity during eyes-closed and not otherwise seen in healthy matched control subjects.)	GFT	P<0.05
(Benar et al., 2002)	4/4	1.5 Tesla, Siemens Vision TE/TR = 50/3000 ms 64 x 64 matrix 25 x 5mm slices	Continuous EEG/fMRI EMR32, Schwarzer	Yes	No	Yes	GLM analysis using *fmristat* (**Conclusions**: The average HRF presented a wider positive lobe in three patients and a longer undershoot in two. There was no clear correlation between the amplitudes of individual BOLD responses and EEG spikes.)	Bonferroni & CT=5 voxels	Arbitrary
(Archer et al., 2003b)	2/1	3 Tesla, GE Signa TE/TR = 30/3000ms 128x128 matrix 22x4mm slices, 1mm gap	EEG-triggered fMRI In House	No	No	Yes	GLM analysis using *SPM99* software (**Conclusions**: Facial somatosensory involvement in BECTS seizures.)	None	P< 0.001
(Archer et al., 2003c)	2/1	3 Tesla, GE Signa TE/TR = 30/3000ms 128x128 matrix 22x4mm slices, 1mm gap	EEG-triggered fMRI In House	No	No	Yes	Unpaired t-test using *iBrain* software (**Conclusions**: Spike activity overlapped with reading activity in the left frontal cortex working memory area.)	None	P< 0.001

Abbreviations: N/I = total number of subjects studied (with EEG/fMRI) / number of illustrated fMRI results, IA = Imaging Artefact Removal, PA = Pulse Artefact Removal, CR = Coregistration (realignment) of fMRI images for motion correction, Threshold = The statistical threshold as actually applied to the illustrated fMRI results, GFT = Gaussian Field Theory, CT = Cluster Threshold level, GLM = General Linear Model

13.2 Appendix II - Recent EEG/fMRI studies in epilepsy

Reference & Citation	n /N	Scanner & Sequence Parameters	Acquisition Mode & EEG System	fMRI Analysis		
				Method & Software	Multiple Comparisons correction	Threshold
(Gotman et al., 2005)	15 25	1.5 Tesla, Siemens Sonata TE/TR = 50/3000 ms 64 x 64 matrix 25 x 5mm slices	EMR32, Schwartzer	FMRISTAT followed by random effects linear model using REML estimate of random effects variance regularized by spatial smoothing to constitute a mixed effects group analysis	Minimum of Bonferroni and GFT, with adjustment for nonisotropic spatial correlation of errors plus non-stationary GFT cluster-size test	P<0.05
				(**Conclusions**: This was a group analysis of the Aghakani 2004 (Aghakhani et al., 2004) data. Activations were described in thalamus, mesial frontal, insula, cerebellum and border of lateral ventricles. Deactivations were seen in anterior frontal and parietal regions, posterior cingulate and left posterior temporal.)		
(Briellmann et al., 2006)	1 2	3.0 Tesla GE TE/TR = 40/3600 ms 128 x 128 matrix 25 slices	In House System	SPM2 Software + iBrain Software	None	P<0.001
				(**Conclusions**: Bilateral deactivations over lesion in a patient with band heterotopia with language-related activation in parts of lesion within language areas.)		
(Bagshaw et al., 2006)	8 8	1.5 Tesla, Siemens Sonata TE/TR = 50/3300 ms 64 x 64 matrix 12 x 5mm slices (1/2 brain)	BrainAmp-MR, Brainproducts	AFNI for realignment after averaging FMRISTAT Smoothing kernel 6mm FWHM	FWE	P<0.05
				(**Conclusions**: No significant increase in the yield of activations in TLE patients when Z-shimming was used.)		
(Kobayashi et al., 2006c)	1 1	1.5 Tesla, Siemens Sonata TE/TR = 50/3000 ms 64 x 64 matrix 25 x 5mm slices	BrainAmp-MR, Brainproducts	FMRISTAT Smoothing kernel 6mm FWHM	Unclear	P<0.05 CT = 5
				(**Conclusions**: 25 brief right temporal electrographic seizures lasting 2-6sec, resulted in large concordant activation with up to 6% BOLD increase, returning to baseline after 30 seconds. IED activation was smaller and within.)		
(Kobayashi et al., 2006b)	13 14	1.5 Tesla, Siemens Sonata TE/TR = 50/3000 ms 64 x 64 matrix 25 x 5mm slices	EMR32, Schwartzer	FMRISTAT Smoothing kernel 6mm FWHM	Unclear	P<0.05 CT = 5
				(**Conclusions**: Activation in 9/12 studies with nodular heterotopia with involvement of heterotopia or adjacent cortex in 6, 3 of which had concomitant distant activations. Deactivation in 9/12 studies with involvement of heterotopia or surrounding cortex in 4, 3 of which had concomitant distal activations. Activation in 11/11 studies of band heterotopia always involving heterotopia and adjacent cortex with concomitant distal activation in 9/11. 11 also had similar deactivations with concomitant distal deactivations in 5.)		
(Kobayashi et al., 2006a)	27 35	1.5 Tesla, Siemens Sonata TE/TR = 50/3000 ms 64 x 64 matrix 25 x 5mm slices	EMR32, Schwartzer	FMRISTAT Smoothing kernel 6mm FWHM	Unclear	P<0.05 CT = 5
				(**Conclusions**: BOLD responses (positive or negative) in 83% of studies, predominantly ipsilateral to EEG but often involving contralateral cortex and frequently also extra-temporally.)		
Di Bonaventura et al (Di et al., 2006)	21 43	1.5 Tesla, Philips Gyroscan TE/TR = 50/3000 ms 64 x 64 matrix 20 x 5mm slices (10min sessions)	Micromed, Italy	SPM99 Software Smoothing kernel 8mm FWHM	FEW-GFT	P<0.05
				(**Conclusions**: Mixture of syndromes including focal and generalized epilepsy. 18 'concordant', 3 illustrated. No new findings.)		
(Leal et al., 2006)	3 3	1.5 Tesla, GE cV1 NV1 TE/TR = 50/3000 ms 64 x 64 matrix 16 x 7mm slices	MagLink, Neuroscan	FSL Software Smoothing kernel 8mm FWHM	Cluster threshold	P<0.05
				(**Conclusions**: 2 patients with late-onset OLE and one with idiopathic photosensitive OLE showed BOLD activations, consistent between the first 2 patients, overall less consistent with source analysis but more consistent with seizure semiology.)		
(Leal et al., 2007)	1 1	1.5 Tesla, GE cV1 NV1 TE/TR = 50/3000 ms 64 x 64 matrix 16 x 7mm slices	MagLink, Neuroscan	ICA using GIFT and temporal sorting by timecourse Smoothing kernel 5mm FWHM	None	none
				(**Conclusions**: Clusters of activity, lateral and interior occipital plus lateral and anterior temporal together with distributed EEG source modeling suggested possible origin in lateral occipital with propagation temporally.)		
(Boor et al., 2007)	4 11	1.5 Tesla, Siemens Vision TE/TR = 66/6000 ms 128 x 128 matrix 16x6mm slices (10% gap)	EMR16, Schwartzer (Periodic-interleaved acquisition)	SPM99 Software HPF = 128s Smoothing kernel 8mm FWHM	GFT	P<0.5 CT = 10
				(**Conclusions**: Unilateral perisylvian activations in 4 patients, concordant with dipole models, but including propagated activity in 3. fMRI could not determine propagation sequence. This was an extension to their data presented in (Boor et al., 2003).)		
(Hawco et al., 2007)	15	1.5 Tesla, Siemens Sonata TE/TR = 50/3000 ms 64 x 64 matrix 25 x 5mm slices	EMR32, Schwartzer	Unspecified software See text for methods	Bonferroni and GFT	CT = 3
				(**Conclusions**: This was a post hoc analysis of previously published data from various studies. 7 data sets contained early HRFs which were a significant part of the conventional activation in 4 out of 15 patients (selected from 130 database patients.)		
(Zijlmans et al., 2007)	29 29	1.5 Tesla, Philips Achieva TE/TR = 46/2500 ms 64 x 63 matrix 29 x 4mm slices (interleaved)	Micromed, Italy	SPM2 Software HPF = 128s Smoothing kernel 7mm FWHM	FWE-GFT	P<0.05 CT = 5
				(**Conclusions**: Of 29 patients (13 MRI negative) previously rejected for surgery, significant BOLD response in 15/29, 11/15 robust, 8/11 concordant. 4/8 new prospects for surgery. 2 had concordant intracranial EEG, and 1 had successful surgery)		
(Kobayashi et al., 2007)	5 8	1.5 Tesla, Siemens Sonata TE/TR = 50/3000 ms 64 x 64 matrix 25 x 5mm slices	EMR32, Schwartzer	FMRISTAT Smoothing kernel 6mm FWHM	Unclear	P<0.05 CT = 5
				(**Conclusions**: Considerable EPI dropout in and around lesions. Responses close to perilesional area in 2. All showed distant responses also.)		

Reference & Citation	n /N	Scanner & Sequence Parameters	Acquisition Mode & EEG System	fMRI Analysis		
				Method & Software	Multiple Comparisons correction	Threshold
De Tiege et al (De. X et al., 2007b)	5 6	1.5 Tesla, Siemens Avanto TE/TR = 50/3080 ms 64 x 64 matrix 36 x 3mm slices (interleaved)	In House	SPM5 Software	FWE - GFT	P<0.05
				(**Conclusions**: Significant concordant activations in 4 (including with intracranial EEG in 1), activations and deactivations in 1, and diffuse deactivations with electrographic seizures in 1.)		
De Tiege et al (De. X et al., 2007a)	1 1	1.5 Tesla, Siemens Avanto TE/TR = 50/3080 ms 64 x 64 matrix 36 x 3mm slices (interleaved)	In House	SPM5 Software	FWE - GFT	P<0.05
				(**Conclusions**: 9.5 yr old child with epileptic encephalopathy and bilaterally synchronous epileptic discharges during sleep and wakefulness showed widespread deactivations with some activations when global scaling was performed.)		
(Lengler et al., 2007)	4 10	3.0 Tesla, Siemens Trio TE/TR = 20/2670 ms 64 x 64 matrix 20 x 4mm slices (1mm gap)	BrainAmp-MR, Brainproducts	SPM2 Software HPF 128sec Smoothing kernel 12mm FWHM	None	P<0.001
				(**Conclusions**: Positive and negative activations in 4 children with benign focal epilepsy of childhood in perisylvian, central, and prefrontal areas with bilateral occipital activations in one.)		
(Jacobs et al., 2007)	13 15	3.0 Tesla, Philips Archeva TE/TR = 45/2250 ms 64 x 64 matrix 30 x 3.5mm slices	BrainAmp-MR, Brainproducts	SPM2 for preprocessing Smoothing kernel 8mm FWHM	FEW-GFT	P<0.05
				(**Conclusions**: In 72% of sessions, rather than subjects, a concordant response was found, 52% were deactivation.)		
(Jacobs et al., 2008a)	37 37	3.0 Tesla, Philips Archeva TE/TR = 45/2250 ms 64 x 64 matrix 30 x 3.5mm slices	BrainAmp-MR, Brainproducts	SPM2 for preprocessing else FMRISTAT Several models compared	FWE-GFT	P<0.05 CT = 5
				(**Conclusions**: Age-related differences seen in HRF peak time and saturation effects noted but patients were mixture of idiopathic and symptomatic, variably sedated, arbitrary age-grouped.)		
(Jacobs et al., 2008b)	5 5	3.0 Tesla, Philips Archeva TE/TR = 45/2250 ms 64 x 64 matrix 30 x 3.5mm slices	BrainAmp-MR, Brainproducts	SPM2 for preprocessing else FMRISTAT Various models compared	Bonferroni correction for models	P<0.05 CT = 10
				(**Conclusions**: BOLD changes (positive and negative) described in 5 children with TS. In 5, at least one tuber in seizure onset lobe showed a response. In all patients more than one tuber was involved. Conversely, different IED types often linked to the same tubers.)		
(Liu et al., 2008)	6 8	3.0 Tesla, GE, EXCITE TE/TR = 40/2000 ms 64 x 64 matrix 30 slices	EBNeuro, Florence	SPM2 Software HPF = 128s Smoothing Kernel 8mm FWHM	Unclear	P<0.001 CT = 3
				(**Conclusions**: Maximally activated areas concordant in 6 patients. No new findings.)		
(Moeller et al., 2008a)	6 10	3.0 Tesla, Philips Archeva TE/TR = 45/2250 ms 64 x 64 matrix 30 x 3.5mm slices	BrainAmp-MR, Brainproducts	SPM2 Software HPF = 128s Smoothing kernel 6mm FWHM 5 separate models tested with a time-shifted HRF and subsequent Bonferroni correction	FWE-GFT	P<0.05 CT = 5
				(**Conclusions**: BOLD increase in mid-thalamus 6 secs prior to GSW with cortical decreases 3-6 sec before. Further studies warranted.)		
(Moeller et al., 2008b)	6 10	3.0 Tesla, Philips Archeva TE/TR = 45/2250 ms 64 x 64 matrix 30 x 3.5mm slices	BrainAmp-MR, Brainproducts	SPM5 Software HPF = 128s Smoothing kernel 6mm FWHM	1st level FWE 2nd level ROI analysis - FDR	P<0.05 CT = 5
				(**Conclusions**: Bilateral BOLD increased in medial thalamus and reductions in posterior parietal cortex, precuneus, and frontal areas in 4-6. Maximum thalamic signal at 6 sec irrespective of seizure duration. No preceding signal changes were found. Findings in drug-naïve children with CAE were no different to adults on medication. BOLD changes did not precede GSW.)		
(Hamandi et al., 2008b)	1 1	1.5 Tesla, GE Horizon TE/TR = 40/3000 ms 64 x 64 matrix 21 x 5mm slices (interleaved)	In House System	SPM2 Software	FEW-GFT	P<0.05
				(**Conclusions**: Activations were found in left parahippocampal and lingual gyrus with left temporal IEDs. Tractography demonstrated anatomical connections. DCM showed stronger connectivity from lingual to parahippocampal than vice versa in both cases but there was stronger evidence for the IED acting on the later.)		
(Manganotti et al., 2008)	8 8	1.5 Tesla, Siemen Vision TE/TR = 50/3700 ms 64 x 64 matrix 36 x 3mm slices	In House System	BrainYoyager QX Software	Bonferroni	P<0.05 CT = 5
				(**Conclusion**: Focal interictal slow waves invariably associated with focal BOLD activations, concordant with EEG focus.)		

Abbreviations: CAE = Childhood absence epilepsy, CT = Cluster Threshold level, DCM = Dynamic Causal Modeling, FDR = False discovery rate error correction, FWE = Family-wise error correction, FWHM = Full-Width Half-Maximum, GFT = Gaussian Field Theory, GLM = General Linear Model, HPF = High pass filter, n/N = total number of subjects from whom the reported EEG fMRI data was obtained / total number studied, Threshold = The statistical threshold as actually applied to the illustrated fMRI results, TS = Tuberous sclerosis (with multiple tubers)

13.3 Appendix III - ICA on Chapter 8 data

Multiple spatial networks subtend generalized spike-wave activity during human absences: An ICA study of simultaneously acquired EEG/fMRI data.

Salek-Haddadi et al. *Epilepsia* 2004; 45(suppl 7):115

Rationale

To determine whether the spatial networks underlying generalized spike-wave activity during human absence seizures are identifiable using fMRI data alone.

Methods

Spatiotemporal Independent Component Analysis (ICA) was performed using MELODIC (Multivariate Exploratory Linear Decomposition into Independent Components) version 2.0, part of the FSL software package (FMRIBs Software Library, http://www.fmrib.ox.ac.uk/fsl), on ictal fMRI data acquired previously from a patient with intractable Idiopathic Generalized Epilepsy.

Pre-processed data (masked, mean corrected and variance normalized) was whitened and projected into a 111-dimensional subspace using probabilistic Principal Component Analysis where the number of dimensions was estimated automatically. The observations were decomposed into a set of time-courses and spatial maps by optimizing for non-Gaussian spatial source distributions using a fixed-point iteration technique. Estimated Component maps were divided by the standard deviation of the residual noise and thresholded by fitting a mixture model to the histogram of intensity values (probabilistic ICA). All time-courses were ranked according to degree of correlation with seizure onset and the corresponding spatial components contrasted with the results of a General Linear Model (GLM) analysis.

Results

At least ten independent components were identified as contributing to the previously reported pattern of thalamic activation and cortical deactivation, each with a timecourse mirroring the ictal EEG activity (see Figure 13-1).

Figure 13-1 Thresholded IC maps.
Five thresholded IC maps (alternative hypothesis test at $p > 0.5$) are shown with their corresponding timecourses underneath. Four absence seizures are indicated with grey shading.

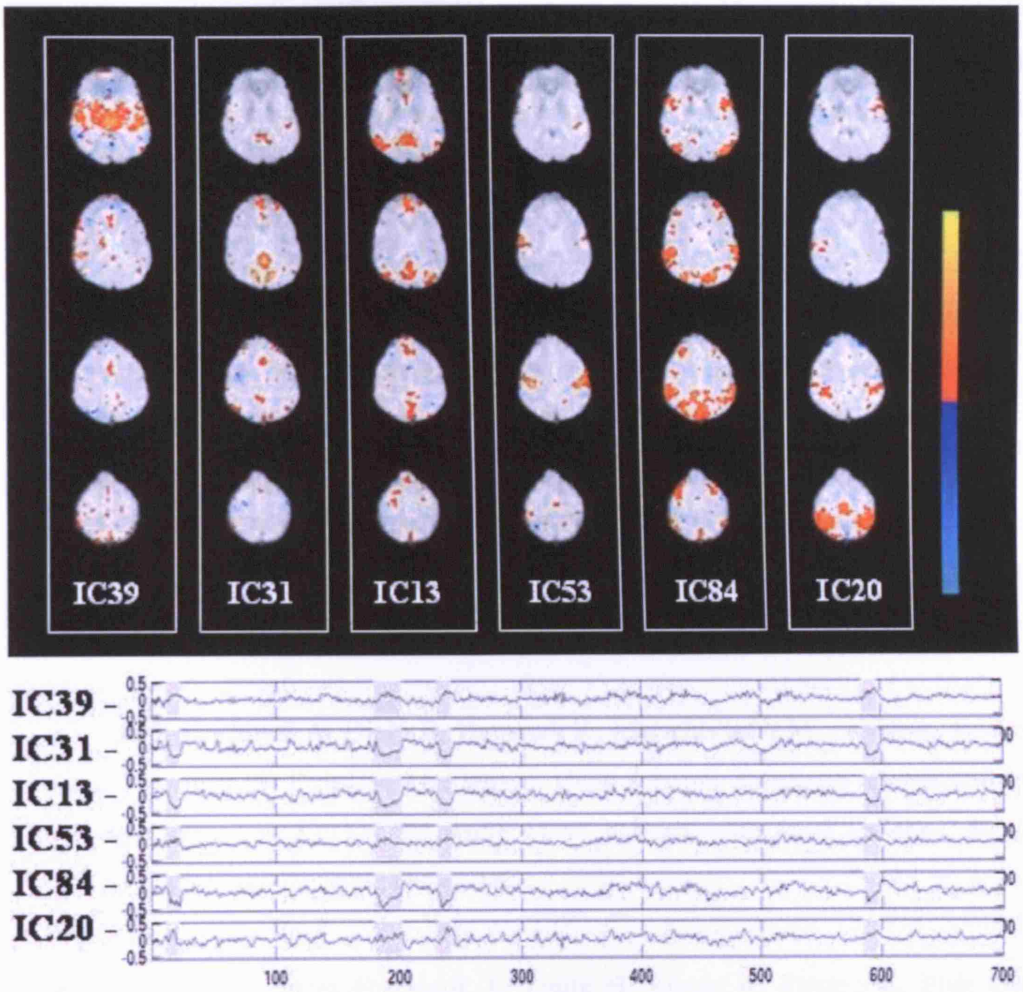

Conclusions

Our observations indicate that a weighted mixture of several *independent* spatial networks may simultaneously subserve the generation of generalized spike-wave activity in man. A mechanism is therefore provided, whereby subject or syndrome-specific changes in this blend, could account for a number of apparent discrepancies in the EEG/fMRI literature. Our results also support the notion that the haemodynamic consequences of prolonged spike-wave activity may be identifiable using fMRI alone.

Original publications

Peer reviewed

- **Salek-Haddadi A**, Mayer T, Hamandi K, Symms, M, Josephs O, Fluegel D, Woermann F, Richardson MP, Noppeney U, Wolf P, Koepp MJ. Imaging seizure activity: a combined EEG/EMG-fMRI study in reading epilepsy. ***Epilepsia.*** 2008 Aug (in press).

- Laufs H, Hamandi K, **Salek-Haddadi A,** Kleinschmidt AK, Duncan JS, Lemieux L. Temporal lobe interictal epileptic discharges affect cerebral activity in "default mode" brain regions. ***Hum Brain Mapp.*** 2007 Oct;28(10):1023-32.

- Lemieux L, **Salek-Haddadi A**, Lund TE, Laufs H, Carmichael D. Modeling large motion events in fMRI studies of patients with epilepsy. ***Magn Reson Imaging.*** 2007 Jul;25(6):894-901.

- **Salek-Haddadi A,** Diehl B, Hamandi K, Merschhemke M, Liston A, Friston K, Duncan JS, Fish DR, Lemieux L. Hemodynamic correlates of epileptiform discharges: an EEG-fMRI study of 63 patients with focal epilepsy. ***Brain Res.*** 2006 May 9;1088(1):148-66.

- Hamandi K, **Salek-Haddadi A,** Laufs H, Liston A, Friston K, Fish DR, Duncan JS, Lemieux L. EEG-fMRI of idiopathic and secondarily generalized epilepsies. ***Neuroimage.*** 2006 Jul 15;31(4):1700-10.

- Liston AD, Lund, TE, **Salek-Haddadi A**, Hamandi K, Friston KJ, Lemieux L. Modeling Cardiac Signal as a Confound in EEG-fMRI and its Application in Focal Epilepsy Studies. ***Neuroimage.*** 2006 Apr 15;30(3):827-34.

- Powell HW, Koepp MJ, Symms MR, Boulby PA, **Salek-Haddadi A** et al. Material-specific lateralization of memory encoding in the medial temporal lobe: blocked versus event-related design. ***Neuroimage.*** 2005 Aug 1;27(1):231-9.

- Hamandi K, **Salek Haddadi A**, Liston A, Laufs H, Fish DR, Lemieux L. fMRI temporal clustering analysis in patients with frequent interictal epileptiform discharges: comparison with EEG-driven analysis. ***Neuroimage***. 2005 May 15;26(1):309-16.

- Liston AD, **Salek-Haddadi A,** Kiebel SJ, Hamandi K, Turner R, Lemieux L. The MR detection of neuronal depolarization during 3-Hz spike-and-wave complexes in generalized epilepsy. ***Magn Reson Imaging***. 2004 Dec;22(10):1441-4.

- **Salek-Haddadi A**, Lemieux L, Merschhemke M, Diehl B, Allen PJ, Fish DR. EEG Quality during simultaneous functional MRI of interictal epileptiform discharges. ***Magn Reson Imaging*** 2003; 21:1159-1166.

- Diehl B, **Salek-Haddadi A**, Lemieux L, Fish DR. Mapping of spikes, slow waves and motor tasks in a patient with malformation of cortical development using simultaneous EEG and fMRI. ***Magn Reson Imaging*** 2003; 21:1167-1173.

- **Salek-Haddadi A**, Lemieux L, Merschhemke M, Friston KJ, Duncan JS, Fish DR. Functional magnetic resonance imaging of human absence seizures. ***Ann Neurol*** 2003; 53(5):663-667.

- Laufs H, Kleinschmidt A, Beyerle A, Eger E, ***Salek-Haddadi A***, Preibisch C et al. EEG-correlated fMRI of human alpha activity. ***Neuroimage*** 2003; 19(4):1463-1476.

- Laufs H, Krakow K, Sterzer P, Eger E, Beyerle A, **Salek-Haddadi A** et al. Electroencephalographic signatures of attentional and cognitive default modes in spontaneous brain activity fluctuations at rest. ***Proc Natl Acad Sci U S A*** 2003; 100(19):11053-11058.

- Guye M, Parker GJ, Symms M, Boulby P, Wheeler-Kingshott CA, **Salek-Haddadi A** et al. Combined functional MRI and tractography to demonstrate the connectivity of the human primary motor cortex in vivo. ***Neuroimage*** 2003; 19(4):1349-1360.

- **Salek-Haddadi A**, Merschhemke M, Lemieux L, Fish DR. Simultaneous EEG-Correlated Ictal fMRI. ***Neuroimage*** 2002; 16(1):32-40.

- Lemieux L, **Salek-Haddadi A**, Josephs O, Allen P, Toms N, Scott C, Krakow K, Turner R, Fish DR. Event-Related fMRI with Simultaneous and Continuous EEG: Description of the Method and Initial Case Report. ***Neuroimage*** 2001; 14(3):780-787.

Reviews

- Hamandi K, **Salek-Haddadi A**, Fish DR, Lemieux L. EEG-correlated fMRI: Update on the Queen Square experience. ***J Clin Neurophysiol*** 2004; 21(4):241-8

- **Salek-Haddadi A**, Friston KJ, Lemieux L, Fish DR. Studying spontaneous EEG activity with fMRI. ***Brain Res Brain Res Rev*** 2003; 43(1):110-133.

- Lemieux L, **Salek-Haddadi A**, Hoffmann A, Gotman J, Fish DR. EEG-Correlated Functional MRI: Recent Methodologic Progress and Current Issues. ***Epilepsia*** 2002; 43(Suppl.1):64-68.

- **Salek-Haddadi A**, Lemieux L, Fish DR. Role of functional magnetic resonance imaging in the evaluation of patients with malformations caused by cortical development. ***Neurosurg Clin N Am*** 2002; 13(1):63-69.

Book Chapters

- **Salek-Haddadi A**, Merlet I, Mauguiere F, Meierkord K, Buchheim K, Fish DR et al. New Physiological and Radiological Investigations in the

Presurgical Evaluation of Epilepsy. In: Shorvon SD, Fish DR, Dodson E, Perucca E, Olivier A, editors. *The Treatment of Epilepsy.* 2nd Edition. Oxford: Blackwell Science, 2004.

- Diehl B, **Salek-Haddadi A,** Fish DR. fMRI in the evaluation of the irritative zone. In: Rosenow F, Lüders HO (volume eds): Pre-surgical assessment of the epilepsies with clinical neurophysiology and functional imaging. In: Daube J, Mauguiere F (handbook eds): *Handbook of Clinical Neurophysiology.* Elsevier New York Amsterdam, 2004.

- Koepp MJ, Noppeney U, **Salek-Haddadi A**, Price C. Functional imaging in reading epilepsy. In: Wolf P, Inoue Y, Zifkin B, editors. *Reflex epilepsies: progress in understanding.* Montrouge: John Libbey, 2004.

- **Salek-Haddadi A,** Lemieux L, Merschhemke M, Allen PJ, Fish DR. Continuous EEG-correlated fMRI in epilepsy. In: Hirata K, editor. 12th World Congress of the International Society of Brain Electromagnetic Topography, Tochigi, 8 - 10 March 2001 – *International Congress Series* 1232. Amsterdam: Elsevier Science B.V., 2002.

Letters

- Lemieux L, **Salek-Haddadi A**, Krakow K. The nature of MR signal changes. **Radiology** 2003; 226(3):922-3.

- Lemieux L, **Salek-Haddadi A**, Hoffmann A, Gotman J, Fish DR. EEG-Correlated Functional MRI: Recent Methodologic Progress and Current Issues. **Epilepsia** 2002; 43(Suppl. 1):64-68.

Abstracts

- **Salek-Haddadi et al.** A 21st century case of unsuccessful exorcism. **JNNP** 2008; 79:347

- **Salek-Haddadi et al.** A killer of a hangover. **JNNP** 2006; 77:1391

- **Salek-Haddadi et al.** Multiple spatial networks subtend generalized spike-wave activity during human absences: An ICA study of simultaneously acquired EEG/fMRI data. **Epilepsia** 2004; 45(suppl 7):115

- **Salek-Haddadi et al.** Physiological imaging of language-induced seizures using simultaneous EEG, EMG & fMRI. **JNNP** 2004; 75:44

- Liston A, **Salek-Haddadi A**, et al. Fast MR signal changes associated with 3Hz spike-and-wave complexes in generalized epilepsy. **Proc Intl Soc Mag Reson Med** 2004;11:2520.

- **Salek-Haddadi et al.** Interictal EEG-correlated fMRI in 50 patients with localization-related epilepsy. **Epilepsia** 2003; 44(s9): 87

- **Salek-Haddadi et al.** Mapping language-induced seizures using EEG, EMG & fMRI. **Neuroimage** 2003;(19):2

- Diehl B, **Salek-Haddadi** A. et al. Simultaneous EEG / fMRI in a patient with malformation of cortical development: activation by spikes, slow waves and motor tasks. **Neuroimage** 2003;(19):2

- **Salek-Haddadi et al.** Imaging absence seizures using functional magnetic resonance imaging. **Epilepsia** 2002;43(s7):123

- **Salek-Haddadi et al.** EEG-Correlated fMRI of Human Generalized Spike-Wave Activity: New evidence for the corticoreticular hypothesis. **Neuroimage** 2002 ('HBM02)

- **Salek-Haddadi et al.** BOLD changes during subclinical electrographic seizures. **Neuroimage** 2001;13(6):S1003

- **Salek-Haddadi et al.** Continuous EEG-Correlated fMRI of Epileptiform Discharges. **Neuroimage** 2001;13(6): S832

- **Salek-Haddadi et al.** Functional Neuroimaging of Epileptiform Discharges. **Proc Intl Soc Mag Reson Med** 2001;9:1270

- **Salek-Haddadi et al.** Simultaneous EEG recording of epileptiform discharges throughout continuous functional MRI: A powerful new alternative to spike-triggered fMRI. **Epilepsia** 2000;

- **Salek-Haddadi et al.** Early Experience with Continuous EEG-Correlated Functional Neuroimaging of Epileptiform Discharges. 3rd *International Magnetic Resonance in Epilepsy Symposium*, Alabama 2000.

References

1. (1989). Proposal for revised classification of epilepsies and epileptic syndromes. Commission on Classification and Terminology of the International League Against Epilepsy. Epilepsia *30*, 389-399.

2. (2004). Human Brain Function (San Diego, CA: Academic Press).

3. Abraham,K., and Ajmone-Marsan,C. (1958). Patterns of cortical discharge and their relation to routine scalp electroencephalography. Electroencephalogr. Clin. Neurophysiol. *10*, 447-461.

4. Achten,E., Jackson,G.D., Cameron,J.A., Abbott,D.F., Stella,D.L., and Fabinyi,G.C. (1999). Presurgical evaluation of the motor hand area with functional MR imaging in patients with tumors and dysplastic lesions. Radiology *210*, 529-538.

5. Aghakhani,Y., Bagshaw,A.P., Benar,C.G., Hawco,C., Andermann,F., Dubeau,F., and Gotman,J. (2004). fMRI activation during spike and wave discharges in idiopathic generalized epilepsy. Brain *127*, 1127-1144.

6. Aguirre,G.K., Zarahn,E., and D'Esposito,M. (1998a). The inferential impact of global signal covariates in functional neuroimaging analyses. Neuroimage *8*, 302-306.

7. Aguirre,G.K., Zarahn,E., and D'Esposito,M. (1998b). The variability of human, BOLD hemodynamic responses. Neuroimage *8*, 360-369.

8. Ajmone-Marsan,C., and Van Buren,J.M. (1958). Epileptiform activity in cortical and subcortical structures in the temporal lobe of man. In Temporal lobe epilepsy., M. Baldwin, and P. Bailey, eds. (Springfield,IL: Charles C Thomas), pp. 78-108.

9. Al-Asmi,A., Benar,C.G., Gross,D.W., Khani,Y.A., Andermann,F., Pike,B., Dubeau,F., and Gotman,J. (2003). fMRI activation in continuous and spike-triggered EEG-fMRI studies of epileptic spikes. Epilepsia *44*, 1328-1339.

10. Alarcon,G., Guy,C.N., Binnie,C.D., Walker,S.R., Elwes,R.D., and Polkey,C.E. (1994). Intracerebral propagation of interictal activity in partial epilepsy: implications for source localisation. J. Neurol. Neurosurg. Psychiatry *57*, 435-449.

11. Alfonso,I., Papazian,O., Litt,R., Villalobos,R., and Acosta,J.I. (1998). Similar brain SPECT findings in subclinical and clinical seizures in two neonates with hemimegalencephaly. Pediatr. Neurol. *19*, 132-134.

12. Allen PJ, Polizzi G, Krakow K, Fish DR, and Lemieux L (1998). Identification of EEG events in the MR scanner: The problem of pulse artifact and a method for its subtraction. Neuroimage *8*, 229-239.

13. Allen,P.J., Josephs,O., and Turner,R. (2000). A Method for Removing Imaging Artifact from Continuous EEG Recorded during Functional MRI. Neuroimage *12*, 230-239.

14. Anami,K., Mori,T., Tanaka,F., Kawagoe,Y., Okamoto,J., Yarita,M., Ohnishi,T., Yumoto,M., Matsuda,H., and Saitoh,O. (2003). Stepping stone sampling for retrieving artifact-free electroencephalogram during functional magnetic resonance imaging. Neuroimage *19*, 281-295.

15. Andersson,J.L., Hutton,C., Ashburner,J., Turner,R., and Friston,K. (2001). Modeling geometric deformations in EPI time series. Neuroimage *13*, 903-919.

16. Archer,J.S., Abbott,D.F., Waites,A.B., and Jackson,G.D. (2003a). fMRI "deactivation" of the posterior cingulate during generalized spike and wave. Neuroimage *20*, 1915-1922.

17. Archer,J.S., Briellman,R.S., Abbott,D.F., Syngeniotis,A., Wellard,R.M., and Jackson,G.D. (2003b). Benign Epilepsy with Centro-temporal Spikes: Spike Triggered fMRI Shows Somato-sensory Cortex Activity. Epilepsia *44*, 200-204.

18. Archer,J.S., Briellmann,R.S., Syngeniotis,A., Abbott,D.F., and Jackson,G.D. (2003c). Spike-triggered fMRI in reading epilepsy: involvement of left frontal cortex working memory area. Neurology *60*, 415-421.

19. Archer,J.S., Waites,A.B., Abbott,D.F., Federico,P., and Jackson,G.D. (2006). Event-related fMRI of myoclonic jerks arising from dysplastic cortex. Epilepsia *47*, 1487-1492.

20. Arnold,S., Jager,L., Reiser,M., Winkler,P., and Noachtar,S. (2002). Visualization of interictal spikes as measured with subdural EEG electrodes using functional magnetic imaging. Epilepsia *43*, 87.

21. Arthurs,O.J., and Boniface,S. (2002). How well do we understand the neural origins of the fMRI BOLD signal? Trends Neurosci. *25*, 27-31.

22. Arthurs,O.J., Williams,E.J., Carpenter,T.A., Pickard,J.D., and Boniface,S.J. (2000). Linear coupling between functional magnetic resonance imaging and evoked potential amplitude in human somatosensory cortex. Neuroscience *101*, 803-806.

23. Ashburner,J., and Friston,K.J. (1999). Nonlinear spatial normalization using basis functions. Hum. Brain Mapp. *7*, 254-266.

24. Ashburner,J., and Friston,K.J. (2000). Voxel-based morphometry--the methods. Neuroimage *11*, 805-821.

25. Ashburner,J., Neelin,P., Collins,D.L., Evans,A., and Friston,K. (1997). Incorporating prior knowledge into image registration. Neuroimage *6*, 344-352.

26. Astrup,J., Sorensen,P.M., and Sorensen,H.R. (1981). Oxygen and glucose consumption related to Na+-K+ transport in canine brain. Stroke *12*, 726-730.

27. Avery,R.A., Spencer,S.S., Spanaki,M.V., Corsi,M., Seibyl,J.P., and Zubal,I.G. (1999). Effect of injection time on postictal SPET perfusion changes in medically refractory epilepsy. Eur. J. Nucl. Med. *26*, 830-836.

28. Avery,R.A., Zubal,I.G., Stokking,R., Studholme,C., Corsi,M., Seibyl,J.P., and Spencer,S.S. (2000). Decreased cerebral blood flow during seizures with ictal SPECT injections. Epilepsy Res. *40*, 53-61.

29. Avoli,M., Gloor,P., Kostopoulos,G., and Naquet,R. (1990). Generalized epilepsy: neurobiological approaches. (Boston: Birkhauser).

30. Avoli,M., Rogawski,M.A., and Avanzini,G. (2001). Generalized epileptic disorders: an update. Epilepsia *42*, 445-457.

31. Bagshaw,A.P., Aghakhani,Y., Benar,C.G., Kobayashi,E., Hawco,C., Dubeau,F., Pike,G.B., and Gotman,J. (2004a). EEG-fMRI of focal epileptic spikes: analysis with multiple haemodynamic functions and comparison with gadolinium-enhanced MR angiograms. Hum Brain Mapp *22*, 179-192.

32. Bagshaw,A.P., Aghakhani,Y., Benar,C.G., Kobayashi,E., Hawco,C., Dubeau,F., Pike,G.B., and Gotman,J. (2004b). EEG-fMRI of focal epileptic spikes: analysis with multiple haemodynamic functions and comparison with gadolinium-enhanced MR angiograms. Hum Brain Mapp *22*, 179-192.

33. Bagshaw,A.P., Hawco,C., Benar,C.G., Kobayashi,E., Aghakhani,Y., Dubeau,F., Pike,G.B., and Gotman,J. (2005). Analysis of the EEG-fMRI response to prolonged bursts of interictal epileptiform activity. Neuroimage. *24*, 1099-1112.

34. Bagshaw,A.P., Torab,L., Kobayashi,E., Hawco,C., Dubeau,F., Pike,G.B., and Gotman,J. (2006). EEG-fMRI using z-shimming in patients with temporal lobe epilepsy. J. Magn Reson. Imaging *24*, 1025-1032.

35. Bahn,M.M., Lin,W., Silbergeld,D.L., Miller,J.W., Kuppusamy,K., Cook,R.J., Hammer,G., Wetzel,R., and Cross,D., III (1997). Localization of language cortices by functional MR imaging compared with intracarotid amobarbital hemispheric sedation. AJR Am. J. Roentgenol. *169*, 575-579.

36. Bandettini,P.A., Jesmanowicz,A., Wong,E.C., and Hyde,J.S. (1993). Processing strategies for time-course data sets in functional MRI of the human brain. Magn Reson. Med. *30*, 161-173.

37. Bandettini,P.A., Wong,E.C., Hinks,R.S., Tikofsky,R.S., and Hyde,J.S. (1992). Time course EPI of human brain function during task activation. Magn Reson. Med. *25*, 390-397.

38. Bartenstein,P.A., Duncan,J.S., Prevett,M.C., Cunningham,V.J., Fish,D.R., Jones,A.K., Luthra,S.K., Sawle,G.V., and Brooks,D.J. (1993). Investigation

of the opioid system in absence seizures with positron emission tomography. J. Neurol. Neurosurg. Psychiatry *56*, 1295-1302.

39. Baudewig,J., Bittermann,H.J., Paulus,W., and Frahm,J. (2001a). Simultaneous EEG and functional MRI of epileptic activity: a case report. Clin. Neurophysiol. *112*, 1196-1200.

40. Baudewig,J., Siebner,H.R., Bestmann,S., Tergau,F., Tings,T., Paulus,W., and Frahm,J. (2001b). Functional MRI of cortical activations induced by transcranial magnetic stimulation (TMS). Neuroreport *12*, 3543-3548.

41. Baumgartner,C., Lindinger,G., Ebner,A., Aull,S., Serles,W., Olbrich,A., Lurger,S., Czech,T., Burgess,R., and Luders,H. (1995). Propagation of interictal epileptic activity in temporal lobe epilepsy. Neurology *45*, 118-122.

42. Baune,A., Sommer,F.T., Erb,M., Wildgruber,D., Kardatzki,B., Palm,G., and Grodd,W. (1999). Dynamical cluster analysis of cortical fMRI activation. Neuroimage *9*, 477-489.

43. Beckmann,C.F., DeLuca,M., Devlin,J.T., and Smith,S.M. (2005). Investigations into resting-state connectivity using independent component analysis. Philos. Trans. R. Soc. Lond B Biol. Sci. *360*, 1001-1013.

44. Benar,C., Aghakhani,Y., Wang,Y., Izenberg,A., Al Asmi,A., Dubeau,F., and Gotman,J. (2003b). Quality of EEG in simultaneous EEG-fMRI for epilepsy. Clin. Neurophysiol. *114*, 569-580.

45. Benar,C., Aghakhani,Y., Wang,Y., Izenberg,A., Al Asmi,A., Dubeau,F., and Gotman,J. (2003a). Quality of EEG in simultaneous EEG-fMRI for epilepsy. Clin. Neurophysiol. *114*, 569-580.

46. Benar,C.G., Gross,D.W., Wang,Y., Petre,V., Pike,B., Dubeau,F., and Gotman,J. (2002). The BOLD Response to Interictal Epileptiform Discharges. Neuroimage *17*, 1182-1192.

47. Benar,C.G., Grova,C., Kobayashi,E., Bagshaw,A.P., Aghakhani,Y., Dubeau,F., and Gotman,J. (2006). EEG-fMRI of epileptic spikes:

concordance with EEG source localization and intracranial EEG. Neuroimage *30*, 1161-1170.

48. Benson,R.R., FitzGerald,D.B., LeSueur,L.L., Kennedy,D.N., Kwong,K.K., Buchbinder,B.R., Davis,T.L., Weisskoff,R.M., Talavage,T.M., Logan,W.J., Cosgrove,G.R., Belliveau,J.W., and Rosen,B.R. (1999). Language dominance determined by whole brain functional MRI in patients with brain lesions. Neurology *52*, 798-809.

49. Berkovic,S.F., Andermann,F., Andermann,E., and Gloor,P. (1987). Concepts of absence epilepsies: discrete syndromes or biological continuum? Neurology *37*, 993-1000.

50. Binder,J.R., Frost,J.A., Hammeke,T.A., Bellgowan,P.S., Rao,S.M., and Cox,R.W. (1999). Conceptual processing during the conscious resting state. A functional MRI study. J. Cogn Neurosci. *11*, 80-95.

51. Binder,J.R., Swanson,S.J., Hammeke,T.A., Morris,G.L., Mueller,W.M., Fischer,M., Benbadis,S., Frost,J.A., Rao,S.M., and Haughton,V.M. (1996). Determination of language dominance using functional MRI: a comparison with the Wada test. Neurology *46*, 978-984.

52. Bittar,R.G., Andermann,F., Olivier,A., Dubeau,F., Dumoulin,S.O., Pike,G.B., and Reutens,D.C. (1999). Interictal spikes increase cerebral glucose metabolism and blood flow: a PET study. Epilepsia *40*, 170-178.

53. Blume,W.T., Borghesi,J.L., and Lemieux,J.F. (1993). Interictal indices of temporal seizure origin. Ann. Neurol *34*, 703-709.

54. Blumenfeld,H., McNally,K.A., Vanderhill,S.D., Paige,A.L., Chung,R., Davis,K., Norden,A.D., Stokking,R., Studholme,C., Novotny,E.J., Jr., Zubal,I.G., and Spencer,S.S. (2004). Positive and negative network correlations in temporal lobe epilepsy. Cereb. Cortex *14*, 892-902.

55. Bode,H. (1992). Intracranial blood flow velocities during seizures and generalized epileptic discharges. Eur. J. Pediatr. *151*, 706-709.

56. Bohning,D.E., Shastri,A., Wassermann,E.M., Ziemann,U., Lorberbaum,J.P., Nahas,Z., Lomarev,M.P., and George,M.S. (2000). BOLD-f MRI response to single-pulse transcranial magnetic stimulation (TMS). J. Magn Reson. Imaging *11*, 569-574.

57. Bonmassar,G., Anami,K., Ives,J., and Belliveau,J.W. (1999). Visual evoked potential (VEP) measured by simultaneous 64-channel EEG and 3T fMRI. Neuroreport *10*, 1893-1897.

58. Bonmassar,G., Hadjikhani,N., Ives,J.R., Hinton,D., and Belliveau,J.W. (2001). Influence of EEG electrodes on the BOLD fMRI signal. Hum. Brain Mapp. *14*, 108-115.

59. Bonmassar,G., Purdon,P., Jaaskelainen,I., Chiappa,K., Solo,V., Brown,E., and Belliveau,J. (2002). Motion and Ballistocardiogram Artifact Removal for Interleaved Recording of EEG and EPs during MRI. Neuroimage *16*, 1127.

60. Bonvento,G., Sibson,N., and Pellerin,L. (2002). Does glutamate image your thoughts? Trends Neurosci. *25*, 359-364.

61. Bookheimer,S.Y. (1996). Functional MRI applications in clinical epilepsy. Neuroimage *4*, S139-S146.

62. Boor,R., Jacobs,J., Hinzmann,A., Bauermann,T., Scherg,M., Boor,S., Vucurevic,G., Pfleiderer,C., Kutschke,G., and Stoeter,P. (2007). Combined spike-related functional MRI and multiple source analysis in the non-invasive spike localization of benign rolandic epilepsy. Clin. Neurophysiol. *118*, 901-909.

63. Boor,S., Vucurevic,G., Pfleiderer,C., Stoeter,P., Kutschke,G., and Boor,R. (2003). EEG-related functional MRI in benign childhood epilepsy with centrotemporal spikes. Epilepsia *44*, 688-692.

64. Born,A.P., Law,I., Lund,T.E., Rostrup,E., Hanson,L.G., Wildschiodtz,G., Lou,H.C., and Paulson,O.B. (2002). Cortical deactivation induced by visual stimulation in human slow-wave sleep. Neuroimage *17*, 1325-1335.

65. Bowtell,R. (2008). Medical imaging: Colourful future for MRI. Nature *453*, 993-994.

66. Breier,J.I., Mullani,N.A., Thomas,A.B., Wheless,J.W., Plenger,P.M., Gould,K.L., Papanicolaou,A., and Willmore,L.J. (1997). Effects of duration of epilepsy on the uncoupling of metabolism and blood flow in complex partial seizures. Neurology *48*, 1047-1053.

67. Briellmann,R.S., Little,T., Harvey,A.S., Abbott,D.F., Jacobs,R., Waites,A.B., and Jackson,G.D. (2006). Pathologic and physiologic function in the subcortical band of double cortex. Neurology *67*, 1090-1093.

68. Bruehl,C., Hagemann,G., and Witte,O.W. (1998). Uncoupling of blood flow and metabolism in focal epilepsy. Epilepsia *39*, 1235-1242.

69. Bruhn,H., Kleinschmidt,A., Boecker,H., Merboldt,K.D., Hanicke,W., and Frahm,J. (1994). The effect of acetazolamide on regional cerebral blood oxygenation at rest and under stimulation as assessed by MRI. J. Cereb. Blood Flow Metab *14*, 742-748.

70. Buchel,C., Holmes,A.P., Rees,G., and Friston,K.J. (1998). Characterizing stimulus-response functions using nonlinear regressors in parametric fMRI experiments. Neuroimage *8*, 140-148.

71. Buchel,C., Wise,R.J., Mummery,C.J., Poline,J.B., and Friston,K.J. (1996). Nonlinear regression in parametric activation studies. Neuroimage *4*, 60-66.

72. Buchheim,K., Obrig,H., Pannwitz,W., Muller,A., Heekeren,H., Villringer,A., and Meierkord,H. (2004). Decrease in haemoglobin oxygenation during absence seizures in adult humans. Neurosci Lett *354*, 119-122.

73. Buckner,R.L., Bandettini,P.A., O'Craven,K.M., Savoy,R.L., Petersen,S.E., Raichle,M.E., and Rosen,B.R. (1996). Detection of cortical activation during averaged single trials of a cognitive task using functional magnetic resonance imaging. Proc. Natl. Acad. Sci. U. S. A *93*, 14878-14883.

74. Buckner,R.L., Koutstaal,W., Schacter,D.L., Dale,A.M., Rotte,M., and Rosen,B.R. (1998). Functional-anatomic study of episodic retrieval. II.

Selective averaging of event-related fMRI trials to test the retrieval success hypothesis. Neuroimage. *7*, 163-175.

75. Burgess,A., and Gruzelier,J. (1993). Individual reliability of amplitude distribution in topographical mapping of EEG. Electroencephalogr. Clin. Neurophysiol. *86*, 219-223.

76. Buxton,R.B., and Frank,L.R. (1997). A model for the coupling between cerebral blood flow and oxygen metabolism during neural stimulation. J. Cereb. Blood Flow Metab *17*, 64-72.

77. Buxton,R.B., Wong,E.C., and Frank,L.R. (1998). Dynamics of blood flow and oxygenation changes during brain activation: the balloon model. Magn Reson. Med. *39*, 855-864.

78. Carmichael,D.W., Hamandi,K., Laufs,H., Duncan,J.S., Thomas,D.L., and Lemieux,L. (2008). An investigation of the relationship between BOLD and perfusion signal changes during epileptic generalised spike wave activity. Magn Reson. Imaging.

79. Cascino,G.D. (2001). Advances in neuroimaging: surgical localization. Epilepsia *42*, 3-12.

80. Chawla,D., Lumer,E.D., and Friston,K.J. (1999). The relationship between synchronization among neuronal populations and their mean activity levels. Neural Comput. *11*, 1389-1411.

81. Chih,C.P., Lipton,P., and Roberts,E.L., Jr. (2001). Do active cerebral neurons really use lactate rather than glucose? Trends Neurosci. *24*, 573-578.

82. Chugani,H.T., Rintahaka,P.J., and Shewmon,D.A. (1994). Ictal patterns of cerebral glucose utilization in children with epilepsy. Epilepsia *35*, 813-822.

83. Chung,M.Y., Walczak,T.S., Lewis,D.V., Dawson,D.V., and Radtke,R. (1991). Temporal lobectomy and independent bitemporal interictal activity: what degree of lateralization is sufficient? Epilepsia *32*, 195-201.

84. Cohen,D., Cuffin,B.N., Yunokuchi,K., Maniewski,R., Purcell,C., Cosgrove,G.R., Ives,J., Kennedy,J.G., and Schomer,D.L. (1990). MEG

versus EEG localization test using implanted sources in the human brain. Ann. Neurol. *28*, 811-817.

85. Cohen,M.S., Goldman,R.I., Stern,J., and Engel,J., Jr. Simultaneous EEG and fMRI made easy. Neuroimage 13[6], S6. 2001.
Ref Type: Abstract

86. Connelly,A. (1995). Ictal imaging using functional magnetic resonance. Magn Reson. Imaging *13*, 1233-1237.

87. Cooper,R., Winter,A.L., Crow,H.J., and Walter,W.G. (1965). Comparison of subcortical, cortical and scalp activity using chronically indwelling electrodes in man. Electroencephalogr. Clin. Neurophysiol. *18*, 217-228.

88. Cover,T.M., and Thomas,J.A. (1991). Elements of Information Theory John Wiley).

89. Cross,J.H. (2002). Epilepsy surgery in childhood. Epilepsia *43 Suppl 3*, 65-70.

90. Cuffin,B.N., Cohen,D., Yunokuchi,K., Maniewski,R., Purcell,C., Cosgrove,G.R., Ives,J., Kennedy,J., and Schomer,D. (1991). Tests of EEG localization accuracy using implanted sources in the human brain. Ann. Neurol. *29*, 132-138.

91. Czisch,M., Wehrle,R., Kaufmann,C., Wetter,T.C., Holsboer,F., Pollmacher,T., and Auer,D.P. (2004). Functional MRI during sleep: BOLD signal decreases and their electrophysiological correlates. Eur. J. Neurosci. *20*, 566-574.

92. Czisch,M., Wetter,T.C., Kaufmann,C., Pollmacher,T., Holsboer,F., and Auer,D.P. (2002). Altered Processing of Acoustic Stimuli during Sleep: Reduced Auditory Activation and Visual Deactivation Detected by a Combined fMRI/EEG Study. Neuroimage *16*, 251-258.

93. D'Esposito,M., Zarahn,E., Aguirre,G.K., and Rypma,B. (1999). The effect of normal aging on the coupling of neural activity to the bold hemodynamic response. Neuroimage *10*, 6-14.

94. Dale,A.M., Greve,D.N., and Burock,M.A. (1999). Optimal stimulus sequences for Event-Related fMRI. Neuroimage *9*, S33.

95. Dale,A.M., and Halgren,E. (2001). Spatiotemporal mapping of brain activity by integration of multiple imaging modalities. Curr. Opin. Neurobiol. *11*, 202-208.

96. Dale,A.M., Liu,A.K., Fischl,B.R., Buckner,R.L., Belliveau,J.W., Lewine,J.D., and Halgren,E. (2000). Dynamic statistical parametric mapping: combining fMRI and MEG for high-resolution imaging of cortical activity. Neuron *26*, 55-67.

97. Damoiseaux,J.S., Rombouts,S.A., Barkhof,F., Scheltens,P., Stam,C.J., Smith,S.M., and Beckmann,C.F. (2006). Consistent resting-state networks across healthy subjects. Proc. Natl. Acad. Sci. U. S. A *103*, 13848-13853.

98. Davis,L.M., Spencer,D.D., Spencer,S.S., and Bronen,R.A. (1999). MR imaging of implanted depth and subdural electrodes: is it safe? Epilepsy Res. *35*, 95-98.

99. de Curtis,M., and Avanzini,G. (2001). Interictal spikes in focal epileptogenesis. Prog. Neurobiol. *63*, 541-567.

100. de Curtis,M., Librizzi,L., and Biella,G. (2001). Discharge threshold is enhanced for several seconds after a single interictal spike in a model of focal epileptogenesis. Eur. J. Neurosci. *14*, 174-178.

101. de Curtis,M., Manfridi,A., and Biella,G. (1998). Activity-dependent pH shifts and periodic recurrence of spontaneous interictal spikes in a model of focal epileptogenesis. J. Neurosci. *18*, 7543-7551.

102. De Munck,J.C., Goncalves,S.I., Huijboom,L., Kuijer,J.P., Pouwels,P.J., Heethaar,R.M., and Lopes da Silva,F.H. (2007). The hemodynamic response of the alpha rhythm: an EEG/fMRI study. Neuroimage *35*, 1142-1151.

103. De Simone,R., Silvestrini,M., Marciani,M.G., and Curatolo,P. (1998). Changes in cerebral blood flow velocities during childhood absence seizures. Pediatr. Neurol *18*, 132-135.

104. de Wit,H., Metz,J., Wagner,N., and Cooper,M. (1991). Effects of diazepam on cerebral metabolism and mood in normal volunteers. Neuropsychopharmacology *5*, 33-41.

105. De Zwart,J.A., Van Gelderen,P., Kellman,P., and Duyn,J.H. (2002). Application of sensitivity-encoded echo-planar imaging for blood oxygen level-dependent functional brain imaging dagger. Magn Reson. Med. *48*, 1011-1020.

106. De,L.M., Beckmann,C.F., De,S.N., Matthews,P.M., and Smith,S.M. (2006). fMRI resting state networks define distinct modes of long-distance interactions in the human brain. Neuroimage *29*, 1359-1367.

107. De,M.F., Gentile,F., Esposito,F., Balsi,M., Di,S.F., Goebel,R., and Formisano,E. (2007). Classification of fMRI independent components using IC-fingerprints and support vector machine classifiers. Neuroimage *34*, 177-194.

108. De,T., X, Harrison,S., Laufs,H., Boyd,S.G., Clark,C.A., Allen,P., Neville,B.G., Vargha-Khadem,F., and Cross,J.H. (2007a). Impact of interictal epileptic activity on normal brain function in epileptic encephalopathy: an electroencephalography-functional magnetic resonance imaging study. Epilepsy Behav. *11*, 460-465.

109. De,T., X, Laufs,H., Boyd,S.G., Harkness,W., Allen,P.J., Clark,C.A., Connelly,A., and Cross,J.H. (2007b). EEG-fMRI in children with pharmacoresistant focal epilepsy. Epilepsia *48*, 385-389.

110. Desmond,J.E., and Glover,G.H. (2002). Estimating sample size in functional MRI (fMRI) neuroimaging studies: statistical power analyses. J. Neurosci. Methods *118*, 115-128.

111. Desmond,J.E., Sum,J.M., Wagner,A.D., Demb,J.B., Shear,P.K., Glover,G.H., Gabrieli,J.D., and Morrell,M.J. (1995). Functional MRI measurement of language lateralization in Wada-tested patients. Brain *118 (Pt 6)*, 1411-1419.

112. Detre,J.A., Alsop,D.C., Aguirre,G.K., and Sperling,M.R. (1996). Coupling of cortical and thalamic ictal activity in human partial epilepsy: demonstration by functional magnetic resonance imaging. Epilepsia *37*, 657-661.

113. Detre,J.A., Sirven,J.I., Alsop,D.C., O'Connor,M.J., and French,J.A. (1995). Localization of subclinical ictal activity by functional magnetic resonance imaging: correlation with invasive monitoring. Ann. Neurol. *38*, 618-624.

114. Devinsky,O., Sato,S., Kufta,C.V., Ito,B., Rose,D.F., Theodore,W.H., and Porter,R.J. (1989). Electroencephalographic studies of simple partial seizures with subdural electrode recordings. Neurology *39*, 527-533.

115. Devlin,J.T., Russell,R.P., Davis,M.H., Price,C.J., Wilson,J., Moss,H.E., Matthews,P.M., and Tyler,L.K. (2000). Susceptibility-induced loss of signal: comparing PET and fMRI on a semantic task. Neuroimage *11*, 589-600.

116. Di,B.C., Vaudano,A.E., Carni,M., Pantano,P., Nucciarelli,V., Garreffa,G., Maraviglia,B., Prencipe,M., Bozzao,L., Manfredi,M., and Giallonardo,A.T. (2006). EEG/fMRI study of ictal and interictal epileptic activity: methodological issues and future perspectives in clinical practice. Epilepsia *47 Suppl 5*, 52-58.

117. Diehl,B., Knecht,S., Deppe,M., Young,C., and Stodieck,S.R. (1998). Cerebral hemodynamic response to generalized spike-wave discharges. Epilepsia *39*, 1284-1289.

118. Diehl,B., Salek-Haddadi,A., Fish,D.R., and Lemieux,L. (2003). Mapping of spikes, slow waves, and motor tasks in a patient with malformation of cortical development using simultaneous EEG and fMRI. Magn Reson. Imaging *21*, 1167-1173.

119. Diekmann,V., Becker,W., Jurgens,R., Grozinger,B., Kleiser,B., Richter,H.P., and Wollinsky,K.H. (1998). Localisation of epileptic foci with electric, magnetic and combined electromagnetic models. Electroencephalogr. Clin. Neurophysiol. *106*, 297-313.

120. Disbrow,E.A., Slutsky,D.A., Roberts,T.P., and Krubitzer,L.A. (2000). Functional MRI at 1.5 tesla: a comparison of the blood oxygenation level-

dependent signal and electrophysiology. Proc. Natl. Acad. Sci. U. S. A *97*, 9718-9723.

121. Draper,N.R., and Smith,H. (1981). Applied Regression Analysis (New York: Wiley).

122. Dreier,J.P., Korner,K., Gorner,A., Lindauer,U., Weih,M., Villringer,A., and Dirnagl,U. (1995). Nitric oxide modulates the CBF response to increased extracellular potassium. J. Cereb. Blood Flow Metab *15*, 914-919.

123. Duchene,M., da Graca Moraes Martin,M., Ricci Arantes,P., de Maria Felix,M., Garcia de Barros,F., Barreiros,M.A.M., Guilherme Caldas,J., Campi de Castro,C., Guido Cerri,G., and Amaro Junior,E. (2001). fMRI findings in AVM. Neuroimage *13*, S788.

124. Duffy,F.H., and Burchfiel,J.L. (1975). Eye movement-related inhibition of primate visual neurons. Brain Res. *89*, 121-132.

125. Dumpelmann,M., and Elger,C.E. (1998). Automatic detection of epileptiform spikes in the electrocorticogram: a comparison of two algorithms. Seizure. *7*, 145-152.

126. Dumpelmann,M., and Elger,C.E. (1999). Visual and automatic investigation of epileptiform spikes in intracranial EEG recordings. Epilepsia *40*, 275-285.

127. Duncan,J.S. (1997a). Idiopathic generalized epilepsies with typical absences. J. Neurol. *244*, 403-411.

128. Duncan,J.S. (1997b). Imaging and epilepsy. Brain *120 (Pt 2)*, 339-377.

129. Dunn,G., and Everitt,B.S. (1982). An Introduction to Mathematical Taxonomy. Cambridge University Press, Cambridge.

130. Dymarkowski,S., Sunaert,S., Van Oostende,S., Van Hecke,P., Wilms,G., Demaerel,P., Nuttin,B., Plets,C., and Marchal,G. (1998). Functional MRI of the brain: localisation of eloquent cortex in focal brain lesion therapy. Eur. Radiol. *8*, 1573-1580.

131. Ebersole,J.S. (1994). Non-invasive localization of the epileptogenic focus by EEG dipole modeling. Acta Neurol. Scand. Suppl *152*, 20-28.

132. Ebersole,J.S. (1997a). Defining epileptogenic foci: past, present, future. J. Clin. Neurophysiol. *14*, 470-483.

133. Ebersole,J.S. (1997b). EEG and MEG Dipole Source Modeling. In Epilepsy: A Comprehensive textbook, J. Engel, and T.A. Pedley, eds. (Philadelphia: Lippincott Williams & Wilkins).

134. Ebersole,J.S., and Wade,P.B. (1990). Spike voltage topography and equivalent dipole localization in complex partial epilepsy. Brain Topogr. *3*, 21-34.

135. Emerson,R.G., Turner,C.A., Pedley,T.A., Walczak,T.S., and Forgione,M. (1995). Propagation patterns of temporal spikes. Electroencephalogr. Clin. Neurophysiol. *94*, 338-348.

136. Engel,J., Jr. (1993). Intracerebral recordings: organization of the human epileptogenic region. J. Clin. Neurophysiol *10*, 90-98.

137. Engel,J., Jr. (2001). A proposed diagnostic scheme for people with epileptic seizures and with epilepsy: report of the ILAE Task Force on Classification and Terminology. Epilepsia *42*, 796-803.

138. Engel,J., Jr. (2006). Report of the ILAE classification core group. Epilepsia *47*, 1558-1568.

139. Engel,J., Jr., Kuhl,D.E., and Phelps,M.E. (1982). Patterns of human local cerebral glucose metabolism during epileptic seizures. Science *218*, 64-66.

140. Engel,J., Jr., Lubens,P., Kuhl,D.E., and Phelps,M.E. (1985). Local cerebral metabolic rate for glucose during petit mal absences. Ann. Neurol. *17*, 121-128.

141. Fandino,J., Kollias,S.S., Wieser,H.G., Valavanis,A., and Yonekawa,Y. (1999). Intraoperative validation of functional magnetic resonance imaging and cortical reorganization patterns in patients with brain tumors involving the primary motor cortex. J. Neurosurg. *91*, 238-250.

142. Featherstone,E., and Josephs,O. (2001). Speech recording during fMRI. Neuroimage *13*, S10.

143. Federico,P., Archer,J.S., Abbott,D.F., and Jackson,G.D. (2005). Cortical/subcortical BOLD changes associated with epileptic discharges: an EEG-fMRI study at 3 T. Neurology *64*, 1125-1130.

144. Felblinger,J., Slotboom,J., Kreis,R., Jung,B., and Boesch,C. (1999). Restoration of electrophysiological signals distorted by inductive effects of magnetic field gradients during MR sequences. Magn Reson. Med. *41*, 715-721.

145. Ferlazzo,E., Zifkin,B.G., Andermann,E., and Andermann,F. (2005). Cortical triggers in generalized reflex seizures and epilepsies. Brain *128*, 700-710.

146. Fernandez Torre,J.L., Alarcon,G., Binnie,C.D., Seoane,J.J., Juler,J., Guy,C.N., and Polkey,C.E. (1999). Generation of scalp discharges in temporal lobe epilepsy as suggested by intraoperative electrocorticographic recordings. J. Neurol. Neurosurg. Psychiatry *67*, 51-58.

147. Fink,G.R., Pawlik,G., Stefan,H., Pietrzyk,U., Wienhard,K., and Heiss,W.D. (1996). Temporal lobe epilepsy: evidence for interictal uncoupling of blood flow and glucose metabolism in temporomesial structures. J. Neurol. Sci. *137*, 28-34.

148. Fish,D.R. (2003). The role of scalp Electroencephalography in presurgical evaluation. In The Treatment of Epilepsy, S.D. Shorvon, D.R. Fish, E. Dodson, E. Perucca, and A. Olivier, eds. (Oxford: Blackwell).

149. FitzGerald,D.B., Cosgrove,G.R., Ronner,S., Jiang,H., Buchbinder,B.R., Belliveau,J.W., Rosen,B.R., and Benson,R.R. (1997). Location of language in the cortex: a comparison between functional MR imaging and electrocortical stimulation. AJNR Am. J. Neuroradiol. *18*, 1529-1539.

150. Forster,A., Juge,O., and Morel,D. (1982). Effects of midazolam on cerebral blood flow in human volunteers. Anesthesiology *56*, 453-455.

151. Frahm,J., Merboldt,K.D., Hanicke,W., Kleinschmidt,A., and Boecker,H. (1994). Brain or vein--oxygenation or flow? On signal physiology in functional MRI of human brain activation. NMR Biomed. *7*, 45-53.

152. Franck,G., Sadzot,B., Salmon,E., Depresseux,J.C., Grisar,T., Peters,J.M., Guillaume,M., Quaglia,L., Delfiore,G., and Lamotte,D. (1986). Regional cerebral blood flow and metabolic rates in human focal epilepsy and status epilepticus. Adv. Neurol. *44*, 935-948.

153. Franck,G., Salmon,E., Sadzot,B., and Maquet,P. (1989). Epilepsy: the use of oxygen-15-labeled gases. Semin. Neurol. *9*, 307-316.

154. Friston,K., Phillips,J., Chawla,D., and Buchel,C. (2000a). Nonlinear PCA: characterizing interactions between modes of brain activity. Philos. Trans. R. Soc. Lond B Biol. Sci. *355*, 135-146.

155. Friston,K.J. (2000). The labile brain. I. Neuronal transients and nonlinear coupling. Philos. Trans. R. Soc. Lond B Biol. Sci. *355*, 215-236.

156. Friston,K.J., Ashburner,J., Poline,J.B., Frith,C.D., Heather,J.D., and Frackowiak,R.S. (1995a). Spatial Registration and Normalization of Images. Hum. Brain Mapp. *2*, 165-189.

157. Friston,K.J., Fletcher,P., Josephs,O., Holmes,A., Rugg,M.D., and Turner,R. (1998a). Event-related fMRI: characterizing differential responses. Neuroimage *7*, 30-40.

158. Friston,K.J., Frith,C.D., Liddle,P.F., Dolan,R.J., Lammertsma,A.A., and Frackowiak,R.S. (1990). The relationship between global and local changes in PET scans. J. Cereb. Blood Flow Metab *10*, 458-466.

159. Friston,K.J., Frith,C.D., liddle,P.F., and Frackowiak,R.S. (1991). Comparing functional (PET) images: the assessment of significant change. J. Cereb. Blood Flow Metab *11*, 690-699.

160. Friston,K.J., Harrison,L., and Penny,W. (2003). Dynamic causal modelling. Neuroimage *19*, 1273-1302.

161. Friston,K.J., Holmes,A.P., and Worsley,K.J. (1999a). How many subjects constitute a study? Neuroimage *10*, 1-5.

162. Friston,K.J., Holmes,A.P., Worsley,K.J., Poline,J.B., Frith,C.D., and Frackowiak,R.S. (1995b). Statistical parametric maps in functional imaging: A general linear approach. Hum. Brain Mapp. *2*, 189-210.

163. Friston,K.J., Josephs,O., Rees,G., and Turner,R. (1998b). Nonlinear event-related responses in fMRI. Magn Reson. Med. *39*, 41-52.

164. Friston,K.J., Josephs,O., Zarahn,E., Holmes,A.P., Rouquette,S., and Poline,J. (2000b). To smooth or not to smooth? Bias and efficiency in fMRI time-series analysis. Neuroimage *12*, 196-208.

165. Friston,K.J., Mechelli,A., Turner,R., and Price,C.J. (2000c). Nonlinear responses in fMRI: the Balloon model, Volterra kernels, and other hemodynamics. Neuroimage *12*, 466-477.

166. Friston,K.J., Stephan,K.E., Lund,T.E., Morcom,A., and Kiebel,S. (2005). Mixed-effects and fMRI studies. Neuroimage *24*, 244-252.

167. Friston,K.J., Williams,S., Howard,R., Frackowiak,R.S., and Turner,R. (1996). Movement-related effects in fMRI time-series. Magn Reson. Med. *35*, 346-355.

168. Friston,K.J., Zarahn,E., Josephs,O., Henson,R.N., and Dale,A.M. (1999b). Stochastic designs in event-related fMRI. Neuroimage *10*, 607-619.

169. Fuchs,M., Wagner,M., Kohler,T., and Wischmann,H.A. (1999). Linear and nonlinear current density reconstructions. J. Clin. Neurophysiol. *16*, 267-295.

170. Fuchs,M., Wagner,M., Wischmann,H.A., Kohler,T., Theissen,A., Drenckhahn,R., and Buchner,H. (1998). Improving source reconstructions by combining bioelectric and biomagnetic data. Electroencephalogr. Clin. Neurophysiol. *107*, 93-111.

171. Gabrieli,J.D., Brewer,J.B., and Poldrack,R.A. (1998). Images of medial temporal lobe functions in human learning and memory. Neurobiol. Learn. Mem. *70*, 275-283.

172. Gaillard,W.D., Fazilat,S., White,S., Malow,B., Sato,S., Reeves,P., Herscovitch,P., and Theodore,W.H. (1995). Interictal metabolism and blood flow are uncoupled in temporal lobe cortex of patients with complex partial epilepsy. Neurology *45*, 1841-1847.

173. Gais,S., Albouy,G., Boly,M., ng-Vu,T.T., Darsaud,A., Desseilles,M., Rauchs,G., Schabus,M., Sterpenich,V., Vandewalle,G., Maquet,P., and Peigneux,P. (2007). Sleep transforms the cerebral trace of declarative memories. Proc. Natl. Acad. Sci. U. S. A *104*, 18778-18783.

174. Gerstein,G.L., and Perkel,D.H. (1969). Simultaneously recorded trains of action potentials: analysis and functional interpretation. Science *164*, 828-830.

175. Gibbs,F.A., Lennox,W.G., and Gibbs,E.L. (1934). Cerebral blood flow preceeding and accompanying epileptic seizures in man. Arch. Neurol. Psychiatr *32*, 257-272.

176. Gloor,P. (1968). Generalized cortico-reticular epilepsies. Some considerations on the pathophysiology of generalized bilaterally synchronous spike and wave discharge. Epilepsia *9*, 249-263.

177. Gloor,P. (1985). Neuronal generators and the problem of localization in electroencephalography: application of volume conductor theory to electroencephalography. J. Clin. Neurophysiol. *2*, 327-354.

178. Goldman,R.I., Stern,J.M., Engel,J., and Cohen,M.S. (2000). Acquiring simultaneous EEG and functional MRI. Clin. Neurophysiol. *111*, 1974-1980.

179. Goldman,R.I., Stern,J.M., Engel,J., Jr., and Cohen,M.S. (2002). Simultaneous EEG and fMRI of the alpha rhythm. Neuroreport *13*, 2487-2492.

180. Good,C.D., Johnsrude,I., Ashburner,J., Henson,R.N., Friston,K.J., and Frackowiak,R.S. (2001). Cerebral asymmetry and the effects of sex and handedness on brain structure: a voxel-based morphometric analysis of 465 normal adult human brains. Neuroimage *14*, 685-700.

181. Gorno-Tempini,M.L., Hutton,C., Josephs,O., Deichmann,R., Price,C., and Turner,R. (2002). Echo time dependence of BOLD contrast and susceptibility artifacts. Neuroimage *15*, 136-142.

182. Gotman,J. (2008). Epileptic networks studied with EEG-fMRI. Epilepsia *49 Suppl 3*, 42-51.

183. Gotman,J., Grova,C., Bagshaw,A., Kobayashi,E., Aghakhani,Y., and Dubeau,F. (2005). Generalized epileptic discharges show thalamocortical activation and suspension of the default state of the brain. Proc. Natl. Acad. Sci. U. S. A *102*, 15236-15240.

184. Gotman,J., and Koffler,D.J. (1989). Interictal spiking increases after seizures but does not after decrease in medication. Electroencephalogr. Clin. Neurophysiol. *72*, 7-15.

185. Gotman,J., and Marciani,M.G. (1985). Electroencephalographic spiking activity, drug levels, and seizure occurrence in epileptic patients. Ann. Neurol *17*, 597-603.

186. Grisar,T., Lakaye,B., Thomas,E., Bettendorf,L., and Minet,A. (1999). The molecular neuron-glia couple and epileptogenesis. Adv. Neurol. *79:591-602*, 591-602.

187. Grootoonk,S., Hutton,C., Ashburner,J., Howseman,A.M., Josephs,O., Rees,G., Friston,K.J., and Turner,R. (2000). Characterization and correction of interpolation effects in the realignment of fMRI time series. Neuroimage *11*, 49-57.

188. Gusnard,D.A., Raichle,M.E., and Raichle,M.E. (2001). Searching for a baseline: functional imaging and the resting human brain. Nat. Rev. Neurosci. *2*, 685-694.

189. Haginoya,K., Munakata,M., Kato,R., Yokoyama,H., Ishizuka,M., and Iinuma,K. (2002). Ictal cerebral haemodynamics of childhood epilepsy measured with near-infrared spectrophotometry. Brain *125*, 1960-1971.

190. Hajnal,J.V., Myers,R., Oatridge,A., Schwieso,J.E., Young,I.R., and Bydder,G.M. (1994). Artifacts due to stimulus correlated motion in functional imaging of the brain. Magn Reson. Med. *31*, 283-291.

191. Hallet,M. (1997). Myoclonus and Myoclonic Syndromes. In Epilepsy: A Comprehensive Textbook, J. Engel, Jr., and T.A. Pedley, eds.

192. Hallett,M. (2000). Transcranial magnetic stimulation and the human brain. Nature *406*, 147-150.

193. Hamandi,K., Laufs,H., Noth,U., Carmichael,D.W., Duncan,J.S., and Lemieux,L. (2008a). BOLD and perfusion changes during epileptic generalised spike wave activity. Neuroimage *39*, 608-618.

194. Hamandi,K., Powell,H.W., Laufs,H., Symms,M.R., Barker,G.J., Parker,G.J., Lemieux,L., and Duncan,J.S. (2008b). Combined EEG-fMRI and tractography to visualise propagation of epileptic activity. J. Neurol. Neurosurg. Psychiatry *79*, 594-597.

195. Hamandi,K., Salek,H.A., Liston,A., Laufs,H., Fish,D.R., and Lemieux,L. (2005a). fMRI temporal clustering analysis in patients with frequent interictal epileptiform discharges: comparison with EEG-driven analysis. Neuroimage *26*, 309-316.

196. Hamandi,K., Salek-Haddadi,A., Laufs,H., Liston,A., Friston,K., Fish,D.R., Duncan,J.S., and Lemieux,L. (2006). EEG-fMRI of idiopathic and secondarily generalized epilepsies. Neuroimage *31*, 1700-1710.

197. Hamandi,K., Salek-Haddadi,A., Laufs,H., Liston,A., Friston,K.J., Fish,D.R., Duncan,J.S., and Lemieux,L. (2005b). EEG-fMRI of Idiopathic and Secondarily Generalized Epilepsies. Neuroimage *in press*.

198. Handforth,A., Cheng,J.T., Mandelkern,M.A., and Treiman,D.M. (1994). Markedly increased mesiotemporal lobe metabolism in a case with PLEDs: further evidence that PLEDs are a manifestation of partial status epilepticus. Epilepsia *35*, 876-881.

199. Hanson,L.G., Lund,T.E., and Hanson,C.G. (2007). Encoding of electrophysiology and other signals in MR images. J. Magn Reson. Imaging *25*, 1059-1066.

200. Harder,D.R., Zhang,C., and Gebremedhin,D. (2002). Astrocytes function in matching blood flow to metabolic activity. News Physiol Sci. *17*, 27-31.

201. Hawco,C.S., Bagshaw,A.P., Lu,Y., Dubeau,F., and Gotman,J. (2007). BOLD changes occur prior to epileptic spikes seen on scalp EEG. Neuroimage *35*, 1450-1458.

202. Hayne,R.A., Belison,I., and gibbs,f.a. (1949). Electrical activity of subcortical areas in epilepsy. Electroencephalogr. Clin. Neurophysiol. *1*, 437-445.

203. Heeger,D.J., Huk,A.C., Geisler,W.S., and Albrecht,D.G. (2000). Spikes versus BOLD: what does neuroimaging tell us about neuronal activity? Nat. Neurosci. *3*, 631-633.

204. Heeger,D.J., and Ress,D. (2002). What does fMRI tell us about neuronal activity? Nat. Rev. Neurosci. *3*, 142-151.

205. Henson,R.N., Price,C.J., Rugg,M.D., Turner,R., and Friston,K.J. (2002). Detecting latency differences in event-related BOLD responses: application to words versus nonwords and initial versus repeated face presentations. Neuroimage *15*, 83-97.

206. Henson,R.N.A., Buchel,C., Josephs,O., and Friston,K.J. (1999). The slice-timing problem in event-related fMRI. Neuroimage *9*, 125.

207. Hertz-Pannier,L., Gaillard,W.D., Mott,S.H., Cuenod,C.A., Bookheimer,S.Y., Weinstein,S., Conry,J., Papero,P.H., Schiff,S.J., Le Bihan,D., and Theodore,W.H. (1997). Noninvasive assessment of language dominance in children and adolescents with functional MRI: a preliminary study [see comments]. Neurology *48*, 1003-1012.

208. Hill,R.A., Chiappa,K.H., Huang-Hellinger,F., and Jenkins,B.G. (1995). EEG during MR imaging: differentiation of movement artifact from paroxysmal cortical activity. Neurology *45*, 1942-1943.

209. Hill,R.A., Chiappa,K.H., Huang-Hellinger,F., and Jenkins,B.G. (1999). Hemodynamic and metabolic aspects of photosensitive epilepsy revealed by functional magnetic resonance imaging and magnetic resonance spectroscopy. Epilepsia *40*, 912-920.

210. Hochman,D.W., Baraban,S.C., Owens,J.W., and Schwartzkroin,P.A. (1995). Dissociation of synchronization and excitability in furosemide blockade of epileptiform activity. Science *270*, 99-102.

211. Hoffmann,A., Jager,L., Werhahn,K.J., Jaschke,M., Noachtar,S., and Reiser,M. (2000). Electroencephalography during functional echo-planar imaging: Detection of epileptic spikes using post-processing methods. Magn Reson. Med. *44*, 791-798.

212. Holmes,G.L., McKeever,M., and Adamson,M. (1987). Absence seizures in children: clinical and electroencephalographic features. Ann. Neurol. *21*, 268-273.

213. Horsely,V. (1886). Brain Surgery. Br Med J *2*, 670-675.

214. Horwitz,B., and Poeppel,D. (2002). How can EEG/MEG and fMRI/PET data be combined? Hum. Brain Mapp. *17*, 1-3.

215. Huang-Hellinger,F., Hans,C., McCormack,G., Cohen,M., Kwong,K.K., Sutton,J.P., Savoy,R.L., Weisskoff,R.M., Davis,T.L., Baker,J.R., Belliveau,J.W., and Rosen,B.R. (1995). Simultaneous functional magnetic resonance imaging and electrophysiological recording. Hum. Brain Mapping *3*, 13-23.

216. Huettel,S.A., and McCarthy,G. (2001). Regional Differences in the Refractory Period of the Hemodynamic Response: An Event-Related fMRI Study. Neuroimage. *14*, 967-976.

217. Hughes,J.R. (1989). The significance of the interictal spike discharge: a review. J. Clin. Neurophysiol. *6*, 207-226.

218. Huppertz,H.J., Hof,E., Klisch,J., Wagner,M., Lucking,C.H., and Kristeva-Feige,R. (2001). Localization of interictal delta and epileptiform EEG activity associated with focal epileptogenic brain lesions. Neuroimage. *13*, 15-28.

219. Iannetti,G.D., Di Bonaventura,C., Pantano,P., Giallonardo,A.T., Romanelli,P.L., Bozzao,L., Manfredi,M., and Ricci,G.B. (2002). fMRI/EEG in paroxysmal activity elicited by elimination of central vision and fixation. Neurology *58*, 976-979.

220. Ives,J.R., Warach,S., Schmitt,F., Edelman,R.R., and Schomer,D.L. (1993). Monitoring the patient's EEG during echo planar MRI. Electroencephalogr. Clin. Neurophysiol. *87*, 417-420.

221. Jack,C.R., Jr., Thompson,R.M., Butts,R.K., Sharbrough,F.W., Kelly,P.J., Hanson,D.P., Riederer,S.J., Ehman,R.L., Hangiandreou,N.J., and Cascino,G.D. (1994). Sensory motor cortex: correlation of presurgical mapping with functional MR imaging and invasive cortical mapping. Radiology *190*, 85-92.

222. Jackson,G.D., Connelly,A., Cross,J.H., Gordon,I., and Gadian,D.G. (1994). Functional magnetic resonance imaging of focal seizures. Neurology *44*, 850-856.

223. Jacobs,J., Hawco,C., Kobayashi,E., Boor,R., LeVan,P., Stephani,U., Siniatchkin,M., and Gotman,J. (2008a). Variability of the hemodynamic response as a function of age and frequency of epileptic discharge in children with epilepsy. Neuroimage *40*, 601-614.

224. Jacobs,J., Kobayashi,E., Boor,R., Muhle,H., Stephan,W., Hawco,C., Dubeau,F., Jansen,O., Stephani,U., Gotman,J., and Siniatchkin,M. (2007). Hemodynamic responses to interictal epileptiform discharges in children with symptomatic epilepsy. Epilepsia *48*, 2068-2078.

225. Jacobs,J., Rohr,A., Moeller,F., Boor,R., Kobayashi,E., LeVan,M.P., Stephani,U., Gotman,J., and Siniatchkin,M. (2008b). Evaluation of epileptogenic networks in children with tuberous sclerosis complex using EEG-fMRI. Epilepsia *49*, 816-825.

226. Jager,L., Hoffmann,A., Joppich,M., and Reiser,M. Simultaneous EEG recording with MR data-acquisition. Proc.ISMRM Sydney, Australia , 286. 1998.
Ref Type: Abstract

227. Jager,L., Werhahn,K.J., Hoffmann,A., Berthold,S., Scholz,V., Weber,J., Noachtar,S., and Reiser,M. (2002). Focal Epileptiform Activity in the Brain: Detection with Spike-related Functional MR Imaging Preliminary Results. Radiology *223*, 860-869.

228. James,W. (1890). Principles of psychology. (New York: Dover).

229. Jasper,H., and Droogleever-Fortuyn,J. (1947). Experimental studies on the functional anatomy of petit mal epilepsy. Res Publ Assoc Res Nerv Ment Dis *26*, 272-298.

230. Jensen,M.S., and Yaari,Y. (1997). Role of intrinsic burst firing, potassium accumulation, and electrical coupling in the elevated potassium model of hippocampal epilepsy. J. Neurophysiol. *77*, 1224-1233.

231. Josephs,O., and Henson,R.N. (1999). Event-related functional magnetic resonance imaging: modelling, inference and optimization. Philos. Trans. R. Soc. Lond B Biol. Sci. *354*, 1215-1228.

232. Josephs,O., Lemieux,L., Krakow,K., and Friston,K.J. (1999). Burst Mode Event-Related fMRI. Neuroimage *9*.

233. Josephs,O., Turner,R., and Friston,K.J. (1997). Event-Related fMRI. Hum. Brain Mapp. *5*, 243-248.

234. Jueptner,M., and Weiller,C. (1995). Review: does measurement of regional cerebral blood flow reflect synaptic activity? Implications for PET and fMRI. Neuroimage *2*, 148-156.

235. Kastrup,A., Kruger,G., Glover,G.H., Neumann-Haefelin,T., and Moseley,M.E. (1999a). Regional variability of cerebral blood oxygenation response to hypercapnia. Neuroimage *10*, 675-681.

236. Kastrup,A., Li,T.Q., Glover,G.H., Kruger,G., and Moseley,M.E. (1999b). Gender differences in cerebral blood flow and oxygenation response during focal physiologic neural activity. J. Cereb. Blood Flow Metab *19*, 1066-1071.

237. Kemna,L.J., and Posse,S. (2001). Effect of respiratory CO(2) changes on the temporal dynamics of the hemodynamic response in functional MR imaging. Neuroimage *14*, 642-649.

238. Kim,B., Boes,J.L., Bland,P.H., Chenevert,T.L., and Meyer,C.R. (1999). Motion correction in fMRI via registration of individual slices into an anatomical volume. Magn Reson. Med. *41*, 964-972.

239. Kleinschmidt,A., Bruhn,H., Kruger,G., Merboldt,K.D., Stoppe,G., and Frahm,J. (1999). Effects of sedation, stimulation, and placebo on cerebral blood oxygenation: a magnetic resonance neuroimaging study of psychotropic drug action. NMR Biomed. *12*, 286-292.

240. Kleinschmidt,A., Steinmetz,H., Sitzer,M., Merboldt,K.D., and Frahm,J. (1995). Magnetic resonance imaging of regional cerebral blood oxygenation changes under acetazolamide in carotid occlusive disease. Stroke *26*, 106-110.

241. Klingelhofer,J., Bischoff,C., Sander,D., Wittich,I., and Conrad,B. (1991). Do brief bursts of spike and wave activity cause a cerebral hyper- or hypoperfusion in man? Neurosci. Lett. *127*, 77-81.

242. Kobayashi,E., Bagshaw,A.P., Benar,C.G., Aghakhani,Y., Andermann,F., Dubeau,F., and Gotman,J. (2006a). Temporal and extratemporal BOLD responses to temporal lobe interictal spikes. Epilepsia *47*, 343-354.

243. Kobayashi,E., Bagshaw,A.P., Gotman,J., and Dubeau,F. (2007). Metabolic correlates of epileptic spikes in cerebral cavernous angiomas. Epilepsy Res. *73*, 98-103.

244. Kobayashi,E., Bagshaw,A.P., Grova,C., Dubeau,F., and Gotman,J. (2005a). Negative BOLD responses to epileptic spikes. Hum. Brain Mapp.

245. Kobayashi,E., Bagshaw,A.P., Grova,C., Dubeau,F., and Gotman,J. (2005b). Negative BOLD responses to epileptic spikes. Hum. Brain Mapp.

246. Kobayashi,E., Bagshaw,A.P., Grova,C., Gotman,J., and Dubeau,F. (2006b). Grey matter heterotopia: what EEG-fMRI can tell us about epileptogenicity of neuronal migration disorders. Brain *129*, 366-374.

247. Kobayashi,E., Bagshaw,A.P., Jansen,A., Andermann,F., Andermann,E., Gotman,J., and Dubeau,F. (2005c). Intrinsic epileptogenicity in polymicrogyric cortex suggested by EEG-fMRI BOLD responses. Neurology *64*, 1263-1266.

248. Kobayashi,E., Hawco,C.S., Grova,C., Dubeau,F., and Gotman,J. (2006c). Widespread and intense BOLD changes during brief focal electrographic seizures. Neurology *66*, 1049-1055.

249. Kochen,S., Giagante,B., and Oddo,S. (2002). Spike-and-wave complexes and seizure exacerbation caused by carbamazepine. Eur. J. Neurol. *9*, 41-47.

250. Koepp,M.J., Hansen,M.L., Pressler,R.M., Brooks,D.J., Brandl,U., Guldin,B., Duncan,J.S., and Ried,S. (1998a). Comparison of EEG, MRI and PET in reading epilepsy: a case report. Epilepsy Res. *29*, 251-257.

251. Koepp,M.J., Richardson,M.P., Brooks,D.J., and Duncan,J.S. (1998b). Focal cortical release of endogenous opioids during reading-induced seizures. Lancet *352*, 952-955.

252. Konn,D., Gowland,P., and Bowtell,R. (2003). MRI detection of weak magnetic fields due to an extended current dipole in a conducting sphere: a model for direct detection of neuronal currents in the brain. Magn Reson. Med. *50*, 40-49.

253. Konn,D., Leach,S., Gowland,P., and Bowtell,R. (2004). Initial attempts at directly detecting alpha wave activity in the brain using MRI. Magn Reson. Imaging *22*, 1413-1427.

254. Kostopoulos,G.K. (2000). Spike-and-wave discharges of absence seizures as a transformation of sleep spindles: the continuing development of a hypothesis. Clin. Neurophysiol. *111 Suppl 2*, S27-S38.

255. Koutroumanidis,M., Koepp,M.J., Richardson,M.P., Camfield,C., Agathonikou,A., Ried,S., Papadimitriou,A., Plant,G.T., Duncan,J.S., and Panayiotopoulos,C.P. (1998). The variants of reading epilepsy. A clinical and video-EEG study of 17 patients with reading-induced seizures. Brain *121 (Pt 8)*, 1409-1427.

256. Krakow,K., Allen,P.J., Lemieux,L., Symms,M.R., and Fish,D.R. (2000a). Methodology: EEG-correlated fMRI. Adv. Neurol. *83*, 187-201.

257. Krakow,K., Allen,P.J., Symms,M.R., Fish,D.R., and Lemieux,L. (2001a). Imaging of Interictal Epileptiform Discharges Using Spike-triggered fMRI. IJBEM *1*, 96-101.

258. Krakow,K., Allen,P.J., Symms,M.R., Lemieux,L., Josephs,O., and Fish,D.R. (2000b). EEG recording during fMRI experiments: Image quality. Hum. Brain Mapping *10*, 10-15.

259. Krakow,K., Baxendale,S.A., Maguire,E.A., Krishnamoorthy,E.S., Lemieux,L., Scott,C.A., and Smith,S.J. (2000c). Fixation-off sensitivity as a model of continuous epileptiform discharges: electroencephalographic, neuropsychological and functional MRI findings. Epilepsy Res. *42*, 1-6.

260. Krakow,K., Lemieux,L., Messina,D., Scott,C.A., Symms,M.R., Duncan,J.S., and Fish,D.R. (2001b). Spatio-temporal imaging of focal interictal epileptiform activity using EEG-triggered functional MRI. Epileptic. Disord. *3*, 67-74.

261. Krakow,K., Messina,D., Lemieux,L., Duncan,J.S., and Fish,D.R. (2001c). Functional MRI Activation of Individual Interictal Epileptiform Spikes. Neuroimage *13*, 502-505.

262. Krakow,K., Symms,M.R., Woermann,F.G., Allen,P.J., Fish,D.R., and Duncan,J.S. (1998). Reproducible localisation of interictal activation in epilepsy patients using spike-triggered fMRI. Epilepsia *39*, 199.

263. Krakow,K., Wieshmann,U.C., Woermann,F.G., Symms,M.R., McLean,M.A., Lemieux,L., Allen,P.J., Barker,G.J., Fish,D.R., and Duncan,J.S. (1999a). Multimodal MR imaging: functional, diffusion tensor, and chemical shift imaging in a patient with localization-related epilepsy. Epilepsia *40*, 1459-1462.

264. Krakow,K., Woermann,F.G., Symms,M.R., Allen,P.J., Lemieux,L., Barker,G.J., Duncan,J.S., and Fish,D.R. (1999b). EEG-triggered functional MRI of interictal epileptiform activity in patients with partial seizures. Brain *122*, 1679-1688.

265. Krings,T., Topper,R., Reinges,M.H., Foltys,H., Spetzger,U., Chiappa,K.H., Gilsbach,J.M., and Thron,A. (2000). Hemodynamic changes in simple partial epilepsy: a functional MRI study. Neurology *54*, 524-527.

266. Kuhl,D.E., Engel,J., Jr., Phelps,M.E., and Selin,C. (1980). Epileptic patterns of local cerebral metabolism and perfusion in humans determined by emission computed tomography of 18FDG and 13NH3. Ann. Neurol. *8*, 348-360.

267. Kuschinsky,W., and Wahl,M. (1978). Local chemical and neurogenic regulation of cerebral vascular resistance. Physiol Rev. *58*, 656-689.

268. Kuschinsky,W., Wahl,M., Bosse,O., and Thurau,K. (1972). Perivascular potassium and pH as determinants of local pial arterial diameter in cats. A microapplication study. Circ. Res. *31*, 240-247.

269. Labate,A., Briellmann,R.S., Abbott,D.F., Waites,A.B., and Jackson,G.D. (2005a). Typical childhood absence seizures are associated with thalamic activation. Epileptic. Disord. *7*, 373-377.

270. Labate,A., Briellmann,R.S., Scheffer,I.E., Waites,A.B., Kalnins,R.M., and Jackson,G.D. (2005b). Amygdala dysplasia with temporal lobe epilepsy and obsessive-compulsive disorder: an fMRI/EEG study. Neurology *64*, 1309-1310.

271. Laufs,H., Hamandi,K., Salek-Haddadi,A., Kleinschmidt,A.K., Duncan,J.S., and Lemieux,L. (2007a). Temporal lobe interictal epileptic discharges affect

cerebral activity in "default mode" brain regions. Hum. Brain Mapp. *28*, 1023-1032.

272. Laufs,H., Hamandi,K., Walker,M.C., Scott,C., Smith,S., Duncan,J.S., and Lemieux,L. (2006a). EEG-fMRI mapping of asymmetrical delta activity in a patient with refractory epilepsy is concordant with the epileptogenic region determined by intracranial EEG. Magn Reson. Imaging *24*, 367-371.

273. Laufs,H., Kleinschmidt,A., Beyerle,A., Eger,E., Salek-Haddadi,A., Preibisch,C., and Krakow,K. (2003a). EEG-correlated fMRI of human alpha activity. Neuroimage *19*, 1463-1476.

274. Laufs,H., Krakow,K., Sterzer,P., Eger,E., Beyerle,A., Salek-Haddadi,A., and Kleinschmidt,A. (2003b). Electroencephalographic signatures of attentional and cognitive default modes in spontaneous brain activity fluctuations at rest. Proc. Natl. Acad. Sci. U. S. A *100*, 11053-11058.

275. Laufs,H., Lengler,U., Hamandi,K., Kleinschmidt,A., and Krakow,K. (2006b). Linking generalized spike-and-wave discharges and resting state brain activity by using EEG/fMRI in a patient with absence seizures. Epilepsia *47*, 444-448.

276. Laufs,H., Walker,M.C., and Lund,T.E. (2007b). 'Brain activation and hypothalamic functional connectivity during human non-rapid eye movement sleep: an EEG/fMRI study'--its limitations and an alternative approach. Brain *130*, e75.

277. Laureys,S., Owen,A.M., and Schiff,N.D. (2004). Brain function in coma, vegetative state, and related disorders. Lancet Neurol. *3*, 537-546.

278. Lazeyras,F., Blanke,O., Perrig,S., Zimine,I., Golay,X., Delavelle,J., Michel,C.M., de Tribolet,N., Villemure,J.G., and Seeck,M. (2000a). EEG-triggered functional MRI in patients with pharmacoresistant epilepsy. J. Magn Reson. Imaging *12*, 177-185.

279. Lazeyras,F., Blanke,O., Zimine,I., Delavelle,J., Perrig,S.H., and Seeck,M. (2000b). MRI, (1)H-MRS, and functional MRI during and after prolonged nonconvulsive seizure activity. Neurology *55*, 1677-1682.

280. Leal,A., Dias,A., Vieira,J.P., Secca,M., and Jordao,C. (2006). The BOLD effect of interictal spike activity in childhood occipital lobe epilepsy. Epilepsia *47*, 1536-1542.

281. Leal,A.J., Nunes,S., Martins,A., Secca,M.F., and Jordao,C. (2007). Brain mapping of epileptic activity in a case of idiopathic occipital lobe epilepsy (Panayiotopoulos syndrome). Epilepsia *48*, 1179-1183.

282. Lee,A.T., Glover,G.H., and Meyer,C.H. (1995). Discrimination of large venous vessels in time-course spiral blood- oxygen-level-dependent magnetic-resonance functional neuroimaging. Magn Reson. Med. *33*, 745-754.

283. Lehericy,S., Cohen,L., Bazin,B., Samson,S., Giacomini,E., Rougetet,R., Hertz-Pannier,L., Le Bihan,D., Marsault,C., and Baulac,M. (2000). Functional MR evaluation of temporal and frontal language dominance compared with the Wada test. Neurology *54*, 1625-1633.

284. Leiderman,D.B., Balish,M., Bromfield,E.B., and Theodore,W.H. (1991). Effect of valproate on human cerebral glucose metabolism. Epilepsia *32*, 417-422.

285. Lemieux,L., Allen,P.J., Franconi,F., Symms,M.R., and Fish,D.R. (1997). Recording of EEG during fMRI experiments: patient safety. Magn Reson. Med. *38*, 943-952.

286. Lemieux,L., Krakow,K., and Fish,D.R. (2001a). Comparison of Spike-Triggered Functional MRI BOLD Activation and EEG Dipole Model Localization. Neuroimage. *14*, 1097-1104.

287. Lemieux,L., Salek-Haddadi,A., Josephs,O., Allen,P., Toms,N., Scott,C., Krakow,K., Turner,R., and Fish,D.R. (2001b). Event-Related fMRI with Simultaneous and Continuous EEG: Description of the Method and Initial Case Report. Neuroimage *14*, 780-787.

288. Lemieux,L., Salek-Haddadi,A., and Krakow,K. (2003). The nature of MR signal changes. Radiology *226*, 922-923.

289. Lengler,U., Kafadar,I., Neubauer,B.A., and Krakow,K. (2007). fMRI correlates of interictal epileptic activity in patients with idiopathic benign focal epilepsy of childhood. A simultaneous EEG-functional MRI study. Epilepsy Res. *75*, 29-38.

290. Lin,F.H., Wald,L.L., Ahlfors,S.P., Hamalainen,M.S., Kwong,K.K., and Belliveau,J.W. (2006). Dynamic magnetic resonance inverse imaging of human brain function. Magn Reson. Med. *56*, 787-802.

291. Lindauer,U., Megow,D., Matsuda,H., and Dirnagl,U. (1999). Nitric oxide: a modulator, but not a mediator, of neurovascular coupling in rat somatosensory cortex. Am. J. Physiol *277*, H799-H811.

292. Liston,A., Lund,T.E., Salek-Haddadi,A., Hamandi,K., Friston,K.J., and Lemieux,L. (2005). Modelling Cardiac Signal as a Confound in EEG-fMRI and its Application in Focal Epilepsy Studies. Neuroimage *in press*.

293. Liston,A.D., De Munck,J.C., Hamandi,K., Laufs,H., Ossenblok,P., Duncan,J.S., and Lemieux,L. (2006). Analysis of EEG-fMRI data in focal epilepsy based on automated spike classification and Signal Space Projection. Neuroimage *31*, 1015-1024.

294. Liu,R.S., Lemieux,L., Bell,G.S., Bartlett,P.A., Sander,J.W., Sisodiya,S.M., Shorvon,S.D., and Duncan,J.S. (2001a). A longitudinal quantitative MRI study of community-based patients with chronic epilepsy and newly diagnosed seizures: methodology and preliminary findings. Neuroimage. *14*, 231-243.

295. Liu,T.T., Frank,L.R., Wong,E.C., and Buxton,R.B. (2001b). Detection Power, Estimation Efficiency, and Predictability in Event- Related fMRI. Neuroimage *13*, 759-773.

296. Liu,Y., Yang,T., Yang,X., Liu,I., Liao,W., Lui,S., Huang,X., Chen,H., Gong,Q., and Zhou,D. (2008). EEG-fMRI study of the interictal epileptic activity in patients with partial epilepsy. J. Neurol. Sci. *268*, 117-123.

297. Llinas,R.R. (1988). The intrinsic electrophysiological properties of mammalian neurons: insights into central nervous system function. Science *242*, 1654-1664.

298. Logothetis,N.K., Pauls,J., Augath,M., Trinath,T., and Oeltermann,A. (2001). Neurophysiological investigation of the basis of the fMRI signal. Nature *412*, 150-157.

299. Logothetis,N.K., and Pfeuffer,J. (2004). On the nature of the BOLD fMRI contrast mechanism. Magn Reson. Imaging *22*, 1517-1531.

300. Lopes da Silva,F.H., Pijn,J.P., Velis,D., and Nijssen,P.C. (1997). Alpha rhythms: noise, dynamics and models. Int. J. Psychophysiol. *26*, 237-249.

301. Lopes,d.S. (1991). Neural mechanisms underlying brain waves: from neural membranes to networks. Electroencephalogr. Clin. Neurophysiol. *79*, 81-93.

302. Lovblad,K.O., Thomas,R., Jakob,P.M., Scammell,T., Bassetti,C., Griswold,M., Ives,J., Matheson,J., Edelman,R.R., and Warach,S. (1999). Silent functional magnetic resonance imaging demonstrates focal activation in rapid eye movement sleep. Neurology *53*, 2193-2195.

303. Luders,H.O., Engel,J., Jr., and Munari,C. (1993). General Principles. In Surgical Treatment of the Epilepsies, J. Engel, Jr., ed. (New York: Raven Press, Ltd.), pp. 137-153.

304. Lund,T.E., Norgaard,M.D., Rostrup,E., Rowe,J.B., and Paulson,O.B. (2005). Motion or activity: their role in intra- and inter-subject variation in fMRI. Neuroimage. *26*, 960-964.

305. Lurito,J.T., Lowe,M.J., Sartorius,C., and Mathews,V.P. (2000). Comparison of fMRI and intraoperative direct cortical stimulation in localization of receptive language areas. J. Comput. Assist. Tomogr. *24*, 99-105.

306. Maes,F., Collignon,A., Vandermeulen,D., Marchal,G., and Suetens,P. (1997). Multimodality image registration by maximization of mutual information. IEEE Trans. Med. Imaging *16*, 187-198.

307. Magistretti,P.J., Pellerin,L., Rothman,D.L., and Shulman,R.G. (1999). Energy on demand. Science *283*, 496-497.

308. Makeig,S., Westerfield,M., Jung,T.P., Enghoff,S., Townsend,J., Courchesne,E., and Sejnowski,T.J. (2002). Dynamic brain sources of visual evoked responses. Science *295*, 690-694.

309. Mandeville,J.B., Marota,J.J., Ayata,C., Moskowitz,M.A., Weisskoff,R.M., and Rosen,B.R. (1999a). MRI measurement of the temporal evolution of relative CMRO(2) during rat forepaw stimulation. Magn Reson. Med. *42*, 944-951.

310. Mandeville,J.B., Marota,J.J., Ayata,C., Zaharchuk,G., Moskowitz,M.A., Rosen,B.R., and Weisskoff,R.M. (1999b). Evidence of a cerebrovascular postarteriole windkessel with delayed compliance. J. Cereb. Blood Flow Metab *19*, 679-689.

311. Manganotti,P., Formaggio,E., Gasparini,A., Cerini,R., Bongiovanni,L.G., Storti,S.F., Mucelli,R.P., Fiaschi,A., and Avesani,M. (2008). Continuous EEG-fMRI in patients with partial epilepsy and focal interictal slow-wave discharges on EEG. Magn Reson. Imaging.

312. Mantini,D., Perrucci,M.G., Del,G.C., Romani,G.L., and Corbetta,M. (2007). Electrophysiological signatures of resting state networks in the human brain. Proc. Natl. Acad. Sci. U. S. A *104*, 13170-13175.

313. Marcar,V.L., Strassle,A.E., Loenneker,T., Schwarz,U., and Martin,E. (2004). The influence of cortical maturation on the BOLD response: an fMRI study of visual cortex in children. Pediatr. Res. *56*, 967-974.

314. Marcus,E.M., and Watson,C.W. (1968). Symmetrical epileptogenic foci in monkey cerebral cortex. Mechanisms of interaction and regional variations in capacity for synchronous discharges. Arch. Neurol. *19*, 99-116.

315. Matsuda,T., Matsuura,M., Ohkubo,T., Ohkubo,H., Atsumi,Y., Tamaki,M., Takahashi,K., Matsushima,E., and Kojima,T. (2002). Influence of arousal level for functional magnetic resonance imaging (fMRI) study: simultaneous

recording of fMRI and electroencephalogram. Psychiatry Clin. Neurosci. *56*, 289-290.

316. Matthew,E., Andreason,P., Pettigrew,K., Carson,R.E., Herscovitch,P., Cohen,R., King,C., Johanson,C.E., Greenblatt,D.J., and Paul,S.M. (1995). Benzodiazepine receptors mediate regional blood flow changes in the living human brain. Proc. Natl. Acad. Sci. U. S. A *92*, 2775-2779.

317. Mauguiere,F., and Ryvlin,P. (2004). The role of PET in presurgical assessment of partial epilepsies. Epileptic. Disord. *6*, 193-215.

318. Mayer,T.A., Schroeder,F., May,T.W., and Wolf,P.T. (2006). Perioral reflex myoclonias: a controlled study in patients with JME and focal epilepsies. Epilepsia *47*, 1059-1067.

319. McCarron,J.G., and Halpern,W. (1990). Potassium dilates rat cerebral arteries by two independent mechanisms. Am. J. Physiol *259*, H902-H908.

320. McCulloch,J., Edvinsson,L., and Watt,P. (1982). Comparison of the effects of potassium and pH on the calibre of cerebral veins and arteries. Pflugers Arch. *393*, 95-98.

321. McGonigle,D.J., Howseman,A.M., Athwal,B.S., Friston,K.J., Frackowiak,R.S., and Holmes,A.P. (2000). Variability in fMRI: an examination of intersession differences. Neuroimage *11*, 708-734.

322. McKeown,M., Hu,Y.J., and Jane,W.Z. (2005). ICA Denoising for Event-Related fMRI Studies. Conf. Proc. IEEE Eng Med. Biol. Soc. *1*, 157-161.

323. McKeown,M.J., Makeig,S., Brown,G.G., Jung,T.P., Kindermann,S.S., Bell,A.J., and Sejnowski,T.J. (1998). Analysis of fMRI data by blind separation into independent spatial components. Hum. Brain Mapp. *6*, 160-188.

324. Meeren,H., van,L.G., Lopes da,S.F., and Coenen,A. (2005). Evolving concepts on the pathophysiology of absence seizures: the cortical focus theory. Arch. Neurol. *62*, 371-376.

325. Merlet,I., and Gotman,J. (1999). Reliability of dipole models of epileptic spikes. Clin. Neurophysiol. *110*, 1013-1028.

326. Michel,C.M., Grave,d.P., Lantz,G., Gonzalez,A.S., Spinelli,L., Blanke,O., Landis,T., and Seeck,M. (1999). Spatiotemporal EEG analysis and distributed source estimation in presurgical epilepsy evaluation. J. Clin. Neurophysiol. *16*, 239-266.

327. Miezin,F.M., Maccotta,L., Ollinger,J.M., Petersen,S.E., and Buckner,R.L. (2000). Characterizing the hemodynamic response: effects of presentation rate, sampling procedure, and the possibility of ordering brain activity based on relative timing. Neuroimage. *11*, 735-759.

328. Miyamoto,A., Takahashi,S., Tokumitsu,A., and Oki,J. (1995). Ictal HMPAO-single photon emission computed tomography findings in reading epilepsy in a Japanese boy. Epilepsia *36*, 1161-1163.

329. Moeller,F., Siebner,H.R., Wolff,S., Muhle,H., Boor,R., Granert,O., Jansen,O., Stephani,U., and Siniatchkin,M. (2008a). Changes in activity of striato-thalamo-cortical network precede generalized spike wave discharges. Neuroimage *39*, 1839-1849.

330. Moeller,F., Siebner,H.R., Wolff,S., Muhle,H., Granert,O., Jansen,O., Stephani,U., and Siniatchkin,M. (2008b). Simultaneous EEG-fMRI in drug-naive children with newly diagnosed absence epilepsy. Epilepsia.

331. Moosmann,M., Ritter,P., Krastel,I., Brink,A., Thees,S., Blankenburg,F., Taskin,B., Obrig,H., and Villringer,A. (2003). Correlates of alpha rhythm in functional magnetic resonance imaging and near infrared spectroscopy. Neuroimage *20*, 145-158.

332. Morgan,V.L., Gore,J.C., and bou-Khalil,B. (2007). Cluster analysis detection of functional MRI activity in temporal lobe epilepsy. Epilepsy Res. *76*, 22-33.

333. Morgan,V.L., Price,R.R., Arain,A., Modur,P., and bou-Khalil,B. (2004). Resting functional MRI with temporal clustering analysis for localization of epileptic activity without EEG. Neuroimage. *21*, 473-481.

334. Morocz,I.A., Karni,A., Haut,S., Lantos,G., and Liu,G. (2003). fMRI of triggerable aurae in musicogenic epilepsy. Neurology *60*, 705-709.

335. Mosher,J.C., Spencer,M.E., Leahy,R.M., and Lewis,P.S. (1993). Error bounds for EEG and MEG dipole source localization. Electroencephalogr. Clin. Neurophysiol. *86*, 303-321.

336. Mullinger,K., Brookes,M., Stevenson,C., Morgan,P., and Bowtell,R. (2008a). Exploring the feasibility of simultaneous electroencephalography/functional magnetic resonance imaging at 7 T. Magn Reson. Imaging.

337. Mullinger,K., Debener,S., Coxon,R., and Bowtell,R. (2008b). Effects of simultaneous EEG recording on MRI data quality at 1.5, 3 and 7 tesla. Int. J. Psychophysiol. *67*, 178-188.

338. Munari,C., Hoffmann,D., Francione,S., Kahane,P., Tassi,L., Lo,R.G., and Benabid,A.L. (1994). Stereo-electroencephalography methodology: advantages and limits. Acta Neurol. Scand. Suppl *152*, 56-67, discussion.

339. Muri,R.M., Felblinger,J., Rosler,K.M., Jung,B., Hess,C.W., and Boesch,C. (1998). Recording of electrical brain activity in a magnetic resonance environment: Distorting effects of the static magnetic field. Magnetic Resonance Medicine *39*, 18-22.

340. Nakasato,N., Levesque,M.F., Barth,D.S., Baumgartner,C., Rogers,R.L., and Sutherling,W.W. (1994). Comparisons of MEG, EEG, and ECoG source localization in neocortical partial epilepsy in humans. Electroencephalogr. Clin. Neurophysiol. *91*, 171-178.

341. Negishi,M., Abildgaard,M., Laufer,I., Nixon,T., and Constable,R.T. (2008). An EEG (electroencephalogram) recording system with carbon wire electrodes for simultaneous EEG-fMRI (functional magnetic resonance imaging) recording. J. Neurosci. Methods.

342. Nehlig,A., Vergnes,M., Waydelich,R., Hirsch,E., Charbonne,R., Marescaux,C., and Seylaz,J. (1996). Absence seizures induce a decrease in cerebral blood flow: human and animal data. J. Cereb. Blood Flow Metab *16*, 147-155.

343. Niedermeyer,E. (1997). Alpha rhythms as physiological and abnormal phenomena. Int. J. Psychophysiol. *26*, 31-49.

344. Niedermeyer,E., Laws,E.R., Jr., and Walker,E.A. (1969). Depth EEG findings in epileptics with generalized spike-wave complexes. Arch. Neurol. *21*, 51-58.

345. Niedermeyer,E., and Lopes da Silva,F.H. (1999). Electroencephalography: Basic Principles, Clinical Applications and Related Fields. (Baltimore, Maryland.: Urban and Schwarzengreg).

346. Niedermeyer,E., and Rocca,U. (1972). The diagnostic significance of sleep electroencephalograms in temporal lobe epilepsy. A comparison of scalp and depth tracings. Eur. Neurol. *7*, 119-129.

347. Noppeney,U., and Price,C.J. (2004). Retrieval of abstract semantics. Neuroimage *22*, 164-170.

348. Norden,A.D., and Blumenfeld,H. (2002). The role of subcortical structures in human epilepsy. Epilepsy Behav. *3*, 219-231.

349. Nunez,P.L. (1981). Electric Fields of the Brain: The Neurophysics of EEG. (New York: Oxford University Press).

350. Nunez,P.L. (1995). Neocortical Dynamics and Human EEG Rhythms. (New York: Oxford University Press).

351. Nunez,P.L., and Silberstein,R.B. (2000). On the relationship of synaptic activity to macroscopic measurements: does co-registration of EEG with fMRI make sense? Brain Topogr. *13*, 79-96.

352. Nunez,P.L., Wingeier,B.M., and Silberstein,R.B. (2001). Spatial-temporal structures of human alpha rhythms: theory, microcurrent sources, multiscale measurements, and global binding of local networks. Hum. Brain Mapp. *13*, 125-164.

353. Ochs,R.F., Gloor,P., Tyler,J.L., Wolfson,T., Worsley,K., Andermann,F., Diksic,M., Meyer,E., and Evans,A. (1987). Effect of generalized spike-and-

wave discharge on glucose metabolism measured by positron emission tomography. Ann. Neurol. *21*, 458-464.

354. Ogawa,S., Lee,T.M., Kay,A.R., and Tank,D.W. (1990). Brain magnetic resonance imaging with contrast dependent on blood oxygenation. Proc. Natl. Acad. Sci. U. S. A *87*, 9868-9872.

355. Ojemann,J.G., Akbudak,E., Snyder,A.Z., McKinstry,R.C., Raichle,M.E., and Conturo,T.E. (1997). Anatomic localization and quantitative analysis of gradient refocused echo-planar fMRI susceptibility artifacts. Neuroimage *6*, 156-167.

356. Palmini,A., Gambardella,A., Andermann,F., Dubeau,F., da Costa,J.C., Olivier,A., Tampieri,D., Gloor,P., Quesney,F., Andermann,E., and . (1995). Intrinsic epileptogenicity of human dysplastic cortex as suggested by corticography and surgical results. Ann. Neurol. *37*, 476-487.

357. Panayiotopoulos,C.P. (2002). A Clnical Guide to Epileptic Syndromes and their Treatment. Blandon Medical Publishing).

358. Parkes,L.M., Fries,P., Kerskens,C.M., and Norris,D.G. (2004). Reduced BOLD response to periodic visual stimulation. Neuroimage *21*, 236-243.

359. Patel,M.R., Blum,A., Pearlman,J.D., Yousuf,N., Ives,J.R., Saeteng,S., Schomer,D.L., and Edelman,R.R. (1999). Echo-planar functional MR imaging of epilepsy with concurrent EEG monitoring. AJNR Am. J. Neuroradiol. *20*, 1916-1919.

360. Paulson,O.B., and Newman,E.A. (1987). Does the release of potassium from astrocyte endfeet regulate cerebral blood flow? Science *237*, 896-898.

361. Pavone,A., and Niedermeyer,E. (2000). Absence seizures and the frontal lobe. Clin. Electroencephalogr. *31*, 153-156.

362. Penfield,W., Kalman,V.S., and Cipriani,A. (1939). Cerebral blood flow during induced epileptiform seizures in animals and man. J. Neurophysiol *2*, 257-267.

363. Petersen,S.E., Fox,P.T., Snyder,A.Z., and Raichle,M.E. (1990). Activation of extrastriate and frontal cortical areas by visual words and word-like stimuli. Science *249*, 1041-1044.

364. Petersson,K.M., Nichols,T.E., Poline,J.B., and Holmes,A.P. (1999a). Statistical limitations in functional neuroimaging. I. Non-inferential methods and statistical models. Philos. Trans. R. Soc. Lond B Biol. Sci. *354*, 1239-1260.

365. Petersson,K.M., Nichols,T.E., Poline,J.B., and Holmes,A.P. (1999b). Statistical limitations in functional neuroimaging. II. Signal detection and statistical inference. Philos. Trans. R. Soc. Lond B Biol. Sci. *354*, 1261-1281.

366. Petridou,N., Plenz,D., Silva,A.C., Loew,M., Bodurka,J., and Bandettini,P.A. (2006). Direct magnetic resonance detection of neuronal electrical activity. Proc. Natl. Acad. Sci. U. S. A *103*, 16015-16020.

367. Pfurtscheller,G., and Aranibar,A. (1977). Event-related cortical desynchronization detected by power measurements of scalp EEG. Electroencephalogr. Clin. Neurophysiol. *42*, 817-826.

368. Pfurtscheller,G., and Lopes da Silva,F.H. (1999). Event-related EEG/MEG synchronization and desynchronization: basic principles. Clin. Neurophysiol. *110*, 1842-1857.

369. Phillips,C., Rugg,M.D., and Friston,K.J. (2002). Anatomically informed basis functions for EEG source localization: combining functional and anatomical constraints. Neuroimage *16*, 678-695.

370. Piredda,S., and Gale,K. (1985). A crucial epileptogenic site in the deep prepiriform cortex. Nature *317*, 623-625.

371. Plonsey,R. (1963). Reciprocity applied to volume conductors and the EEG. IEEE Trans. Biomed. Eng. *10*, 9-12.

372. Polack,P.O., Guillemain,I., Hu,E., Deransart,C., Depaulis,A., and Charpier,S. (2007). Deep layer somatosensory cortical neurons initiate spike-and-wave

discharges in a genetic model of absence seizures. J. Neurosci. *27*, 6590-6599.

373. Poldrack,R.A., Wagner,A.D., Prull,M.W., Desmond,J.E., Glover,G.H., and Gabrieli,J.D. (1999). Functional specialization for semantic and phonological processing in the left inferior prefrontal cortex. Neuroimage *10*, 15-35.

374. Portas,C.M., Krakow,K., Allen,P., Josephs,O., Armony,J.L., and Frith,C.D. (2000). Auditory processing across the sleep-wake cycle: simultaneous EEG and fMRI monitoring in humans. Neuron *28*, 991-999.

375. Postle,B.R., Zarahn,E., and D'Esposito,M. (2000). Using event-related fMRI to assess delay-period activity during performance of spatial and nonspatial working memory tasks. Brain Res. Brain Res. Protoc. *5*, 57-66.

376. Prevett,M.C., Duncan,J.S., Jones,T., Fish,D.R., and Brooks,D.J. (1995). Demonstration of thalamic activation during typical absence seizures using H2(15)O and PET. Neurology *45*, 1396-1402.

377. Prince,D.A., and Connors,B.W. (1986). Mechanisms of interictal epileptogenesis. Adv. Neurol. *44*, 275-299.

378. Puce,A., Constable,R.T., Luby,M.L., McCarthy,G., Nobre,A.C., Spencer,D.D., Gore,J.C., and Allison,T. (1995). Functional magnetic resonance imaging of sensory and motor cortex: comparison with electrophysiological localization. J. Neurosurg. *83*, 262-270.

379. Pujol,J., Conesa,G., Deus,J., Lopez-Obarrio,L., Isamat,F., and Capdevila,A. (1998). Clinical application of functional magnetic resonance imaging in presurgical identification of the central sulcus. J. Neurosurg. *88*, 863-869.

380. Radhakrishnan,K., Silbert,P.L., and Klass,D.W. (1995). Reading epilepsy. An appraisal of 20 patients diagnosed at the Mayo Clinic, Rochester, Minnesota, between 1949 and 1989, and delineation of the epileptic syndrome. Brain *118 (Pt 1)*, 75-89.

381. Raichle,M.E., MacLeod,A.M., Snyder,A.Z., Powers,W.J., Gusnard,D.A., and Shulman,G.L. (2001). A default mode of brain function. Proc. Natl. Acad. Sci. U. S. A *98*, 676-682.

382. Raichle,M.E., and Mintun,M.A. (2006). Brain work and brain imaging. Annu. Rev. Neurosci. *29*, 449-476.

383. Rao,T.S. (1992). Indentification of Bilinear Time Series Models 5. Statistica Sinica *2*, 465-478.

384. Rezai,A.R., Finelli,D., Nyenhuis,J.A., Hrdlicka,G., Tkach,J., Sharan,A., Rugieri,P., Stypulkowski,P.H., and Shellock,F.G. (2002). Neurostimulation systems for deep brain stimulation: in vitro evaluation of magnetic resonance imaging-related heating at 1.5 tesla. J. Magn Reson. Imaging *15*, 241-250.

385. Rezai,A.R., Lozano,A.M., Crawley,A.P., Joy,M.L., Davis,K.D., Kwan,C.L., Dostrovsky,J.O., Tasker,R.R., and Mikulis,D.J. (1999). Thalamic stimulation and functional magnetic resonance imaging: localization of cortical and subcortical activation with implanted electrodes. Technical note. J. Neurosurg. *90*, 583-590.

386. Richter,W., and Richter,M. (2003). The shape of the fMRI BOLD response in children and adults changes systematically with age. Neuroimage *20*, 1122-1131.

387. Robson,M.D., Dorosz,J.L., and Gore,J.C. (1998). Measurements of the temporal fMRI response of the human auditory cortex to trains of tones. Neuroimage. *7*, 185-198.

388. Rodin,E. (1999). Decomposition and mapping of generalized spike-wave complexes. Clin. Neurophysiol. *110*, 1868-1875.

389. Rodionov,R., De,M.F., Laufs,H., Carmichael,D.W., Formisano,E., Walker,M., Duncan,J.S., and Lemieux,L. (2007). Independent component analysis of interictal fMRI in focal epilepsy: comparison with general linear model-based EEG-correlated fMRI. Neuroimage *38*, 488-500.

390. Rosenow,F., and Luders,H. (2001). Presurgical evaluation of epilepsy. Brain *124*, 1683-1700.

391. Rostrup,E., Law,I., Blinkenberg,M., Larsson,H.B., Born,A.P., Holm,S., and Paulson,O.B. (2000). Regional differences in the CBF and BOLD responses to hypercapnia: a combined PET and fMRI study. Neuroimage *11*, 87-97.

392. Rowe,J., Friston,K., Frackowiak,R., and Passingham,R. (2002). Attention to action: specific modulation of corticocortical interactions in humans. Neuroimage *17*, 988-998.

393. Rumsey,J.M., Horwitz,B., Donohue,B.C., Nace,K., Maisog,J.M., and Andreason,P. (1997). Phonological and orthographic components of word recognition. A PET-rCBF study. Brain *120 (Pt 5)*, 739-759.

394. Rutten,G.J., van Rijen,P.C., van Veelen,C.W., and Ramsey,N.F. (1999). Language area localization with three-dimensional functional magnetic resonance imaging matches intrasulcal electrostimulation in Broca's area. Ann. Neurol. *46*, 405-408.

395. Salek-Haddadi,A., Diehl,B., Hamandi,K., Merschhemke,M., Liston,A., Friston,K., Duncan,J.S., Fish,D.R., and Lemieux,L. (2006). Hemodynamic correlates of epileptiform discharges: an EEG-fMRI study of 63 patients with focal epilepsy. Brain Res. *1088*, 148-166.

396. Salek-Haddadi,A., Friston,K.J., Lemieux,L., and Fish,D.R. (2003a). Studying spontaneous EEG activity with fMRI. Brain Res Brain Res Rev *43*, 110-133.

397. Salek-Haddadi,A., Hamandi,K., Lemieux,L., Duncan,J.S., and Fish,D.R. (2004). Multiple spatial networks subtend generalised spike-wave activity during human absences: An ICA study of simultaneously acquired EEG/fMRI data. Epilepsia *45*, 115.

398. Salek-Haddadi,A., Lemieux,L., Merschhemke,M., Friston,K.J., Duncan,J.S., and Fish,D.R. (2003c). Functional magnetic resonance imaging of human absence seizures. Ann. Neurol *53*, 663-667.

399. Salek-Haddadi,A., Lemieux,L., Merschhemke,M., Friston,K.J., Duncan,J.S., and Fish,D.R. (2003b). Functional magnetic resonance imaging of human absence seizures. Ann. Neurol *53*, 663-667.

400. Salek-Haddadi,A., Lemieux,L., Merschhemke,M., Friston,K.J., Duncan,J.S., and Fish,D.R. (2003g). Functional magnetic resonance imaging of human absence seizures. Ann. Neurol *53*, 663-667.

401. Salek-Haddadi,A., Lemieux,L., Merschhemke,M., Friston,K.J., Duncan,J.S., and Fish,D.R. (2003f). Functional magnetic resonance imaging of human absence seizures. Ann. Neurol *53*, 663-667.

402. Salek-Haddadi,A., Lemieux,L., Merschhemke,M., Friston,K.J., Duncan,J.S., and Fish,D.R. (2003d). Functional magnetic resonance imaging of human absence seizures. Ann. Neurol *53*, 663-667.

403. Salek-Haddadi,A., Lemieux,L., Merschhemke,M., Friston,K.J., Duncan,J.S., and Fish,D.R. (2003e). Functional magnetic resonance imaging of human absence seizures. Ann. Neurol. *53*, 663-667.

404. Salek-Haddadi,A., Merschhemke,M., Lemieux,L., and Fish,D.R. (2002). Simultaneous EEG-Correlated Ictal fMRI. Neuroimage *16*, 32-40.

405. Sammaritano,M., Gigli,G.L., and Gotman,J. (1991). Interictal spiking during wakefulness and sleep and the localization of foci in temporal lobe epilepsy. Neurology *41*, 290-297.

406. Sanada,S., Murakami,N., and Ohtahara,S. (1988). Changes in blood flow of the middle cerebral artery during absence seizures. Pediatr. Neurol. *4*, 158-161.

407. Scannell,J.W., and Young,M.P. (1999). Neuronal population activity and functional imaging. Proc. R. Soc. Lond B Biol. Sci. *266*, 875-881.

408. Schabus,M., ng-Vu,T.T., Albouy,G., Balteau,E., Boly,M., Carrier,J., Darsaud,A., Degueldre,C., Desseilles,M., Gais,S., Phillips,C., Rauchs,G., Schnakers,C., Sterpenich,V., Vandewalle,G., Luxen,A., and Maquet,P. (2007). Hemodynamic cerebral correlates of sleep spindles during human

non-rapid eye movement sleep. Proc. Natl. Acad. Sci. U. S. A *104*, 13164-13169.

409. Schacter,D.L., Buckner,R.L., Koutstaal,W., Dale,A.M., and Rosen,B.R. (1997). Late onset of anterior prefrontal activity during true and false recognition: an event-related fMRI study. Neuroimage. *6*, 259-269.

410. Schlosser,M.J., Luby,M., Spencer,D.D., Awad,I.A., and McCarthy,G. (1999). Comparative localization of auditory comprehension by using functional magnetic resonance imaging and cortical stimulation. J. Neurosurg. *91*, 626-635.

411. Schomer,D.L., Bonmassar,G., Lazeyras,F., Seeck,M., Blum,A., Anami,K., Schwartz,D., Belliveau,J.W., and Ives,J. (2000). EEG-Linked functional magnetic resonance imaging in epilepsy and cognitive neurophysiology. J. Clin. Neurophysiol. *17*, 43-58.

412. Schulder,M., Maldjian,J.A., Liu,W.C., Holodny,A.I., Kalnin,A.T., Mun,I.K., and Carmel,P.W. (1998). Functional image-guided surgery of intracranial tumors located in or near the sensorimotor cortex. J. Neurosurg. *89*, 412-418.

413. Seeck,M., Lazeyras,F., Michel,C.M., Blanke,O., Gericke,C.A., Ives,J., Delavelle,J., Golay,X., Haenggeli,C.A., de Tribolet,N., and Landis,T. (1998). Non-invasive epileptic focus localization using EEG-triggered functional MRI and electromagnetic tomography. Electroencephalogr. Clin. Neurophysiol. *106*, 508-512.

414. Shmuel,A., Yacoub,E., Pfeuffer,J., Van de Moortele,P.F., Adriany,G., Hu,X., and Ugurbil,K. (2002). Sustained negative BOLD, blood flow and oxygen consumption response and its coupling to the positive response in the human brain. Neuron *36*, 1195-1210.

415. Sibson,N.R., Dhankhar,A., Mason,G.F., Rothman,D.L., Behar,K.L., and Shulman,R.G. (1998). Stoichiometric coupling of brain glucose metabolism and glutamatergic neuronal activity. Proc. Natl. Acad. Sci. U. S. A *95*, 316-321.

416. Siesjo,B.K. (1978). Brain Energy Metabolism. New York, Wiley.

417. Sijbers,J., Michiels,I., Verhoye,M., Van Audekerke,J., Van Der Linden,A., and Van Dyck,D. (1999). Restoration of MR-induced artefacts in simultaneously recorded MR/EEG data. Magn Reson. Imaging *17*, 1383-1391.

418. Snead,O.C., III (1995). Basic mechanisms of generalized absence seizures. Ann. Neurol. *37*, 146-157.

419. Sodickson,D.K., and McKenzie,C.A. (2001). A generalized approach to parallel magnetic resonance imaging. Med. Phys. *28*, 1629-1643.

420. spiegel,e.a., wycis,h.t., and reyes,v. (1951). Diencephalic mechanisms in petit mal epilepsy. Electroencephalogr. Clin. Neurophysiol. *3*, 473-475.

421. Sporns,O., and Zwi,J.D. (2004). The small world of the cerebral cortex. Neuroinformatics. *2*, 145-162.

422. Stefan,H., Schuler,P., Abraham-Fuchs,K., Schneider,S., Gebhardt,M., Neubauer,U., Hummel,C., Huk,W.J., and Thierauf,P. (1994). Magnetic source localization and morphological changes in temporal lobe epilepsy: comparison of MEG/EEG, ECoG and volumetric MRI in presurgical evaluation of operated patients. Acta Neurol. Scand. Suppl *152*, 83-88.

423. Stefanovic,B., Warnking,J.M., Kobayashi,E., Bagshaw,A.P., Hawco,C., Dubeau,F., Gotman,J., and Pike,G.B. (2005). Hemodynamic and metabolic responses to activation, deactivation and epileptic discharges. Neuroimage. *28*, 205-215.

424. Sterman,M.B., Howe,R.C., and Macdonald,L.R. (1970). Facilitation of spindle-burst sleep by conditioning of electroencephalographic activity while awake. Science *167*, 1146-1148.

425. Stone,J.V., Porrill,J., Porter,N.R., and Wilkinson,I.D. (2002). Spatiotemporal independent component analysis of event-related fMRI data using skewed probability density functions. Neuroimage *15*, 407-421.

426. Symms,M.R., Allen,P.J., Woermann,F.G., Polizzi,G., Krakow,K., Barker,G.J., Fish,D.R., and Duncan,J.S. (1999). Reproducible localization of

interictal epileptiform discharges using EEG-triggered fMRI. Phys. Med. Biol. *44*, N161-N168.

427. Tao,J.X., Ray,A., Hawes-Ebersole,S., and Ebersole,J.S. (2005). Intracranial EEG substrates of scalp EEG interictal spikes. Epilepsia *46*, 669-676.

428. Theodore,W.H., Bairamian,D., Newmark,M.E., DiChiro,G., Porter,R.J., Larson,S., and Fishbein,D. (1986a). Effect of phenytoin on human cerebral glucose metabolism. J. Cereb. Blood Flow Metab *6*, 315-320.

429. Theodore,W.H., Balish,M., Leiderman,D., Bromfield,E., Sato,S., and Herscovitch,P. (1996). Effect of seizures on cerebral blood flow measured with 15O-H2O and positron emission tomography. Epilepsia *37*, 796-802.

430. Theodore,W.H., Bromfield,E., and Onorati,L. (1989). The effect of carbamazepine on cerebral glucose metabolism. Ann. Neurol. *25*, 516-520.

431. Theodore,W.H., Brooks,R., Margolin,R., Patronas,N., Sato,S., Porter,R.J., Mansi,L., Bairamian,D., and DiChiro,G. (1985). Positron emission tomography in generalized seizures. Neurology *35*, 684-690.

432. Theodore,W.H., DiChiro,G., Margolin,R., Fishbein,D., Porter,R.J., and Brooks,R.A. (1986b). Barbiturates reduce human cerebral glucose metabolism. Neurology *36*, 60-64.

433. Tiihonen,J., Hari,R., Kajola,M., Karhu,J., Ahlfors,S., and Tissari,S. (1991). Magnetoencephalographic 10-Hz rhythm from the human auditory cortex. Neurosci. Lett. *129*, 303-305.

434. Tiihonen,J., Kajola,M., and Hari,R. (1989). Magnetic mu rhythm in man. Neuroscience *32*, 793-800.

435. Timofeev,I., and Steriade,M. (2004). Neocortical seizures: initiation, development and cessation. Neuroscience *123*, 299-336.

436. Tronnier,V.M., Staubert,A., Hahnel,S., and Sarem-Aslani,A. (1999). Magnetic resonance imaging with implanted neurostimulators: an in vitro and in vivo study. Neurosurgery *44*, 118-125.

437. Tseng,S.Y., Chong,F.C., Chen,R.C., and Kuo,T.S. (1995). Source localization of averaged and single EEG spikes using the electric dipole model. Med. Eng Phys. *17*, 64-70.

438. Turner,R. (2002). How much cortex can a vein drain? Downstream dilution of activation-related cerebral blood oxygenation changes. Neuroimage *16*, 1062-1067.

439. Turner,R., Howseman,A., Rees,G.E., Josephs,O., and Friston,K. (1998). Functional magnetic resonance imaging of the human brain: data acquisition and analysis. Exp. Brain Res. *123*, 5-12.

440. Vazquez,A.L., and Noll,D.C. (1998). Nonlinear aspects of the BOLD response in functional MRI. Neuroimage *7*, 108-118.

441. Velasco,M., Velasco,F., Velasco,A.L., Lujan,M., and Vazquez,d.M. (1989). Epileptiform EEG activities of the centromedian thalamic nuclei in patients with intractable partial motor, complex partial, and generalized seizures. Epilepsia *30*, 295-306.

442. Villringer,A., and Dirnagl,U. (1995). Coupling of brain activity and cerebral blood flow: basis of functional neuroimaging. Cerebrovasc. Brain Metab Rev. *7*, 240-276.

443. von Stein,A., Chiang,C., and Konig,P. (2000). Top-down processing mediated by interareal synchronization. Proc. Natl. Acad. Sci. U. S. A *97*, 14748-14753.

444. Wagner,M., Fuchs,M., Wischmann,H.A., Ottenburge,K., and Dossel,O. (1995). Cortex segmentation from 3-D MR images for MEG reconstructions. In Biomagnetism: Fundamental Research and Clinical Applications., C.e.al. Baumgartner, ed. (Amsterdam: Elsevier Science IOS Press), pp. 433-438.

445. Waldvogel,D., van Gelderen,P., Muellbacher,W., Ziemann,U., Immisch,I., and Hallett,M. (2000). The relative metabolic demand of inhibition and excitation. Nature *406*, 995-998.

446. Warach,S., Ives,J.R., Schlaug,G., Patel,M.R., Darby,D.G., Thangaraj,V., Edelman,R.R., and Schomer,D.L. (1996). EEG-triggered echo-planar functional MRI in epilepsy. Neurology *47*, 89-93.

447. Wenzel,R., Wobst,P., Heekeren,H.H., Kwong,K.K., Brandt,S.A., Kohl,M., Obrig,H., Dirnagl,U., and Villringer,A. (2000). Saccadic suppression induces focal hypooxygenation in the occipital cortex. J. Cereb. Blood Flow Metab *20*, 1103-1110.

448. Wieshmann,U.C., Krakow,K., Symms,M.R., Parker,G.J., Clark,C.A., Barker,G.J., and Shorvon,S.D. (2001). Combined functional magnetic resonance imaging and diffusion tensor imaging demonstrate widespread modified organisation in malformation of cortical development. J. Neurol Neurosurg. Psychiatry *70*, 521-523.

449. Williams,D. (1953). A study of thalamic and cortical rythms in petit mal. Brain *76*, 50-69.

450. Wilson,S.B., Harner,R.N., Duffy,F.H., Tharp,B.R., Nuwer,M.R., and Sperling,M.R. (1996). Spike detection. I. Correlation and reliability of human experts. Electroencephalogr. Clin. Neurophysiol. *98*, 186-198.

451. Wolf,P. (1992). Reading Epilepsy. In Epileptic syndromes in infancy, childhood and adolescence., J. Roger, M. Bureau, Ch. Dravet, F.E. Dreifuss, A. Perret, and P. Wolf, eds. (London: Libbey), pp. 281-298.

452. Wolf,P., Mayer,T., and Reker,M. (1998). Reading epilepsy: report of five new cases and further considerations on the pathophysiology. Seizure. *7*, 271-279.

453. Wong,P.K. (1989). Stability of source estimates in rolandic spikes. Brain Topogr. *2*, 31-36.

454. Wong,P.K. (1991). Source modelling of the rolandic focus. Brain Topogr. *4*, 105-112.

455. Worthington,C., Vincent,D.J., Bryant,A.E., Roberts,D.R., Vera,C.L., Ross,D.A., and George,M.S. (1997). Comparison of functional magnetic

resonance imaging for language localization and intracarotid speech amytal testing in presurgical evaluation for intractable epilepsy. Preliminary results. Stereotact. Funct. Neurosurg. *69*, 197-201.

456. Yeni,S.N., Kabasakal,L., Yalcinkaya,C., Nisli,C., and Dervent,A. (2000). Ictal and interictal SPECT findings in childhood absence epilepsy. Seizure. *9*, 265-269.

457. Yetkin,F.Z., Mueller,W.M., Morris,G.L., McAuliffe,T.L., Ulmer,J.L., Cox,R.W., Daniels,D.L., and Haughton,V.M. (1997). Functional MR activation correlated with intraoperative cortical mapping. AJNR Am. J. Neuroradiol. *18*, 1311-1315.

458. Yetkin,F.Z., Swanson,S., Fischer,M., Akansel,G., Morris,G., Mueller,W., and Haughton,V. (1998). Functional MR of frontal lobe activation: comparison with Wada language results. AJNR Am. J. Neuroradiol. *19*, 1095-1098.

459. Yousry,T., Schmid,U.D., Schmidt,D., Heiss,D., Jassoy,A., Eisner,W., Reulen,H.J., and Reiser,M. (1995). [The motor hand area. Noninvasive detection with functional MRI and surgical validation with cortical stimulation]. Radiologe *35*, 252-255.

460. Zarahn,E., and Slifstein,M. (2001). A reference effect approach for power analysis in fMRI. Neuroimage. *14*, 768-779.

461. Zeineh,M.M., Engel,S.A., and Bookheimer,S.Y. (2000). Application of cortical unfolding techniques to functional MRI of the human hippocampal region. Neuroimage *11*, 668-683.

462. Zijlmans,M., Huiskamp,G., Hersevoort,M., Seppenwoolde,J.H., van Huffelen,A.C., and Leijten,F.S. (2007). EEG-fMRI in the preoperative work-up for epilepsy surgery. Brain *130*, 2343-2353.

463. Zubal,I.G., Spanaki,M.V., MacMullan,J., Corsi,M., Seibyl,J.P., and Spencer,S.S. (1999). Influence of technetium-99m-hexamethylpropylene amine oxime injection time on single-photon emission tomography perfusion changes in epilepsy. Eur. J. Nucl. Med. *26*, 12-17.